CERN 67-24
Volume II
20 December 1967

ORGANISATION EUROPÉENNE POUR LA RECHERCHE NUCLÉAIRE
CERN EUROPEAN ORGANIZATION FOR NUCLEAR RESEARCH

PROCEEDINGS OF THE 1967 CERN SCHOOL OF PHYSICS

Rättvik, May 21 - June 3, 1967

Volume II
Lectures by:

B.E.Y. Svensson

G E N E V A
1967

CERN - Service d'Information scientifique - H/293 - 3000 - janvier 1968
750 - mai 1978

SCIENTIFIC ORGANIZING COMMITTEE

Dr. J.S. Bell	(CERN)
Prof. G. von Dardel	(CERN and University of Lund)
Prof. A.G. Ekspong Chairman	(University of Stockholm and Swedish Atomic Research Council)
Dr. W.O. Lock	(CERN)
Prof. J. Nilsson	(University of Göteborg)
Prof. B. Ronne	(University of Stockholm)
Miss E.W.D. Steel Organizing Secretary	(CERN)
Prof. L. Van Hove	(CERN)
Dr. K. Winter	(CERN)

EDITORIAL BOARD FOR THE PROCEEDINGS

Dr. W.O. Lock	(CERN)
Prof. J. Nilsson	(University of Göteborg)

PREFACE TO VOLUME II

The 1967 CERN School at Rättvik was the sixth in a series that began in 1962. The lectures of the 1967 School started on the moring of 22 May and were attended by 84 students from 21 countries in Western Europe, Eastern Europe, the Middle East, and India. The School closed on 2 June with the traditional banquet.

The purpose of the School was to familiarize young post-graduate students of experimental physics with the current theoretical and experimental situation in elementary particle studies. Eleven lecturers contributed to this end by giving a total of 34 seminars, lectures, or after-dinner talks.

This volume contains the lectures given by Dr. B. E. Y. Svensson on "High-Energy Phenomenology and Regge Poles". In the interests of speed we have photographed the typescripts given to us by the authors and used the photo-offset reproduction process to produce the four volumes of the Proceedings. We trust that what has been lost in beauty of presentation will be compensated by the fact that the Proceedings will be available to the scientific community in a much shorter time than previously after the end of the School. We would be pleased to receive comments from readers on this change in our publishing policy.

Our thanks are due to the authors who have worked very hard to provide us with their manuscripts either at the School itself or a very few weeks afterwards, and to the Scientific Information Service for their careful and rapid work of publication.

Editorial Board.

CONTENTS

HIGH-ENERGY PHENOMENOLOGY AND REGGE POLES

B. E. Y. Svensson

Department of Theoretical Physics,
University of Lund

and

Theoretical Study Division, CERN, Geneva.

LIST OF CONTENTS

ACKNOWLEDGEMENTS

It is a pleasure to aknowledge discussions with Professor L. Van Hove, Drs. A.M. Wetherell, P. Carlsson, H. Högaasen and J.T. Donohue on different aspects of the topics treated. Several discussions with the participants at the School have had their influence on the final version of the notes, as have many of the nearly horse-winning questions. I want to express my appreciation to Professor G. Ekspong for the stimulating atmosphere I found at Rättvik. I am also very grateful to Professor L. Van Hove and to Professor J. Prentki for the kind hospitality extended to me at the CERN Theoretical Study Division, where the greater part of the lecture notes was written.

CHAPTER 1 - INTRODUCTION AND SURVEY. UNITS

The aim of these lecture notes on "High-Energy Phenomenology and Regge Poles" is to present the basic theoretical arguments underlying the Regge pole model, as well as its applications to particle (= stable particle or resonance) classification and to high-energy reactions. My point of view has been to try to explain the basic theoretical concepts and the general assumptions that underlie the model in as simple a language as possible, rather than to treat the most tricky aspects of the model or its most recent developments. In this attempt, I have tried always to remain close to the experimental findings. This seems to me almost indispensable, since the success of the Regge pole approach lies on the phenomenological level. Only experiment can decide whether a certain hypothesis of the model is correct or not.

In order to understand the current phenomenological treatments of high-energy hadronic reactions (hadron = strongly interacting particle) at all, whether they are discussed in terms of the Regge pole model or within any other framework, a certain amount of basic theory is necessary. In Part I of these notes an attempt is made to present this theoretical background. The presentation is kept as simple as possible; these chapters could just be glanced through and only used for reference by those who already have a working knowledge of relativistic kinematics, connection between amplitudes, cross-sections and polarization, partial wave and impact parameter expansions, etc. To give one example of the simple discussion, let me mention that the S-matrix is never used but the whole presentation is carried through in the wave function description. Such a procedure has certainly some drawbacks. For instance, the optical theorem in the general form can be justified only by plausibility arguments. Moreover, the treatment might seem unnecessarily cumbersome to those having a good knowledge of the S-matrix language. Nevertheless, I thought it pedagogically advantageous to use the wave description, since it is nearest to the conventional treatment of quantum mechanics in elementary text-books. To elucidate some mathematical topics encountered three Appendices at the end of the notes treat analytic functions, Bessel functions and Legendre functions, respectively.

In a phenomenological discussion, knowledge of the present experimental situation at high energy is needed. Part II is devoted to a survey of experimental results on total cross-sections, most aspects of elastic scattering, and some representative inelastic two-body processes. Among things not treated are large-angle ($\Theta_{cms} \sim 90°$) elastic scattering, and collisions leading to genuine many-body final states.

By high energy we mean throughout this text an incident laboratory momentum p_{lab} greater than 5 GeV/c. There is no fundamental reason for choosing this particular energy as the limit. But it is necessary to have some definition of the concept "high energy", and the one chosen is connected with the fact that most experimental quantities seem to have a smooth energy-dependence for $p_{lab} \gtrsim 5$ GeV/c. The reason is, presumably, the almost negligible contribution from resonance formation at these energies. Moreover, so many different channels are already open that it should not matter very much if a few more channels become kinematically accessible. Both these phenomena, resonance formation and passing the threshold for an inelastic channel, are known to have important influence on cross-sections, etc., at lower energies. It should be noted, though, that they do not seem to be completely out of the picture even at rather high energies.

While the high-energy region thus extends from $p_{lab} \sim 5$ GeV/c to the highest momenta within reach with the present day accelerators, the asymptotic energy region starts much further away. It is defined as those energies where the data satisfy general theoretical high-energy expectations, like the Pomeranchuk theorem, the vanishing of the real part of the forward scattering amplitude, and maybe spin independence. Based on extrapolation of the present findings, it seems as if at least a 4000 GeV accelerator, or a 45 GeV storage rings arrangement, would be needed in order to perform experiments in this asymptotic energy region.

Parts III and IV are devoted to the Regge pole model. The presentation is rather standard. It makes no claims whatsoever to be rigorous even at a rather modest physical level. For example, the results obtained in potential theory are merely stated, although a few of the important points are discussed at some length. The results are then taken over to hadronic interactions without much further motivation. The signature concept, for instance, is introduced by considering an exchange potential, not from a dispersion relation.

The basis for classification of hadrons on Regge trajectories is discussed, and illustrated by the non-strange mesons and fermions. At this School, these topics have been thoroughly discussed in the lectures by Professor G. Goldhaber and by Professor G. Giacomelli. Their lectures notes (report CERN 67-24, Vol. III, 1967) should therefore be consulted for more details.

The application of the Regge pole model to high-energy reactions is rather extensively illustrated for pion-nucleon elastic and, in particular, charge-exchange scattering. Nucleon-nucleon and kaon-nucleon reactions are on the other hand treated much more briefly. Some more or less disconnected theoretical topics, not discussed in the previous treatment, are collected in the last chapter.

It should be remarked that the contents of Chapters 2-7 and Appendices 1-3 of these notes are in fact extended versions of the corresponding lectures given at the School. On the other hand Chapters 8-16 are more or less the same wording as in the actual lectures, only slightly re-arranged at some places. During the last lecture an attempt was made to estimate the present status of the Regge pole model, which in these notes is put at the appropriate places.

There is very little reference to the literature in the text. In lecture notes like these I think this is an advantage, since it means that one may read them without having to look into the list of references continuously. Instead, I have appended a bibliography of the Regge pole literature. It is not complete, despite the fact that it contains some 300 different entries, but is hopefully at least a representative selection. It was completed on June 30, 1967.

We close this introductory chapter by specifying the conventions concerning units. They are, as usual in elementary-particle physics, such that $\hbar$, the Planck's constant divided by 2π, and c, the velocity of light, equals unity

$$\hbar = c = 1 \ . \tag{1.1}$$

Energy and mass are measured in MeV or GeV, but momentum in units of GeV/c merely to distinguish it from an energy. The unit of length is fermi (or femtometer), denoted fm, with

$$1 \text{ fm} = 10^{-15} \text{ m} . \tag{1.2}$$

The unit of time is sec. Cross-sections are measured in mb with

$$1 \text{ mb} = 10^{-31} \text{ m}^2 = 0.1(\text{fm})^2 . \tag{1.3}$$

Some useful conversion factors are

$$1 \text{ GeV} \approx 5 \text{ fm}^{-1} , \tag{1.4}$$

$$1 (\text{GeV})^{-1} \approx 0.2 \text{ fm} , \tag{1.5}$$

$$1 (\text{GeV})^{-2} \approx 0.389 \text{ mb} , \tag{1.6}$$

$$1 (\text{MeV})^{-1} \approx 7 \times 10^{-22} \text{ sec} . \tag{1.7}$$

Exercise 1.1: Derive these conversion factors.
[Hint: $\hbar = 6.582 \times 10^{-22}$ MeV sec, $c = 2.998 \times 10^{8}$ m/sec.]

My way to try to remember the first two relations is to observe that the pion Compton wavelength m_π^{-1} approximately equals $\sqrt{2}$ fm:

$$\frac{1}{m_\pi} \approx \frac{1}{140 \text{ MeV}} \approx \frac{10}{\sqrt{2}} (\text{GeV})^{-1} \approx \sqrt{2} \text{ fm} . \tag{1.8}$$

PART I

(Chapters 2-4)

SOME BASIC THEORETICAL TOOLS

In this part we shall introduce the fundamental theoretical concepts used in analysing scattering experiments, particularly at high energies. Most of what will be treated here should be well known to you. Nevertheless, we thought it worthwhile to repeat these things, since they will be used over and over again in the subsequent chapters. Thus a firm knowledge of the basic facts is indispensable, and this part will, we hope, at least serve as a reminder. Furthermore, it gives us the possibility to specify the conventions and the notation to be used.

CHAPTER 2 - KINEMATICS OF TWO-BODY REACTIONS

We shall almost exclusively consider two-body reactions. That is, in the collision of two particles, say a pion and a nucleon, we shall be particularly interested in those final states which also contain two particles. In the case of negative pions incident on protons, examples of such reactions are

$\pi^- p \to \pi^- p$ elastic scattering,

$\pi^- p \to \pi^0 n$ charge-exchange scattering,

$\pi^- p \to K^0 \Lambda$ associated production (or strangeness-exchange reaction).

Single production processes like

$$\pi^- p \to \eta(550) n ,$$

or even more like

$$\pi^- p \to \rho^0(760) n ,$$
$$\hookrightarrow \pi^+ \pi^-$$

and double production reactions like

$$\pi^- p \to \rho^0(760) + N^{*0}(1240) ,$$
$$\hookrightarrow \pi^+ \pi^- \quad \hookrightarrow \pi^- p$$

in which either or both final particles have very short lifetimes (of the order of 10^{-19} sec for η, 10^{-23} sec for ρ and N^*), are commonly called quasi-two-body reactions, in order to distinguish them from ordinary two-body processes and from genuine many-particle reactions like

$$\pi^- p \to \pi^+ \pi^- \pi^- p ,$$

in which by definition no formation of resonances occurs.

The reason for considering only two-body (and quasi-two-body) reactions is a purely pragmatic one: they are by far the least difficult to analyse theoretically, if for no other reason than because the kinematical considerations are much simpler than for other processes. As we shall see, though, one is forced to take all inelastic reactions into account,

including genuine many-particle reactions, when discussing elastic scattering. This is due to the conservation of probability or, to use a more fancy name, to "unitarity", which links together all possible final states.

Since we shall consider high-energy reactions, it is better to use relativistic kinematics. In particular, we must be able to transform relevant physical quantities, like momenta, cross-sections, etc., from the laboratory system (to be called "the lab.") to the centre-of-momentum system (c.m.s.), which is appropriate for theoretical considerations. The lab. is, by definition, the Lorentz frame where the nucleon is at rest; it is usually but not always (e.g. intersecting storage rings!) the system where experiments are performed. The theorist's preference for the c.m.s., in which the total momentum of the particles is zero, originates in the simple fact that only the relative motion of the particles is of interest in discussing their interaction, not the over-all motion of them.

2.1 πN scattering

To be more precise, let us first consider the kinematics of pion-nucleon elastic scattering; it goes without saying that what we really require is a two-body process where the masses of the particles in the initial state [let them be m for the one (pion) and M for the other (nucleon)] are the same as the masses in the final state. The notation for the four-momenta, energies and three-momenta are shown in Table 2.1,

Table 2.1

Notation for kinematical quantities

Particle (mass)	Lab.	c.m.s.	Arbitrary Lorentz frame
π_{in} (m)	$p_1 = (\omega_{lab}, \vec{p}_{lab})$	$k_1 = (\omega, -\vec{k})$	q_1
N_{in} (M)	$p_2 = (M, \vec{0})$	$k_2 = (\epsilon, \vec{k})$	q_2
π_{out} (m)	$p_1' = (\omega'_{lab}, \vec{p}\,'_{lab})$	$k_1' = (\omega', -\vec{k}')$	q_1'
N_{out} (M)	$p_2' = (\epsilon'_{lab}, \vec{p}_2')$	$k_2' = (\epsilon', \vec{k}')$	q_2'

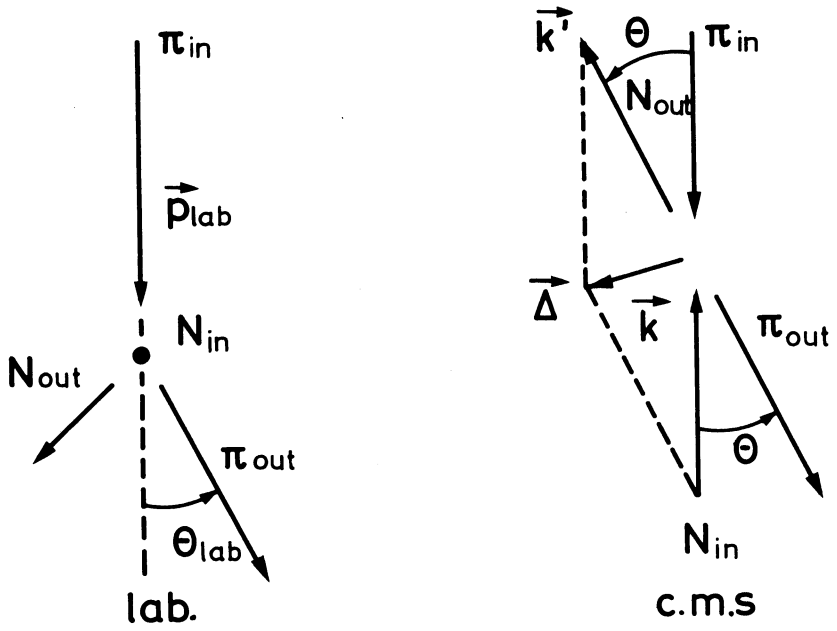

Fig. 2.1

The momentum configuration in the laboratory (lab.) and the centre-of-momentum (c.m.s.) systems.

and the kinematical situation in the lab. and in the c.m.s. is illustrated in Fig. 2.1.

The four-momenta are not independent, since conservation of energy and momentum requires

$$q_1 + q_2 = q_1' + q_2' \ . \tag{2.1}$$

Consider first the c.m.s. Our notation for the three-momenta already conforms with momentum conservation. The conservation of energy gives the relation

$$\omega + \epsilon = \omega' + \epsilon' = E = \sqrt{s} \ , \tag{2.2}$$

which also serves to define the total c.m.s. energy, E, and its square s; these two related variables will be used repeatedly. Finally, one defines, as in Fig. 2.1, a c.m.s. scattering angle Θ by the relation

$$\vec{k} \cdot \vec{k}' = |\vec{k}| \cdot |\vec{k}'| \cdot \cos \Theta \ . \tag{2.3}$$

It is now easy to prove that all kinematical quantities in the c.m.s. (to be more exact all those which are independent of the orientation of the particular three-dimensional coordinate system used) can be expressed in terms of the c.m.s. energy E and the scattering angle Θ. Namely, the direction of $\vec{k}'$ with respect to $\vec{k}$ is given by Θ. Moreover, the absolute values $|\vec{k}| = k$ and $|\vec{k}'| = k'$, as obtained from the energy-conservation relation

$$E = \sqrt{(-\vec{k})^2 + m^2} + \sqrt{\vec{k}^2 + M^2} = \sqrt{(-\vec{k}')^2 + m^2} + \sqrt{\vec{k}'^2 + M^2} \ , \qquad (2.4)$$

are given by

$$k = k' = \frac{1}{2E} \sqrt{\lambda(E^2, M^2, m^2)} \ . \qquad (2.5)$$

Here, we have introduced the convenient notation

$$\lambda(x, y, z) = (x - y - z)^2 - 4yz = x^2 + y^2 + z^2 - 2xy - 2yz - 2zx \ ; \qquad (2.6)$$

it represents a function symmetric in all its three arguments.

Exercise 2.1: Prove Eq. (2.5). Furthermore, express the energies ω, ω', ϵ and ϵ' in terms of E and the masses, and show that $\omega = \omega'$, $\epsilon = \epsilon'$.

One could thus be satisfied with, say, the variables E and cos Θ. However, some combinations of these variables are often more convenient. For instance, defining the three-momentum transfer by the equation

$$\vec{\Delta} = \vec{k}' - \vec{k} \qquad (2.7)$$

(see also Fig. 2.1), one finds for its square

$$\Delta^2 = (\vec{k}' - \vec{k})^2 = k^2 + k'^2 - 2kk' \cos\Theta = -t \ . \qquad (2.8)$$

This relation also defines "minus the momentum transfer squared", t. Consequently, the variables s and t could be used as well in specifying the kinematical configuration. In particular, the relation between t and cos Θ reads

$$\cos\Theta = 1 + \frac{t}{2k^2} = 1 + \frac{2ts}{\lambda(s, M^2, m^2)} \quad . \tag{2.9}$$

Why use s and t? Simply because these are relativistic variables; this can be seen as follows (note Exercise 2.1):

$$s = (\epsilon + \omega)^2 = (\epsilon + \omega)^2 - [\vec{k} + (-\vec{k})]^2 = (k_1 + k_2) = (q_1 + q_2)^2 \ , \tag{2.10}$$

$$t = -(\vec{k}' - \vec{k})^2 = (\epsilon' - \epsilon)^2 - (\vec{k}' - \vec{k})^2 = (k_2' - k_2)^2 = (q_2' - q_2)^2 \ . \tag{2.11}$$

The last equalities in these two equations are due to the relativistic invariance of the square $a^2 = a_0^2 - \vec{a}^2$ of a four vector $a = (a_0, \vec{a})$.

It follows that the invariant variables s and t, or "Mandelstam variables" as they are often called, are particularly convenient in transforming kinematical quantities from the c.m.s. to the lab., or vice versa. For example

$$s = M^2 + m^2 + 2M\omega_{lab} \tag{2.12}$$

which at high energy, $p_{lab} \gg M, m$, gives

$$s \approx 2Mp_{lab} \ . \tag{2.13}$$

This expresses the well-known fact that the square of the c.m.s. energy grows linearly with the laboratory momentum at high energies. For the variable t one finds

$$t = -2M(\epsilon'_{lab} - M) \ , \tag{2.14}$$

which shows that the momentum transfer squared is proportional to the kinetic energy of the recoil nucleon in the lab.

Exercise 2.2: Prove relations (2.12 - 2.14).

What is the range of variation of the variables s and t? Obviously

$$s \geq (M+m)^2 \ , \tag{2.15}$$

while for a given value of s one has

$$0 \leq -t \leq 4k^2 = \frac{1}{s}\lambda(s, M^2, m^2) \approx s \ , \tag{2.16}$$

the last approximate equality being valid at high energy. The possible values for s and t are conveniently illustrated in the s-t plane, or "Mandelstam plane", of Fig. 2.2. Here the shaded region corresponds to s and t fulfilling the restrictions (2.15), (2.16); it is called the physical region for the process in question. We shall later be interested also in values of s and t outside this physical region.

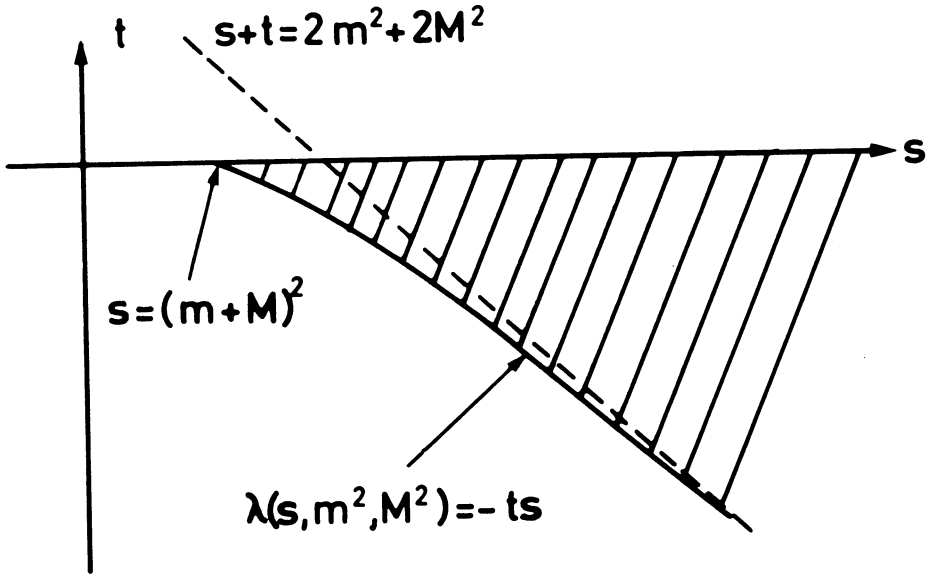

Fig. 2.2

An illustration of the domain of variation for s and t in the "Mandelstam plane".

2.2 General masses

It only remains to generalize the relations obtained for an elastic scattering process to an arbitrary process

$$a + b \to c + d \tag{2.17}$$

m_a	m_b	m_c	m_d	masses
ϵ_a	ϵ_b	ϵ_c	ϵ_d	c.m.s. energies
$\vec{k}$	$-\vec{k}$	$\vec{k}'$	$-\vec{k}'$	c.m.s. three-momenta .

Very often one represents such a process by the diagram in Fig. 2.3, which at his stage has no deeper significance but merely serves as a convenient way to keep track of the notation

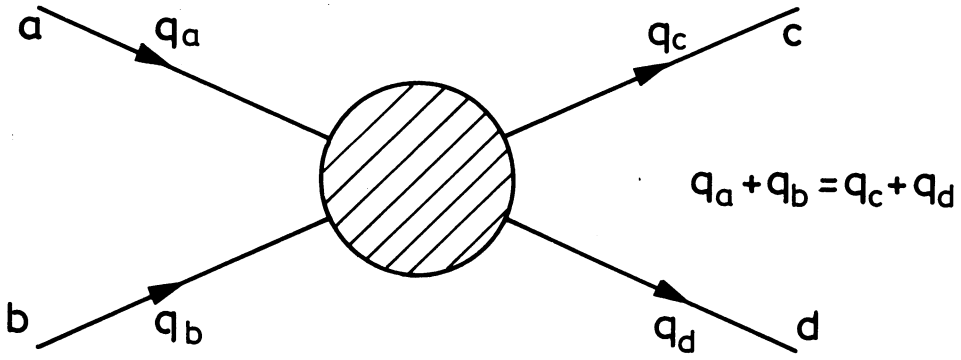

Fig. 2.3

An illustration of the reaction (2.17) and the notation for the four-momenta.

In analogy with elastic scattering, one defines

$$s = (q_a + q_b)^2 = (q_c + q_d)^2 , \tag{2.18}$$

$$t = (q_a - q_c)^2 = (q_b - q_d)^2 , \tag{2.19}$$

where again s is the total c.m.s. energy squared and t is the square of the four-momentum transfer from particle a to c, or from particle b to d. Then one finds

$$k = |\vec{k}| = \frac{1}{2\sqrt{s}} \sqrt{\lambda(s, m_a^2, m_b^2)} , \tag{2.20}$$

$$k' = |\vec{k}'| = \frac{1}{2\sqrt{s}} \sqrt{\lambda(s, m_c^2, m_d^2)} , \tag{2.21}$$

$$\epsilon_a = \sqrt{s} - \epsilon_b = \frac{1}{2\sqrt{s}} (s + m_a^2 - m_b^2) , \tag{2.22}$$

$$\epsilon_c = \sqrt{s} - \epsilon_d = \frac{1}{2\sqrt{s}} (s + m_c^2 - m_d^2) . \tag{2.23}$$

Exercise 2.3: Derive the relations (2.20) to (2.23).

Furthermore, one introduces the c.m.s. scattering angle Θ by the definition

$$\vec{k} \cdot \vec{k}' = kk' \cos \Theta ; \tag{2.24}$$

$\cos \Theta$ can of course be expressed in terms of s and t. We give this relation in the form

$$t = 2kk' \cos \Theta + m_a^2 + m_c^2 - 2\epsilon_a \epsilon_c . \tag{2.25}$$

Exercise 2.4: Derive Eq. (2.25) and use it to give $\cos \Theta$ as function of s and t.

Let us note one more thing before we are through with the kinematics. For symmetry reasons, one often introduces a third invariant, or Mandelstam variable u defined by

$$u = (q_a - q_d)^2 = (q_b - q_c)^2 . \tag{2.26}$$

Since all kinematical quantities are functions of s and t, so is u. In fact, one has

$$\begin{aligned} s+t+u &= (q_a+q_b)^2 + (q_c-q_a)^2 + (q_a-q_d)^2 \\ &= q_a^2 + q_b^2 + q_c^2 + q_d^2 \\ &\quad + 2q_aq_b - 2q_aq_c + q_a^2 + q_a^2 - 2q_aq_d \\ &= m_a^2 + m_b^2 + m_c^2 + m_d^2 \\ &\quad + 2q_a(q_b + q_a - q_c - q_d) \\ &= \sum_{i=a}^{d} m_i^2 \ , \end{aligned} \tag{2.27}$$

which is the desired relation. The interpretation of u is similar to that of t, viz., as a four-momentum transfer squared, now between particles a and d, or between particles b and c.

Exercise 2.5: If the masses of all four particles are equal, prove that

$$u = -2k^2(1 + \cos\Theta) \ .$$

What is the result if $m_a = m_c = m$, $m_b = m_d = M$, particularly at high energy?

CHAPTER 3 - SCATTERING AMPLITUDES AND CROSS-SECTIONS

Consider once more the particular example of $\pi^- p$ collisions. At first, we shall assume that p_{lab} is below the (effective) threshold for pion production; this requires $p_{lab} \lesssim 350$ MeV/c, and is not a high energy in our terminology. However, we shall later generalize the results at the appropriate places. By assumption, then, the only reactions possible are

$\pi^- p \to \pi^- p$ elastic scattering

$\pi^- p \to \pi^0 n$ charge-exchange scattering .

The last process is included merely to have an explicit example of an inelastic reaction.

3.1 The spinless case

We treat the process in the c.m.s., and choose the coordinate system such that the incoming nucleon has its momentum $\vec{k}$ along the positive z axis as indicated in Fig. 3.1. The collision is assumed to take place at the

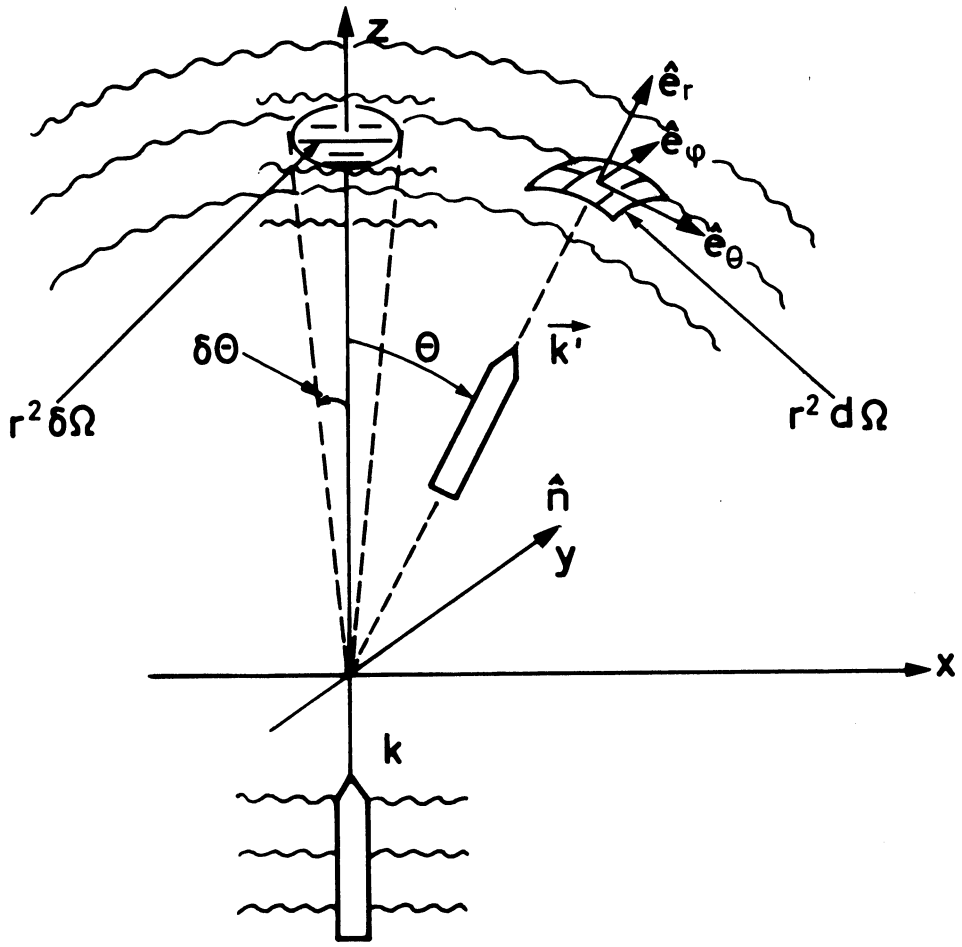

Fig. 3.1

The choice of the coordinate system used for the wave function (3.1).

origin. The scattering angle Θ is then the polar angle of the outgoing nucleon momentum $\vec{k}'$. We shall furthermore assume that the problem has complete cylindrical symmetry around the direction of the incoming particles, i.e., the z axis. Then, no measurable quantities should depend on the azimuthal angle φ for $\vec{k}'$, and we may, as in Fig. 3.1., choose the x axis so that $\vec{k}'$ lies in the x-z plane, i.e., such that $\varphi = 0$. Finally, we shall assume that the interaction is of finite range, i.e., the particles can be treated as free ones outside the radius R of interaction.

Under these assumptions, the asymptotic wave function consists of three parts (here, asymptotic means for a distance r from the origin much bigger than the interaction radius):

i) An incoming plane wave exp (ikz) in the z direction describing the initial state. To avoid misconceptions, note that this wave also represents an outgoing wave along the positive z axis, i.e., a wave that passes the scattering centre unchanged.

ii) A wave $F_{el}(\cos\Theta, E)r^{-1}\exp(ikr)$, describing the elastically scattered π^-p system. Here, the radial dependence is characteristic of an outgoing spherical wave. Observe that the absolute value of the outgoing nucleon momentum is the same as in the initial state, since it is an elastic scattering process. The factor F_{el} multiplying the spherical wave is called the elastic scattering amplitude. It is, in general, a function of both $\cos\Theta$ and the total c.m.s. energy E, but not of the azimuth angle φ, from the cylinder symmetry argument.

iii) An outgoing spherical wave $F_{c.e.}(\cos\Theta, E)r^{-1}\exp(ik''r)$ describing the emerging π^0n system. Here, the r dependent factor differs from the corresponding factor in the elastic wave with respect to the momentum k'' of the outgoing neutron; since $m_{\pi^-} \neq m_{\pi^0}$ and $m_p \neq m_n$ one has indeed $k = |\vec{k}| \neq k'' = |\vec{k}''|$. Although the difference becomes negligibly small at high energy, for pedagogical reasons it is convenient to keep $k \neq k''$. The factor $F_{c.e.}$ in front is the charge-exchange scattering amplitude, again a function of angle and energy.

Summarizing, the asymptotic form of the wave function reads

$$\psi(\vec{r}) \simeq \exp(ikz) + F_{el}(\cos\Theta, E)\frac{1}{r}\exp(ikr) + F_{c.e.}(\cos\Theta, E)\frac{1}{r}\exp(ik''r) \quad . \tag{3.1}$$

We next derive the differential cross-section $d\sigma/d\Omega$, defined by (cf. Fig. 3.1)

$$\frac{d\sigma}{d\Omega} = \frac{\text{outgoing flux through the area } r^2 d\Omega}{\text{incoming flux perpendicular to } \vec{k}} . \tag{3.2}$$

Here, the fluxes may be calculated knowing the probability current density $\vec{j}(\vec{r})$. For a wave function satisfying the Klein-Gordon equation, appropriate for scalar particle scattering at relativistic energies, $\vec{j}$ may be taken as

$$\vec{j} = \frac{i}{2} [\psi \nabla \psi^* - \psi^* \nabla \psi] = \text{Im} [\psi^* \nabla \psi] . \tag{3.3}$$

Indeed, what fixes $\vec{j}$ is the requirement that it should satisfy a continuity equation

$$\nabla \vec{j} + \frac{\partial \rho}{\partial t} = 0 , \tag{3.4}$$

where ρ is the probability density; this relation follows from conservation of probability, but it determines $\vec{j}$ only up to a (constant) multiplicative factor, which is, however, of no physical importance.

Exercise 3.1: Assume that ψ satisfies a Klein-Gordon equation

$$(\Box - m^2)\psi \equiv \left(\nabla^2 - \frac{\partial^2}{\partial t^2} - m^2\right)\psi = 0 .$$

Then, prove that $\vec{j}$ of Eq. (3.3) satisfies the continuity equation (3.4) with

$$\rho = \text{Im}\left[\psi^* \frac{\partial \psi}{\partial t}\right] .$$

Using Eq. (3.3), the incoming flux through unit area normal to the momentum $\vec{k}$ is

$$\hat{e}_z \cdot \vec{j}_{inc} = \text{Im}\left[\exp(-ikz) \frac{d}{dz} \{\exp(ikz)\}\right] = k . \tag{3.5}$$

To calculate the outgoing flux through the area $r^2 d\Omega$, one needs the radial part of the current density for the outgoing spherical wave. Since in polar coordinates

$$\nabla = \hat{e}_r \frac{\partial}{\partial r} + \hat{e}_\Theta \frac{\partial}{r \partial \Theta} + \hat{e}_\varphi \frac{\partial}{r \sin \Theta \, \partial \varphi} , \tag{3.6}$$

where the unit vectors $\hat{e}_r$, $\hat{e}_\Theta$, $\hat{e}_\varphi$ are specified in Fig. 3.1, it follows that

$$\hat{e}_r \cdot \vec{j}_{out;\,el} \simeq |F_{el}(\cos \Theta, E)|^2 \frac{k}{r^2} . \tag{3.7}$$

Here, we have neglected terms tending to zero like r^{-3} when $r \to \infty$. This implies an elastic cross-section given by

$$\frac{d\sigma_{el}}{d\Omega} = |F_{el}(\cos \Theta, E)|^2 . \tag{3.8}$$

Analogously, one obtains for large r

$$\hat{e}_r \cdot j_{out;\,c.e.} \simeq |F_{c.e.}(\cos \Theta, E)|^2 \frac{k''}{r^2} , \tag{3.9}$$

which gives the cross-section for charge-exchange

$$\frac{d\sigma_{c.e.}}{d\Omega} = \frac{k''}{k} |F_{c.e.}(\cos \Theta, E)|^2 \tag{3.10}$$

Note the difference between the expressions for the elastic and the charge-exchange cross-section: the ratio of the momenta in the final and initial states multiplies the square of the amplitude in the case of charge-exchange.

The scattering amplitudes, both the elastic and the charge-exchange ones, can thus be measured (up to a phase) by measuring the differential cross-sections. As we shall see below, this will no longer be true when one treats the spin of the nucleon consistently.

We note a few trivial consequences of the formulae (3.8) and (3.10). First, since the scattering amplitude does not depend on the azimuth angle φ, we may integrate over that angle to obtain

$$\frac{d\sigma_{el}}{d(\cos\Theta)} = \int_0^{2\pi} d\varphi \, \frac{d\sigma_{el}}{d\Omega} = 2\pi |F_{el}(\cos\Theta, E)|^2 \, , \qquad (3.11)$$

with a similar result for the charge-exchange cross-section. Going one step further, the total elastic cross-section is given by

$$\sigma_{el} = \int d\Omega \, \frac{d\sigma_{el}}{d\Omega} = 2\pi \int_{-1}^{+1} d(\cos\Theta) |F_{el}(\cos\Theta, E)|^2 \, . \qquad (3.12)$$

Again, there is a corresponding formula for $\sigma_{c.e.}$, the total charge-exchange cross-section.

The derivation of the formulae for the cross-sections might look as if it were only applicable in the low-energy limit, i.e., for non-relativistic kinematics. However, this is not true. In fact, we have referred all quantities to the c.m.s., so there is so far no question of transforming from one reference frame to another. But one is indeed interested in transforming the c.m.s. cross-section to, say, the lab. or vice versa. The simplest way to accomplish this is to write it in terms of relativistic variables. This may be done as follows. From the definition (2.8) of t, the negative of the momentum transfer squared, we find for elastic scattering

$$t = -2k^2(1 - \cos\Theta) \rightarrow dt = 2k^2 d(\cos\Theta) \, , \qquad (3.13)$$

which immediately gives

$$\frac{d\sigma_{el}}{d(\cos\Theta)} = 2k^2 \, \frac{d\sigma_{el}}{dt} \, . \qquad (3.14)$$

Consequently

$$\frac{d\sigma_{el}}{dt} = \frac{\pi}{k^2} |F_{el}(\cos\Theta, E)|^2 \, . \qquad (3.15)$$

This is the differential elastic cross-section per interval in the momentum transfer squared. Since t may be expressed in terms of quantities measured in the lab. system [see Eq. (2.14)] this formula gives directly the scattering amplitude as a function of lab. quantities.

To derive the corresponding formula for the charge-exchange reaction, we must observe that the connection between t and cos Θ for an inelastic reaction as given by Eq. (2.25) reads

$$t = 2kk'' \cos\Theta + (\text{terms independent of } \cos\Theta) , \tag{3.16}$$

so that

$$dt = 2kk'' \, d(\cos\Theta) , \tag{3.17}$$

and, consequently,

$$\frac{d\sigma_{c.e.}}{dt} = \frac{1}{2kk''} \frac{d\sigma_{c.e.}}{d(\cos\Theta)} = \frac{\pi}{k^2} |F_{c.e.}(\cos\Theta, E)|^2 . \tag{3.18}$$

Note the similarity between the elastic and the charge-exchange cross-sections if $d\sigma/dt$ is considered instead of $d\sigma/d\Omega$.

From the point of view of kinematical variables, the formulae for $d\sigma/dt$ are a sort of hybrid: they involve both c.m.s. variables Θ and E, and the relativistic variable t. It would be more consistent to have a scattering amplitude which is also a function of the Mandelstam variables s and t. Of course, this is no problem, since we know the relation between these variables and cos Θ and E. However, one usually changes the normalization somewhat, defining a relativistic scattering amplitude, or T matrix element, by the relations

$$T_{el}(s, t) = 8\pi\sqrt{s} \, F_{el}(\cos\Theta, E) , \tag{3.19}$$

$$T_{c.e.}(s, t) = 8\pi\sqrt{s} \, F_{c.e.}(\cos\Theta, E) . \tag{3.20}$$

Here, we shall not enter into a discussion on why to use such a normalization. Let us only remark that several other conventions concerning factors of 2's and π's, and even of the momenta, are used in the literature. Thus, one must

be careful and check the conventions used by each particular author. This is most easily done by looking at the expression for the cross-section. With the conventions we use one finds

$$\frac{d\sigma_{el}}{dt} = \frac{1}{64\pi sk^2} |T_{el}(s,t)|^2 , \tag{3.21}$$

$$\frac{d\sigma_{c.e.}}{dt} = \frac{1}{64\pi sk^2} |T_{c.e.}(s,t)|^2 . \tag{3.22}$$

These expressions will be used as alternatives to the forms (3.18) in our subsequent discussions of high-energy reactions. We observe that at those energies where the masses of the incoming particles may be neglected compared to the total c.m.s. energy, we have $k = \frac{1}{2}\sqrt{s}$ so that

$$\frac{d\sigma}{dt} \approx \frac{1}{16\pi s^2} |T(s,t)|^2 \quad \text{for} \quad s >> m^2, M^2 . \tag{3.23}$$

For instance, in pion-nucleon collisions at $p_{lab} = 10$ GeV/c, the approximation $k = \frac{1}{2}\sqrt{s}$ is good to about 5%; in nucleon-nucleon collisions at the same momentum to about 10%.

3.2 The optical theorem

In deriving the cross-sections above in terms of the scattering amplitudes we were really not quite consistent. Actually, we should calculate the probability current density $\vec{j}$ using the full asymptotic wave function, not merely the separate contributions from the incoming and the outgoing waves. In other words, since $\vec{j}$ is quadratic in ψ, there could be interference terms between the different waves. As we shall now show, such an interference term between the incoming plane wave and the elastically scattered wave does indeed occur. Moreover, this term has a definite physical interpretation. In fact, it gives the attenuation of the incoming wave due to the reactions taking place and is thus related to the total cross-section. The relation which expresses this fact is known as the optical theorem. Our derivation of this relation follows closely the treatment by K. Gottfried in his book "Quantum Mechanics. Vol. I: Fundamentals" (W.A. Benjamin, Inc., New York and Amsterdam, 1966), p. 106-108.

To derive this relation within the wave function description, let us first simplify the problem to the extent that we neglect the charge-exchange reaction, i.e., we assume that only elastic scattering takes place; this would actually be the case if, instead of $\pi^- p$ collisions, we considered $\pi^+ p$ collisions below the threshold for pion production. Then, the radial part of the current density is

$$\hat{e}_r \cdot \vec{j} \simeq \mathrm{Im}\left[\left\{\exp(-ikr\cos\Theta) + F_{el}^*(\cos\Theta, E)\frac{1}{r}\exp(-ikr)\right\} \times \frac{\partial}{\partial r}\left\{\exp(ikr\cos\Theta) + F_{el}(\cos\Theta, E)\frac{1}{r}\exp(ikr)\right\}\right] \qquad (3.24)$$

$$= \hat{e}_r[\vec{j}_{inc} + \vec{j}_{out;el} + \vec{j}_{int}] .$$

Here, $\vec{j}_{inc}$ and $\vec{j}_{out;el}$ are those current densities already calculated [see Eqs. (3.5) and (3.7)], while

$$\hat{e}_r \cdot \vec{j}_{int} \simeq \mathrm{Im}\left[ikF_{el}(\cos\Theta, E)\frac{1}{r}\exp\{ikr(1-\cos\Theta)\} + ik\cos\Theta\, F_{el}^*(\cos\Theta, E)\frac{1}{r}\exp\{-ikr(1-\cos\Theta)\}\right] . \qquad (3.25)$$

This interference term has an angular dependence which is drastically different from the other two terms in the current; while j_{inc} and $j_{out;el}$ are smooth functions, j_{int} oscillates wildly as a function of the distance r when $\vec{r} \to \infty$ in all directions other than the very forward one, $\cos\Theta = 1$. If, instead of waves with sharp momentum we had considered wave packets, i.e., superposition of waves with momenta in a certain interval $\Delta\vec{k}$ around $\vec{k}$, such oscillating terms would have disappeared in the k integration. For example

$$\int_{k}^{k+\Delta k} dk \exp\{ikr(1-\cos\Theta)\} = \begin{cases} \Delta k & \text{if } \cos\Theta = 1 \\ \dfrac{1}{ir(1-\cos\Theta)}\left[\exp\{ikr(1-\cos\Theta)\}\right]_{k}^{k+\Delta k} \to & \\ \to 0 \text{ as } r \to \infty \text{ if } \cos\Theta \neq 1 . & \end{cases} \tag{3.26}$$

With this in mind, terms oscillating in r with a frequency proportional to k may always be neglected when $r \to \infty$.

What happens then in the forward direction? Let us consider the flux through a small area $r^2\delta\Omega$, corresponding to a cone around the z axis in Fig. 3.1, with a small opening angle $\delta\Theta$. We integrate the expression for the interference current over this angular interval. All smoothly varying factors can be taken out of the integral and put equal to their value at $\Theta = 0$. The integral to be evaluated is thus

$$\int_{\cos\delta\Theta}^{1} d(\cos\Theta) \exp\{ikr(1-\cos\Theta)\} =$$

$$= \exp(ikr)\frac{1}{-ikr}\left[\exp(-ikr) - \exp(-ikr\cos\delta\Theta)\right] = \tag{3.27}$$

$$= \frac{i}{kr} + \text{oscillating terms} .$$

Consequently, as $r \to \infty$,

$$r^2 \int_{\delta\Omega} d\Omega\, \hat{e}_r \cdot \vec{j}_{int} \simeq r^2 2\pi\, \mathrm{Im}\left[i\frac{k}{r}\left\{\frac{i}{kr} F_{el}(\cos\Theta = 1, E) - \frac{i}{kr} F_{el}^{*}(\cos\Theta = 1, E)\right\}\right] = \tag{3.28}$$

$$= -4\pi\, \mathrm{Im}\, F_{el}(\cos\Theta = 1, E) .$$

To relate this to something measurable, we note that the conservation of probability in the stationary case under consideration may be expressed by requiring the net flux out of a sufficiently big sphere around the origin to be zero; the probability that particles enter into the sphere equals the probability that something comes out of it. Mathematically, this is expressed by the relation

$$r^2 \int d\Omega \hat{e}_r \cdot \vec{j} \simeq 0 \; ; \tag{3.29}$$

it may also be derived from the continuity equation (3.4) by noting that $\partial\rho/\partial t$ vanishes for a stationary process.

Of the three terms that compose the current, $\vec{j}_{inc}$ gives itself a vanishing contribution to the integral (3.29). What remains can be written

$$-4\pi \, \mathrm{Im} \, F_{el}(\cos\Theta = 1, E) + \int d\Omega \, k |F_{el}(\cos\Theta, E)|^2 = 0 \, , \tag{3.30}$$

or, from the definition (3.12) of the elastic cross-section,

$$\sigma_{el}(E) = \frac{4\pi}{k} \, \mathrm{Im} \, F_{el}(\cos\Theta = 1, E) \, . \tag{3.31}$$

This is (a special case of) the optical theorem, valid in the absence of inelastic reactions. It relates the total (elastic) cross-section to the imaginary part of the forward elastic scattering amplitude.

The essence of this result is the following. Due to the fact that scattering takes place, the outgoing wave along the positive z axis is not merely the incoming one. On the contrary, it is attenuated by an amount corresponding to the scattering that occurs; what has been taken away from the incident beam due to the collision appears as an outgoing scattered wave. Or in still other words: the scattering centre casts a shadow behind it.

Next we have to generalize the optical theorem to the case when inelastic reactions also occur. Let us at first include only the charge-exchange reaction. It is then easy to see that the interference terms

in the probability current between the outgoing $\pi^0 n$ wave and any of the parts describing the $\pi^- p$ system are oscillating as $r \to \infty$; remember that $k'' \neq k$. Thus, the only effect of including charge-exchange is to add to the total current $\vec{j}$ the term $\vec{j}_{out;\,c.e.}$ of Eq. (3.9). This modifies Eq. (3.30) to read

$$-4\pi \,\mathrm{Im}\, F_{el}(\cos\Theta = 1, E) + \int d\Omega\, k |F_{el}(\cos\Theta, E)|^2 + \int d\Omega\, k'' |F_{c.e.}(\cos\Theta, E)|^2 = 0 \,, \tag{3.32}$$

so that, remembering Eq. (3.10),

$$\frac{4\pi}{k} \,\mathrm{Im}\, F_{el}(\cos\Theta = 1, E) = \sigma_{el}(E) + \sigma_{c.e.}(E) = \sigma_{tot}(E) \,. \tag{3.33}$$

Consequently the imaginary part of the forward <u>elastic</u> scattering amplitude is in this case directly related to the sum of the elastic and the charge-exchange cross-sections, i.e., to the <u>total</u> cross-sections σ_{tot}.

In view of the fact that the optical theorem is a way of expressing the attenuation of the incoming beam in the forward direction as given by everything that is taken out of it, it is natural that the optical theorem generalizes to processes where several inelastic channels are open. To discuss this problem, involving as it does two-body, quasi-two-body and many-body final states, it is indispensable to use the S-matrix formulation instead of the wave-function language. In fact, from the unitarity of the S-matrix one may prove the general relation

$$\sigma_{tot}(E) = \frac{4\pi}{k} \,\mathrm{Im}\, F_{el}(\cos\Theta = 1, E) \,, \tag{3.34}$$

where $\sigma_{tot}(E)$ is the total cross-section, i.e., the sum of all cross-sections for every possible reaction occurring in the collision of the two incident particles at the c.m.s. energy E. This is the form of the optical theorem which we shall use frequently.

Let us finally note that in terms of the relativistic amplitude (3.19), the optical theorem reads

$$\sigma_{tot}(s) = \frac{1}{2k\sqrt{s}} \, \mathrm{Im} \, T_{el}(s, t = 0) \, , \tag{3.35}$$

from which one obtains the high-energy form

$$\sigma_{tot}(s) \approx \frac{1}{s} \, \mathrm{Im} \, T_{el}(s, t = 0) \, , \qquad s >> m^2, \, M^2 \, . \tag{3.36}$$

3.3 A consistent treatment of the spin

Using the same picture as before, Fig. 3.1, the spin of the nucleon is described by the usual (Pauli) spinors

$$\xi(m_s) = \begin{cases} \begin{pmatrix} 1 \\ 0 \end{pmatrix} & \text{for} \quad m_s = +\tfrac{1}{2} \\ \begin{pmatrix} 0 \\ 1 \end{pmatrix} & \text{for} \quad m_s = -\tfrac{1}{2} \end{cases} \tag{3.37}$$

on which act the conventional spin matrices

$$\sigma_x = \begin{pmatrix} 0 & 1 \\ 1 & 0 \end{pmatrix} , \quad \sigma_y = \begin{pmatrix} 0 & -i \\ i & 0 \end{pmatrix} , \quad \sigma_z = \begin{pmatrix} 1 & 0 \\ 0 & -1 \end{pmatrix} , \tag{3.38}$$

$$\sigma_{\pm} = \sigma_x \pm i\sigma_y \, . \tag{3.39}$$

These conventions assume that the z axis is chosen as the spin quantization axis.

The incoming wave is now the product of the usual plane wave $\exp(ikz)$ and a spin wave function ξ, in general a linear combination of $\xi(\pm \tfrac{1}{2})$. The outgoing spherical wave has one part where the spinor is the same as for the incoming wave (spin-non-flip part) and another where the spin is reversed (spin-flip part). Neglecting, for simplicity, a possible charge-exchange reaction, the asymptotic wave-function for $m_s = \pm \tfrac{1}{2}$ may thus be written

$$\psi_{m_s}(\vec{r}) \simeq \xi(m_s) \exp(ikz) + [G_{m_s}(\cos\Theta, E)\xi(m_s) + H_{m_s}(\cos\Theta, E)\xi(-m_s)]\frac{1}{r}\exp(ikr) . \tag{3.40}$$

We now anticipate a result which we shall prove when we discuss the partial wave expansion: the spin-non-flip and spin-flip parts for the two possible m_s values are related by

$$G_{+1/2}(\cos\Theta, E) = G_{-1/2}(\cos\Theta, E) \equiv G(\cos\Theta, E) , \tag{3.41}$$

$$H_{+1/2}(\cos\Theta, E) = -H_{-1/2}(\cos\Theta, E) \equiv H(\cos\Theta, E) . \tag{3.42}$$

Since

$$\xi(-m_s) = 2m_s i\sigma_y \xi(m_s) , \tag{3.43}$$

we may write

$$\psi_{m_s}(\vec{r}) \simeq \xi(m_s) \exp(ikz) + F(\cos\Theta, E)\xi(m_s)\frac{1}{r}\exp(ikr) , \tag{3.44}$$

where the scattering amplitude $F(\cos\Theta, E)$ now is a 2×2 matrix,

$$F(\cos\Theta, E) = G(\cos\Theta, E) + i\vec{\sigma} \cdot \hat{n}\, H(\cos\Theta, E) , \tag{3.45}$$

$$\hat{n} = \frac{\vec{k} \times \vec{k}'}{|\vec{k}| \cdot |\vec{k}'|} = \hat{e}_y . \tag{3.46}$$

Here, G should be thought of as multiplied by the 2×2 unit matrix. Moreover, we have written $\vec{\sigma} \cdot \hat{n}$ instead of σ_y, with $\hat{n}$ the unit normal to the scattering plane, which in Fig. 3.1 is the x-z plane. The fact that only σ_y enters into F, and not σ_x and σ, may be seen to follow from parity conservation. We also note that the form (3.45) is applicable to elastic as well as to charge-exchange scattering.

Now let us consider cross-sections. Since both the initial and final nucleon has two spin degrees of freedom, there are several different cross-sections to be considered, depending on the spin direction of the

target and the outgoing nucleon. Let us as a particularly important example consider the case of a target nucleon polarized in the direction $\hat{n}$. We describe this situation by introducing the eigenvectors $\chi(\pm \frac{1}{2})$ to $\vec{\sigma} \cdot \hat{n} = \sigma_y$:

$$\vec{\sigma} \cdot \hat{n} \chi(\pm \tfrac{1}{2}) = \pm \chi(\pm \tfrac{1}{2}) , \tag{3.47}$$

and by writing the incoming wave as

$$\psi_{inc}(\vec{r}) = [\alpha \chi(+\tfrac{1}{2}) + \beta \chi(-\tfrac{1}{2})] \exp (ikz) , \tag{3.48}$$

normalized so that

$$|\alpha|^2 + |\beta|^2 = 1 . \tag{3.49}$$

Here, one conventionally introduces the degree of polarization P_n of the target along the normal $\hat{n}$ by the definition

$$P_n = |\alpha|^2 - |\beta|^2 . \tag{3.50}$$

The corresponding outgoing wave is

$$\begin{aligned} \psi_{out}(\vec{r}) &\simeq [G + i\vec{\sigma} \cdot \hat{n} H] \times [\alpha \chi(+\tfrac{1}{2}) + \beta \chi(-\tfrac{1}{2})] \frac{1}{r} \exp (ikr) = \\ &= [\alpha \{G + iH\} \chi(+\tfrac{1}{2}) + \beta \{G - iH\} \chi(-\tfrac{1}{2})] \frac{1}{r} \exp (ikr) . \end{aligned} \tag{3.51}$$

We could now proceed by calculating the cross-section using the current density in the same way as above. However, we shall take for granted that those results derived for the spin-zero case also apply here. Moreover, we shall only be interested in the differential cross-section when the spin of the final nucleon is not observed. Since the outgoing wave (3.51) is expanded in eigenvectors to $\vec{\sigma} \cdot \hat{n}$, the usual quantum mechanical procedure to obtain probabilities immediately yields the result

$$\frac{d\sigma}{d\Omega} = |\alpha(G + iH)|^2 + |\beta(G - iH)|^2 = |G|^2 + |H|^2 + (|\alpha|^2 - |\beta|^2) 2 \text{ Im } [GH^*] . \tag{3.52}$$

If the target is unpolarized we have $P_n = 0$, and the cross-section reads

$$\left(\frac{d\sigma}{d\Omega}\right)_{unpol} = |G|^2 + |H|^2 , \tag{3.53}$$

while with $P_n \neq 0$ it reads

$$\frac{d\sigma}{d\Omega} = \left(\frac{d\sigma}{d\Omega}\right)_{unpol} [1 + P_n P] . \tag{3.54}$$

Here, conventionally, the polarization parameter P is defined by

$$P = \frac{2\ \mathrm{Im}\ [GH^*]}{|G|^2 + |H|^2} . \tag{3.55}$$

Note that P is really a quantity characterizing the interaction, in contrast to P_n, which specifies the experimental arrangement.

To summarize, with an unpolarized target one measures the combination $|G|^2 + |H|^2$ of the flip and non-flip amplitudes; with a polarized target, it is also possible to measure Im (GH^*). However, these two measurements are not sufficient to derive the amplitudes themselves, since these constitute four real functions (or, if an over-all phase is disregarded, three real functions). On the other hand, there are other experimental set-ups. For example, one may have the target polarized in the scattering plane and analyse the polarization of the outgoing nucleon in the scattering plane. More detailed considerations, into which we shall not enter, show that such experiments measure two other polarization parameters known as the R and the A parameters. They are expressed in terms of the combinations Re (GH^*) and $|G|^2 - |H|^2$. The exact relations may be found, for example, in R.J.N. Phillips and W. Rarita, UCRL 16185 (unpublished). It is not difficult to see that a complete determination of G and H, up to a common phase, requires measurements of all three polarization parameters P, R and A as well as of the unpolarized cross-sections.

Finally, we note that the results derived so far apply equally well to elastic and to charge-exchange scattering, with the usual exception of the ratio between the momenta multiplying the charge-exchange cross-section [cf., Eq. (3.10)]. Moreover, the optical theorem now reads

$$\sigma_{tot}(E) = \frac{4\pi}{k} \text{Im } G_{el}(\cos\Theta = 1, E) . \tag{3.56}$$

It relates the imaginary part of the forward non-flip elastic amplitude to the total cross-section; in fact, one may as well write the full amplitude F_{el} instead of G_{el} in Eq. (3.56), since the spin-flip amplitude vanishes for $\Theta = 0$, as we shall see when making the partial-wave analysis [cf. Eq. (4.39)].

3.4 Potential scattering

So far, we have not discussed any dynamical question, i.e., problems related to the details of the interaction. The only thing required in order that the formalism presented should be correct is that the interaction between elementary particles, whatever its nature, is of finite range. In fact, this is necessary in order that the asymptotic form of the wave function should have the simple appearance (3.1). The problem of the underlying dynamics for strong interaction at high energy is very far from a solution; we shall later on see at what preliminary stage it is. In the case of low-energy scattering, however, one has at least a framework in which to formulate the dynamical questions, viz., the Schrödinger equation with a potential, which reads

$$-\frac{1}{2\mu}\nabla^2\psi(\vec{r}) + V(r)\psi(\vec{r}) = E\psi(\vec{r}) . \tag{3.57}$$

Here $V(r)$ is a spherical symmetric potential and μ is the (reduced) mass. By requiring the asymptotic form

$$\psi(\vec{r}) \simeq \exp(ikz) + F(\cos\Theta, E)\frac{1}{r}\exp(ikr) \tag{3.58}$$

for the solution to the Schrödinger equation, one is in principle able to express the scattering amplitude $F(\cos\Theta, E)$ in terms of the potential. In practice, needless to say, this may be difficult. However, if the potential is weak, one may use the Born approximation to arrive at an approximate expression for the scattering amplitude. This reads

$$F_{Born}(\cos\Theta, E) = -\frac{\mu}{2\pi}\int d^3x[\exp(-i\vec{k}'\vec{x})]V(r)[\exp(i\vec{k}\vec{x})] =$$

$$= -\frac{2\mu}{|\vec{k}-\vec{k}'|}\int_0^\infty r\,dr\,V(r)\sin(r|\vec{k}-\vec{k}'|)\ ; \tag{3.59}$$

the momenta $\vec{k}$ and $\vec{k}'$ are those defined in Fig. 3.1.

In the particular case of a Coulomb interaction between two particles of charge $Z_1 e$ and $Z_2 e$, the potential is

$$V(r) = \frac{Z_1 Z_2 \alpha}{r}\ , \tag{3.60}$$

where $\alpha = (e^2/4\pi) \approx 1/137$ is the fine structure constant (the units are such that $\epsilon_0 = 1$). One then finds

$$F_{Coulomb;\,Born}(\cos\Theta, E) = \frac{-\mu Z_1 Z_2 \alpha}{k^2(1-\cos\Theta)} = \frac{2\mu Z_1 Z_2 \alpha}{t}\ . \tag{3.61}$$

In fact, the Coulomb potential is <u>not</u> of finite range, and the treatment above is, in a strict sense, not valid for it. However, by modifying the r dependence of the potential by a factor $\exp(-\beta r)$, $\beta > 0$, i.e., by transforming the Coulomb potential into a Yukawa one, it is possible to circumvent this problem. The result (3.61) must indeed be derived by keeping $\beta > 0$ in the calculations and in the very last step let β tend to zero.

The result for the Coulomb scattering amplitude is definitely applicable only in the non-relativistic limit. However, in the high-energy and low momentum transfer limit, one obtains almost the same result assuming that the Coulomb interaction takes place via one-photon exchange (o.ph.e.). The only modification is that the (reduced) mass μ should be replaced by the particle's c.m.s. energy $\sim \frac{1}{2}\sqrt{s}$. Thus

$$F_{Coulomb;\,o.ph.e.}(\cos\Theta, E) = Z_1 Z_2 \alpha \frac{\sqrt{s}}{t}\ , \qquad (\sqrt{s} >> m, M, |t| \text{ small}). \tag{3.62}$$

We note that elementary particles accessible for experiment have $|Z_1| = |Z_2| = 1$, and that $F_{Coulomb;\,o.ph.e.}$ is negative (positive) if the particles electrically repel (attract) each other.

CHAPTER 4 - PARTIAL WAVE ANALYSIS

By combining the law of probability conservation, as expressed, for example, by the optical theorem, with that of angular momentum conservation, one obtains more information on the structure of the scattering amplitude.

4.1 The spinless case

Since the incoming wave satisfies

$$L_z \exp(ikz) = -i\left(x\frac{\partial}{\partial y} - y\frac{\partial}{\partial x}\right)\exp(ikz) = 0 , \qquad (4.1)$$

conservation of L_z implies that the outgoing waves are also eigenstates of L_z with eigenvalue zero. Consequently, they can be expanded in terms of the Legendre polynomials $P_\ell(\cos\Theta)$, which also are eigenfunctions to $\vec{L}^2$ with eigenvalue $\ell(\ell+1)$; they are normalized so that

$$\frac{1}{2}\int_{-1}^{+1} d(\cos\Theta)P_\ell(\cos\Theta)P_{\ell'}(\cos\Theta) = \frac{1}{2\ell+1}\delta_{\ell\ell'} . \qquad (4.2)$$

Thus one writes, extracting for convenience some momentum-dependent factors explicitly

$$F_{el}(\cos\Theta, E) = \frac{1}{k}\sum_{\ell=0}^{\infty}(2\ell+1)f_{el}(\ell, E)P_\ell(\cos\Theta) , \qquad (4.3)$$

$$F_{c.e.}(\cos\Theta, E) = \frac{1}{\sqrt{kk''}}\sum_{\ell=0}^{\infty}(2\ell+1)f_{c.e.}(\ell, E)P_\ell(\cos\Theta) . \qquad (4.4)$$

By using the orthogonality relation (4.2), one may conversely express the partial-wave amplitudes $f(\ell, E)$ as angle integrals over the full amplitude $F(\cos\Theta, E)$.

In terms of the amplitudes $f(\ell, E)$, the different cross-sections read

$$\sigma_{el} = \frac{4\pi}{k^2} \sum_{\ell=0}^{\infty} (2\ell + 1) |f_{el}(\ell, E)|^2 , \tag{4.5}$$

$$\sigma_{c.e.} = \frac{4\pi}{kk''} \frac{k''}{k} \sum_{\ell=0}^{\infty} (2\ell + 1) |f_{c.e.}(\ell, E)|^2 , \tag{4.6}$$

$$\sigma_{tot} = \frac{4\pi}{k^2} \sum_{\ell=0}^{\infty} (2\ell + 1) \, \mathrm{Im} \, f_{el}(\ell, E) . \tag{4.7}$$

Exercise 4.1: Prove the relations (4.5) to (4.7). [Hint: Remember Eq. (4.2) and, to prove Eq. (4.7), that $P_\ell(\cos \Theta = 1) = 1$.]

If for the time being we assume that no other reactions occur, the fact that σ_{tot} equals the sum of σ_{el} and $\sigma_{c.e.}$ implies

$$\frac{4\pi}{k^2} \sum_{\ell=0}^{\infty} (2\ell + 1)[\mathrm{Im} \, f_{el} - |f_{el}|^2 - |f_{c.e.}|^2] = 0 . \tag{4.8}$$

Now, the conservation of angular momentum means that each term in the sum (4.8) can be treated separately. In other words, there can be no cancellations between the different terms in the sum. Thus each term must vanish

$$\mathrm{Im} \, f_{el}(\ell, E) = |f_{el}(\ell, E)|^2 + |f_{c.e.}(\ell, E)|^2 , \quad \ell = 0, 1, 2, \ldots . \tag{4.9}$$

Although the result (4.9) is absolutely correct, the argument leading to it may not be completely convincing. We shall postpone that problem and proceed immediately to draw conclusions from the "partial-wave unitarity condition" (4.9).

To this end, we observe that

$$|f_{el}|^2 - \mathrm{Im}\, f_{el} = |f_{el} - \tfrac{i}{2}|^2 - \tfrac{1}{4} , \tag{4.10}$$

so that Eq. (4.9) may be written

$$|f_{el} - \tfrac{i}{2}|^2 + |f_{c.e.}|^2 = \tfrac{1}{4} . \tag{4.11}$$

This is the form of the partial wave unitarity condition which will be used subsequently.

From (4.10) it follows that

$$|f_{el} - \tfrac{i}{2}|^2 \leq \tfrac{1}{4} , \tag{4.12}$$

implying a parametrization of the elastic partial-wave amplitude given by

$$f_{el}(\ell, E) - \tfrac{i}{2} = \frac{1}{2i}\, \eta_\ell(E)\, \exp\,[2i\delta_\ell(E)] , \tag{4.13}$$

or

$$f_{el}(\ell, E) = \frac{1}{2i}\, \{\eta_\ell(E)\, \exp\,[2i\delta_\ell(E)] - 1\} . \tag{4.14}$$

Here, the "phase shift" $\delta_\ell(E)$ and the "inelasticity" or "absorption coefficient" $\eta_\ell(E)$ are real functions of the energy E. Moreover, the inelasticity is positive by definition; a possible ambiguity of sign can be absorbed into the phase shift. It thus satisfies

$$0 \leq \eta_\ell \leq 1 \tag{4.15}$$

in order that Eq. (4.12) should be fulfilled. It is related to the occurrence of inelastic reactions, as may be seen by calculating

$$\sigma_{inel} = \sigma_{tot} - \sigma_{el} = \frac{\pi}{k^2} \sum_{\ell=0}^{\infty} (2\ell + 1)(1 - \eta_\ell^2) . \tag{4.16}$$

Exercise 4.2: Prove the relation (4.16).

We may now see the reason for introducing δ_ℓ and η_ℓ as was done in Eq. (4.13). In the case of no inelastic scattering, η_ℓ equals unity for all ℓ values. This is for instance the case in potential scattering with a real potential. In fact, it is the requirement that the general form (4.13) should reduce to the more well-known one from potential theory that lies behind the definition of the phase shift. We shall consider a few questions related to partial waves in potential scattering towards the end of this chapter.

On the other hand, if $\eta_\ell \neq 0$, the inelastic cross-section does not vanish. In a very direct sense the inelasticity measures the amount of inelastic scattering, or "absorption", that occurs. To get some more insight into this problem, we have to consider the partial-wave expansion of the whole asymptotic wave function (3.1), not only the outgoing parts as up till now.

To this end, one expands

$$\exp(ikz) = \sum_{\ell=0}^{\infty} (2\ell+1) i^\ell j_\ell(kr) P_\ell(\cos\Theta) , \qquad (4.17)$$

where, from the orthonormality relation (4.2),

$$i^\ell j_\ell(kr) = \frac{1}{2} \int_{-1}^{+1} d(\cos\Theta) P_\ell(\cos\Theta) \exp(ikr\cos\Theta) . \qquad (4.18)$$

Since we are only interested in the expansion at large distances, we may use partial integrations to obtain

$$i^\ell j_\ell(kr) = \frac{1}{k}\left[\frac{1}{2ir}\exp(ikr) - (-)^\ell \frac{1}{2ir}\exp(-ikr)\right] + O\left(\frac{1}{r^2}\right). \qquad (4.19)$$

Exercise 4.3: Prove Eq. (4.18). [Hint: Perform one partial integration using $P_\ell(-1) = (-1)^\ell P_\ell(1) = (-1)^\ell$; then make another partial integration to prove that the remaining integral behaves as r^{-2}.]

In this way we see that the incoming plane wave exp (ikz) is a superposition of all possible angular momenta, and that each partial wave asymptotically is a linear combination of one incoming spherical wave r^{-1} exp (-ikr) and one outgoing spherical wave r^{-1} exp (ikr). This is not quite as astonishing as it sounds, if one keeps in mind that the incoming plane wave exp (ikz) in reality, despite the name we have given to it, also describes an outgoing plane wave representing that part of the incident beam that is not scattered.

Observing the expansions (4.3) and (4.4), we may now write the total asymptotic wave function as a superposition of angular momentum eigenfunctions

$$\psi(\vec{r}) \simeq \frac{1}{k} \sum_{\ell=0}^{\infty} (2\ell+1)\varphi_\ell(r)P_\ell(\cos\Theta) \ , \qquad (4.20)$$

where each partial wave $\varphi_\ell(r)$ is a sum of one incoming π^-p spherical wave

$$-(-)^\ell \frac{1}{2ir} \exp(-ikr) \ , \qquad (4.21)$$

and outgoing spherical waves

$$\left[f_{el}(\ell, E) - \frac{i}{2}\right]\frac{1}{r}\exp(ikr) + \sqrt{\frac{k}{k''}}\, f_{c.e.}(\ell, E)\frac{1}{r}\exp(ik''r) \ , \qquad (4.22)$$

one part of which is the elastic wave; the other describes the outgoing π^0n system.

We are now able to give a more rigorous proof of the partial wave unitarity condition (4.9) or, equivalently, (4.11). It is as follows. The square of the coefficient for the incoming spherical wave (4.21) is proportional to the probability of finding an incoming particle system with angular momentum ℓ. In the same way, the square of the coefficient in front of each of the outgoing waves in expression (4.22) gives the probability of finding the outgoing π^-p and π^0n system, respectively. Conservation of probability and angular momentum tells that the total probability of finding a particle system with angular momentum ℓ in the final state should equal the probability of finding a particle system with the same

angular momentum in the initial state. This gives immediately the condition (4.11), if one observes that it is in reality the probability current that matters, not merely the probability, and that this always [cf. Eq. (3.7) and Eq. (3.9)] gives the momentum as a factor in front of the coefficient squared.

There is now an alternative way to look upon the parametrization of the elastic partial wave amplitude in terms of a real phase shift and an inelasticity. Compare the incoming part of $\varphi_\ell(r)$ to the outgoing elastic wave, Eqs. (4.20)-(4.22). The coefficient for the latter is proportional to $\eta_\ell \exp(2i\delta_\ell)$, from Eq. (4.13). Consequently, the incoming spherical wave is modified by the interaction and appears as an outgoing spherical wave having in general both another phase (as represented by the phase shift) and a smaller absolute value (as given by the absorption coefficient); this remark will be of importance for our derivation of the partial wave expansion below treating the spin of the nucleon consistently. In particular, if $\eta_\ell = 1$, there is so to speak, no probability left for any inelastic reactions. On the other hand, if $\eta_\ell < 1$ probability conservation requires that part of the initial wave is transformed into inelastic final states. Maximum absorption obviously occurs for $\eta_\ell = 0$, in which case the whole initial probability goes into inelastic channels.

What happens when several other inelastic reactions also occur? It should be clear from the preceding discussion that the only change needed is to include terms in the partial wave unitarity condition (4.11) representing those other inelastic reactions. We shall not enter into any detailed consideration of this point, since the only thing we subsequently need is the form Eq. (4.14) of the elastic partial wave amplitude, and the interpretation of the absorption coefficient just presented. These items are not influenced by the presence of several open channels.

Exercise 4.4: How do you reconcile the following two statements:

a) there is complete absorption, $\eta_\ell = 0$, in the ℓth partial wave, so there is no outgoing elastic ℓ wave;

b) if $\eta_\ell = 0$, the elastic partial wave amplitude equals $i/2 \neq 0$, so there is scattering in the ℓth partial wave.

4.2 Consistent treatment of nucleon spin

For the incoming plane wave we now write, in analogy with the spinless case,

$$\psi_{inc}(\vec{r}) = \xi \exp(ikz)\,\tilde{\sim}$$

$$\tilde{\sim}\ \frac{1}{2ik}\sum_{\ell=0}^{\infty}(2\ell+1)\left[-(-)^{\ell}\frac{1}{r}\exp(-ikr)+\frac{1}{r}\exp(ikr)\right]P_{\ell}(\cos\Theta)\xi\ . \tag{4.23}$$

In applying angular momentum conservation, we must keep in mind that the total angular momentum $\vec{J}$, which is the quantity conserved, is the sum of the orbital angular momentum $\vec{L}$ and the spin angular momentum $\frac{1}{2}\vec{\sigma}$

$$\vec{J} = \vec{L} + \frac{1}{2}\vec{\sigma}\ . \tag{4.24}$$

In particular, for each eigenvalue $j(j+1)$ of $\vec{J}^2$ there exist two values $\ell = j \pm \frac{1}{2}$ of the orbital angular momentum. These two values correspond to different parities of the pion-nucleon system, given by $-(-)^{\ell}$; the extra minus sign is due to the negative intrinsic parity of the pion. Consequently, for interactions that conserve parity, ℓ is also conserved. In other words, if one expands the wave function in terms of eigenfunctions both of the total angular momentum and of the orbital angular momentum, then each partial wave corresponding to definite j and ℓ can be treated separately in the same way as each partial wave was treated separately in the case of no nucleon spin considered previously.

We may then arrive at the partial wave expansion in two steps. The first step is to expand ψ_{inc} in terms of eigenfunctions of definite j and ℓ. The next step is to conclude that each incoming partial wave is modified by the interaction both in respect of the phase (represented by a phase shift) and, if inelastic reactions occur, also in respect of the absolute value (represented by an inelasticity).

One could use conventional Clebsch-Gordan gymnastics for the first step. For our purpose, however, it is easier to use a projection operator technique (cf. N. Nishijima "Fundamental Particles", W.A. Benjamin, New York and Amsterdam, 1963). To this end, consider the two operators

$$\Pi_{\ell,+} = \frac{\ell + 1 + \vec{L}\cdot\vec{\sigma}}{2\ell+1} , \tag{4.25}$$

$$\Pi_{\ell,-} = \frac{\ell - \vec{L}\cdot\vec{\sigma}}{2\ell+1} , \tag{4.26}$$

related by

$$\Pi_{\ell,+} + \Pi_{\ell,-} = 1 . \tag{4.27}$$

Applying $\Pi_{\ell,+}$ to an eigenstate $|j, \ell>$ of $\vec{J}^2$ and $\vec{L}^2$, gives

$$\begin{aligned} \Pi_{\ell,+}|j = \ell + \tfrac{1}{2}, \ell> &= |j = \ell + \tfrac{1}{2}, \ell> , \\ \Pi_{\ell,+}|j = \ell - \tfrac{1}{2}, \ell> &= 0 . \end{aligned} \tag{4.28}$$

This means that $\Pi_{\ell,+}$ projects out of any mixture of $j = \ell \pm \frac{1}{2}$ that part which has $j = \ell + \frac{1}{2}$. In the same way, since $\Pi_{\ell,+}$ and $\Pi_{\ell,-}$ add up to unity, the operator $\Pi_{\ell,-}$ projects out that part which corresponds to $j = \ell - \frac{1}{2}$. Summarizing, $\Pi_{\ell,\pm}$ are projection operators onto the states $|j = \ell \pm \frac{1}{2}, \ell>$.

Exercise 4.5: Prove the relation (4.28). [Hint: Obtain $\vec{\sigma}\cdot\vec{L}$ by squaring Eq. (4.24).]

Now, we proceed as follows. The incoming spherical ℓ wave is written

$$-(-)^{\ell}\frac{1}{2ik}\frac{1}{r}[\exp(-ikr)][\Pi_{\ell,+} + \Pi_{\ell,-}]P_{\ell}(\cos\Theta)\xi . \tag{4.29}$$

The outgoing elastic spherical ℓ wave produced by this incoming wave is then of the form

$$\frac{1}{2ik}\frac{1}{r}[\exp(ikr)] \times$$

$$\times [\eta_{\ell,+}\{\exp(2i\delta_{\ell,+})\}\Pi_{\ell,+} + \eta_{\ell,-}\{\exp(2i\delta_{\ell,-})\}\Pi_{\ell,-}]P_\ell(\cos\Theta)\xi \ , \tag{4.30}$$

where the phase shifts $\delta_{\ell,\pm}$ and the inelasticities $\eta_{\ell,\pm}$, $0 \leq \eta_{\ell,\pm} \leq 1$, are real functions of the energy. Indeed, this form merely expresses the fact that probability is conserved for each value of ℓ and $j = \ell \pm \frac{1}{2}$, taking into account possible inelastic reactions.

For the outgoing wave (4.30), we may write

$$\frac{1}{2ik}\frac{1}{r}[\exp(ikr)]P_\ell(\cos\Theta)\xi +$$

$$+ \frac{1}{r}[\exp(ikr)]\frac{1}{k}[f_{el}(\ell,+,E)\Pi_{\ell,+} + f_{el}(\ell,-,E)\Pi_{\ell,-}]P_\ell(\cos\Theta)\xi \tag{4.31}$$

where

$$f_{el}(\ell,\pm,E) = \frac{1}{2i}[\eta_{\ell,\pm}\exp(2i\delta_{\ell,\pm}) - 1] \ . \tag{4.32}$$

That is, the total outgoing elastic spherical wave consists of two parts. The first term in (4.31) gives the outgoing spherical wave of ψ_{inc}, Eq. (4.23). The second part represents the elastically scattered wave. In fact, by summing over ℓ and comparing with Eqs. (3.44) and (3.45), one identifies

$$F_{el}(\cos\Theta, E) = G_{el} + i\vec{\sigma}\cdot\hat{n}H_{el} =$$

$$= \frac{1}{k}\sum_{\ell=0}^{\infty}(2\ell+1)[f_{el}(\ell,+,E)\Pi_{\ell,+} + f_{el}(\ell,-,E)\Pi_{\ell,-}]P_\ell(\cos\Theta) \ . \tag{4.33}$$

This is the partial wave expansion of the elastic scattering amplitude in the present case. It only remains to split the sum into two terms, the one independent of $\vec{\sigma}$ and the other proportional to $\vec{\sigma}\cdot\hat{n}$; in so doing, we also establish Eqs. (3.41)-(3.42) needed in deriving Eq. (3.45).

To this end, one rewrites the expression (4.33), collecting together those terms involving $\vec{\sigma}\cdot\vec{L}$, to get

$$F_{el}(\cos\Theta,E) = \frac{1}{k}\sum_{\ell=0}^{\infty}[(\ell+1)f_{el}(\ell,+,E)+\ell f_{el}(\ell,-,E)]P_\ell(\cos\Theta) + \tag{4.34}$$

$$+\frac{1}{k}\sum_{\ell=0}^{\infty}[f_{el}(\ell,+,E)-f_{el}(\ell,-,E)]\vec{\sigma}\cdot\vec{L}P_\ell(\cos\Theta)\,.$$

From this, using

$$\vec{L} = -i\vec{r}\times\nabla = -i\vec{r}\times\left[\hat{e}_r\frac{\partial}{\partial r}+\hat{e}_\Theta\frac{\partial}{r\,\partial\Theta}+\hat{e}_\varphi\frac{\partial}{r\sin\Theta\,\partial\varphi}\right], \tag{4.35}$$

we find

$$\vec{L}P_\ell(\cos\Theta) = -i\vec{r}\times\hat{e}_\Theta\frac{\partial}{r\,\partial\Theta}P_\ell(\cos\Theta) = -i\hat{e}_y(-\sin\Theta)\frac{d}{d(\cos\Theta)}P_\ell(\cos\Theta) = \tag{4.36}$$

$$= i\hat{n}\sin\Theta\,P_\ell'(\cos\Theta)\,.$$

Here, use was made of the particular coordinate system chosen (see Fig. 3.1), to conclude that

$$\hat{e}_r\times\hat{e}_\Theta = \hat{e}_\varphi = -\hat{e}_x\sin\varphi+\hat{e}_y\cos\varphi = \hat{e}_y\,, \quad \text{for} \quad \varphi = 0. \tag{4.37}$$

Inserting the result Eq. (4.36) into Eq. (4.34) yields the following partial wave expansion of the non-flip and the flip amplitudes

$$G_{el}(\cos\Theta,E) = \frac{1}{k}\sum_{\ell=0}^{\infty}[(\ell+1)f_{el}(\ell,+,E)+\ell f_{el}(\ell,-,E)]P_\ell(\cos\Theta), \tag{4.38}$$

$$H_{el}(\cos\Theta, E) = \frac{1}{k}\sum_{\ell=1}^{\infty}[f_{el}(\ell,+,E) - f_{el}(\ell,-,E)]\,\sin\Theta\,P_\ell'(\cos\Theta)\,. \quad (4.39)$$

This is the result wanted. Similar results apply to the charge-exchange amplitudes with the usual replacement of k^{-1} by $(kk'')^{-1/2}$ [see Eq. (4.4)].

The cross-sections in terms of the partial wave amplitudes read

$$\sigma_{el}(E) = \frac{4\pi}{k^2}\sum_{\ell=0}^{\infty}[(\ell+1)|f_{el}(\ell,+,E)|^2 + \ell|f_{el}(\ell,-,E)|^2]\,, \quad (4.40)$$

$$\sigma_{tot}(E) = \frac{4\pi}{k^2}\sum_{\ell=0}^{\infty}[(\ell+1)\,\mathrm{Im}\,f_{el}(\ell,+,E) + \ell\,\mathrm{Im}\,f_{el}(\ell,-,E)]\,, \quad (4.41)$$

$$\sigma_{inel}(E) = \frac{\pi}{k^2}\sum_{\ell=0}^{\infty}[(\ell+1)(1-\eta_{\ell,+}^2) + \ell(1-\eta_{\ell,-}^2)]\,. \quad (4.42)$$

Exercise 4.6: Derive the results in Eqs. (4.40) to (4.42). [Hint (if you do not find another way): Consider σ_{tot} first. Then, specialize to $\eta_{\ell,\pm} = 1$ to get σ_{el}.]

4.3 Impact parameter representation

As is well known, the partial wave analysis is a powerful tool at low energy, due to the small number of terms that contribute. At high energy, on the other hand, many partial waves must be considered and the slow convergence of the sum causes difficulties. In fact, one may estimate the maximum angular momentum ℓ_{max} required from a semi-classical argument as follows. If the wavelength $1/k$ (recall that $\hbar = 1$ in our units) of the incident wave is much smaller than the range R of the forces responsible

for the scattering, the path of the incoming particle may be specified with an accuracy $\sim 1/k \ll R$ without violating the uncertainty principle; this would correspond to the limit of geometrical optics if the waves had represented light. Consequently, one may define the impact parameter b as the distance of the line of flight for the incident particle to the scattering centre, see Fig. 4.1.

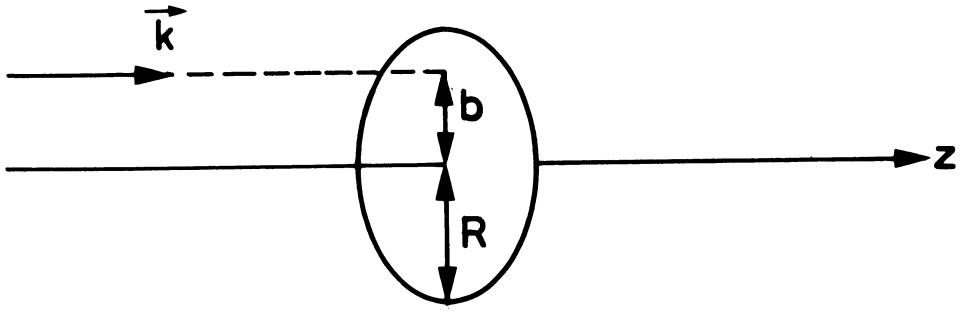

Fig. 4.1

The impact parameter b and
the range R of interaction.

Classically, the angular momentum of the particle is bk. The condition for scattering is that the incoming particle hits the interaction region, which implies

$$\ell_{max} \sim Rk \, . \tag{4.43}$$

For example, if $R \sim 1$ fm as is appropriate for hadronic interactions, and if $k \sim 5$ GeV/c $\approx 25\,(\text{fm})^{-1}$, one needs at least 25 partial waves, very probably more. In that case it is often more convenient to transform the partial wave sum into an integral representation of the scattering amplitude, known as the impact parameter expansion. We now proceed to derive this expansion.

Let us start from the partial wave expansion

$$F(\cos\Theta, E) = \frac{1}{k} \sum_{\ell=0}^{\infty} (2\ell + 1) f(\ell, E) P_\ell(\cos\Theta) \, . \tag{4.44}$$

Instead of ℓ, we introduce as a new summation variable the impact parameter b now defined by

$$b = \frac{1}{k}\,(\ell + \tfrac{1}{2})\,. \tag{4.45}$$

Then

$$F(\cos\Theta, E) = 2k \sum_{b=1/2k}^{\infty} b\,\Delta b\, f(bk - \tfrac{1}{2}, E) P_{bk-\frac{1}{2}}(\cos\Theta)\,. \tag{4.46}$$

Notice that b increases in steps $\Delta b = 1/k$ as ℓ increases in unit steps. Thus, as k grows large, Δb becomes small, and we get, approximately,

$$F(\cos\Theta, E) = 2k \int_0^{\infty} b\,db\, f(bk - \tfrac{1}{2}, E) P_{bk-\frac{1}{2}}(\cos\Theta) \tag{4.47}$$

Besides the definition of an integral, this approximation requires that

i) The Legendre polynomials $P_\ell(\cos\Theta)$ can be generalized to arbitrary positive values of ℓ, not only integer ones. In other words we need functions $P_\nu(\cos\Theta)$ depending on a parameter ν, which interpolate the Legendre polynomials between integers. Such functions do indeed exist and are known as Legendre functions (of the first kind). In Appendix 3 we discuss some properties of these functions.

ii) The partial wave amplitudes $f(\ell, E)$, which a priori are defined only for non-negative integers ℓ, could be interpolated to all positive ℓ values. If $f(\ell, E)$ is a smooth function of ℓ in the sense that it does not vary too much from one ℓ value to a subsequent one, this is possible. Later, when we define partial wave amplitudes also for complex values of ℓ, we shall consider this interpolation in more detail (see Chapter 9, in particular Fig. 9.1).

Very often one is interested in the impact parameter expansion (4.47) only for small angles Θ. Then one may approximate the Legendre functions by a Bessel function of order zero

$$P_\nu(\cos\Theta) = J_0(2\nu \sin\Theta/2)\,, \qquad \Theta \text{ small}\,, \tag{4.48}$$

a relation which is discussed in Appendix 3. Defining the impact parameter amplitude by

$$B(b, E) = f(bk - \tfrac{1}{2}, E) , \tag{4.49}$$

the integral (4.47) assumes the form (we approximate $bk - \frac{1}{2}$ by bk)

$$F(\cos\Theta, E) = 2k \int_0^\infty b\, db\, B(b, E) J_0(b\Delta) , \qquad \Theta \text{ small} , \tag{4.50}$$

where the momentum transfer, $\Delta = 2k \sin\Theta/2 = \sqrt{-t}$, is introduced from Eq. (2.9).

The representation (4.50) constitutes the impact parameter representation in the form we shall need it. Remember that our way of deriving it requires high energy (many partial waves contributing) and small angles. Mathematically, it constitutes a Fourier-Bessel integral representation of the scattering amplitude [cf. Appendix 2, in particular Eqs. (A2.8-9)].

We note that the inversion formula for Bessel functions, as given in Appendix 2, may be used to express the impact parameter amplitude B(b, E) in terms of the scattering amplitude as

$$B(b, E) = \frac{1}{2k} \int_0^\infty \Delta\, d\Delta\, F\left(1 - \frac{\Delta^2}{2k^2}, E\right) J_0(b\Delta) . \tag{4.51}$$

Moreover, if $f(\ell, E)$ is a continuous function of ℓ, so are the phase shift and the inelasticity. By writing them as functions of b instead, one obtains from Eq. (4.14)

$$B(b, E) = \frac{1}{2i} \left[\eta(b, E) \exp\{2i\delta(b, E)\} - 1\right] . \tag{4.52}$$

The cross-sections (4.5), (4.7) and (4.16) become in the impact parameter representation

$$\sigma_{el}(E) = 8\pi \int_0^\infty b\, db |B_{el}(b, E)|^2 , \tag{4.53}$$

$$\sigma_{tot}(E) = 8\pi \int_0^\infty b\, db\, \mathrm{Im}\, B_{el}(b,E)\,, \tag{4.54}$$

$$\sigma_{inel}(E) = 2\pi \int_0^\infty b\, db[1-\eta(b)^2]\,. \tag{4.55}$$

Finally, if the spin of the nucleon is taken into account, the non-flip amplitude can be treated as above. For the flip amplitude, however, a slight modification is appropriate since it is an expansion in terms of the derivatives $P_\ell'(\cos\Theta)$ of the Legendre polynomials. It is not difficult to prove that at small angles

$$P_\nu'(\cos\Theta) = \frac{\nu}{2\sin\Theta/2} J_1(2\nu \sin\Theta/2)\,, \quad \Theta \text{ small}\,. \tag{4.56}$$

Exercise 4.7: Derive the approximation (4.56). [Hint: Use Eq. (4.48) and the relation (A2.2) between the Bessel functions of order zero and one.]

Thus, the impact parameter representation for the spin-flip amplitude becomes an integral involving Bessel functions of order one.

4.4 Resonances

Consider first the case of a resonance in a purely elastic partial wave, i.e., one of unit inelasticity. A resonance is said to occur at an energy $E = E_{res}$ if the contribution to the total cross-section from the partial wave studied has a maximum at that energy; since this contribution is proportional to $\sin^2\delta(E)$, where $\delta(E)$ is the phase shift (indices j and ℓ are suppressed), this implies

$$\delta(E_{res}) = \frac{\pi}{2}\,(+n\pi)\,. \tag{4.57}$$

Proceeding further, one writes the (elastic) partial wave amplitude as

$$f_{el}(E) = \exp(i\delta)\sin\delta = \frac{1}{\cot\delta - i}\,, \tag{4.58}$$

and expands $\cot\delta(E)$ in a Taylor series around the resonance energy

$$\cot\delta(E) = \cot\delta(E_{res}) + (E - E_{res})\left\{\frac{d}{dE}\left[\cot\delta(E)\right]\right\}_{E=E_{res}} + \ldots \approx$$

$$\approx (E - E_{res})\left(-\frac{2}{\Gamma}\right)\,, \tag{4.59}$$

where

$$\frac{2}{\Gamma} = -\left\{\frac{d}{dE}\left[\cot\delta(E)\right]\right\}_{E=E_{res}} = \delta'(E = E_{res})\,. \tag{4.60}$$

The partial wave amplitude for energies near to the resonance thus reads

$$f_{el}(E) = \frac{\frac{1}{2}\Gamma}{E_{res} - E - i\frac{1}{2}\Gamma}\,, \tag{4.61}$$

implying a cross-section in the resonating partial-wave that is proportional to

$$\Gamma^2 \frac{\frac{1}{4}}{(E - E_{res})^2 + \frac{1}{4}\Gamma^2} = \Gamma^2\,BW(E)\,. \tag{4.62}$$

This is the Breit-Wigner form of the partial-wave cross-section for a resonance at $E = E_{res}$ of full width Γ. It requires Γ to be positive. Indeed, one may prove that the phase shift must <u>increase</u> through 90° as the energy increases through E_{res} in order to give a resonance.

For our purpose, this heuristic treatment of a resonance in an elastic partial wave suffices. However, we must generalize the results to the case of a resonance in a partial wave with inelasticity smaller than one. For a complete treatment, this would require the whole multi-channel formalism. We shall instead give a crude, phenomenological discussion.

For an inelastic resonance, there is a certain probability $x < 1$ for the resonance to decay into the elastic channel. One calls x the "elasticity" of the resonance. It follows that the resonance has the probability $1 - x$ to decay into an inelastic channel. Moreover, from time reversal invariance, x is also the probability for the resonance to be formed in the collision of the two incident particles. From this simple-minded approach, we expect the elastic, total and inelastic cross-sections to be obtained from the purely elastic form (4.62) through multiplication by, respectively, x^2, x and $x(1-x)$. Adopting the notation

$$\begin{aligned} \Gamma_{tot} &= \Gamma && = \text{total width}, \\ \Gamma_{el} &= x\Gamma && = \text{elastic partial width}, \\ \Gamma_{inel} &= (1-x)\Gamma && = \text{inelastic partial width}, \end{aligned} \tag{4.63}$$

the contribution to the different cross-sections from the resonating partial wave is

$$\begin{aligned} &\text{elastic} && \propto \Gamma_{el}^2 BW(E), \\ &\text{total} && \propto \Gamma_{el}\Gamma\, BW(E), \\ &\text{inelastic} && \propto \Gamma_{el}\Gamma_{inel} BW(E). \end{aligned} \tag{4.64}$$

A form for the partial wave amplitude that gives these cross-sections is

$$f_{el}(E) = \frac{\frac{1}{2}\Gamma_{el}}{E_{res} - E - i\frac{1}{2}\Gamma}, \tag{4.65}$$

Exercise 4.8: Prove that the amplitude (4.65) reproduces the cross-sections (4.64).

4.5 Resonances and bound states as poles of the amplitude

Anticipating our future treatment, we state that the partial wave scattering amplitude may be continued to complex values of the energy E. If this is so, the simple Breit-Wigner form (4.65) implies that the amplitude has a pole at the energy $E = E_{res} - i\,\tfrac{1}{2}\Gamma$. This is of course not a physical energy. In fact, the procedure involves an extrapolation of the expression (4.65) from $E = E_{res}$ to $E = E_{res} - i\,\tfrac{1}{2}\Gamma$, which is reliable only if Γ is small. Still, it is of great interest from the mathematical point of view to be able to classify a resonance as a pole of the partial wave amplitude. Indeed, the concept of a pole for the amplitude as a function of energy constitutes a unified description of resonances and of stable particles, i.e., bound states appearing for energies below the scattering threshold. In a very rough way, one may see how a bound state also gives poles for the scattering amplitude, as follows.

The asymptotic form of the partial wave $\varphi_\ell(r)$ as given by Eqs. (4.20)-(4.22) is (we neglect the charge-exchange part)

$$r\varphi_\ell(r) \simeq \left[f(\ell, E) - \frac{i}{2} \right] \exp(ikr) - (-)^\ell \frac{1}{2i} \exp(-ikr) . \qquad (4.66)$$

As it was constructed [cf. Eq. (3.1)], it is only appropriate for energies where scattering occurs, $E \geq M + m$. If the energy goes below this limit, the momentum k becomes imaginary, $k = i|k|$ (with non-relativistic kinematics k equals $i\sqrt{-2\mu E}$). If one still insists on the form (4.66), it now becomes a linear combination of the two exponentials $\exp(\pm|k|r)$. Such an asymptotic wave function has, in general, no physical sense, since it is not normalizable. However, if for a certain energy $E = E_b$ and the corresponding momentum $k = i|k_b|$ it so happens that only the decreasing term $\exp(-|k_b|r)$ is present, then the wave function is normalizable and represents, consequently, a bound state of energy E_b.

In fact, this situation occurs if the partial wave amplitude $f(\ell, E)$ has a pole for $E = E_b$, $k = i|k_b|$, so that $f(\ell, E)$ is proportional to $(E - E_b)^{-1}$ for $E \sim E_b$. In that case the wave proportional to $\exp(-ikr)$ can be neglected near $E = E_b$. One might wonder whether the whole wave function does not become infinite for such an energy where the scattering

amplitude has a pole. However, since the wave function allows multiplication by an arbitrary factor [in our previous considerations it is only the relative normalization between the different terms in $\psi(\vec{r})$, Eq. (3.1), that matters], one may multiply it by $E - E_b$ before letting the energy tend to E_b.

Summarizing, the partial wave amplitude may, under certain circumstances, be continued to complex values of the energy E. In fact, one may show that $f(\ell, E)$ is an analytic function of E except for:

i) a cut along the positive real axis starting (at least) at $E = M + m$;
ii) poles;

there are in general, further singularities, for example, those connected with the range of the forces (cf. Chapter 2 in the book by Omnès-Froissart cited in the bibliography).

A pole of the amplitude allows a simple interpretation: if it occurs at an energy such that the corresponding momentum lies on the positive imaginary axis, it corresponds to a stable particle, i.e. a bound state. If it occurs at a value $E = E_{res} - i\,\frac{1}{2}\Gamma$, $E_{res} > M + m$, $\Gamma > 0$, it corresponds to a resonance at $E = E_{res}$ with full width Γ. It should be noted that there may exist poles of $f(\ell, E)$ which do not have this interpretation. The situation in the complex E plane is illustrated in Fig. 4.2.

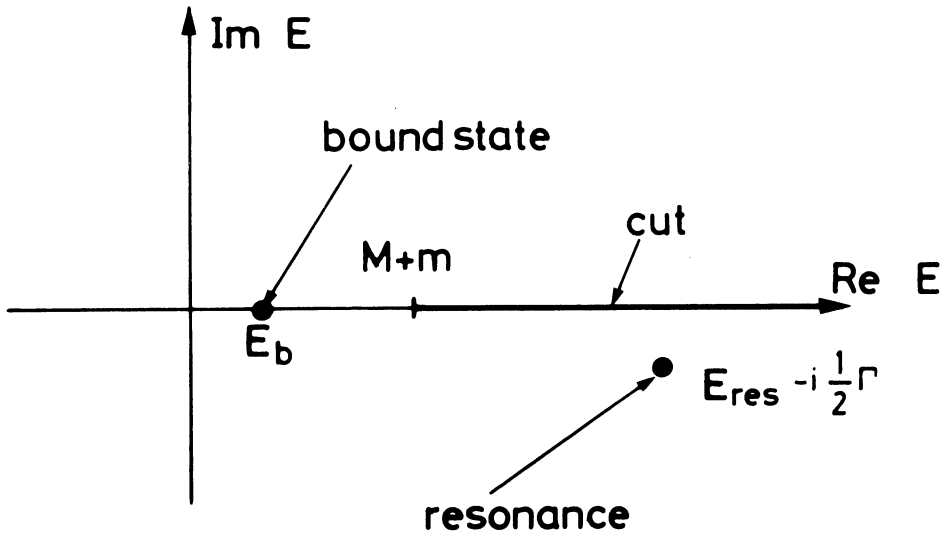

Fig. 4.2

An illustration of the (simplest) singularities of the partial wave amplitude as function of E.

4.6 Potential scattering

Potential scattering is one case where these "certain circumstances" occur under which $f(\ell, E)$ may be continued to complex E. Writing the complete wave function

$$\psi(\vec{r}) = \frac{1}{k} \sum_{\ell=0}^{\infty} (2\ell + 1) \frac{1}{r} u_\ell(r) P_\ell(\cos \Theta) , \tag{4.67}$$

one finds by substitution into the Schrödinger equation (3.57) that $u_\ell(r)$ satisfies the radial Schrödinger equation

$$- \frac{1}{2\mu} \left[\frac{d^2}{dr^2} - \frac{\ell(\ell+1)}{r^2} \right] u_\ell(r) + V(r) u_\ell(r) = E u_\ell(r) . \tag{4.68}$$

For a scattering problem, this equation should be solved requiring the asymptotic form of the partial wave to be

$$u_\ell(r) \simeq \kappa_+(\ell, E) \exp (ikr) + \kappa_-(\ell, E) \exp (-ikr) . \tag{4.69}$$

In that case, $u_\ell(r)$ becomes proportional to $\varphi_\ell(r)$ of Eq. (4.20) at large r, if one identifies

$$2if(\ell, E) = (-)^{\ell+1} \frac{\kappa_+(\ell, E)}{\kappa_-(\ell, E)} - 1 . \tag{4.70}$$

Under suitable restrictions on the potential, one may now prove that the two functions $\kappa_\pm(\ell, E)$ are analytic functions (except for cuts) of E; This is essentially due to the simple dependence on E of Eq. (4.68), to be more precise that the equation involves E analytically. It follows that $f(\ell, E)$ is also analytic, except where $\kappa_-(\ell, E)$ vanishes. If this happens for an energy E_b such that $k = i|k_b|$, then $u_\ell(r)$ represents a bound state of energy E_b and $f(\ell, E)$ has a pole at that energy.

P A R T II

(Chapters 5-7)

EXPERIMENTAL DATA AND THEIR PRELIMINARY INTERPRETATION

We now turn to a discussion of the relevant experimental data, trying to systematize them using simple phenomenological approaches. We keep in mind that high energy corresponds, for our purpose, to laboratory momenta $p_{lab} \gtrsim 5$ GeV/c. However, in some cases where data at higher energies are lacking, or when some interesting phenomena only occur at a lower energy, we shall also go below this limit. Let me also confess that I have taken a rather liberal attitude towards the experimental data in the sense that in many diagrams I present only curves drawn freehand through the experimental points, all of which are not exhibited; typical statistical errors are, however, shown. Moreover, I have at some places preferred the experimental results from one group to others for the mere reason that the data chosen had the least statistical errors.

Besides the review talk by L. Van Hove, and the accompanying experimental survey by A.M. Wetherell from the 1966 Berkeley Conference (see point I. in the bibliography), I should like to mention two articles which are particularly relevant to this chapter. The first is the lecture notes "Theoretical problems in strong interactions at high energies" by L. Van Hove given at CERN in 1964 (report CERN 65-22, 1965), the other is the review article "High-energy strong interactions of elementary particles" by L. Bertocchi and E. Ferrari in the book "High-energy physics, Vol. II" (editor E.H.S. Burhop), (Acad. Press, New York/London, 1967).

CHAPTER 5 - TOTAL CROSS-SECTIONS

This is an experimental quantity which has been measured to very high accuracy (total absorbing techniques). It is also the simplest one to discuss theoretically since, from the optical theorem (3.34), it is related to the imaginary part of the forward elastic amplitude, not to an amplitude squared.

The experimental results for all reactions measured up till now are shown in Fig. 5.1. The data seem to indicate a smooth behaviour of the cross-sections as functions of energy without those large variations which characterize, for example, low energy $\pi^{\pm}p$ scattering. This fact should not be over-emphasized, though, since some variations could have escaped detection; note in this context the relatively large distance on the energy scale between adjacent points.

As is seen, all cross-sections lie in the interval $\sim$ 15 mb to $\sim$ 60 mb, with $\bar{p}p$ being the largest and K^+p the smallest. The fact that σ_{tot} is bigger for $\bar{p}p$ than for pp is qualitatively explained by the larger number of inelastic channels open in $\bar{p}p$ collisions (annihilation, baryon-antibaryon final states, etc.). A similar explanation works for π^-p as compared with π^+p, and for K^-p versus K^+p scattering.

The fact that the cross-sections are finite is already an indication that the range R of the forces responsible for the interaction is finite. Namely, in the crudest of models one expects a total cross-section of the order of the geometrical one

$$\sigma_{tot} \sim \pi R^2 \quad . \tag{5.1}$$

A value of 40 mb for σ_{tot} implies $R \sim 10^{-15}$ m = 1 fm, which approximately equals the pion Compton wavelength, a reasonable number. We shall in a moment substantiate this remark somewhat.

Let us, however, first note that an extrapolation of the curves, up to energies above the highest now available, seems not inconsistent with the view that they all tend to constant, non-vanishing values as p_{lab} tends to infinity. At least, it seems as if the cross-sections will not become infinite as the energy increases. In other words, the range R of the interaction seems to stay finite as $p_{lab} \to \infty$. There is also a theoretical

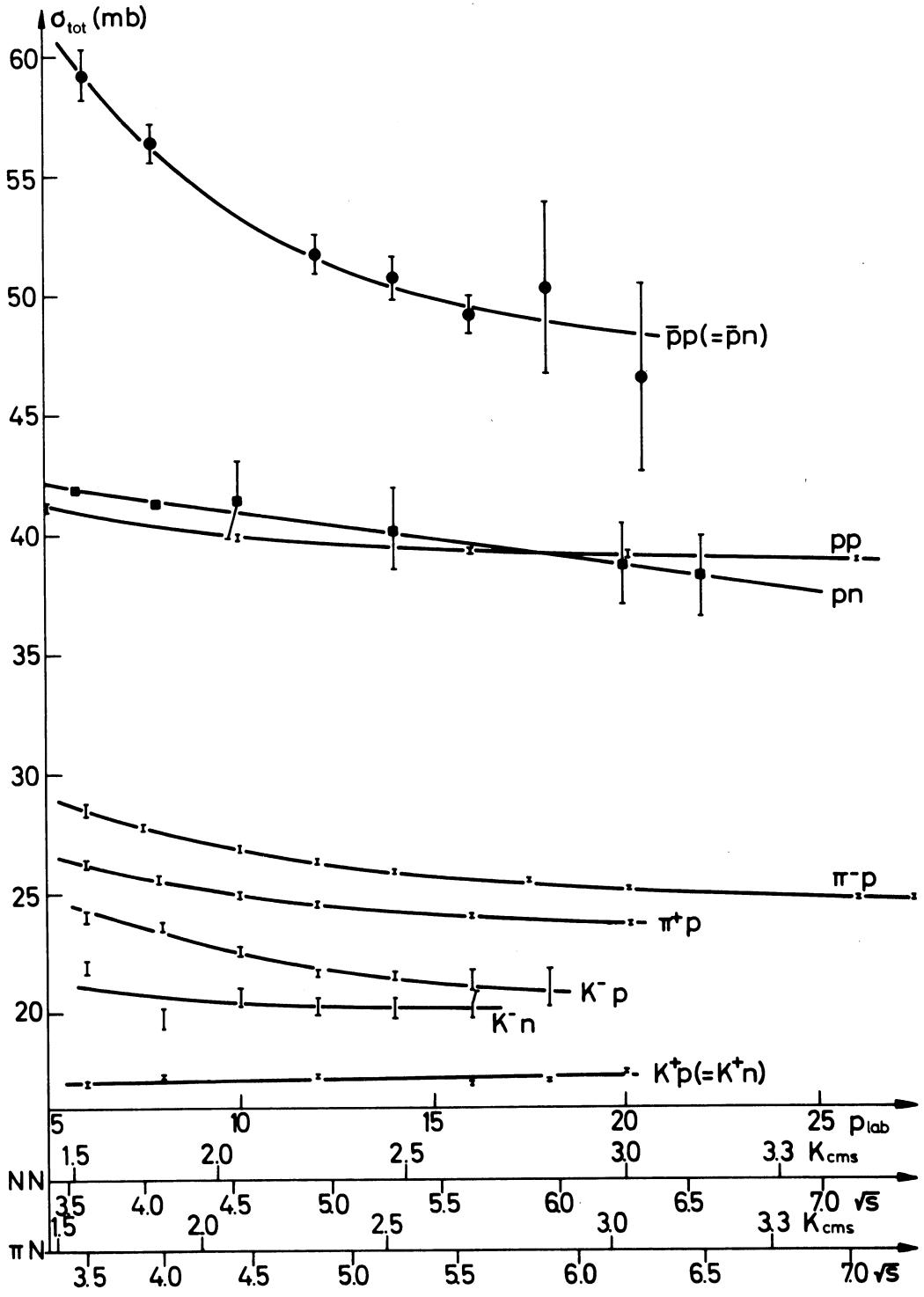

Fig. 5.1

Total cross-sections for $5 \leq p_{lab} \leq 25$ GeV/c. The $\pi^{\pm}$p and pp data are from S.J. Lindenbaum, Invited paper presented at the Coral Gables Conference on Symmetry Principles at High Energies, January 1967. The two points at lowest energy for pn are from D.V. Bugg et al., Phys.Rev. 146, 980 (1966). All other results are from W. Galbraith et al., Phys.Rev. 138, B913 (1965). The curves are freehand fits to the data. Note also the conversion scale from lab. to c.m.s. quantities, all in units of GeV, at the bottom of the figure.

argument supporting this fact, although slightly weaker in its formulation. By exploiting the consequences of quantum field theory, one is able to show that σ_{tot} may grow at most as the second power of $\log(p_{lab})$ as energy increases

$$\sigma_{tot} < C[\log (p_{lab})]^2 \quad , \quad p_{lab} \to \infty \tag{5.2}$$

where C is a constant, the value of which is not known. This relation is called the Froissart bound, and was originally proved by Froissart in 1961 [Phys.Rev. 123, 1053] using unitarity and the Mandelstam representation of the scattering amplitude. The proof based on the axioms of quantum field theory was given by Martin in 1966 [Nuovo Cimento 42A, 930 (1966); see also Phys.Rev. 129, 1432 (1963)].

There is one more observation to be made: straightforward extrapolation of the data seems to indicate that the total cross-sections for collision of a particle and its antiparticle with the same target will eventually become equal. For example, $\sigma_{tot}(\pi^+p)$ and $\sigma_{tot}(\pi^-p)$ could very well become equal at higher energies. In fact, this rule has theoretical justification as well. Namely, if one assumes that the total cross-sections tend to constant non-vanishing values (logarithmic energy-variations are allowed, though) one is able to prove, using theorems from field theory of essentially the same kind as those used in proving the Froissart bound (5.2), that these constant values must be the same for particle and antiparticle reactions. This result is known as the Pomeranchuk theorem, originally proved from dispersion relations by Pomeranchuk in 1956 [Zhur.Eksp.i Teor.Fiz. 30, 423, English translation in Soviet Phys. - JETP (USA) 3, 306], and with less assumptions by Martin [Nuovo Cimento 44, 704 (1965)].

These two theorems, the Froissart bound and, in particular, the Pomeranchuk theorem, are restrictions a theorist wants the experimental data to obey. One even introduces the concept of the "asymptotic region" for those energies where the assumptions and consequences of the Pomeranchuk theorem are satisfied. Where would this asymptotic region be? One could get a feeling for that from the recent results by Lindenbaum and co-workers on the total $\pi^{\pm}p$ cross-sections as given in Fig. 5.1. They assumed a parametrization

$$\sigma_{tot}(\pi^{\pm}p) = a + b_{\pm}\left(\frac{p_o}{p_{lab}}\right)^{m_{\pm}} , \qquad (5.3)$$

where p_o = 1 GeV/c and p_{lab} is in units of GeV/c, and fitted the values of the constants to obtain a = 22.57 mb, m_+ = 1.02, m_- = 0.664, b_+ = 24.51 mb and b_- = 19.55 mb (no errors quoted). It then follows that the difference $\sigma_{tot}(\pi^-p) - \sigma_{tot}(\pi^+p)$ becomes less than the present errors for each of them ($\sim$ 0.1 mb) at p_{lab} of the order of 4×10^3 GeV/c, i.e., $k_{cms} \sim 45$ GeV/c. Summarizing, the theorist's wonderful Asymptopia could be within reach with a 4000 GeV/c machine, or with 45 GeV/c intersecting storage rings [cf. Phys.Rev.Letters 19, 330 (1967)].

In this context it should also be mentioned that there has been put forward the idea that the total cross-sections should tend to zero at infinite energies. In fact, the data were found to be consistent with a high-energy decrease of σ_{tot} as p_{lab}^{-n} with n = 0.075 ± 0.008 [see N. Cabibbo et al., Nuovo Cimento 45A, 275 (1966)]. However, if Lindenbaum assumes that the "constant" a in the parametrization (5.3) has such an energy-dependence, he gets $0 \leq n < 0.03 - 0.05$. A more clear-cut answer will be obtained with the Serpukhov machine, since if $n \approx 0.07$ the cross-sections will be down by $\sim$ 2 mb from p_{lab} = 20 GeV/c to 70 GeV/c.

Above, we introduced a range R of interaction by requiring the total cross-section to be of the order of the geometrical one. Let us now try to make this idea somewhat more precise. To do this, let us consider $\pi^{\pm}p$ scattering, neglecting the influence of the nucleon spin, i.e., assuming that the two partial wave amplitudes (4.32) are (approximately) equal

$$f(\ell, +, E) = f(\ell, -, E) \equiv f(\ell, E) . \qquad (5.4)$$

This means that the spin-flip amplitude H, Eq. (4.39), vanishes, and that the non-flip one, Eq. (4.38), has the same partial wave expansion as if the nucleon had no spin. In an impact parameter picture, we could define R as the maximum impact parameter b_{max} for which scattering occurs. For the impact parameter amplitude B(b, E) this assumption takes the form

$$B(b, E) = 0 \quad \text{for} \quad b > b_{max} = R . \qquad (5.5)$$

It simply means that all pions that pass the nucleon at a distance larger than R will not feel any influence from the nucleon and will thus pass untouched; see also Fig. 4.1.

What would be a reasonable assumption concerning scattering at impact parameters less than R? At the high energies under considerations it is an experimental fact that inelastic reactions occur very frequently. Referring to the discussion in Chapter 4, this means that the absorption parameter $\eta(b)$ might be quite small. The simplest assumption which is in line with this argument is to assume that $\eta(b) = 0$ for those b-values at which scattering occurs. From Eq. (4.25) the impact parameter then takes the form

$$B(b, E) = \frac{1}{2i}(0 - 1) = \frac{i}{2} \quad \text{for} \quad b < R \; . \tag{5.6}$$

In particular, the value of the (real) phase shift $\delta(b)$ does not matter, since the inelasticity vanishes. The assumptions (5.5, 5.6) define the "black disc model", so called because all particles hitting the disc $b < R$ are completely absorbed by it.

The result of the black disc model for the elastic scattering amplitude (4.50) is then

$$F_{el;\,\text{black disc}}(\cos\Theta, E) = ik \int_0^R b \, db \, J_0(b\Delta) \tag{5.7}$$

Here, the integral can be evaluated explicitly. We postpone this, however, until discussing $d\sigma_{el}/dt$ in the next chapter. Right now, we are only interested in the total cross-section, which is most easily derived directly from the optical theorem in the form (4.54)

$$\sigma_{tot} = \frac{4\pi}{k} \, \text{Im} \left[ik \int_0^R b \, db \right] = 2\pi R^2 \; . \tag{5.8}$$

In somewhat more precise terms, this is the relation between the range R of interaction and the total cross-section σ_{tot}. In particular, σ_{tot} is twice the geometrical cross-section. We shall comment on this point later when considering elastic scattering. In anticipation, we mention that the black disc model given here will turn out to be too crude to fit the experimental results on $d\sigma_{el}/dt$; in fact, essentially all its predictions are violated by the data. It must therefore necessarily be modified in order to describe, at least approximately, the experimental findings. We shall consider these problems in the next chapter.

As a summary of this chapter we note that:

i) σ_{tot} is a slowly varying function of energy for $p_{lab} \geq 5$ GeV/c;
ii) σ_{tot} corresponds to a range of interaction of about 1 fm; it is largest (60-50 mb) for $\bar{p}p$, smallest ($\sim$ 15 mb) for K^+p;
iii) all total cross-sections seem to be asymptotically constant; in particular, they seem to obey the Froissart bound;
iv) σ_{tot} for particle and antiparticle reactions with the same target seem to approach the same constant limit (Pomeranchuk's theorem).

CHAPTER 6 - ELASTIC SCATTERING

The black disc model introduced in the previous chapter gave the very definite expression (5.7) for the elastic scattering amplitude. The model can therefore be compared with the experimentally determined elastic cross-sections. In fact, one may evaluate the integral over the Bessel function to get

$$F_{el;\,black\ disc}(\cos\Theta, E) = ikR^2\,\frac{J_1(R\Delta)}{R\Delta} \simeq ikR^2\,\frac{1}{2}\exp\left[-\frac{1}{8}R^2\Delta^2\right], \quad (6.1)$$

the last approximation being valid at small angles, $\Delta \lesssim 1/R$. In this

---

Exercise 6.1: Prove Eq. 6.1 using the findings of Appendix 2.

---

model, the cross-sections then read

$$\frac{d\sigma_{el;\,\text{black disc}}}{dt} = \pi R^4 \left| \frac{J_1(R\Delta)}{R\Delta} \right|^2 \simeq \frac{\pi R^4}{4} \exp\left[\left(\frac{R}{2}\right)^2 t \right], \qquad (6.2)$$

where we introduced $t = -\Delta^2$, and

$$\sigma_{el;\,\text{black disc}} = \pi R^2 = \frac{1}{2}\,\sigma_{tot;\,\text{black disc}}\,. \qquad (6.3)$$

The small-angle approximation in Eq. (6.2) is good to $\leq 20\%$ for $|t| \leq 0.25\,(\text{GeV/c})^2$ (if $R \geq 1$ fm).

Exercise 6.2: Prove the relations (6.2) and (6.3). [Hint for σ_{el}: use Eq. (4.53)!]

The black disc model is invoked essentially to account for the finite range of the interaction and for the large amount of inelastic reactions at high energies. We may summarize its predictions as follows:

i) No spin effects.

ii) The scattering amplitude is purely imaginary.

iii) $d\sigma_{el}/dt$ decreases exponentially for small $|t|$ with a logarithmic slope $(R/2)^2$. For larger $|t|$ it should show minima ("dips") and maxima ("bumps"); the first dip is expected at $-t \sim 0.7\,(\text{GeV/c})^2$ (for $R \sim 1$ fm) and the first bump at $-t \sim 1.0\,(\text{GeV/c})^2$, as may be inferred from from Fig. A2.1 of Appendix 2.

iv) σ_{el}/σ_{tot} should be 0.5.

Let us make two remarks about these results before we compare them to the data. First, the pattern of minima and maxima predicted for the elastic differential cross-section is well-known both from optics (for example, the intensity pattern for light passing a sharp edge) and from low energy nuclear physics. It is in fact characteristic for a wave incident on a totally absorbing object with sharp boundaries, having an extension much larger than the wavelength. It is known in optics as diffraction; this name is then also used for the analogous phenomena in nuclear and elementary-particle physics.

Second, you might be astonished by the fact that there is elastic scattering at all, since one of the properties of the black disc model, Eq. (5.6), was that there should be no outgoing elastic wave with $b < b_{max} = R$. This apparent contradiction is solved by carefully investigating what total absorption, $\eta_\ell = 0$, really means. To this end we note that the outgoing spherical ℓ-wave, from Chapter 4, in particular Eqs. (4.22) and (4.13), is proportional to $1 + 2if_{el}(\ell, E) = \eta_\ell \exp(2i\delta_\ell)$. Here, the first term, the number 1, comes from the expansion of the plane wave exp (ikz), while the second represents the amount of scattering. Now, if one requires η_ℓ to vanish, this by no means implies the absence of scattering. Actually, it implies complete destructive interference between the ℓth partial wave part of the plane wave exp (ikz) and the corresponding scattered elastic partial wave. In other words, since the plane wave must always be there, from the asymptotic form (3.1) of the total wave function, the absence of an outgoing spherical wave means a scattered wave completely out of phase compared to the incoming one. Or in still other terms: a completely absorbing obstacle may be considered as an emitter of elastic partial waves 180° out of phase compared to the incoming ones. One calls this "shadow scattering".

These considerations also throw some light on the fact that σ_{tot} is twice the geometrical value πR^2. Namely, σ_{tot} comprises σ_{el} and σ_{inel}. Due to absorption, the inelastic cross-section equals πR^2. For the same reason, as we just saw, the elastic cross-section equals πR^2 as well. This explains the factor of two in the total cross-section.

With the predictions from the black disc model in mind, in particular point (iii) above, we now turn to the experimental findings. Some typical elastic differential cross-sections (in this case for $\pi^{\pm}p$ scattering) are shown in the logarithmic plots of Figs. 6.1 and 6.2. They do not follow the expected behaviour particularly well. Even if at "low" energies ($p_{lab} \sim 2.5$-4 GeV/c) there is a dip at $-t \sim 0.8\,(\text{GeV/c})^2$ and a bump at $-t \sim 1.4\,(\text{GeV/c})^2$, this structure seems completely absent at higher momenta where the black disc model in fact should be more appropriate. Instead, $d\sigma_{el}/dt$ seem to decrease roughly exponentially with $|t|$ out to at least $\sim 1\,(\text{GeV/c})^2$, may be even to $\sim 2\,(\text{GeV/c})^2$. One usually refers to this exponential peak for near forward elastic scattering as the "diffraction peak".

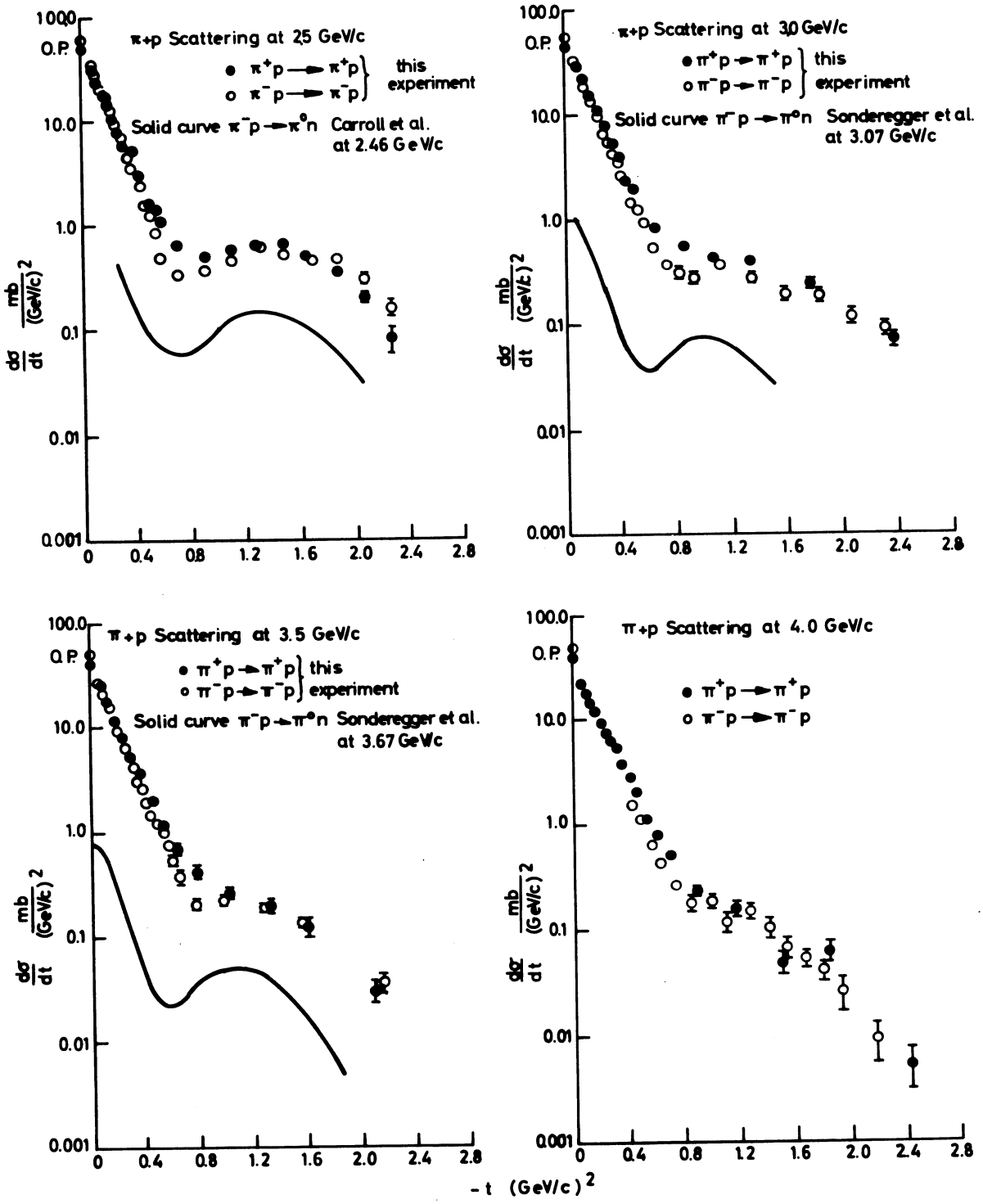

Fig. 6.1

$d\sigma_{el}/dt$ for $\pi^{\pm}p$ in the interval $2 \leq p_{lab} \leq 4$ GeV/c. Data from C.T. Coffin et al. [Phys.Rev.Letters 17, 458 (1966)].

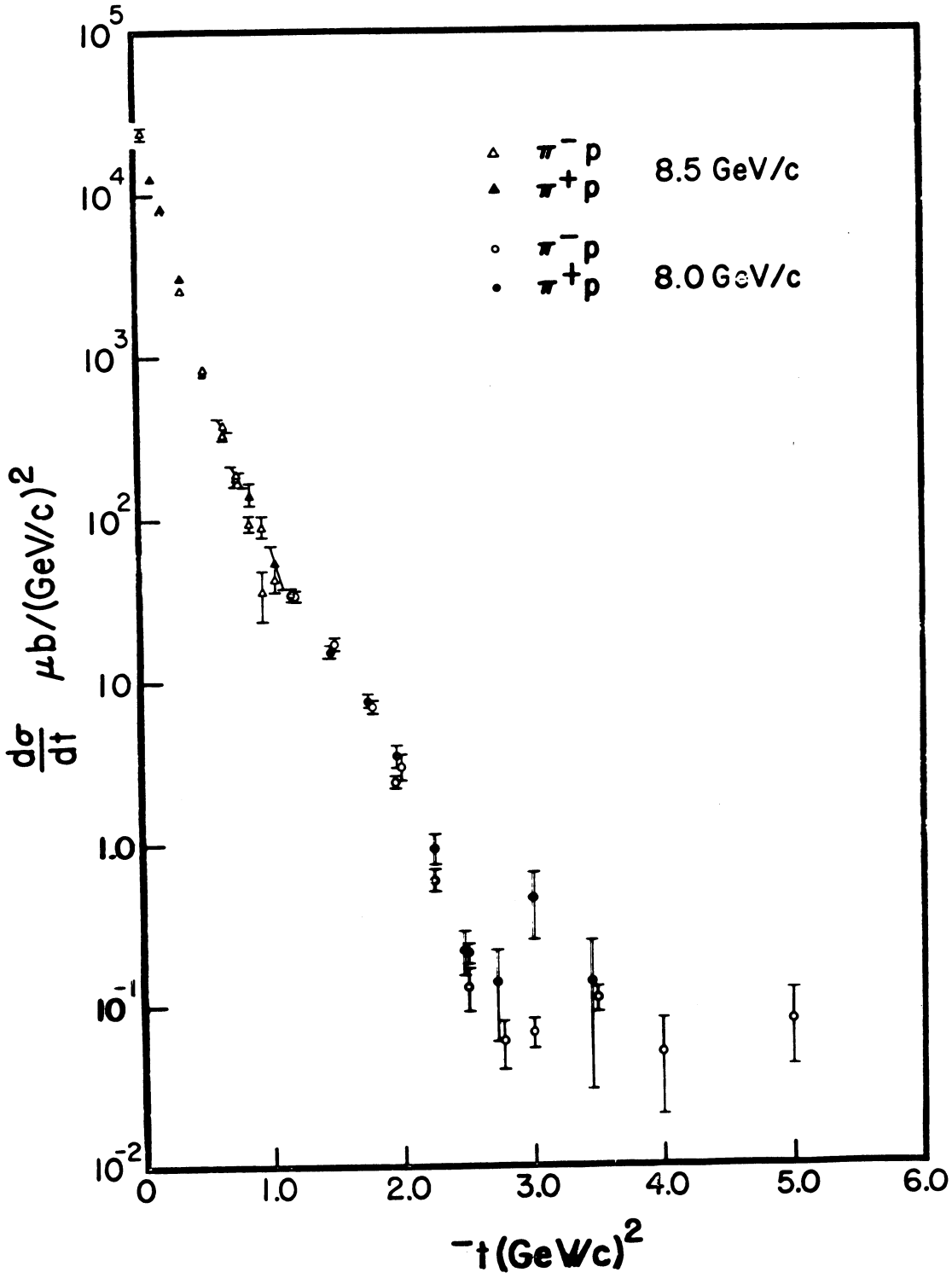

Fig. 6.2

$d\sigma_{el}/dt$ for $\pi^{\pm}p$ at $p_{lab} \sim 8$ GeV/c. Data from J. Orear et al. [Phys.Rev.Letters 15, 309 (1965)].

Actually, a very good parametrization of the data for $p_{lab} \gtrsim 5$ GeV/c, is given by

$$\frac{d\sigma_{el}}{dt} = \frac{d\sigma_{el}}{dt}\,(t = 0)\,\exp\,[At + Bt^2]\,, \qquad (6.4)$$

valid for $0.05 \lesssim |t| < 1 - 1.5\,(\mathrm{GeV/c})^2$; over this range the cross-section decreases by four orders of magnitude. The form (6.4) fits all measured elastic differential cross-sections at high energy with approximately energy-independent parameters A and B that vary slightly from reaction to reaction but are always positive.

In more detail, A is in all cases of the order of $10\,(\mathrm{GeV/c})^{-2}$; the experimental results are given in Figs. 6.4-6.6 (see p. 3-68 to 3-70). Note that the approximate energy-independence of A is linked to our use of the variable t in the parametrization (6.4). Had we used, say, $\cos\Theta$ as the variable, the coefficient in the exponent would have shown a strong dependence on the energy. Moreover, the parameter B is fairly small, $B/A^2 \lesssim 0.03$. Thus the B-term is comparable to the A-term only for $-t \gtrsim 10/A \sim 1\,(\mathrm{GeV/c})^2$, and may often be completely neglected for $|t| < 0.5\,(\mathrm{GeV/c})^2$. Since the cross-section is almost entirely confined to the smallest momentum transfers, one then obtains

$$\sigma_{el} = \int_{-t_{min}}^{0} dt\,\frac{d\sigma_{el}}{dt} \approx \frac{d\sigma_{el}}{dt}\,(t = 0) \int_{-\infty}^{0} dt\,\exp At = A^{-1}\,\frac{d\sigma_{el}}{dt}\,(t = 0)\,. \qquad (6.5)$$

The parametrization (6.4), with A and B positive, means that the differential cross-section on a logarithmic plot is like a parabola open upwards. Note that the black disc model would indeed in a second approximation give the form (6.4) but with B negative, since on a logarithmic plot it gives a convex cross-section (~ parabola open downwards) as may be inferred from Fig. A2.1.

The prediction of diffraction minima and maxima in the black disc model is closely related to the sharp edge of the disc, i.e., the fact that $B(b, E)$ jumps from i/2 to 0 at $b = R$. Such a discontinuity is in fact rather unlikely physically. Actually, still keeping to the spirit of the

model, the absence of a dip-bump structure indicates that the disc should have a diffuse edge. In other words, one expects a transition region in b around b = R where B(b, E) drops to zero. The more refined theoretical framework in which to discuss such a behaviour is the optical model. In fact, the black disc model is a particularly simple case of the optical model. We shall not discuss that model any more here but only refer to, for example, the CERN lecture notes by Van Hove (report CERN 65-22, 1965) for a more detailed treatment.

Instead, we shall take a purely phenomenological standpoint and try to extract information on the scattering amplitude and its impact parameter expansion directly from the experimental findings as given by the form (6.4). To this end, however, one needs an assumption on the phase of $F_{el}(\cos\Theta, E)$ since only its absolute value is determined from the cross-section. As a first approximation we shall assume that the amplitude is still purely imaginary. The validity of that assumption will be discussed in a moment. From Eqs. (6.4) and (6.5) one then derives

$$F_{el}(\cos\Theta, E) = ik\sqrt{\frac{A\sigma_{el}}{\pi}}\exp\left(\frac{1}{2}At\right), \tag{6.6}$$

where we neglected the B-term in the exponent. This form may be for the time being regarded as the experimentally determined scattering amplitude.

In passing we note that the form (6.6) gives, via the optical theorem, a total cross-section that reads

$$\sigma_{tot} = \frac{4\pi}{k}\,\mathrm{Im}\,F_{el}(t=0) = \sqrt{16\pi A\sigma_{el}}\,. \tag{6.7}$$

Here, it is convenient to introduce the parameter $a = \sigma_{el}/\sigma_{tot}$ to relate the elastic cross-section to the total one. This parameter, or perhaps even better $1 - a = \sigma_{inel}/\sigma_{tot}$, is a direct measure of the amount of absorption occuring in the interaction; in fact, 2a is often called the absorptivity or the opacity of the interaction region. Inserting the definition of a into Eq. (6.6) yields

$$F_{el}(\cos\Theta, E) = 4ikaA\,\exp\left[\frac{1}{2}At\right]. \tag{6.8}$$

Finally, calculation of the impact parameter amplitude from this elastic amplitude, using the relation (4.51) and the formula (A2.11) of Appendix 2, gives

$$B(b,E) = 2ia \exp\left[-\frac{b^2}{2A}\right]. \qquad (6.9)$$

Exercise 6.3: Prove Eq. (6.9).

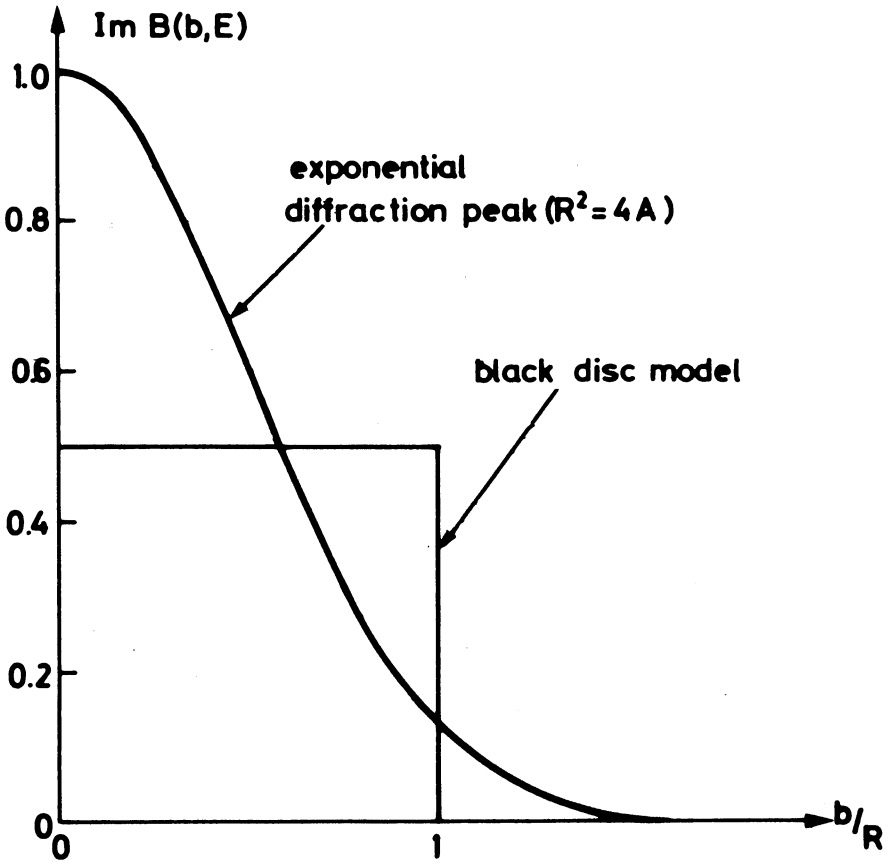

Fig. 6.3

The impact parameter amplitude B(b, E), assumed purely imaginary, for the black disc model and for an exponential diffraction peak. In both cases a = ½.

We illustrate in Fig. 6.3 the impact parameter amplitude (6.9) and compare it to the result of the black disc model in the case of $a = \frac{1}{2}$. It should be clear from the discussion that the result (6.9) is valid only for b when it is not too different from R. Namely, at very small b, corresponding to central collisions and therefore to large momentum transfers, as well as for very large b, corresponding to peripheral and therefore very small momentum transfer collisions, the parametrization (6.4) is not necessarily appropriate.

Summarizing, we may conclude that:

i) If the scattering amplitude is purely imaginary, the fact that $d\sigma_{el}/dt$ behaves as exp (At) implies that the impact parameter amplitude decreases with b as exp $(-b^2/2A)$. Comparing the black disc model prediction for the elastic amplitude at small $|t|$, Eq. (6.1), to the parametrization (6.6) gives

$$A = \left(\frac{R}{2}\right)^2 . \qquad (6.10)$$

Thus, the slope A of the exponential diffraction peak may still be considered as a measure of the extension of the interaction region.

ii) Besides A, there is now one more parameter, viz., $a = \sigma_{el}/\sigma_{tot}$, which may be used to characterize the experimental findings. It obeys $a \leq 1$, with equality only for purely elastic scattering, and is a measure of the amount of absorption, or inelastic reactions. It equals 0.5 for the black disc model.

Let us then turn to the experimental results as given in terms of the slope A and the ratio σ_{el}/σ_{tot}. They are given in Figs. 6.4, 6.5 and 6.6 for different reactions. Also shown in these figures are the ratios of the real to the imaginary parts of the forward scattering amplitude; we shall discuss these data in a moment.

From the figures we note that:

i) The slope A lies between $\sim 5\,(\mathrm{GeV/c})^{-2}$ and $14\,(\mathrm{GeV/c})^{-2}$, being smallest for K^+p, which also has the smallest σ_{tot}, and largest for $\bar{p}p$, which has the largest σ_{tot}. In terms of $R = 2\sqrt{A}$ it implies $0.9 \leq R \leq 1.4$ fm.

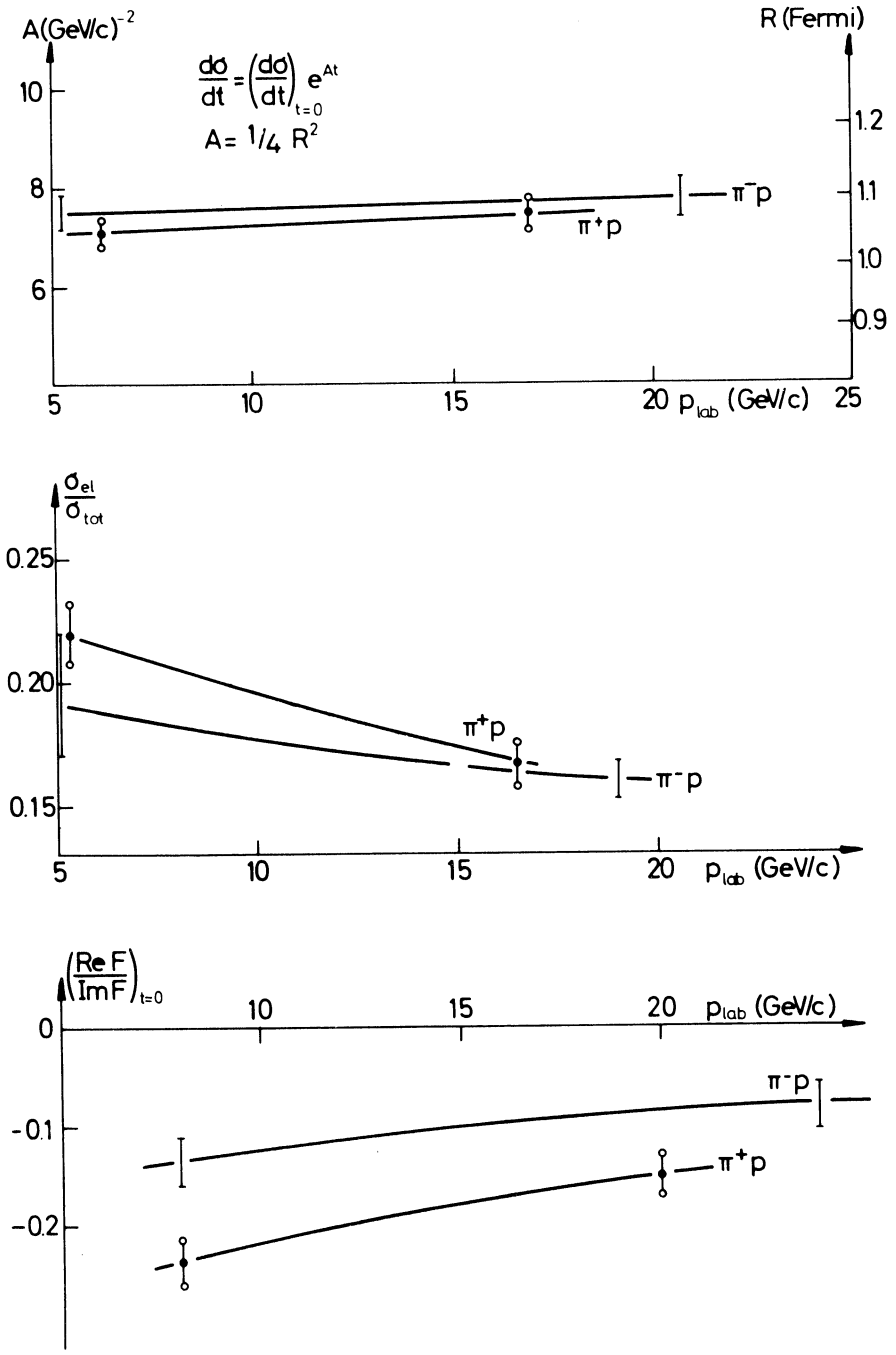

Fig. 6.4

The slope A of the forward diffraction peak, the ratio σ_{el}/σ_{tot} of the elastic to the total cross-section, and the ratio $(\mathrm{Re}\ F/\mathrm{Im}\ F)_{t=0}$ of the real to the imaginary part of the forward scattering amplitude as functions of $p_{lab} \geq 5$ GeV/c for $\pi^{\pm}p$. The curves are freehand fits to the data and the error bars only indicate typical statistical errors. σ_{el}/σ_{tot} and A are taken from the compilation by M.N. Focacci and G. Giacomelli (report CERN 66-18, 1966). $(\mathrm{Re}\ F/\mathrm{Im}\ F)_{t=0}$ is from Lindenbaum's 1967 Coral Gables paper [see caption to Fig. 5.1; cf. also Phys.Rev.Letters 19, 193 (1967)].

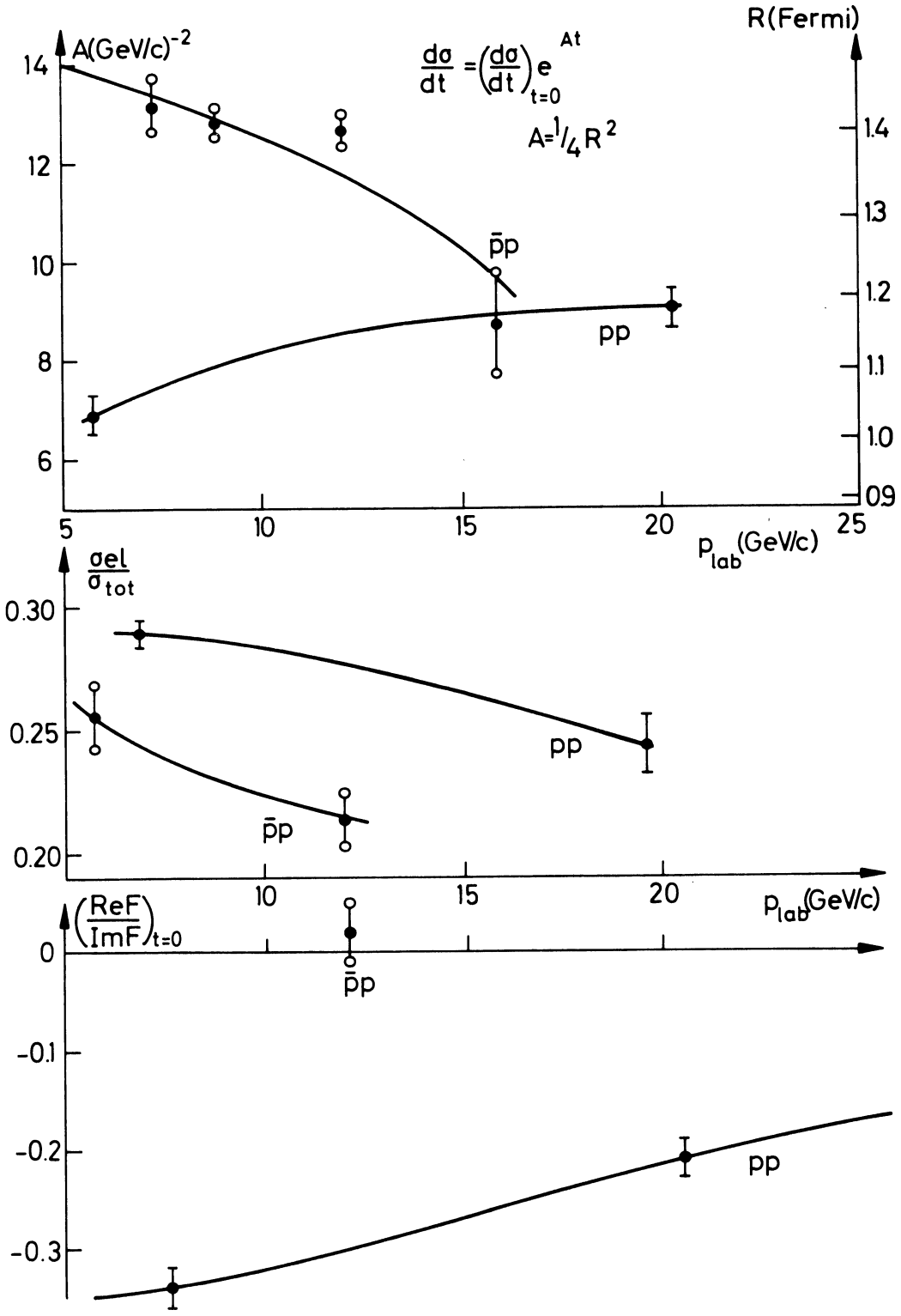

Fig. 6.5

Data for pp and $\bar{p}p$ analogous to those for $\pi^{\pm}p$ in Fig. 6.4. The slope A for pp is from Focacci and Giacomelli (cf. caption to Fig. 6.4); A for $\bar{p}p$ and σ_{el}/σ_{tot} are from K.J. Foley et al. [Phys.Rev.Letters 11, 425, 503 (1963)] while $(\mathrm{Re}\ F/\mathrm{Im}\ F)_{t=0}$ is from Lindenbaum's 1967 Coral Gables paper [see caption to Fig. 5.1; cf. also Phys.Rev.Letters 19, 857 (1967)].

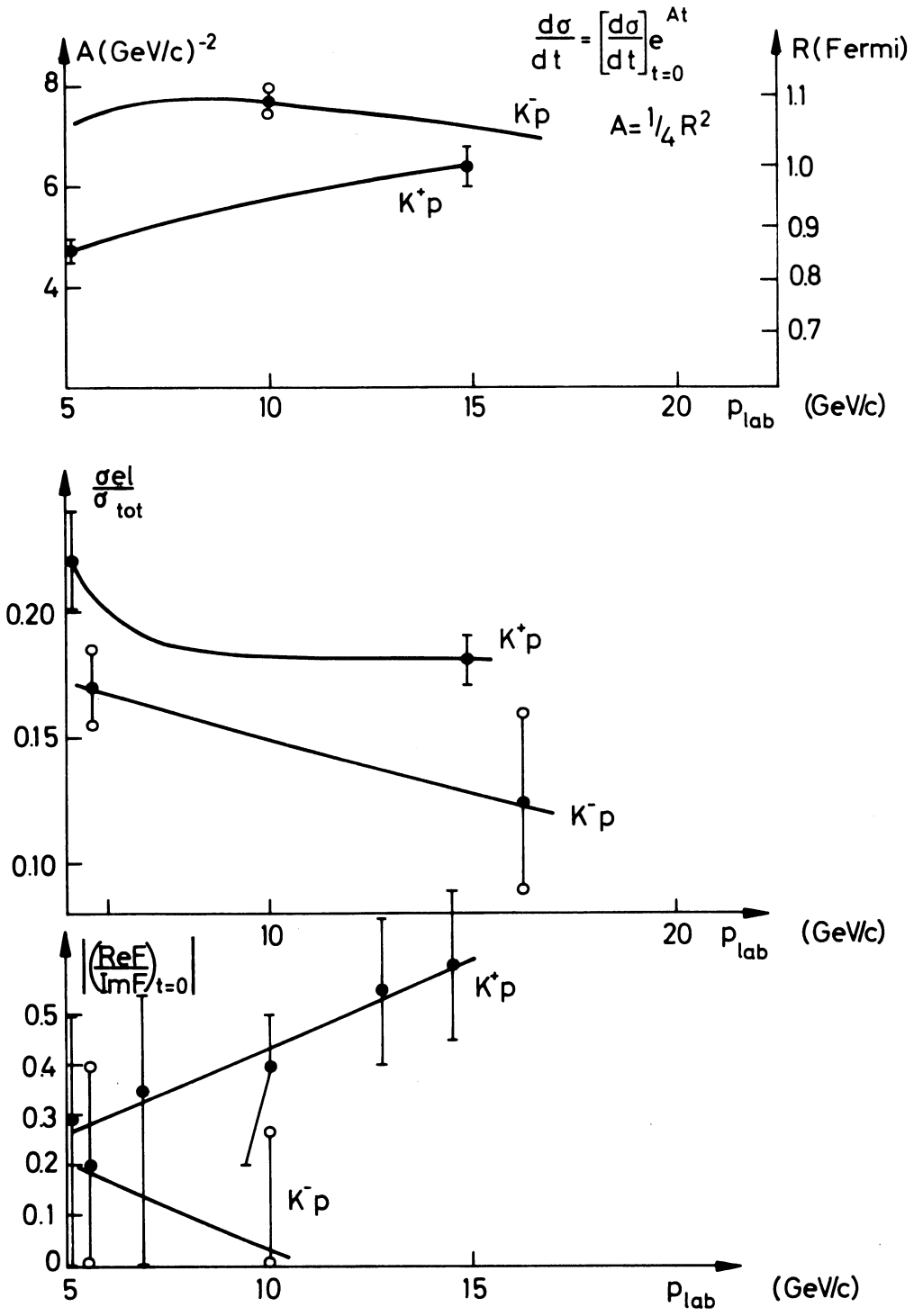

Fig. 6.6

Data for $K^{\pm}p$ analogous to those for $\pi^{\pm}p$ in Fig. 6.4. The findings for K^-p, and σ_{el}/σ_{tot} for K^+p, are taken from M. Aderholz et al. [Physics Letters 24B, 434 (1967)], the slope A for K^+p from K.J. Foley et al. [Phys.Rev.Letters 11, 503 (1963)] and $|(\mathrm{Re}\ F/\mathrm{Im}\ F)_{t=0}|$ from M. Lusignolli et al. [Nuovo Cimento 45A, 792 (1966)].

ii) For $\pi^{\pm}p$ and K^-p there is no significant energy variation of A when p_{lab} varies from ~ 5 GeV/c to the highest available energies. On the other hand, A increases for K^+p and pp while it decreases for $\bar{p}p$. As is seen from the definition (6.4) of A (neglecting the B-term), an increasing A means a steeper decrease of the differential cross-section as a function of $|t|$ ("shrinking diffraction peak") while a decrease in A implies a flatter $|t|$ distribution ("expanding diffraction peak").

iii) The value of σ_{el}/σ_{tot} lies between ~ 0.3 and ~ 0.15, i.e., about half the value predicted by the black disc model. It is larger for π^+p than for π^-p, for K^+p than for K^-p and for pp than for $\bar{p}p$. This is connected to the circumstance that more inelastic channels are open for π^-p scattering compared to π^+p, for K^-p compared to K^+p, and for $\bar{p}p$ compared to pp.

There are two essential ingredients which go into the analysis presented so far, viz., that F_{el} (cos Θ, E) is purely imaginary and that spin effects may be neglected. Do the data support these assumptions? Let us treat them one at a time to see how they can be tested.

The real part of F_{el} in the forward direction could be obtained as follows. Write the forward amplitude

$$F_{el} = \text{Re } F_{el} + i \text{ Im } F_{el} = i(1 - i\rho) \text{ Im } F_{el} \tag{6.11}$$

where

$$\rho = \frac{\text{Re } F_{el}(\Theta = 0)}{\text{Im } F_{el}(\Theta = 0)} . \tag{6.12}$$

Now, in the very forward direction the optical theorem implies

$$\text{Im } F_{el}(\cos \Theta = 1, E) = \frac{k}{4\pi} \sigma_{tot} . \tag{6.13}$$

Consequently,

$$\frac{d\sigma_{el}}{dt} (t = 0) = \frac{(\sigma_{tot})^2}{16\pi} (1 + \rho^2) \geq \frac{(\sigma_{tot})^2}{16\pi} . \tag{6.14}$$

The value $(\sigma_{tot})^2/16\pi$ for the forward differential cross-section is often referred to as the optical point. Since $(d\sigma_{el}/dt)(t = 0)$ can be obtained by extrapolating the measured differential cross-section to zero scattering angle, and since σ_{tot} is measured separately, the relation (6.14) provides knowledge of $|\rho|$. However, besides leaving the sign of ρ undetermined, the extrapolation required is not very accurate. Therefore, the procedure outlined gives a poor determination of $|\rho|$, the more so because $|\rho|$ is a small quantity, in general. However, data indicate that the extrapolated forward cross-section is within 20% of the optical point, implying that $|\rho|$ is less than $\sim$ 40%.

A better procedure to obtain ρ, including its sign, is afforded by measurements of $d\sigma_{el}/dt$ at very small but non-zero angles (Θ_{lab} of the order of milliradians), where interference between the hadronic and the Coulomb part of the scattering amplitude occurs. The argument is as follows. So far, we have neglected the electromagnetic interaction between the particles. Since this is small compared to the strong (= hadronic) interaction, one might expect it to be negligible. However, in the very forward direction, the Coulomb scattering amplitude (3.61) goes to infinity as t^{-1}. This is merely a reflection of the long range character of the electromagnetic forces. Since one expects the hadronic amplitude to remain finite, it should be possible to detect the Coulomb interaction by going to very small values of $|t|$. Moreover, since the Coulomb amplitude is explicitly known, one may be able to measure the relative phase between it and the hadronic amplitude, in other words to measure ρ.

More quantitatively, one writes

$$F_{el} = F_C + F_h \ . \tag{6.15}$$

Here, for the small t-values of interest

$$F_C \equiv F_{Coulomb} = \pm \alpha \frac{\sqrt{s}}{t} \ , \tag{6.16}$$

where the positive sign is appropriate for particles of equal charges (for example, $\pi^+ p$), the negative sign for particles of opposite charges (for example, $\pi^- p$). Furthermore, for the hadronic amplitude $F_h(\cos\Theta, E)$ at small $|t|$, one assumes

$$F_h = 2i\sqrt{s}\, aA(1 - i\rho)\, \exp\left[\frac{1}{2} At\right] \qquad (6.17)$$

in accordance with Eqs. (6.8) and (6.11); here we also approximated k by $\frac{1}{2}\sqrt{s}$. Now, since $\alpha \approx 1/137$ and $aA \sim 0.2 \times 10\,(\mathrm{GeV/c})^{-2}$, it follows that the two terms in Eq. (6.15) are comparable in magnitude for

$$|t| \sim \frac{1}{137} \times \frac{1}{4}\,(\mathrm{GeV/c})^2 \approx 0.002\,(\mathrm{GeV/c})^2 \ .$$

In the lab. this corresponds to a recoil nucleon kinetic energy of 1 MeV(!), but it has since 1964 nevertheless been possible to measure $d\sigma_{el}/dt$ at such very small momentum transfers.

Summarizing, at very small scattering angles one expects

$$\frac{d\sigma_{el}}{dt} = \frac{\pi}{k^2}|F_C + F_h|^2 \approx \frac{4\pi}{s}\left[|F_C|^2 + |F_h|^2 + 2\,\mathrm{Re}\,(F_C F_h^*)\right] = \qquad (6.18)$$

$$= 4\pi\left[\frac{\alpha^2}{t^2} + 4a^2A^2(1+\rho^2)\,\exp\,(At) \pm 4aA\rho\,\frac{\alpha}{t}\,\exp\left(\frac{1}{2}At\right)\right] \ ,$$

with the same sign conventions as in Eq. (6.16). Here, for $|t| \leq 0.001\ (\mathrm{GeV/c})^2$ the Coulomb term α^2/t^2 should dominate, while for $|t| \geq 0.05\,(\mathrm{GeV/c})^2$ only the second term, i.e., the hadronic part, is important. In the region $0.001 \leq |t| \leq 0.05\,(\mathrm{GeV/c})^2$, however they are comparable in magnitude and it should thus also be possible to measure the interference term, i.e., $\rho = (\mathrm{Re}\ F_h)/(\mathrm{Im}\ F_h)$.

Two additional remarks may appropriately be added to the preceding discussion. First, in the actual data analysis, ρ is usually taken as a constant. Its t-dependence is not known, and the procedure followed is adequate only if ρ does not vary appreciably in the momentum transfer interval studied. Second, several refinements in the expression (6.18) can be made to account for deviations of F_{Coulomb} from the simple form (6.16) and for corrections to the simple assumption (6.15) that the Coulomb

and the hadronic amplitudes just add to give the total amplitude. We may refer to Lindenbaum's 1967 Coral Gables talk (see caption to Fig. 5.1) for a more detailed discussion of these corrections as well as further references.

What would $d\sigma_{el}/dt$ look like according to Eq. (6.18)? We have in the schematic diagram of Fig. 6.7 illustrated the situation in $\pi^{\pm}p$ scattering assuming $\rho = 0$ (dashed line), and $\rho < 0$ (full lines) for both processes; the parameters a and A were here assumed equal for π^+ and π^-. Examples of experimentally determined cross-sections are given in Fig. 6.8. It is seen that the data show a behaviour expected for ρ negative in both reactions. The actual numerical value here is $\rho \sim -0.1$ for π^- and ~ -0.2 for π^+.

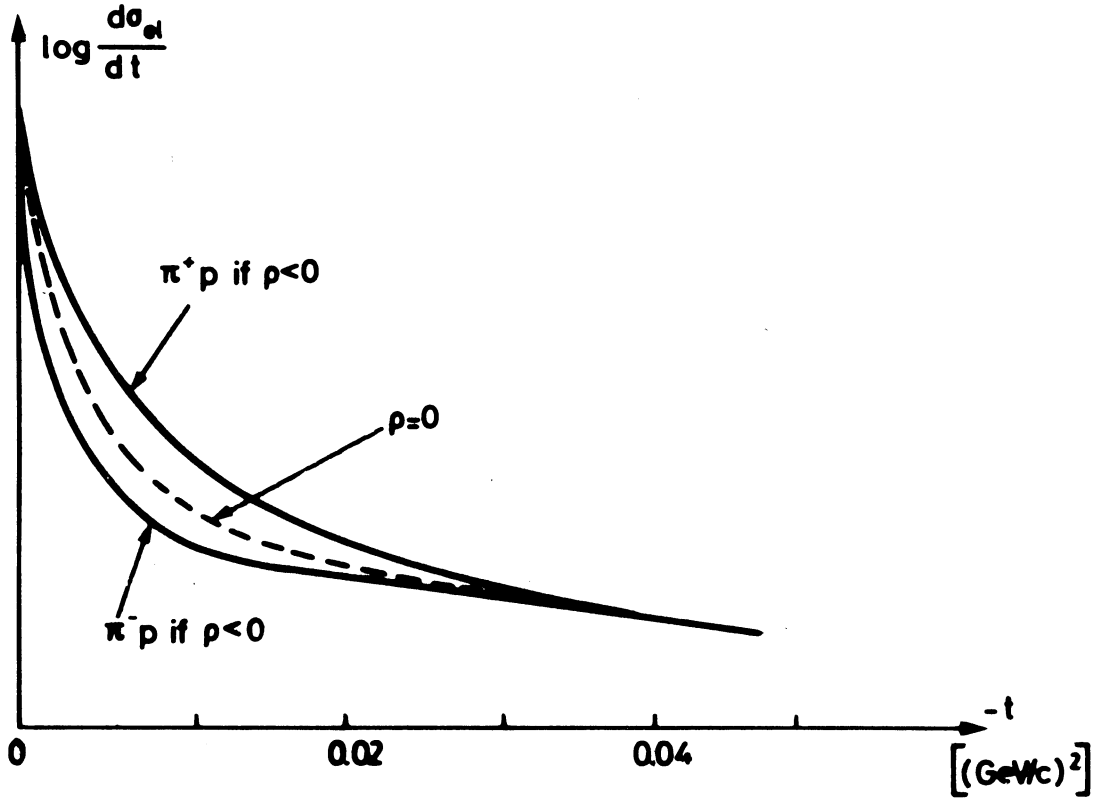

Fig. 6.7

The elastic differential cross-section for very small $|t|$-values according to Eq. (6.18).

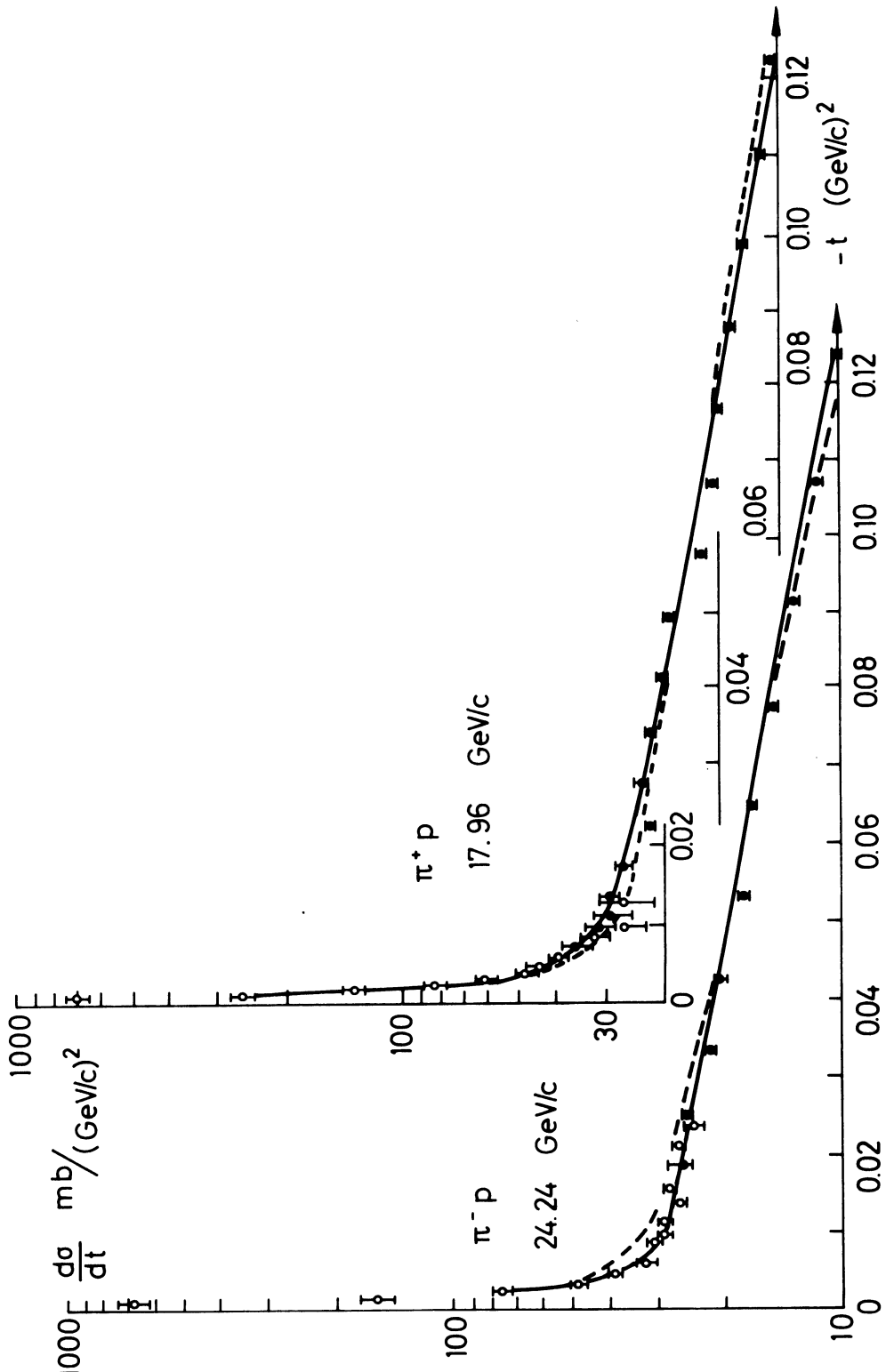

Fig. 6.8

$\pi^{\pm}$p elastic scattering in the Coulomb interference region. Data are from Lindenbaum's 1967 Coral Gables paper (see caption to Fig. 5.1). Note the scale displacements between the two graphs.

In this way, one has measured ρ = (Re F/Im F)(t = 0) as function of energy for $\pi^{\pm}$p and pp elastic scattering. Very recently, a result for $\bar{p}p$ at one energy was also reported. The experimental results are given in Figs. 6.4 and 6.5. The ρ parameter for $K^{\pm}$p scattering has not yet been measured from Coulomb interference experiments, but only through extrapolation of $d\sigma_{el}/dt$ to t = 0, comparing it with the optical point. The results for $|\rho|$ are presented in Fig. 6.6 but should be taken with great caution since the value is very sensitive even to small systematic errors in the cross-sections.

As the experimental results show, the assumption of a purely imaginary (hadronic) scattering amplitude is not correct, except possibly for $\bar{p}p$ scattering. On the contrary, (Re F/Im F)(t = 0) is negative and of the order of 10-30% for both $\pi^{\pm}$p and pp, implying a phase of $90° + \sim 15°$. The sign of the ratio corresponds, in the Born approximation (3.48), to a repulsive interaction, V(r) > 0; in fact, this argument generalizes beyond the Born approximation. It seems as if the ratio could tend to zero for $p_{lab} \to \infty$, though. Actually, as we shall see later, the phase of the scattering amplitude is closely related to its energy dependence. More precisely, if the π^+p and π^-p elastic amplitudes become equal at high energies and if they imply a constant total cross-section then they must both be purely imaginary. This means roughly that the Pomeranchuk theorem has as a consequence that (Re F/Im F)(t = 0) should vanish in the asymptotic region.

Now, we turn to the question whether spin effects can be neglected at high energies. We remember that in the analysis so far we have assumed that the spin flip amplitude H(cos Θ, E) vanishes, so that the total elastic amplitude F(cos Θ, E) equals the non-flip one G(cos Θ, E). An obvious way to test this assumption is to measure the polarization parameter P, which from Eq. (3.55) is proportional to Im (GH^*). Thus, P should vanish if H = 0 (the opposite conclusion is not true!). These considerations really only apply to $\pi^{\pm}$p (and $K^{\pm}$) scattering, since in pp and $\bar{p}p$ reactions the beam particle also has spin, which complicates the spin analysis. We shall not go into details but merely state that the NN polarization may be discussed along much the same lines as in πN scattering, and that, in particular, one may define a polarization parameter P also here.

Some results of the recent experiments concerning P are shown in Fig. 6.9. Indeed, even if P turns out to be small, of the order of 0.1, it is certainly not zero. Consequently, spin effects cannot be ignored even for p_{lab} in the region of 10 GeV/c, unless as a first approximation.

How would spin effects influence the preceding analysis of $\pi^{\pm}p$ elastic scattering? Clearly, the derivation of the scattering amplitude and its impact parameter expansion, Eqs. (6.8) and (6.9), is no longer true, except qualitatively as a rough approximation. Indeed, things become complicated and only additional measurement of the R and A polarization parameters can give the complete answer. However, for the analysis of (Re F/Im F) (t = 0) the situation is better, since in the very forward direction the spin flip amplitude necessarily vanishes [see Eq. (4.39)].

For pp scattering, many polarization measurements (actually at least nine) are required for a complete determination of the scattering amplitude. Furthermore, there are several (in fact three) terms with different spin structure even in the forward amplitude, complications which are usually ignored in the data analysis of Coulomb interference experiments.

So far we have only discussed elastic scattering at relatively small scattering angles. We now treat very briefly what happens outside the forward diffraction peak. For the c.m.s. scattering angle Θ near to 90°, the cross-section turns out to be extremely small, typically 6-12 orders of magnitude smaller than in the forward direction $[(d\sigma_{el}/dt)\,(\Theta = 90°) \sim (10^{-4} - 10^{-10})\,\mathrm{mb/(GeV/c)^2}]$. We may refer to Van Hove's report at the 1966 Berkeley Conference, as quoted in the bibliography, for some recent results on such large angle scattering.

An interesting question is what happens at still larger angles, near to the backward direction in the c.m.s. Keeping in mind that the identity of particles in pp scattering forbids elastic scattering at larger angles than 90°, one must go to, for example, πN reactions to study this question. Some experimental results for $\pi^{\pm}p$ scattering are shown in Figs. 6.10 and 6.11; recall (Exercise 2.5) that in the backward direction the variable $u \sim -2k^2(1 + \cos\Theta)$ is approximately zero. One notes that $(d\sigma_{el}/dt)\,(180°)$ reaches $\sim 10\ \mu\mathrm{b/(GeV/c)^2}$ which, although a factor of about 10^3 less than in the forward direction, is still some 100 times bigger than the cross-section around 90°. Thus the backward peak is indeed significant. In

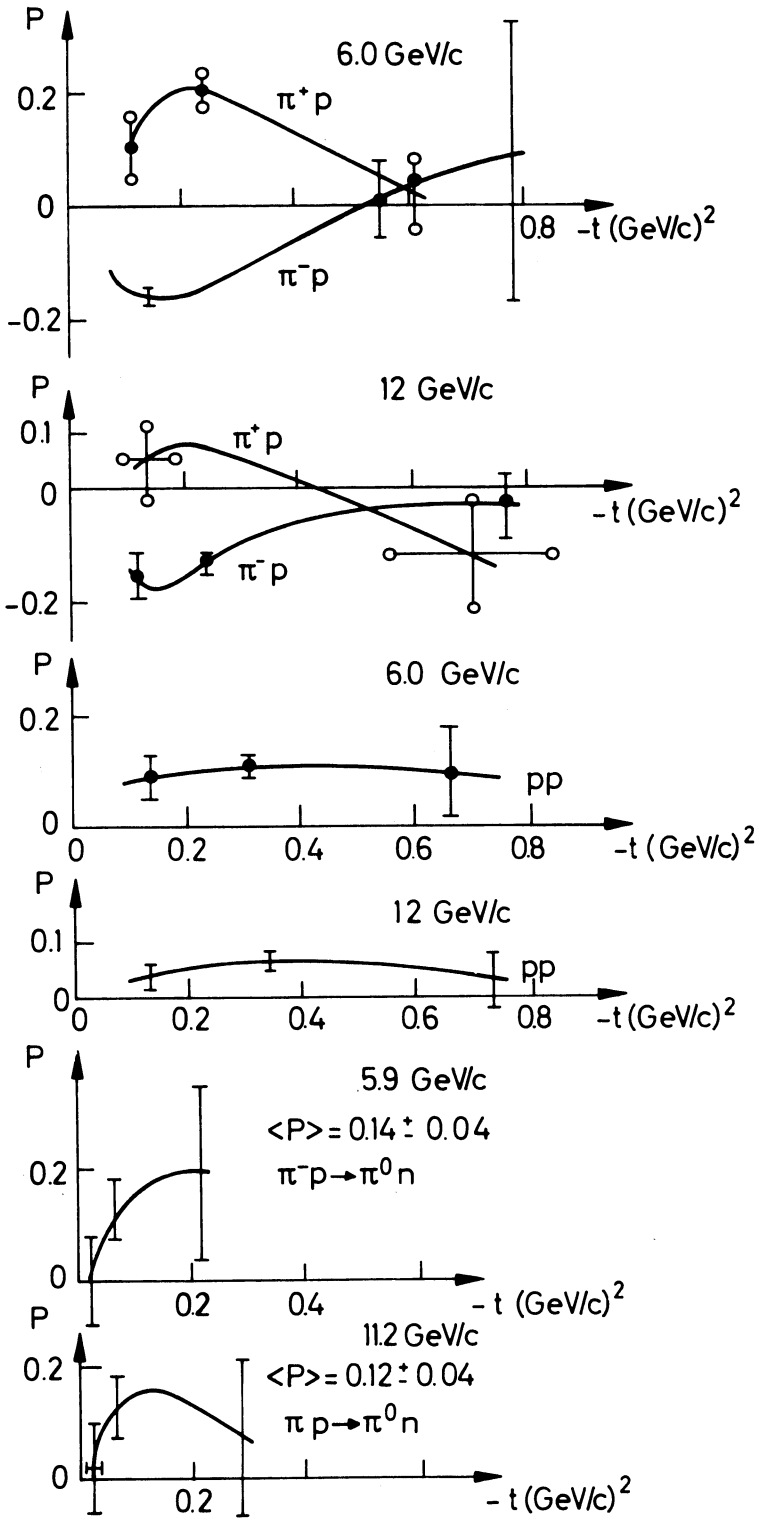

Fig. 6.9

The polarization parameter P in elastic $\pi^{\pm}$p and pp scattering, and in π^{-}p charge exchange. The elastic scattering data are from M. Borghini et al. [Physics Letters 24B, 77 (1967)], the charge exchange data from P. Bonamy et al. [Physics Letters 23, 501 (1966)]. Curves are freehand fits to the data, and the error bars only indicate typical statistical errors.

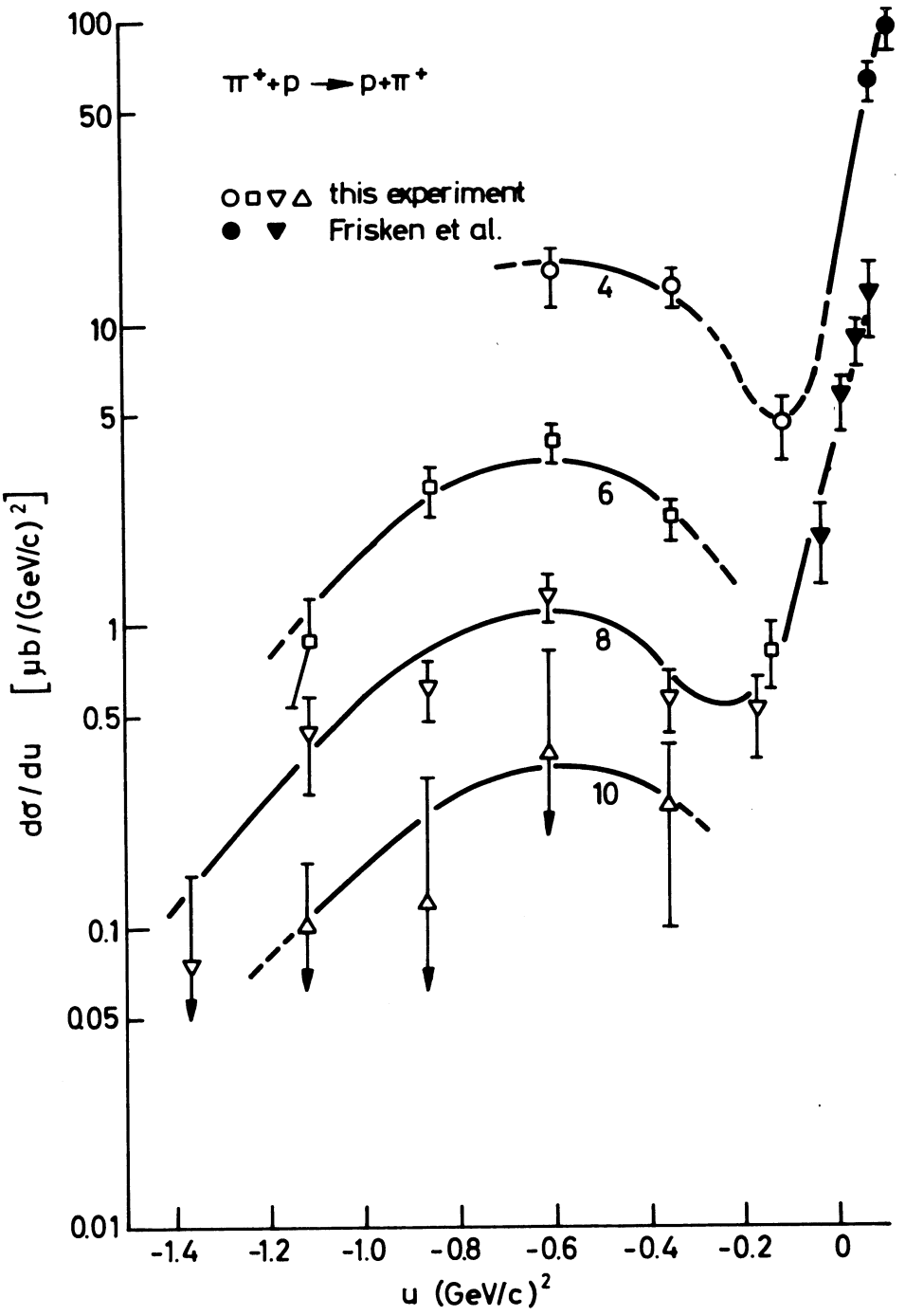

Fig. 6.10

Backward elastic $\pi^+ p$ scattering for $4 \leq p_{lab} \leq 10$ GeV/c as measured by W. Selove et al., and by W.R. Frisken et al., taken from L. Van Hove's Rapporteur's Report in the Proceedings of the XIIIth International Conference on High-Energy Physics, Berkeley, California, Aug. 31-Sept.7, 1966 (University of California Press, 1967), p. 253.

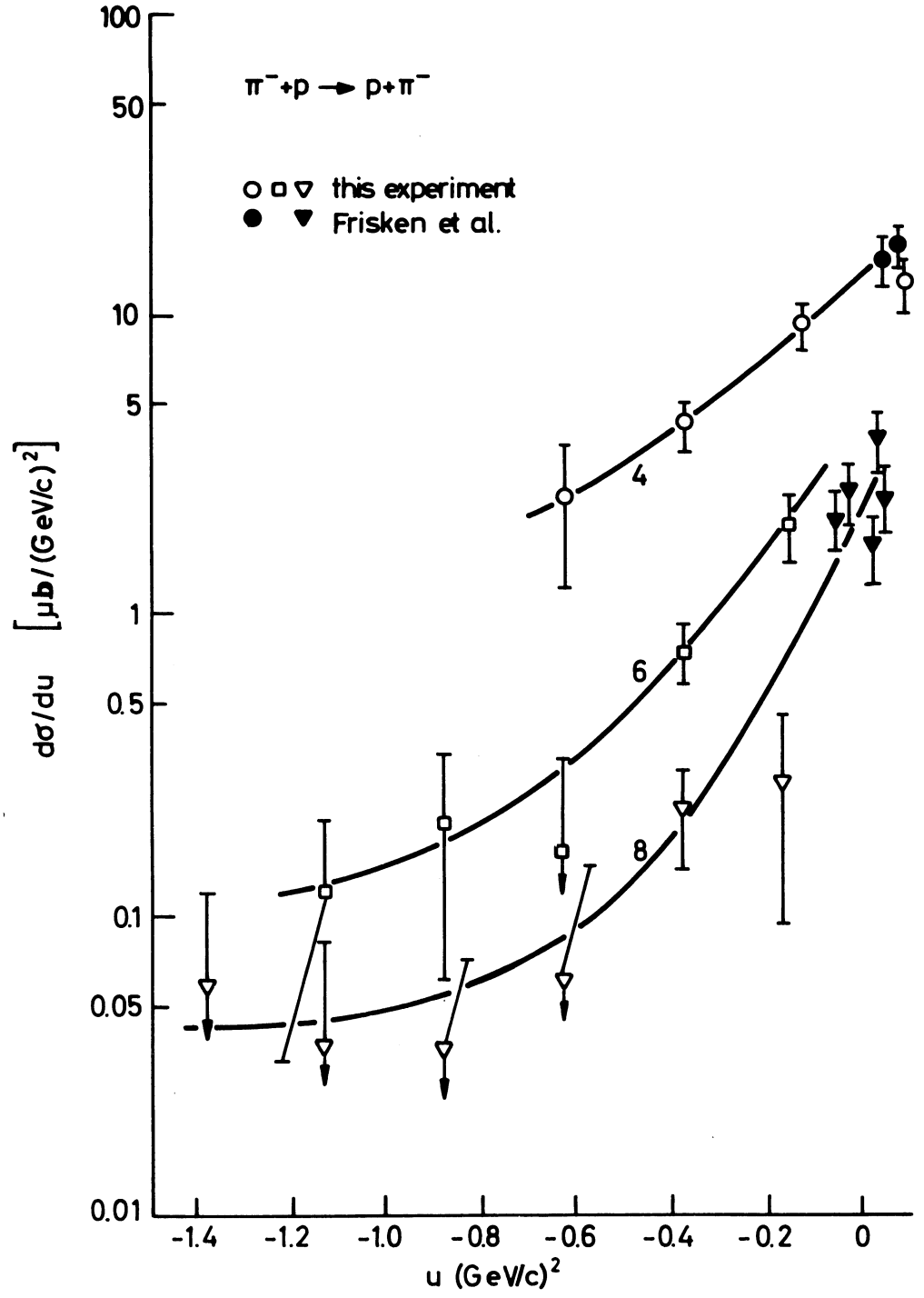

Fig. 6.11

Backward elastic $\pi^- p$ scattering for $4 \leq p_{lab} \leq 8$ GeV/c as measured by W. Selove et al., and by W.R. Frisken et al., taken from Van Hove's 1966 Berkeley report (see caption to Fig. 6.10).

more detail, it seems as if the backward scattering also shows an exponential peak. Its slope is slightly bigger than for the forward peak $\sim$ (10-20) $(\text{GeV/c})^{-2}$. We also note the dip-bump structure in the $\pi^+ p$ case, which seems absent for $\pi^- p$ scattering. On the other hand, the $\pi^- p$ cross-section could flatten out, or even turn over, very near to $\Theta = 180°$. Note also that the backward cross-section seems to decrease rather fast with energy, something like p_{lab}^{-3}.

A summary of this chapter may be given as follows. Elastic scattering shows a diffraction character in the sense that the differential cross-section has a pronounced, approximately energy-independent, peak in the forward direction and decreases exponentially as a function of the momentum transfer squared with an approximately energy-independent slope of about $10\,(\text{GeV/c})^{-2}$, and also in the sense that the forward scattering amplitude is approximately imaginary. However, the cross-section shows no trend of diffraction minima and maxima at high energy. Instead, on a logarithmic plot it is more like a parabola open upwards. Moreover, the phase of the elastic amplitude (for $\pi^{\pm} p$ and pp) is about 105°. Finally, one cannot ignore spin effects, the polarization parameter P being about 10% even at $p_{lab} = 12$ GeV/c. Therefore, any simple diffraction model can be used only to reproduce the gross features of elastic scattering.

The essential experimental results on total and elastic scattering are collected in Table 6.1, following the way of presenting the data given by Wetherell at the 1966 Berkeley Conference.

Colliding particles	σ_{tot}	$\frac{\sigma_{el}}{\sigma_{tot}}$	$-\left(\frac{\mathrm{Re}\ F}{\mathrm{Im}\ F}\right)_{t=0}$	$\frac{d\sigma}{dt} \propto e^{At}$ $\lvert t\rvert \lesssim 0.5$ (GeV/c)^2 A in (GeV/c)$^{-2}$	$\frac{d\sigma}{dt} \propto e^{Bt+Ct^2}$ $\lvert t\rvert \lesssim 1$ (GeV/c)^2 $\frac{C}{B^2} \cdot 100$	Polarization (P)	Further characteristics of forward scattering	Backward scattering		
								$\frac{(d\sigma/dt)\ (180°)}{(d\sigma/dt)\ (0°)}$	Slope (GeV/c)$^{-2}$	Structure
pp	41 ↘ 39 mb (5 - 25 GeV/c)	0.29 ↘ 0.24 (6 - 20 GeV/c)	0.35 ↘ 0.15 (5 - 26 GeV/c)	7 ↗ 9 (6 - 20 GeV/c) shrinks	5 ↘ 2 (5 - 20 GeV/c)	Positive [$\lvert t\rvert <$ ~ 0.8 (GeV/c)^2] P_{max} = 20% ↘ 8% at 6 - 12 GeV/c	Smooth t-dependence for all energies	-	-	-
$\bar{p}p$	65 ↘ ~ 48 mb (5 - 20 GeV/c)	0.26 ↘ 0.21 (5 - 12 GeV/c)	~ - 0.05 (12 GeV/c)	14 ↘ 9 (5 - 16 GeV/c) expands	~ 0 (5 - 16 GeV/c)	Not measured	At 1 - 2.5 GeV/c, dip at -t ~ 0.45 (GeV/c)^2, bump at -t ~ 0.8 (GeV/c)^2; structure seems to vanish at higher energies	Not observed		
π^+p	26 ↘ 24 mb (5 - 20 GeV/c)	0.22 ↘ 0.17 (5 - 16 GeV/c)	0.25 ↘ 0.15 (7 - 20 GeV/c)	~ 7.3 (5 - 17 GeV/c) constant	~ 3 (5 - 17 GeV/c)	Positive [$\lvert t\rvert <$ ~ 0.6 (GeV/c)^2] P_{max} = 30% ↘ 8% at -t ~ 0.2 (GeV/c)^2 (6 - 12 GeV/c)	At 2 - 4 GeV/c, dip at -t ~ 0.7 (GeV/c)^2, bump at -t ~ 1.2 (GeV/c)^2; structure vanishes at higher energies	(8 ↘ 2) × 10^{-3} (4 - 8 GeV/c)	~ 15 - 20 (4 - 8 GeV/c)	Dip - bump structure
π^-p	29 ↘ 25 mb (5 - 25 GeV/c)	0.19 ↘ 0.16 (5 - 20 GeV/c)	0.15 ↘ 0.07 (7 - 25 GeV/c)	~ 7.8 (5 - 21 GeV/c) constant	~ 3 (5 - 19 GeV/c)	Negative [$\lvert t\rvert <$ ~ 0.6 (GeV/c)^2] $\lvert P\rvert_{max}$ ~ 17% at -t ~ 0.2 GeV/c (6 - 12 GeV/c)	As for π^+p	(10 ↘ 2) × 10^{-4} (4 - 8 GeV/c)	~ 10 (4 - 8 GeV/c)	$d\sigma/dt$ might flatten out near 180°
K^+p	~ 17 mb (5 - 20 GeV/c)	0.22 ↘ 0.18 (5 - 15 GeV/c)	Absolute value might be ~ 0.4 (5 - 15 GeV/c)	4.5 ↗ 6.5 (5 - 15 GeV/c) shrinks	~ 3 (7 - 15 GeV/c)	Not measured	No structure observed	~ 4 × 10^{-3} (3.6 GeV/c)	< 27 (3.6 GeV/c)	Not observed
K^-p	25 ↘ 21 mb (5 - 18 GeV/c)	0.17 ↘ 0.12 (5 - 16 GeV/c)	Absolute value $\lesssim$ 0.2 (10 GeV/c)	~ 7 (5 - 16 GeV/c) constant	3 - 4 (7 - 16 GeV/c)	Not measured	No structure observed	< 4 × 10^{-3} (3.6 GeV/c)	-	-

Table 6.1

Survey of total and elastic scattering data, extending the presentation given by A.M. Wetherell at the 1966 Berkeley Conference. The sources of information are those listed in the captions to Figs. 5.1, 6.4-6.6, and 9.11. Furthermore C/B^2 for $\pi^{\pm}p$ and pp are taken from Focacci and Giacomelli (cf. caption to Fig. 6.4), for $\bar{p}p$ and $K^{\pm}p$ from Foley et al. (cf. captions to Figs. 6.5-6.6). The $K^{\pm}p$ backward data are from J. Banaigs et al. [Physics Letters 24B, 317 (1967)].

CHAPTER 7 - SOME OTHER TWO-BODY REACTIONS

The two-body reactions most closely connected to elastic scattering are the charge exchange processes like $\pi^- p \to \pi^0 n$, $K^- p \to \bar{K}^0 n$, $np \to pn$ and $\bar{p}p \to \bar{n}n$. Consider first the pion-nucleon charge-exchange reaction. From isospin invariance it is related to πN elastic scattering. To see that let the πN scattering amplitudes in the isospin channels $I = \frac{1}{2}, \frac{3}{2}$, be denoted F_{2I}. Then

$$F_{el}^{(+)} \equiv F(\pi^+ p \to \pi^+ p) = F_3 \ , \tag{7.1}$$

$$F_{el}^{(-)} \equiv F(\pi^- p \to \pi^- p) = \frac{1}{3} F_3 + \frac{2}{3} F_1 \ , \tag{7.2}$$

$$F_{c.e.} \equiv F(\pi^- p \to \pi^0 n) = \frac{\sqrt{2}}{3} [F_3 - F_1] = \frac{1}{\sqrt{2}} \left[F_{el}^{(+)} - F_{el}^{(-)} \right] . \tag{7.3}$$

Exercise 7.1: Check the relations (7.1)-(7.3) from a table of Clebsch-Gordan coefficients.

Thus, the charge exchange amplitude is proportional to the difference between the $\pi^{\pm} p$ elastic amplitudes. Since, from the experimental data, these two amplitudes are not very different, one expects $d\sigma_{c.e.}/dt$ to be rather small compared to $d\sigma_{el}(\pi^{\pm} p)/dt$. Moreover, the difference $F_{el}^{(+)} - F_{el}^{(-)}$ need not have the same t-dependence as either term separately, so there is a priori no reason why $d\sigma_{c.e.}/dt$ should have the same variation with t as has $d\sigma_{el}/dt$.

The experimental results are shown in Figs. 6.1 and 7.1. As is seen, $d\sigma_{c.e.}/dt$ in the forward direction is a factor of 30 smaller than the elastic cross-section at $p_{lab} \sim 3$ GeV/c. It decreases with increasing energy as $p_{lab}^{-0.86}$ to become about 200 times smaller as $(d\sigma_{el}/dt)(t = 0)$ at $p_{lab} \sim 18$ GeV/c.

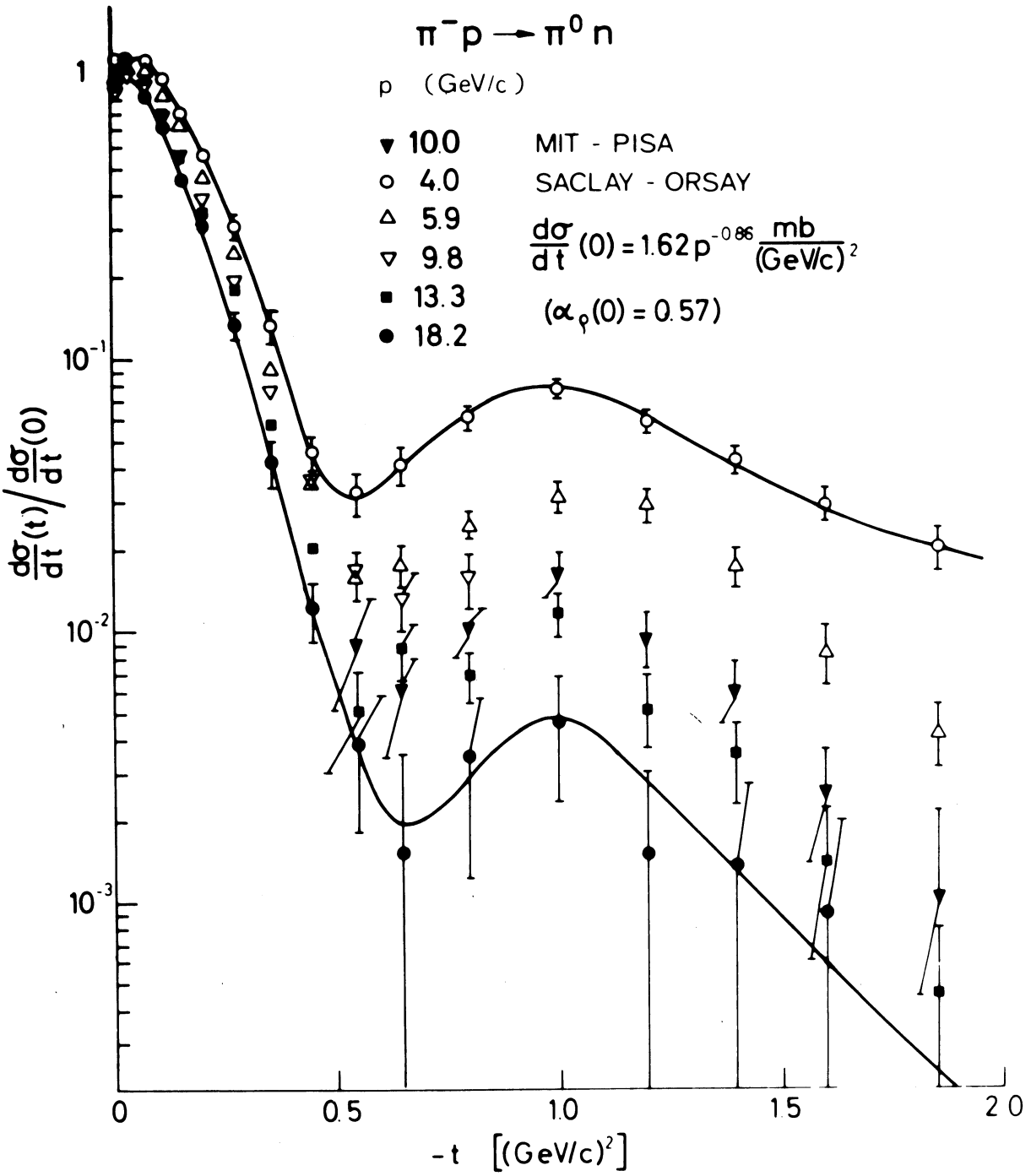

Fig. 7.1

Differential cross-section for $\pi^- p \to \pi^0 n$ in the range $4 \leq p_{lab} \leq 18$ GeV/c taken from P. Sonderegger et al. [Physics Letters 20, 75 (1966)]

This decrease of the forward charge exchange cross-section is related to the decrease of the difference $\sigma_{tot}(\pi^- p) - \sigma_{tot}(\pi^+ p)$. Namely, the charge symmetry relation (7.3) and the optical theorem (3.34) implies

$$F_{c.e.}(\Theta = 0) = \text{Re } F_{c.e.}(\Theta = 0) + i \text{ Im } F_{c.e.}(\Theta = 0) = \tag{7.4}$$

$$= \text{Re } F_{c.e.}(\Theta = 0) - i \frac{k}{4\pi} \frac{1}{\sqrt{2}} [\sigma_{tot}(\pi^- p) - \sigma_{tot}(\pi^+ p)] ,$$

so that

$$\frac{d\sigma_{c.e.}}{dt} (\Theta = 0) = \frac{1}{32\pi} [\sigma_{tot}(\pi^- p) - \sigma_{tot}(\pi^+ p)]^2 + \frac{\pi}{k^2} [\text{Re } F_{c.e.}(\Theta = 0)]^2 . \tag{7.5}$$

Consequently, if Re $F_{c.e.}(\Theta = 0)$ has (approximately) the same energy dependence as Im $F_{c.e.}(\Theta = 0)$, the forward charge exchange cross-section should decrease roughly as $p_{lab}^{-1.2}$, if we invoke the Lindenbaum result for the total cross-sections as discussed in Chapter 5, in particular Eq. (5.3). The difference between the exponents, -1.2 versus -0.86, can presumably be blamed on the errors in the data and on the possibility of getting slightly different results when using different parametrizations. In fact, if Lindenbaum fits directly the difference $\sigma_{tot}(\pi^- p) - \sigma_{tot}(\pi^+ p)$ he finds a decrease as $p_{lab}^{-0.3}$, implying a charge exchange cross-section behaving like $p_{lab}^{-0.6}$. In passing we note that the form (7.5) can be invoked to measure $|\text{Re } F_{c.e.}(\Theta = 0)|$; the results are that it is roughly equal to the corresponding imaginary part, so the phase of the forward charge exchange amplitude is about 45° (modulus 90°).

The experiment shows a characteristic structure of $d\sigma_{c.e.}/dt$ as a function of t: in the very forward direction a flat top, and possibly even a decrease for $\Theta \to 0$, then a roughly exponential peak with logarithmic slope of about 11 $(\text{GeV/c})^{-2}$ followed by a minimum at $-t \sim 0.6\,(\text{GeV/c})^2$ and a secondary maximum at $-t \sim 1.0\,(\text{GeV/c})^2$. The forward flat top is usually ascribed to the contribution from a large spin-flip term. Since this is proportional to sin Θ, it is bound to vanish for $\Theta = 0$. It may, however, raise quickly as soon as Θ is away from the forward direction and could thus give rise to the observed structure in the very forward cross-section.

Concerning the dip-bump structure at larger $|t|$ we note that it is present even at the highest energies. Thus one finds a cross-section that seems to show a diffraction pattern in a case where diffraction cannot occur; remember that diffraction depends upon the interference between the incoming plane wave and the outgoing scattered one describing the same type of particles.

The word "à la mode" to describe a forward peak in an inelastic reaction is instead "peripheral". In a very qualitative, semi-classical picture this means that an inelastic πp reaction occurs only for incident pions hitting the non-central, or peripheral part of the proton. The pion is therefore only slightly deflected by the interaction and should in the majority of cases be scattered at very small angles, which explains the peak. Since the nuclear forces of longest range are those mediated by particles having the smallest masses (largest Compton wavelengths), this interpretation means that the incoming pion interacts only with the meson cloud surrounding the proton. In particular, the charge-exchange reaction could be described along these lines by saying that the proton is transformed into a neutron by virtual emission of a positive ρ-meson, which is absorbed by the negative pion to become a neutral pion. Note that the incident pion cannot absorb a virtual pion to become a pion, since this would violate conservation of G-parity and even ordinary (space) parity.

These considerations form the intuitive basis of the one-particle-exchange (OPE) model. The ideas can be substantiated in terms of, for example, Feynman diagrams. The graph describing the ρ-meson exchange contribution to the reaction $\pi^- p \to \pi^0 n$ is given in Fig. 7.2. We shall consider the OPE model in some detail later on. Here, let me only warn you against two things. First, a Feynman diagram like that in Fig. 7.2 does really not describe the space-time development of the interaction. Even if it is of great didactic help to think of the ρ-meson as being emitted and reabsorbed, the physical theory underlying the Feynman graphs is much more sophisticated than that, as you have learned, for example, from Prof. Veltman's lectures. Second, straight-forward calculations from the simple Feynman diagram of Fig. 7.2 give results in definite disagreement with the experimental findings. Thus, it is at best a qualitative way of visualizing how the charge-exchange reaction could take place.

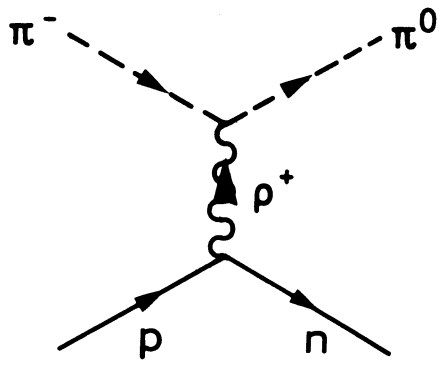

Fig. 7.2

Feynman diagram for ρ-meson exchange in pion-nucleon charge exchange.

Before we leave the experimental results on the pion-nucleon charge-exchange scattering, we mentioned that the polarization parameter $P_{c.e.}$ has also been measured. The results are exhibited in the two last drawings of Fig. 6.9. Although the errors are rather large, the data evidently show a non-vanishing polarization. We shall come back to this point later, in connection with the Regge pole model. In fact, the pion-nucleon charge-exchange reaction thoroughly studied experimentally as it is is, constitutes a very adequate test for that model.

The other three charge exchange reactions which have been measured so far may be discussed in an analogous fashion. In particular, the amplitude for charge exchange can always be related to a difference of elastic amplitudes by invoking isospin invariance.

Exercise 7.2: Prove that the amplitudes for charge-exchange are related to the elastic amplitudes by, in an obvious notation,

i) $\quad K^- p \to \bar{K}^0 n = (K^- n)_{el} - (K^- p)_{el}$,

ii) $\quad np \to pn = (pp)_{el} - (np)_{el}$,

iii) $\quad \bar{p}p \to \bar{n}n = (\bar{p}p)_{el} - (\bar{p}n)_{el}$.

The experimental results are given in Figs. 7.3-7.5 and summarized in Table 7.1. The general trend of the data is the same as for pion-nucleon charge exchange: decreasing cross-section as function of the incident momentum, and a pronounced forward peak in the differential cross-section. Minor differences, as shown in Table 7.1, should, however, be noted.

Exercise 7.3: Assume a one-particle exchange mechanism for charge-exchange scattering. Which particles can be exchanged in the different reactions? [Hint: Consider exchange of the pseudoscalar mesons π, η and K, the vector mesons ρ, ω, φ and K^* and the 2^+ mesons $A_2(1310)$, $f^0(1250)$, $f^{0\prime}(1500)$ and $K^{**}(1410)$. Use the known conservation laws for strong interactions to rule out all but the ρ-, the A_2- and, in the NN and $\bar{N}N$ cases, the π-meson.]

Many other two-body and quasi-two-body reactions have been studied extensively. Let us just mention a few of them to see the general character of the results. Figures 7.6 and 7.7 show the differential cross-section for the associated production, or strangeness exchange reaction $\pi^+ p \to K^+\Sigma^+$, as well as the corresponding polarization parameter P, in this case measured by investigating the decay of the Σ^+. The forward peak in the cross-section could, in the spirit of the OPE model, be due to exchange of a K^*-meson; the K-meson is ruled out from parity conservation. Note also that there is some trace of a minimum in $d\sigma/dt$ at $-t \sim 0.6\,(\mathrm{GeV/c})^2$, followed by a secondary maximum. Moreover, there seems to be a backward peak, where the outgoing baryon prefers the direction of the incoming meson. In the OPE model, this would mean that the incoming pion is transformed into an outgoing sigma, and would require the exchange of a baryon, in this particular case having strangeness different from zero. Possible candidates are the Λ- and the Σ-hyperon and the Y^*-resonances. The corresponding Feynman diagram is given in Fig. 7.8.

Reaction	Structure in angular distribution	Forward peak $\sim e^{bt}$ b $(GeV/c)^{-2}$	Shrinking	$(d\sigma/dt)_0$ > optical theorem value	Variation of $\sigma_{tot} \propto (momentum)^{-n}$	Cross-sections		Polarization effects
						Momentum (GeV/c)	σ_{tot} (μb)	
$p + n \to n + p$	Very sharp forward peak	For forward peak $\lvert t\rvert \lesssim 0.02$ $(GeV/c)^2$ b ≈ 50; for larger $\lvert t\rvert$ b ≈ 5	Yes (between ~ 2 and 8 GeV/c)	Yes	Rapid decrease	3.0	1100 ± 25	
						3.67	430 ± 16	
						8.00	60 ± 30	
$\bar{p} + p \to \bar{n} + n$	No	≈ 4.5	No (5 - 9 GeV/c)	Not clear	$\sim p^{-1.5}$	5	598 ± 86	
						6	563 ± 32	
						7	373 ± 54	
						9	284 ± 41	
$\pi^- + p \to \pi^0 + n$	Forward dip Minimum at $t \approx -0.6$ $(GeV/c)^2$ Bump at $t \approx -1$ $(GeV/c)^2$	≈ 11	Yes	Yes	$\sim p^{-1.3}$	3.67	191 ± 18	≈ + 14 ± 4% at 6 GeV/c ≈ ± 12 ± 4% at 11 GeV/c Maximum at $t \approx -0.15$ $(GeV/c)^2$
						4.83	128 ± 15	
						5.83	96 ± 5	
						13.3	37 ± 2	
						18.2	25 ± 3	
$K^- + p \to \bar{K}^0 + n$	Forward dip	≈ 5	Yes	Probably not	$\sim p^{-1.0}$	5	124 ± 20	
						7	94 ± 10	
						9.5	70 ± 10	

Table 7.1

Descriptive survey of data on high-energy charge exchange process taken from the compilation by A.M. Wetherell in the Proceedings of the XIIIth International Conference on High-Energy Physics, Berkeley, California, Aug. 31 - Sept. 7, 1966 (University of California Press, 1967).

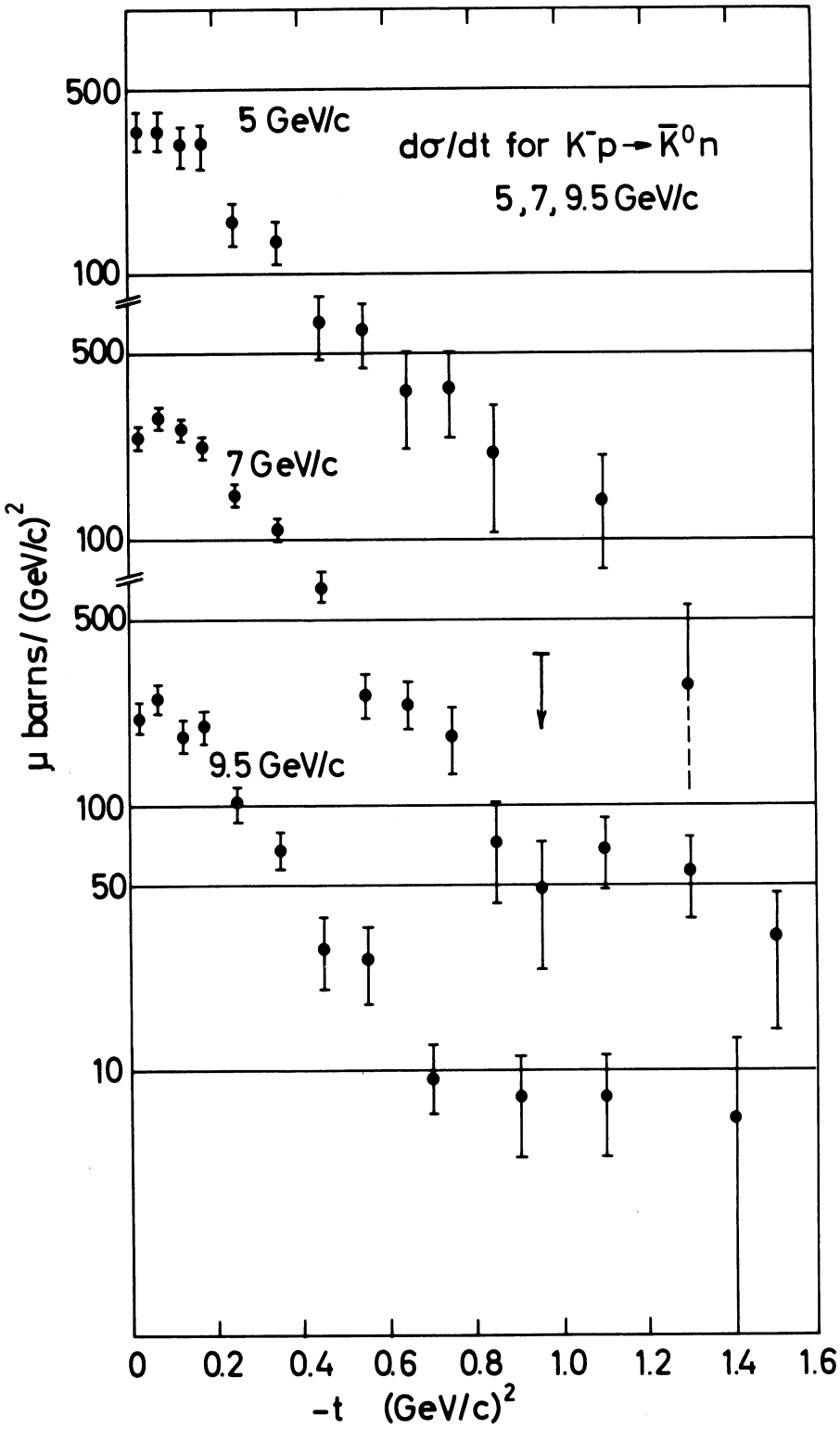

Fig. 7.3

Differential cross-section for $K^- p \to \bar{K}^0 n$ in the range $5 \leq p_{lab} \leq 9.5$ GeV/c taken from P. Astbury et al. [Physics Letters 23, 396 (1966)].

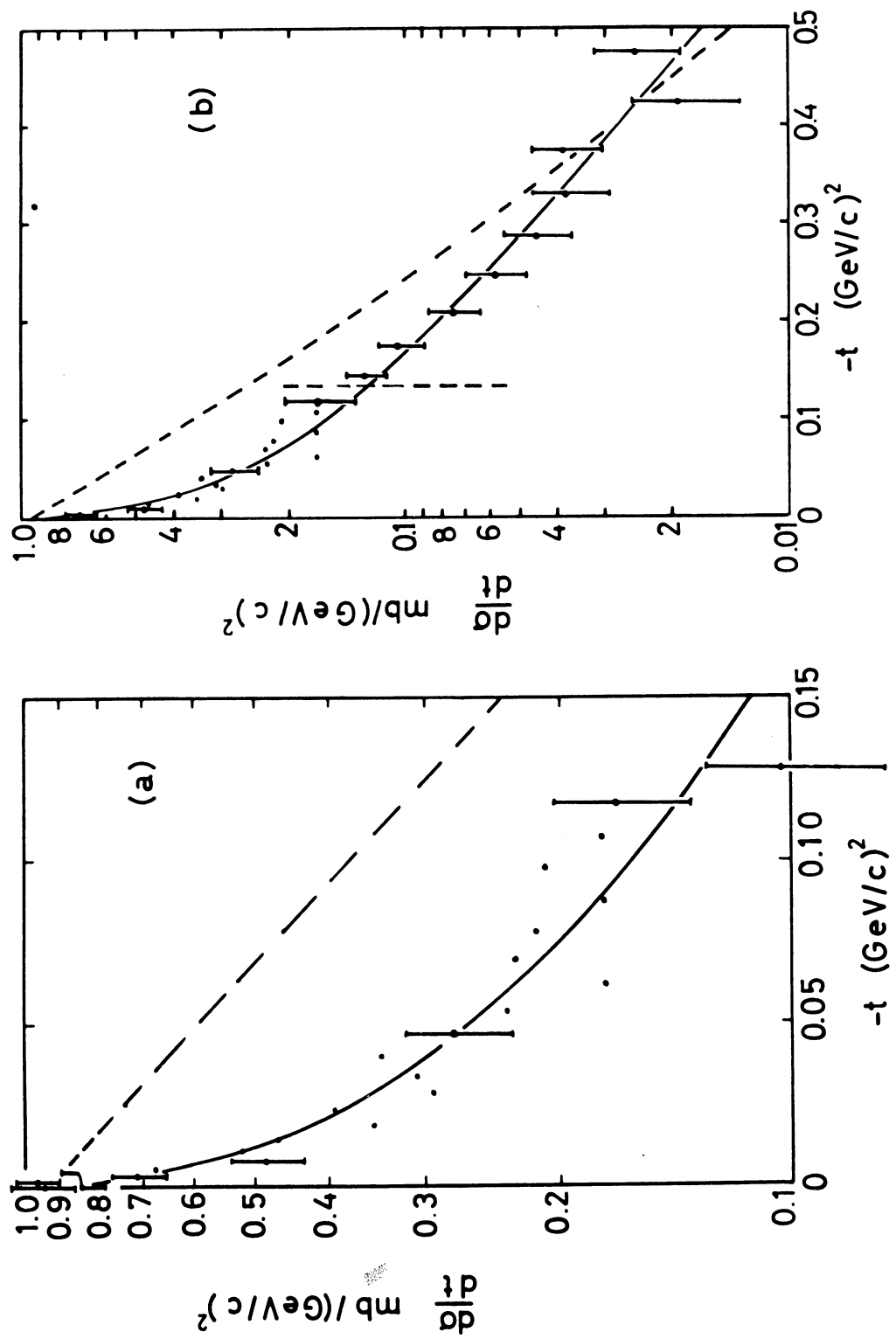

Fig. 7.4

Differential cross-section for pn → np at 8 GeV/c taken from G. Manning et al. [Nuovo Cimento 41A, 167(1966)]. The broken line shows the trend of the pp elastic cross-section at 8.9 GeV/c. Note the different scales in (a) and (b).

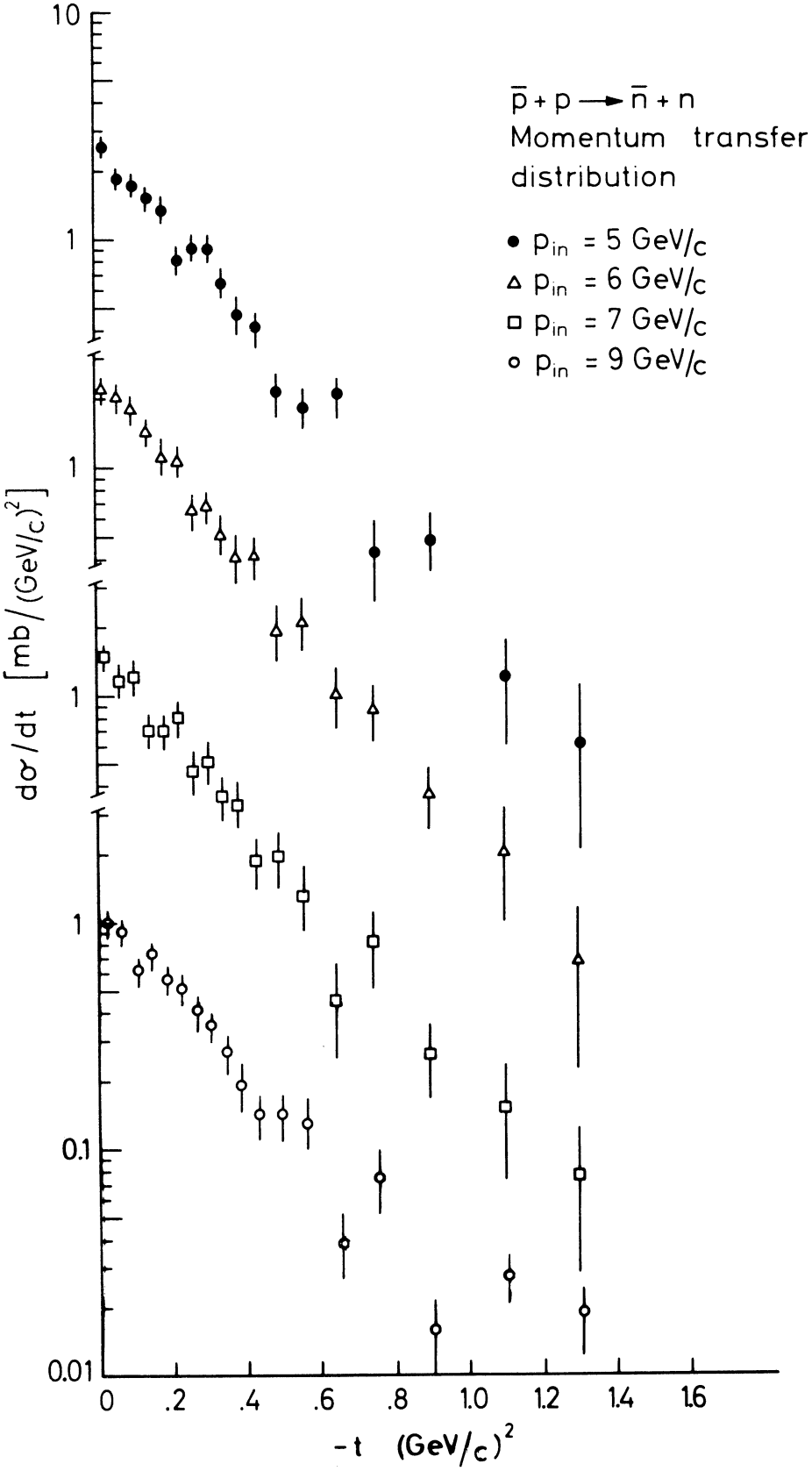

Fig. 7.5

Differential cross-section for $\bar{p}p \to \bar{n}n$ in the range $5 \leq p_{lab} \leq 9$ GeV/c taken from P. Astbury et al. [Physics Letters 22, 537, and 23, 160 (1966)].

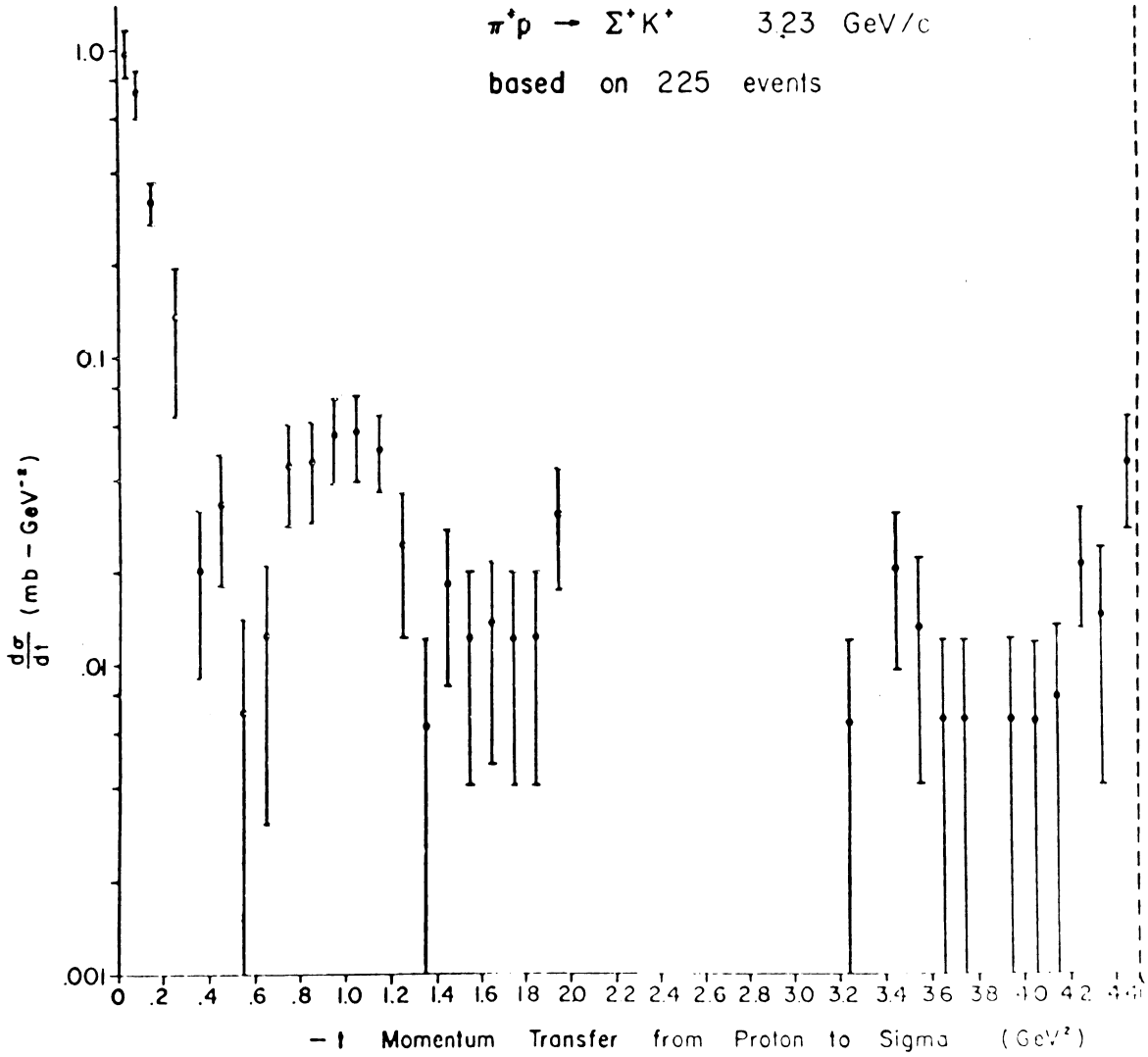

Fig. 7.6

Differential cross-section for $\pi^+p \rightarrow K^+\Sigma^+$ at 3.23 GeV/c as measured by R.R. Kofler et al., taken from Van Hove's 1966 Berkeley Report (see caption to Fig. 6.10).

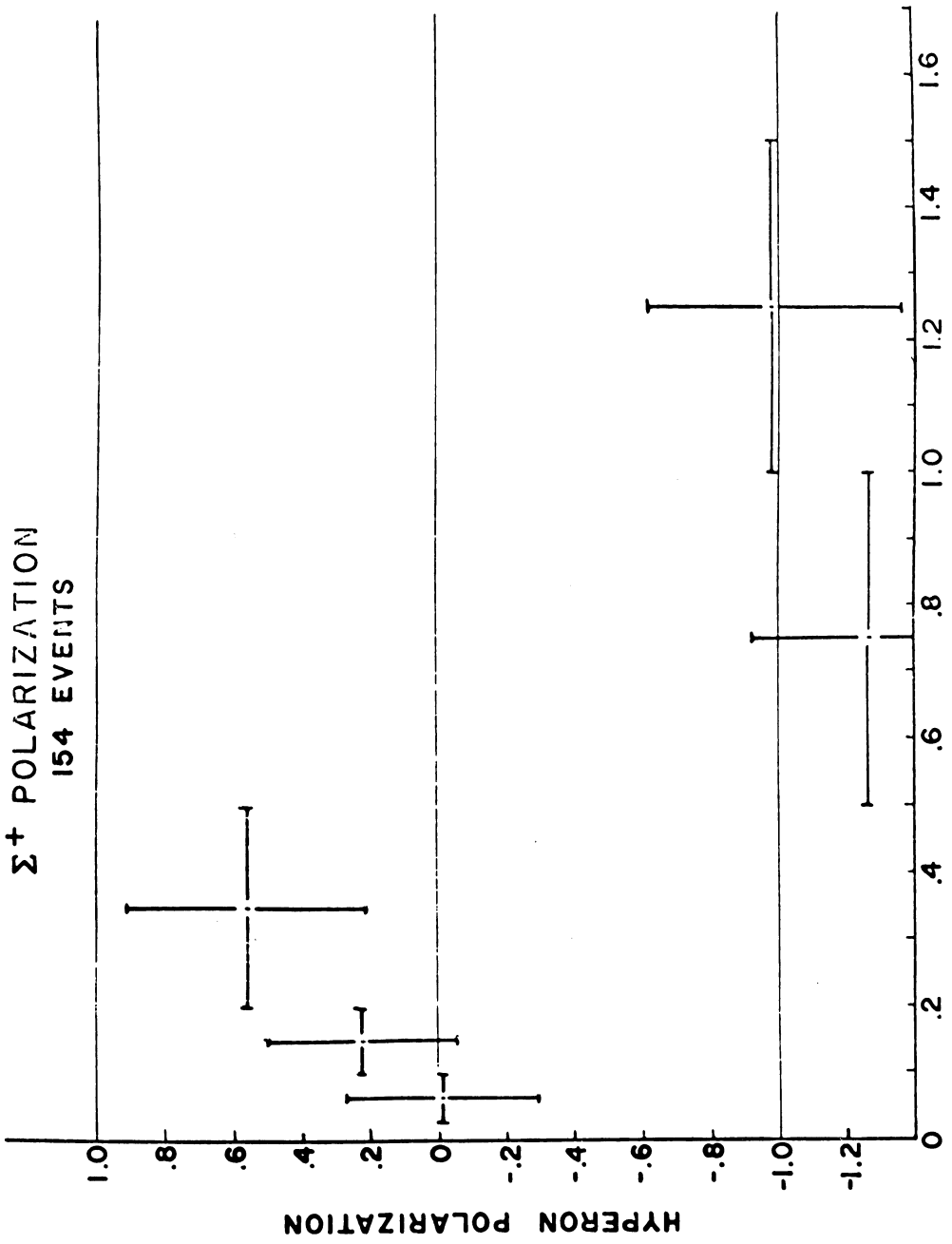

Fig. 7.7

The polarization of Σ^+ in $\pi^+ p \to K^+\Sigma^+$ at 3.23 GeV/c (see caption to Fig. 7.6 for reference).

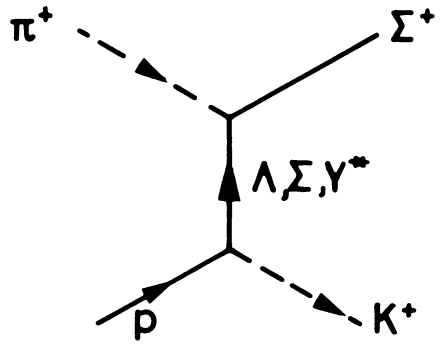

Fig. 7.8

Feynman diagram with baryon exchange that contributes to a backward peak in the reaction $\pi^+p \to K^+\Sigma^+$.

We note in passing that the same mechanism, baryon exchange, could be invoked to explain the backward peaks in $\pi^{\pm}p$ elastic scattering. In particular, both the nucleon and the N*(1236) could be exchanged in π^+p backward scattering, while the π^-p case need a particle carrying two units of charge, thus requiring $N^*_{I=3/2}$-exchange. This could be the origin of the experimentally observed difference between the two reactions.

It should be noted, as pointed out to me by Dr. P. Carlsson, that the baryon exchange model is not the only possible explanation of a backward peak, since such a structure may also result from resonance formation and decay in the direct channel.

An interesting reaction from the point of view of the Regge pole model is the process $\pi^-p \to \eta n$. Experimentally, it is investigated by the same techniques as the pion-nucleon charge exchange scattering, involving the detection of the decay of the final meson into two gamma-quanta. The experimental cross-section as given in Fig. 7.9 is also rather similar to the charge exchange one. Note in particular the flattening off for very small momentum transfers. In a OPE model, the only known meson that could be invoked to explain the forward peaking is the A_2-meson.

To illustrate the result on quasi-two-body production, we reproduce in Fig. 7.10 some results obtained in π^+p collision at 8 GeV/c. For comparison, the elastic cross-section is also given in the figure. The

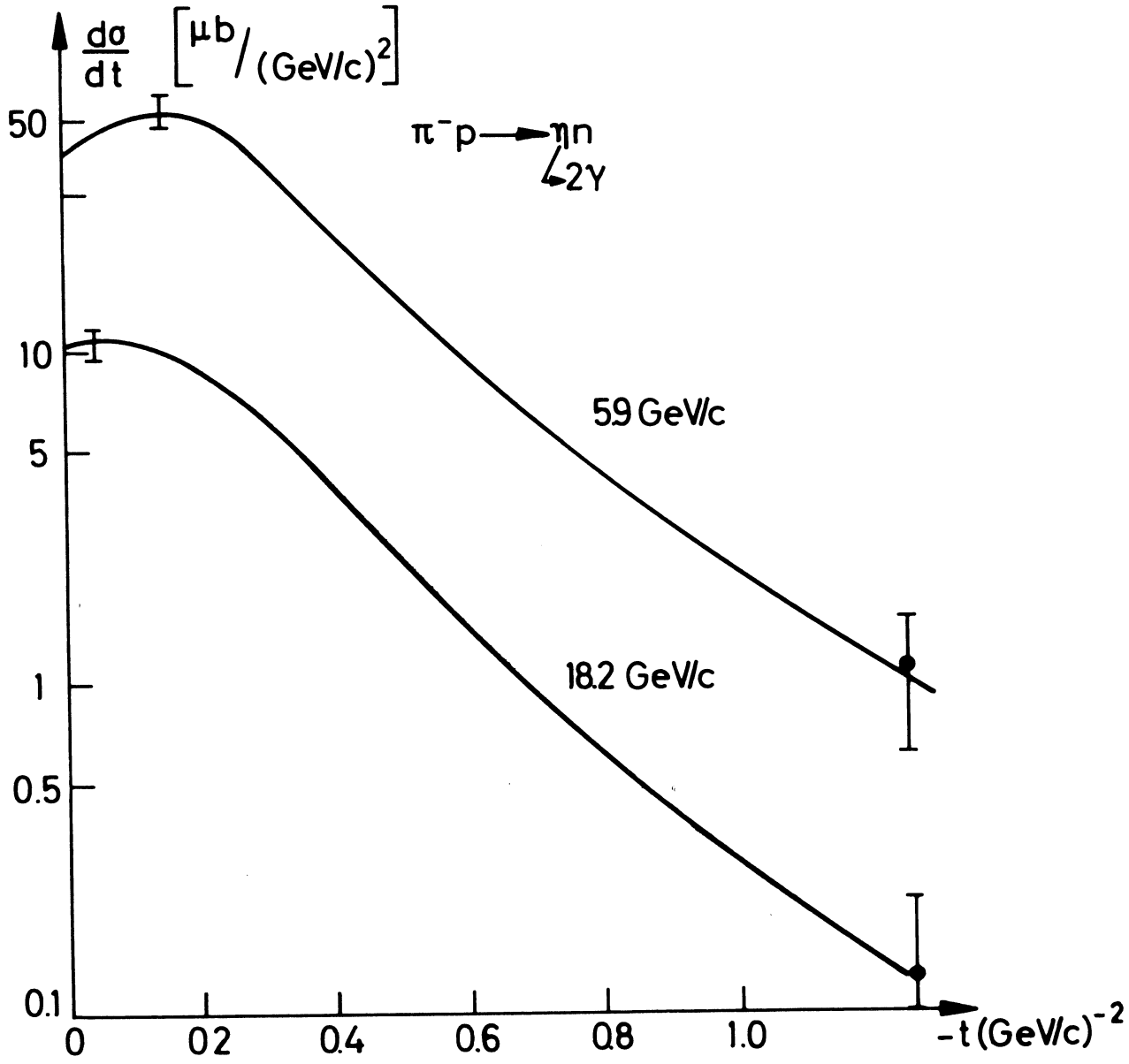

Fig. 7.9

Differential cross-section for $\pi^- p \to \eta n$, $\eta \to 2\gamma$, at 5.9 and 18.2 GeV/c from O. Guisan et al. [Physics Letters 18, 200 (1965)]. Curves are freehand fits to the data, and error bars only indicate typical statistical errors.

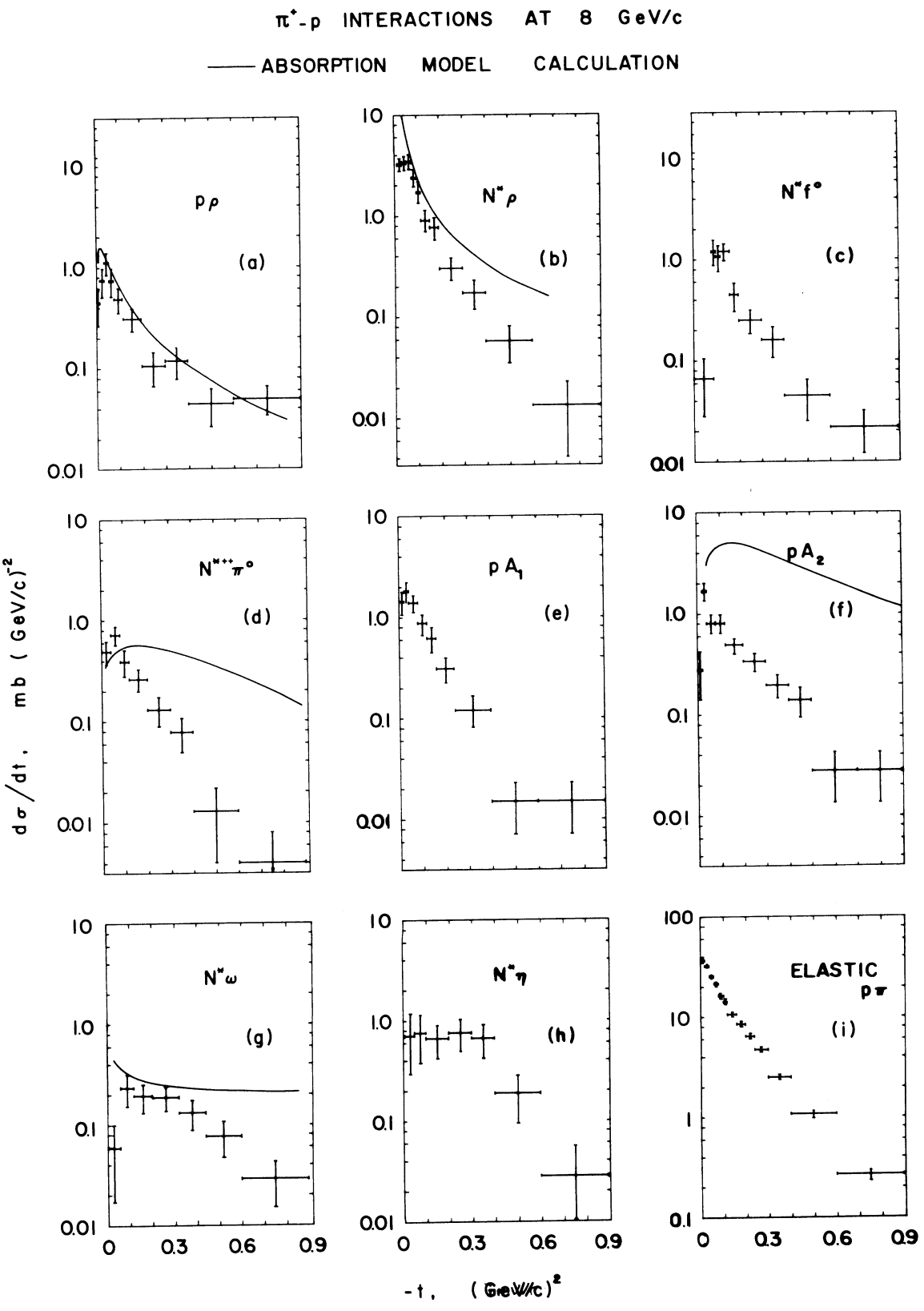

Fig. 7.10

Differential cross-sections for various (quasi-)two-body reactions in $\pi^+ p$ interactions at 8 GeV/c from D.R.O. Morrison's invited paper at the Conference on High Energy Two Body Reactions, Stony Brook, April 1966 [preprint CERN/TC/Physics 66-20, 10.8.1966].

solid lines represent the predictions of the OPE model (with absorptive corrections). The general experimental trend in all reactions are the same: a more or less pronounced forward peak. This property is shared by almost all quasi-two-body reactions.

In fact, the experimental results on inelastic reactions reviewed in this chapter may be summarized in two main empirical rules:

i) The differential cross-section for a two-body (or quasi-two-body) reaction has an approximately exponential forward peak as soon as there exists a meson which can be exchanged in the reaction, but not otherwise. A similar statement is true concerning a backward peak, where baryon exchange is needed in meson-baryon processes, meson exchange in baryon-baryon processes.

ii) Most cross-sections for inelastic two-body (or quasi-two-body) processes decrease as the energy increases. The decrease can be parametrized as p_{lab}^{-n}, where the exponent n varies from reaction to reaction, ranging between ~ 1 and ~ 4.

A few final comments on these points. We have seen many examples of forward peaks in reactions where some meson may be exchanged. Are there any processes in which this is not allowed? Consider for example the reaction $K^- p \to K^+ \Xi^-$. Since the incident K^-, of strangeness $S = -1$, is transformed into an outgoing K^+, of strangeness $S = +1$, exchange of an $S = 2$-meson is required. Such an object has not been discovered so far. Thus, if the rule (i) is correct, one expects no forward peak in this reaction, and experiments show indeed no such peak. In fact, I know of no exception to the rule (i).

All inelastic cross-sections we have discussed so far have shown a decrease with energy. But there are other ones that seem to have roughly constant cross-sections over a fairly large energy interval. The most important examples are the reactions $pp \to pN^*_{1/2}$, where $N^*_{1/2}$ is one of the isospin-$\frac{1}{2}$ nucleon resonances of mass and spin-parity 1410 MeV ($\frac{1}{2}^+$), 1520 MeV ($\frac{3}{2}^-$) and 1688 MeV ($\frac{5}{2}^+$). This process has been measured by a missing mass technique up to energies corresponding to $p_{lab} = 30$ GeV/c. The results for the total cross-sections are shown in Fig. 7.11, together with the data for production of $N^*_{3/2}(1236)$ in the same reaction. The

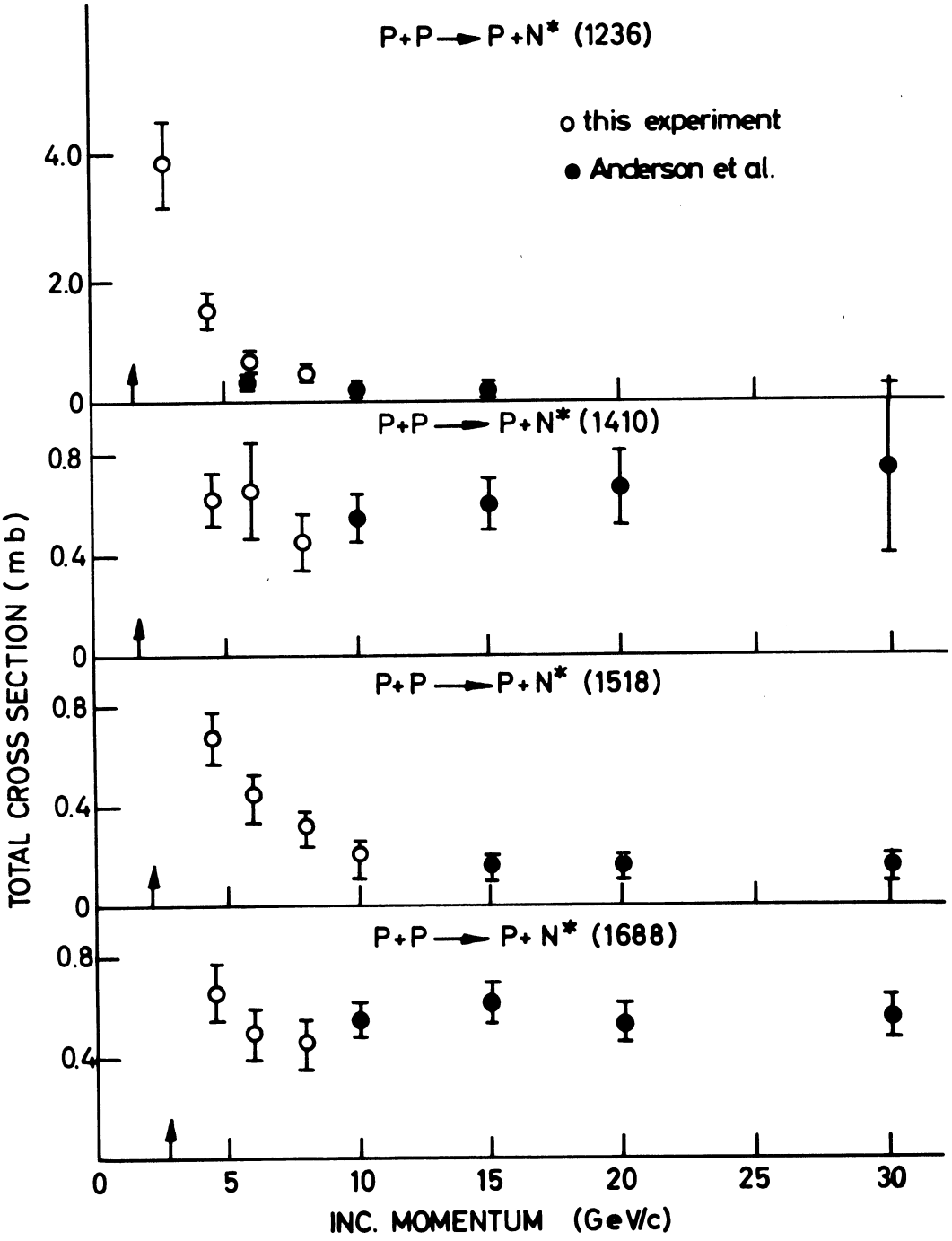

Fig. 7.11

The total cross-sections for isobar production in the process pp → pN* as functions of p_{lab}, taken from I.M. Blair et al. [Phys.Rev.Letters 17, 789 (1966)].

latter shows a decreasing cross-section and is in fact below the detection limit at $p_{lab} \sim 15$ GeV/c. There might be a few meson-induced inelastic reactions also having roughly energy-independent total cross-sections, but the energy intervals in which they have been investigated are not wide enough to allow a firm conclusion.

A detailed treatment of inelastic two-body processes, in particular illustrating the two rules (i)-(ii), may be found in the report by D.R.O. Morrison at the Conference on High Energy Two Body Reactions, Stony Brook, April 1966 (see caption to Fig. 7.10).

P A R T III

(Chapters 8-10)

COMPLEX ANGULAR MOMENTUM IN POTENTIAL THEORY
HADRON REGGE TRAJECTORIES

CHAPTER 8 - BRIEF DESCRIPTION AND HISTORICAL SURVEY

Let me first in rather general terms try to give a description of what the Regge pole model deals with. It appears in two different, although closely connected contexts.

i) By means of a "Regge trajectory", it correlates particles (bound states and resonances) of the same internal quantum numbers (baryon number, isospin, G-parity, strangeness, etc.) and of the same parity, but with spins that differ in units of two.

ii) High energy (quasi-)two-body reactions are predicted to be dominated by the exchange of a few of these trajectories.

Let us illustrate the first point by some examples. Consider the nucleon N(938) and its isobar $N^*(1688)$ of isospin $\frac{1}{2}$ and spin-parity $\frac{5}{2}^+$, and plot them in the diagram of Fig. 8.1 with the spin, J, considered as a function of the energy squared, E^2; such a picture is known as a Chew-Frautschi diagram.

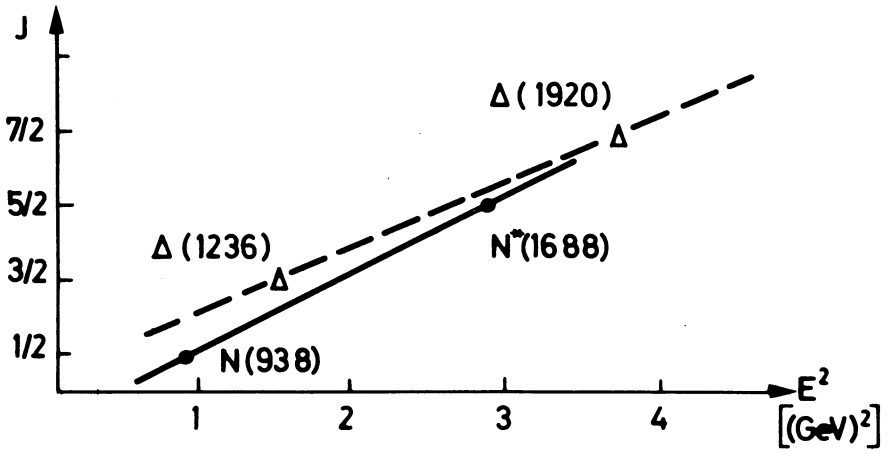

Fig. 8.1

The Chew-Frautschi diagram for the N- and Δ-trajectories.

The Regge pole model then states that there exists a (complex) function, $\alpha_N(E)$, such that

$$\text{Re } \alpha_N(E = 938 \text{ MeV}) = \tfrac{1}{2} , \tag{8.1}$$

$$\text{Re } \alpha_N(E = 1688 \text{ MeV}) = \tfrac{5}{2} . \tag{8.2}$$

This function is called a "Regge trajectory"; in the Chew-Frautschi plot it links the two, a priori separate points. It can, in fact, be looked upon as a function that interpolates the angular momentum between the physical values. Usually, the dependence of the Regge trajectory on the energy is assumed to be

$$\text{Re } \alpha_N(E) = a_N + b_N E^2 , \tag{8.3}$$

which means a straight line in the Chew-Frautschi diagram. If this is true, one has

$$\frac{d}{d(E^2)} \text{Re } \alpha_N(E) = b_N = \frac{\tfrac{5}{2} - \tfrac{1}{2}}{(1688)^2 - (938)^2} (\text{MeV})^{-2} \approx 1.0\,(\text{GeV})^{-2} . \tag{8.4}$$

Take another example, the isospin $\tfrac{3}{2}$ resonances $N^*_{3/2}(1236)$ or, as it is often called, the $\Delta(1236)$, and the $\Delta(1920)$, of spin-parity $\tfrac{3}{2}^+$ and $\tfrac{7}{2}^+$, respectively. They are also marked in Fig. 8.1, but cannot be connected by the nucleon trajectory, since the isospins are different. By the Regge hypothesis, they are instead connected by another trajectory, $\alpha_\Delta(E)$, such that

$$\text{Re } \alpha_\Delta(E = 1236 \text{ MeV}) = \tfrac{3}{2} , \tag{8.5}$$

$$\text{Re } \alpha_\Delta(E = 1920 \text{ MeV}) = \tfrac{7}{2} . \tag{8.6}$$

If one again assumes a linear trajectory in the Chew-Frautschi plot, one obtains

$$\frac{d}{d(E^2)} \alpha_\Delta(E) \approx 0.9\,(\text{GeV})^{-2} , \tag{8.7}$$

which is roughly the same slope as for α_N.

Similar considerations also apply to, for example, the mesons, among them the ρ-meson, although it is less certain here whether there are at least two particles on each of the trajectories, simply because the spins and parities of the higher boson resonances are not well established.

In summary, the first claim of the Regge pole model is the existence of trajectories $\alpha(E)$ such that whenever E equals the mass of a particle on the trajectory, Re $\alpha(E)$ equals the spin of that particle. Several particles with identical internal quantum numbers and parity may lie on the same trajectory, provided their spins differ by two units. Experimentally, the slopes of the trajectories are about $1\,(\mathrm{GeV})^{-2}$.

To illustrate the second application of the Regge pole model, consider the reaction $\pi^- p \to \pi^0 n$. The model claims that the object being exchanged in this process is not really the ρ-meson as we discussed previously, but instead something which is related to the ρ-meson trajectory α_ρ, for which

$$\mathrm{Re}\ \alpha_\rho(E = 760\ \mathrm{MeV}) = 1\ . \qquad (8.8)$$

In particular, the energy-dependence of the cross-section $d\sigma_{c.e.}/dt$ is immediately given by this trajectory.

In this way, the Regge pole model constitutes a connection between low-energy phenomena (resonances) and high-energy ones (differential cross-sections, etc., at large energies). It requires detailed considerations to really understand the two points, and also the connection between them. Before we seriously dive into the Regge pool, let us however give a few historical facts.

The Regge pole model originates in potential theory. In fact, the whole story was started by Regge and his collaborators in the late 1950's when they asked the question whether, and under what circumstances one could consider the partial wave amplitude $f(\ell, E)$ not only as an analytic function of the energy E but also as an analytic function of the angular momentum ℓ. Regge remained all the time within the context of potential theory and could there strictly prove what he did. It was soon (around 1961) realized by other physicists (Chew, Frautschi, Gribov, Froissart, just to mention a few of them) that the Regge ideas would have important consequences for the interaction between elementary particles. However,

since a complete theory for hadronic interaction is lacking, one must here be content with plausibility arguments and guided guesses. These are, however, based, on what is strictly proved in potential theory, and on those general requirements which the strong interaction fulfils. In short, while the Regge approach can be strictly proved in potential theory, it remains a suggestion, or a model, for elementary particle interactions. "The Schrödinger equation is the theorist's laboratory."

The Regge pole model first drew maximum attention around 1962 (see, for example, the Proceedings of the 1962 Int. Conf. on High-Energy Physics held at CERN). This was primarily due to the fact that the most simple-minded approach, viz., one Regge trajectory exchange, predicted the shrinkage of the pp diffraction peak, in agreement with experiment. Soon, however, experiments revealed a constant forward peak in $\pi^{\pm}p$ elastic scattering, and even an expanding diffraction peak for $\bar{p}p$ interaction, in definite disagreement with the assumption of one trajectory dominance. Due also to other difficulties (occurence of Regge cuts, contributions from several Regge trajectories), the Regge pole model lost most of its flavour. This can be followed from the Conference proceedings. At the 1963 Sienna Conference, Regge himself gave a pessimistic outlook. At the 1964 Dubna Conference the Regge pole model was indeed discussed at one session, but with emphasis on rather subtle theoretical problems. And at the 1965 Oxford Conference, the word Regge pole was hardly mentioned at all, although it was about this time that the model started to become "à la mode" again. Finally, at the 1966 Berkeley Conference, the Regge pole approach was once more taken seriously.

Why did an almost dead model revive like that? I think the answer to this question is two-fold. First, the ingenuity of the experimenters provided the theorists with a large amount of accurate high-energy data, in particular on reactions which are crucial to the model, like pion-nucleon charge-exchange scattering. Among other things, the numerous experimental results allowed the theorists to use expressions containing several unknown parameters which could be fitted to the data. In fact, it turned out that one of the virtues of the Regge pole model was its elasticity, in the sense that the really clean-cut predictions of the model at present accelerator energies were rather few. Instead, it afforded a theoretical framework, convenient for parametrization of the scattering amplitude and thus for a phenomenological discussion of the data.

The second point contributing to the Regge pole boom was the fact that most other approaches (optical model, peripheral model, etc.) gave predictions which were in disagreement with the data, and thus had to be ruled out.

In other words, the present interest in the Regge pole model is mostly due to its success on a phenomenological level, while it is still rather incomplete from a strictly theoretical point of view. Furthermore, it has some internal anomalies, like the seemingly inevitable angular momentum cuts (see Chapter 16). We shall in the following try to indicate both the phenomenological successes of the model and its theoretical weakness.

CHAPTER 9 - REGGE POLES IN POTENTIAL SCATTERING

We shall always consider a (real) Yukawa potential

$$V_Y(r) = g \frac{1}{r} \exp(-\nu r) , \tag{9.1}$$

or, more generally, a superposition of Yukawa potentials

$$V(r) = \int_{\omega>0}^{\infty} d\nu\, g(\nu) \frac{1}{r} \exp(-\nu r) . \tag{9.2}$$

We adopt the convention that whenever we talk of a potential we mean such a superposition. There are both mathematical and physical reasons for considering this particular type. Mathematically, it makes possible the proofs of statements (i)-(iv) below in the simplest way. Physically, it is presumably the kind of potential which best reproduces elementary-particle interactions, since exchange of a particle having mass ν gives the same form of the scattering amplitude as the Yukawa potential (9.1) in the Born approximation.

Let us recall our discussion of the partial wave scattering amplitude $f(\ell, E)$ as an analytic function of the energy E, given at the very end of Chapter 4. Since the radial Schrödinger equation (4.68), from which $f(\ell, E)$ is to be determined, contains E in a "simple" way one may investigate

solutions to the equation also for complex values of E. Such considerations led to the conclusion that $f(\ell, E)$ is an analytic function of E, except for cuts and possible poles which may correspond to bound states and resonances. The idea of Regge was now to observe that the radial Schrödinger equation also depends in a simple way on the angular momentum ℓ. One could thus try to explore its solutions for values of ℓ other than non-negative integer ones, in fact for arbitrary complex ℓ-values. This is at first sight a purely mathematical game, since physical (orbital) angular momentum occurs in quantum mechanics only as an integer. It will turn out, though, that the mathematical investigation also gives a great deal of physical insight.

It will take us much too far to follow the details of Regge's discussion. We only state those results which are most important to our subsequent applications (we assume E real):

i) The radial Schrödinger equation (4.68) has solutions for arbitrary complex ℓ, provided Re $\ell \geq -\frac{1}{2}$. In particular, this means that one may define a partial wave amplitude $f(\ell, E)$ for complex ℓ-values.

ii) $f(\ell, E)$ is a meromorphic function of ℓ (analytic except for poles) for Re $\ell > -\frac{1}{2}$, but is continuous for Re $\ell = -\frac{1}{2}$.

iii) The poles of $f(\ell, E)$ are called Regge poles and occur:
- on the real ℓ-axis if E is below the scattering threshold E_{th}, viz., $E < 0$ in the non-relativistic case; the residue at the pole is real here;
- in the upper half plane, Im $\ell > 0$, if E is above E_{th} ($E > 0$ in the non-relativistic case).

Moreover, the number of poles to the right of Re $\ell = -\frac{1}{2}$ is finite.

iv) As $|\ell| \to \infty$, $|f(\ell, E)|$ is suitably well-behaved; this property will be needed only in connection with Eq. (9.18) below.

Let us add a few comments to these results. First, since it is possible to define $f(\ell, E)$ for arbitrary complex ℓ, it means in particular that $f(\ell, E)$ may be defined for all real ℓ-values greater than $-\frac{1}{2}$. In other words, one is able to interpolate the partial wave amplitude between integer ℓ-values, where it was first defined. This is illustrated in Fig. 9.1. Such a result, although only a special case of the continuation to arbitrary ℓ, is of importance for the impact parameter representation as we discussed it in Chapter 4, in particular for the transition from Eq. (4.46) to Eq. (4.47).

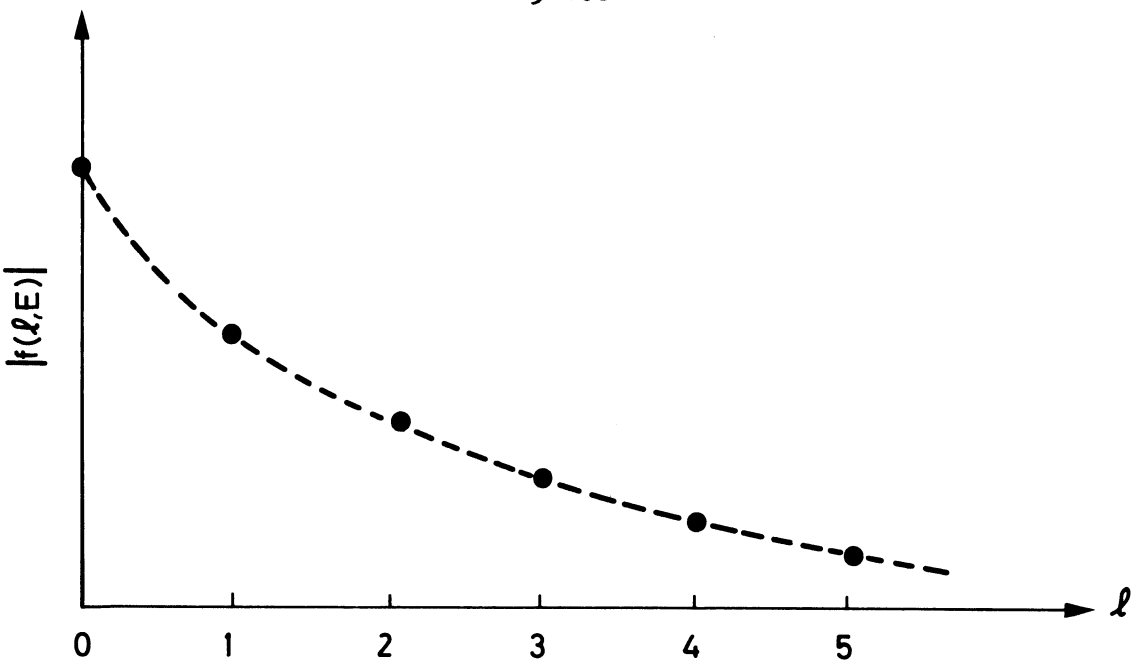

Fig. 9.1

An illustration of the interpolation of the partial wave amplitudes between integer ℓ-values; since $f(\ell, E)$ is in general complex, we have plotted $|f(\ell, E)|$.

The analyticity of $f(\ell, E)$ as function of ℓ is illustrated in Fig. 9.2. In the complex ℓ-plane we have also marked the position of one Regge pole and how the pole position moves as the energy E varies. Detailed considerations show that the pole, which for $E \ll E_{th}$ lies to the left of the line Re $\ell = -\frac{1}{2}$, could for some ℓ-value cross this line and enter into the meromorphic domain; whether it does so or not depends among other things on the strength of the potential. If E is still below the scattering threshold E_{th}, the pole moves along the real axis as indicated in the figure. As E passes E_{th}, the position of the pole acquires a positive imaginary part, and the trajectory moves off into the upper half-plane. As E increases to $+\infty$, further considerations show that the trajectory turns back and eventually returns to the left of Re $\ell = -\frac{1}{2}$.

Let us now more carefully define the commonly used concepts, already introduced above:

i) A <u>Regge pole</u> is a pole of the partial wave amplitude $f(\ell, E)$ in the complex ℓ-plane. If it occurs at $\ell = \alpha$, and if it is a single pole (pole of order one), then in the neighbourhood of $\ell = \alpha$ one has

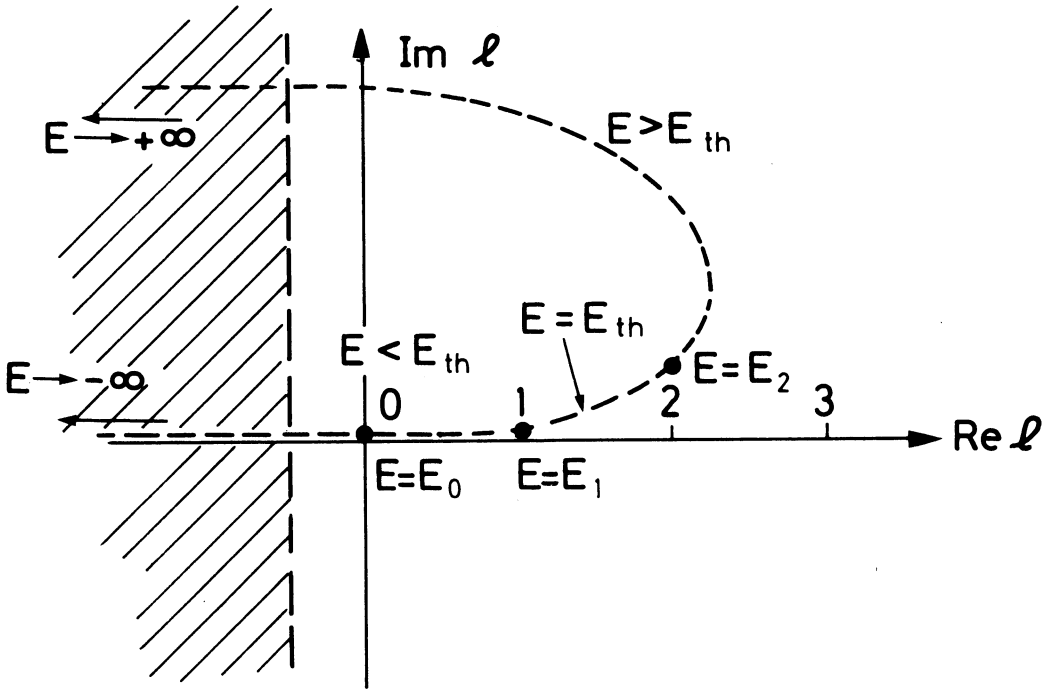

Fig. 9.2

An example of the motion of one Regge pole in the complex angular momentum plane as the energy E varies from numerically large, negative values through the scattering threshold E_{th} to large positive values.

$$f(\ell, E) = \frac{R}{\ell - \alpha} + \quad \text{(terms, finite at } \ell = \alpha) \ . \tag{9.3}$$

Since $f(\ell, E)$ also depends on E, so do in general the pole position $\alpha = \alpha(E)$ and the residue $R = R(E)$.

ii) As E varies, the pole moves in the complex ℓ-plane. Therefore, $\alpha = \alpha(E)$ is called the trajectory of the pole, or the Regge trajectory.

So far, it is pure mathematics. Physics is still confined to integer, non-negative ℓ-values. We shall see, however, that the concept of a Regge pole has definite physical implications. In a rough way this may be done as follows.

Consider the pole position α as function of the energy E. Suppose there is an energy E_n such that $\alpha(E_n)$ is a non-negative integer n

$$\alpha(E_n) = n \ . \tag{9.4}$$

Obviously, this requires E_n to be less than E_{th}, since otherwise α would have an imaginary part. For energies near to $E = E_n$, a Taylor series expansion gives

$$\alpha(E) = \alpha(E_n) + (E - E_n)\alpha'(E_n) + \ldots \approx n + (E - E_n)\alpha'(E_n) \ , \qquad (9.5)$$

so that for ℓ near to n and E near to E_n the amplitude reads

$$f(\ell, E) \approx \frac{R}{\ell - n - (E - E_n)\alpha'(E_n)} = \frac{R}{\alpha'(E_n)} \left[\frac{\ell - n}{\alpha'(E_n)} - (E - E_n) \right]^{-1} . \qquad (9.6)$$

But this means that $f(\ell = n, E)$ has a pole <u>as function of the energy</u> at $E = E_n$, which corresponds to a bound state at that energy of angular momentum $\ell = n$. Summarizing, if the Regge trajectory passes a non-negative integer n for an energy $E_n < E_{th}$, then it implies a bound state of energy E_n and angular momentum n. Since one and the same trajectory may pass through several integers, it may give rise to several bound states; for example, the trajectory of Fig. 9.2 gives bound states with n = 0 and n = 1.

What happens for $E > E_{th}$? We can of course not get a bound state. But how about a resonance? To see how it may come about, let us suppose that there is an energy $E_m > E_{th}$ such that

$$\text{Re } \alpha(E_m) = m \ , \qquad (9.7)$$

where m is a non-negative integer. As before, we expand

$$\alpha(E) = \text{Re } \alpha(E) + i \ \text{Im } \alpha(E) \approx$$

$$\approx m + (E - E_m) \left[\frac{d}{dE} [\text{Re } \alpha(E)] \right]_{E=E_m} + i \ \text{Im } \alpha(E_m) \ . \qquad (9.8)$$

Here, we assumed Im (E_m) to be so small that no further terms are needed in the expansion of the imaginary part. It is convenient to introduce the notation

$$\kappa = \left[\frac{d}{dE} [\text{Re } \alpha(E)] \right]_{E=E_m} \qquad (9.9)$$

$$\tfrac{1}{2}\Gamma = \frac{1}{\kappa}\,\mathrm{Im}\;\alpha(E_m) \tag{9.10}$$

to be able to write, for E near to E_m and ℓ near to $\alpha(E_m)$

$$f(\ell, E) \approx -\frac{R}{\kappa}\left[E - E_m + i\,\tfrac{1}{2}\Gamma - \frac{\ell - m}{\kappa}\right]^{-1} . \tag{9.11}$$

Consequently, if the form (9.11) is valid also for $\ell = m$, the partial wave amplitude $f(\ell = m, E)$ has now a dependence on the energy which is characteristic for a resonance of angular momentum $\ell = m$, energy E_m and width Γ [cf. Eq. (4.61)]. Some conditions must be fulfilled, though, for this interpretation to be true. First of all Im α (E_m) must be so small that $\alpha(E_m) = m + i\ \mathrm{Im}\ \alpha(E_m)$ does not differ too much from m in order to allow the above-mentioned extrapolation to the physical ℓ-value. Second, Γ must be positive, which requires κ to be greater than zero since Im $\alpha(E_m)$ is positive. In order that a Regge trajectory should give a resonance, it must thus <u>increase</u> through the value Re α = m as the energy increases through E_m. For example, the trajectory of Fig. 9.2 gives a d-wave resonance at $E = E_2$, but none as the trajectory bends over and <u>decreases</u> through the values Re α = 2, 1 and 0.

In summary, a Regge trajectory $\alpha(E)$, the real part of which passes through a non-negative integer n at an energy $E = E_n$, gives rise to:

i) a bound state if $E_n < E_{th}$,
ii) a resonance if $E_n > E_{th}$, if Im $\alpha(E_n)$ is small, and if Re $\alpha(E)$ increases through its value at $E = E_n$.

In this manner, one and the same trajectory not only connects bound states of different angular momenta to each other, but also possible resonances to each other and to the bound states. The trajectory of Fig. 9.2, for example, represents two bound states and one resonance. In this sense one may say that the Regge trajectory interpolates the angular momentum between integers.

Instead of picturing the Regge trajectory in the complex ℓ-plane with the energy E as a parameter, it is very often convenient to concentrate on Re $\alpha(E)$ and plot it as a function of E. This gives the diagram in

Fig. 9.3, which represents the same trajectory as that of Fig. 9.2. Essentially, this is the Chew-Frautschi plot already mentioned in Chapter 8. Two things must be done first, though. Instead of E one should take E^2 as a variable. Moreover, one should extend the Regge ideas from the safe realms of potential theory to the more exciting but less certain context of elementary-particle interactions. This will be done in the next chapter.

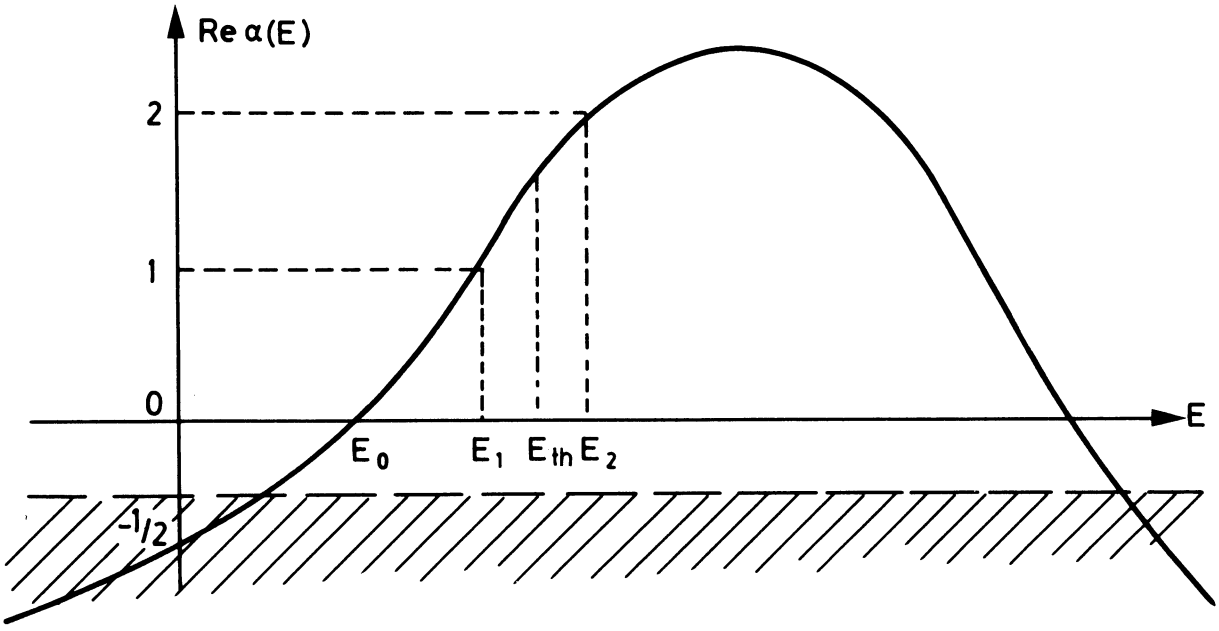

Fig. 9.3

The Regge trajectory of Fig. 9.2 now with Re $\alpha(E)$ plotted as a function of E.

Before that, however, we shall return for a while to mathematics and explore the consequences of the Regge ideas on the partial wave sum

$$k F(\cos\Theta, E) = \sum_{\ell=0}^{\infty} (2\ell + 1) f(\ell, E) P_\ell(\cos\Theta) \ . \qquad (9.12)$$

The aim is to investigate what the analycity properties of $f(\ell, E)$ as a function of ℓ, and in particular the Regge poles, means for the total amplitude $F(\cos\Theta, E)$. For that purpose, we apply a trick known as the Sommerfeld-Watson transform. Its starting-point is to consider the partial wave expansion as the sum of residues of an analytic function, and then to use the Cauchy integral theorem in order to transform the sum into an integral. Finally, by deforming the integration contour, one is able to exhibit the contributions from the Regge poles explicitly.

To this end, consider the function

$$g(\ell) = \frac{\pi(2\ell+1)f(\ell,E)P_\ell(-\cos\Theta)}{\sin\pi\ell} \,. \tag{9.13}$$

From the treatment above we know that $f(\ell, E)$ is an analytic function of ℓ, except for Regge poles. As is indicated in Appendix 3, $P_\ell(-\cos\Theta)$ is also an (entire) analytic function of ℓ, and so is $\sin\pi\ell$. Consequently, $g(\ell)$ is analytic for Re $\ell > -\frac{1}{2}$, except for poles. These are:

i) the Regge poles;

ii) the poles at $\ell = n$, $n = 0, 1, 2, \ldots$, arising from the vanishing of $\sin\pi\ell$. The residue of $g(\ell)$ at $\ell = n$ is obtained by noting that, for ℓ near to n, one has

$$\sin\pi\ell = \sin\pi n + (\ell - n)\left[\frac{d}{d\ell}\sin\pi\ell\right]_{\ell=n} + \ldots \approx$$

$$\approx (\ell - n)\pi\cos\pi n = (\ell - n)\pi(-)^n \,. \tag{9.14}$$

Remembering that $P_n(-x) = (-)^n P_n(x)$ for integer n, we thus get

$$\text{Res } g(\ell = n) = (2n+1)f(n,E)P_n(\cos\Theta) \,, \tag{9.15}$$

i.e., exactly the term in the sum (9.12). This is one reason why one considers $g(\ell)$, Eq. (9.13).

Now, let C be a path that encircles the zeros of sin $\pi\ell$ but not the Regge poles. For instance, the curve C of Fig. 9.4 will do if we assume its far right ends to be closed at infinity. Cauchy's integral theorem (cf. Appendix 1) then implies

$$\frac{1}{2\pi i}\int_C g(\ell)d\ell = \sum_{n=0}^{\infty} \text{Res } g(\ell = n) = \tag{9.16}$$

$$= \sum_{n=0}^{\infty} (2n+1) f(n,E) P_n(\cos\Theta) = kF(\cos\Theta, E) .$$

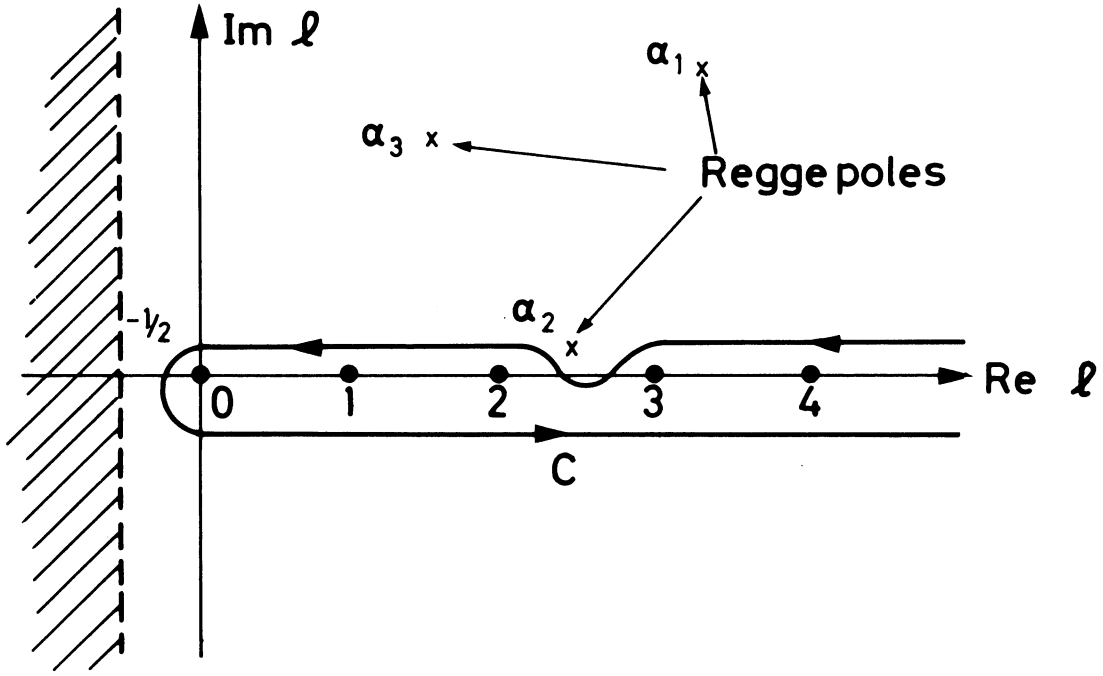

Fig. 9.4

The choice of the path C in Eq. (9.16). Three Regge poles are exhibited, the positions of which correspond to $E > E_{th}$.

Summarizing, we have derived an integral representation for the scattering amplitude $F(\cos\Theta, E)$, in which the sum over partial waves at integral angular momenta is replaced by an integral along a path C in the complex angular momentum plane.

How does this formula exhibit the Regge poles when we even avoided them in order to get Eq. (9.16)? The point here is that we may use the Cauchy theorem once more to deform the contour C and pick up the contributions from the Regge poles. To this end, consider the curve C′ of Fig. 9.5. It consists partly of the previous path C, but also of pieces of a circle in the first and fourth quandrant. The circle radius will eventually tend to infinity. Moreover, the contour C′ comprises the straight line $\mathrm{Re}\ \ell = -\frac{1}{2} + \epsilon$, $\epsilon > 0$ small; ϵ is there only to assure that the path of integration stays within the domain of analyticity for $f(\ell, E)$ and, as a consequence, for $g(\ell)$. Applying the Cauchy theorem to the contour integral of $g(\ell)$ along this new path C′ gives

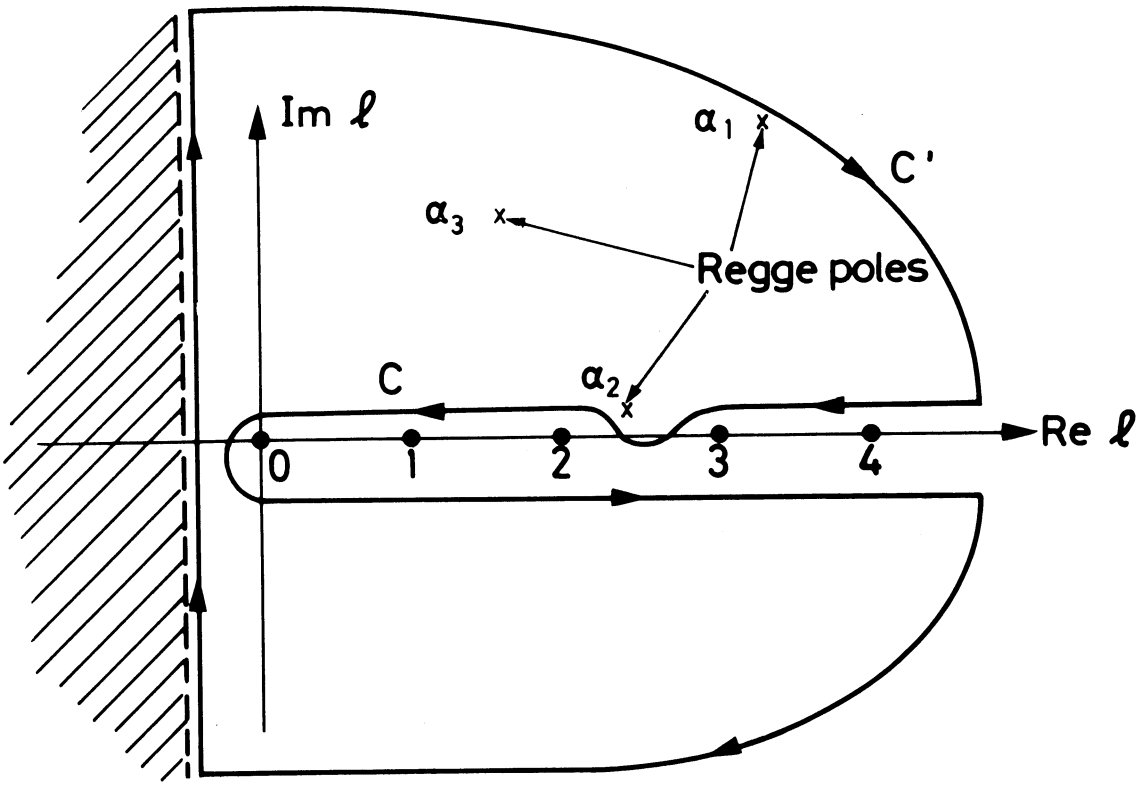

Fig. 9.5

The path C′ of integration used in deforming the contour C to pick up the contributions from the Regge poles.

$$\frac{1}{2\pi i}\oint_{C'} g(\ell)\,d\ell = -\sum_{i} \text{Res } g(\ell = \alpha_i)\ , \tag{9.17}$$

where the sum runs over all Regge poles inside C′. Note the minus sign in front of the sum, since C′ is encircled clockwise, i.e., in the negative direction.

On the other hand, we have in a self-evident notation

$$\oint_{C'} g(\ell)\,d\ell = \left[\int_{C} + \int + \int + \int\right] g(\ell)\,d\ell\ . \tag{9.18}$$

Now, using the property (iv) on page 3-107 above, one is able to prove that the integrals along the circular pieces of C′ vanish as the radius of the circle tends to infinity. For this to be true, it is essential that $g(\ell)$ of Eq. (9.13) is defined with the factor $\sin \pi\ell$ in the denominator. For instance, a factor $\tan \pi\ell$ will not do, although it could give the result (9.15). I am indebted to Dr. H. Högaasen for this remark. We shall not carry through the proof but merely take the vanishing for granted. Introducing the "background integral" from the definition

$$BI(\cos\Theta, E) = \frac{i}{2k} \int_{\text{Re } \ell = -\frac{1}{2}+\epsilon} d\ell\ \frac{(2\ell+1)f(\ell, E)P_\ell(-\cos\Theta)}{\sin \pi\ell} \tag{9.19}$$

we obtain, by combining Eqs. (9.16) and (9.18),

$$\begin{aligned} kF(\cos\Theta, E) &= \frac{1}{2\pi i}\int_{C} g(\ell)\,d\ell = \frac{1}{2\pi i}\oint_{C'} g(\ell)\,d\ell - \frac{1}{2\pi i}\int g(\ell)\,d\ell = \\ &= -\sum_{i} \text{Res } g(\ell = \alpha_i) + k\,BI(\cos\Theta, E)\ . \end{aligned} \tag{9.20}$$

This constitutes a new representation of the scattering amplitude as a sum over the Regge poles to the right of Re $\ell = -\frac{1}{2}$, and a background integral. To exhibit more clearly the Regge pole sum, we calculate the residue of $g(\ell)$ at $\ell = \alpha_i$. The form for $f(\ell, E)$ is given by Eq. (9.3). Since all other factors in $g(\ell)$ are finite at $\ell = \alpha_i$, provided α_i is not an integer, we have

$$\text{Res } g(\ell = \alpha_i) = \frac{\pi[2\alpha_i(E) + 1]R_i(E)P_{\alpha_i(E)}(-\cos\Theta)}{\sin \pi\alpha_i(E)} . \qquad (9.21)$$

For economy in writing we introduce

$$\beta_i = \beta_i(E) = -\frac{\pi}{k}[2\alpha_i(E) + 1]R_i(E) . \qquad (9.22)$$

Both here and in Eq. (9.21) the energy dependence is explicitly exhibited. The final result then reads

$$F(\cos\Theta, E) = \sum_i \frac{\beta_i(E)P_{\alpha_i(E)}(-\cos\Theta)}{\sin \pi\alpha_i(E)} + BI(\cos\Theta, E) . \qquad (9.23)$$

We shall call this formula the Regge-Sommerfeld-Watson (RSW) representation of the scattering amplitude. It will be used extensively in our subsequent discussion.

What are the advantages of the RSW representation? A general answer to this question can be given as follows. The partial wave expansion is of immediate value only when a few terms in the sum contribute. As soon as many terms must be taken into account, the sum becomes difficult to handle. In that case it could happen that the RSW representation is simpler in the sense that only a few Regge poles appear in the sum and that the background integral either can be neglected or be handled in one way or another. For instance, provided the background integral may be neglected and only one Regge pole contributes, one knows explicitly the $\cos\Theta$-dependence of the scattering amplitude since $P_\alpha(-\cos\Theta)$ is a known function. Although in a different context, these considerations form the basis for the use of the RSW representation in high-energy scattering phenomenology, as we shall subsequently see.

We have now developped the necessary formalism in order to give a more stringent discussion of how a Regge pole may give bound states and resonances. Let us concentrate on the contribution to $F(\cos\Theta, E)$ from one Regge pole $\alpha(E)$

$$F(\cos\Theta, E) = \frac{\beta(E) P_{\alpha(E)}(-\cos\Theta)}{\sin \pi\alpha(E)} + \ldots . \qquad (9.24)$$

By using Eq. (A3.11) of Appendix 3, one finds a contribution to the nth partial wave from this Regge pole that reads

$$f(\ell = n, E) = \frac{k\beta(E)}{\pi[\alpha(E) + n + 1]} \frac{1}{\alpha(E) - n} + \ldots . \qquad (9.25)$$

The dots here correspond to the dots in Eq. (9.25). It shows that <u>one</u> Regge pole contributes to <u>all</u> partial waves, in general.

<u>Exercise 9.1</u>: Derive Eq. (9.25), using Eq. (A3.11).

One may now discuss, in exactly the same way as above, what happens at such an energy $E = E_n < E_{th}$ that $\alpha(E_n) = n$. The conclusion is that $f(\ell = n, E)$ has a pole <u>in energy</u> at $E = E_n$. One may also repeat the previous treatment to discuss the case when $E = E_m > E_{th}$ and $\mathrm{Re}\ \alpha(E_m) = m$. The conclusion one arrives at is that this represents a resonance provided $\mathrm{Re}\ \alpha(E)$ increases through the value m as E increases through E_m. The only difference in the present and previous treatments is that we now consider the physical partial wave amplitudes, i.e., $f(\ell, E)$ for non-negative integers $\ell = n$, while previously we considered $f(\ell, E)$ in the neighbourhood of the Regge pole, i.e., for $\ell \approx \alpha$, and extrapolated to the physical ℓ-value (in the case of a resonance).

<u>Exercise 9.2</u>: Discuss what happens for $f(\ell = n, E)$, Eq. (9.25), at an energy E_n such that $\mathrm{Re}\ \alpha(E_n) = n$ in the two cases (i) $E_n < E_{th}$, (ii) $E_n > E_{th}$. Hint: Repeat the treatment of pages 3-109 to 3-111.

CHAPTER 10 - HADRONS ON REGGE TRAJECTORIES

The ideas presented so far are well-established ones in the sense that from well-defined mathematical assumptions one arrives by logical steps at watertight conclusions. However, the results, interesting and original as indeed they are, are perhaps not terribly exciting, since we at least feel that we have a pretty good understanding of the Schrödinger equation without invoking the Regge investigations.

The really exciting things come into play if one conjectures that the Regge idea generalizes to hadronic interactions. It cannot be much more than a conjecture, since there exists no complete, firmly established dynamical framework from which logical conclusions can be drawn. However, the experimental consequences of the conjecture are certainly so interesting that from a purely phenomenological point of view much has been learned by applying the Regge pole model to hadronic interactions.

The results from the potential approach that are taken over to hadronic interactions are, essentially, the following:

i) The partial wave amplitude $f(\ell, E)$ can be defined for complex ℓ-values. It is analytic, except for a finite number of isolated Regge poles of order one, at least in the half-plane Re $\ell > -\frac{1}{2}$. Sometimes we shall need analyticity further to the left of the line Re $\ell = -\frac{1}{2}$.

ii) As $|\ell| \to \infty$, the amplitude $|f(\ell, E)|$ behaves in such a way that the contribution from the circle at infinity to the RSW transform vanishes.

These assumptions imply the RSW representation

$$F(\cos\Theta, E) = \sum_i \frac{\beta_i(E) P_{\alpha_i(E)}(-\cos\Theta)}{\sin \pi\alpha_i(E)} + BI(\cos\Theta, E) \qquad (10.1)$$

of the scattering amplitude. It follows that a Regge pole gives bound states and resonances in exactly the same way as it did in potential scattering.

When applying the Regge ideas to hadrons, it must also be kept in mind that a scattering amplitude now carries quantum numbers like baryon number, isospin, G-parity (when it applies), strangeness, etc. In other words, one

must tell which particular scattering process one considers. Consequently, each Regge trajectory also carries the same attributes. Particles can lie on the same trajectory only if they have the same set of quantum numbers except for spin.

10.1 Boson Regge trajectories

To discuss the classification of hadrons on Regge trajectories, let us first consider the simple case of $\pi\pi$-scattering in the isospin I = 1 state. Experimentally, there exists a $\pi\pi$, I = 1 resonance with $\ell = 1$, viz., the ρ-meson. The assumption is now that this particle lies on a Regge trajectory $\alpha_\rho(E)$, which then satisfies

$$\text{Re } \alpha_\rho(E = m_\rho) = 1 \ . \tag{10.2}$$

Im $\alpha_\rho(m_\rho)$ is related to the width of the ρ-meson. In a Chew-Frautschi plot i.e., a diagram like that in Fig. 9.3 but with E^2 instead of E on the abscissa, we then know one point on the ρ-trajectory (see Fig. 10.1).

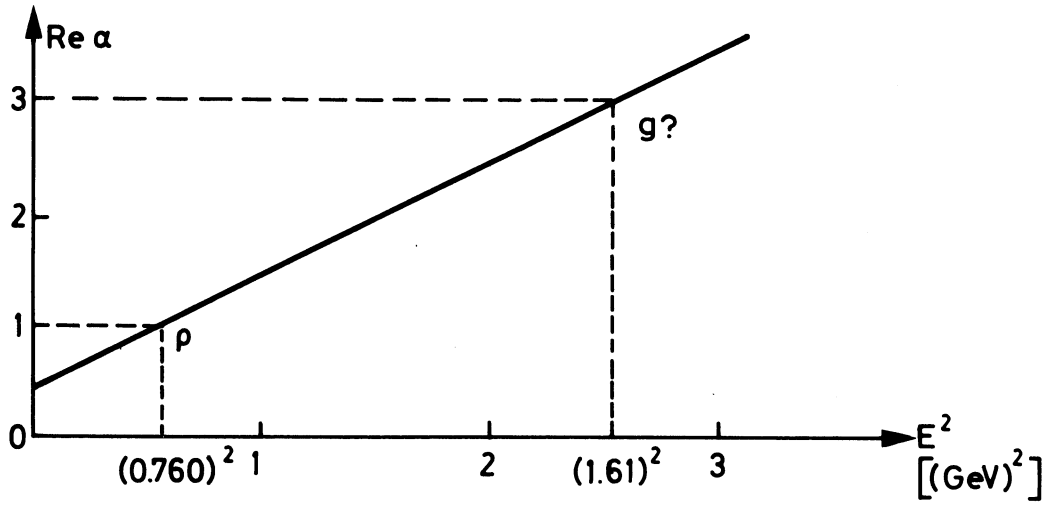

Fig. 10.1

The Chew-Frautschi diagram for the ρ-trajectory, assuming a constant slope of 1 $(\text{GeV})^{-2}$.

Are there any more particles on the ρ-trajectory? In this approach we need a $\pi\pi$, I = 1 resonance, so from Bose-Einstein statistics it cannot have spin 0 or spin 2. The first possible candidate for a "Regge recurrence" of the ρ-meson would then have spin 3. What do we know about its mass? The only thing we can be sure of is that if it exists it must be heavier than the ρ-meson; recall that a trajectory must increase through an integer in order to give a resonance. However, the following admittedly crude argument may be applied. As we saw in Chapter 8, the N- and the Δ-trajectories have slopes approximately equal to $1\,(\mathrm{GeV})^{-2}$. If the same slope applies to the ρ-trajectory, we may extract the mass m_3 of the first Regge recurrence of the ρ-meson from

$$\frac{3-1}{m_3^2 - m_\rho^2} \approx 1 \qquad (10.3)$$

to get

$$m_3^2 \approx 2 + m_\rho^2 = (1.61)^2 \ . \qquad (10.4)$$

Consequently, a straight-line ρ-trajectory with a slope of $1\,(\mathrm{GeV})^{-2}$ predicts the first Regge recurrence of the ρ-meson at $\sim$ 1.6 GeV with spin-parity 3^-. Indeed, as you know from Prof. Goldhaber's lectures, the g-meson of mass $\sim$ 1.65 GeV seems to have the right quantum numbers.

In the same simple-minded way one may discuss any scattering process. Take for example $\pi\rho$-scattering in the isospin I = 1 state, and neglect for the sake of simplicity the spin of the ρ-meson. Here, we know of at least one resonance, the A_2-meson, of spin-parity 2^+ and mass 1.310 GeV. The A_2-trajectory would then satisfy

$$\mathrm{Re}\ \alpha_{A_2}(E = m_{A_2}) = 2 \ . \qquad (10.5)$$

Which could be the other particles on that trajectory? One might expect mesons with spins 1 and 3, since Bose-Einstein statistics do not apply for non-identical particles. However, there is now another argument which is invoked in order to force the first Regge recurrence of the A_2-meson to have spin 4 [spin 0 will be excluded; see Eq. (10.13) below]. This is the concept of signature, intimately linked to the existence of exchange forces. It requires a small detour back to the mathematics of the Schrödinger equation to explain these concepts.

From nuclear physics one is familiar with the existence of a (space-) exchange potential $V_{ex}^{op}(r)$. By definition, it exchanges the space coordinates of the two interacting particles. That it to say, if $\psi(\vec{r})$ is the wave function for the relative motion $\vec{r} = \vec{r}_1 - \vec{r}_2$, then

$$V_{ex}^{op}(r)\psi(\vec{r}) = V_{ex}(r)\psi(-\vec{r}) = \tag{10.6}$$

$$= V_{ex}(r)\,\frac{1}{kr}\sum_{\ell=0}^{\infty}(2\ell+1)f(\ell,E)u_\ell(r)(-)^\ell P_\ell(\cos\Theta)\ ,$$

where $V_{ex}(r)$ now is an ordinary function of $r = |\vec{r}|$. Here, we also introduced the partial wave expansion (4.67), using the fact that $\vec{r} \to -\vec{r}$ implies $(r, \cos\Theta) \to (r, -\cos\Theta)$.

Such an exchange potential is in fact expected to occur in all elementary-particle interactions, if a potential description is at all appropriate. Without further discussion we mention that in field theory it is connected to the appearance of crossed (u-channel) diagrams, as is illustrated in Fig. 10.2.

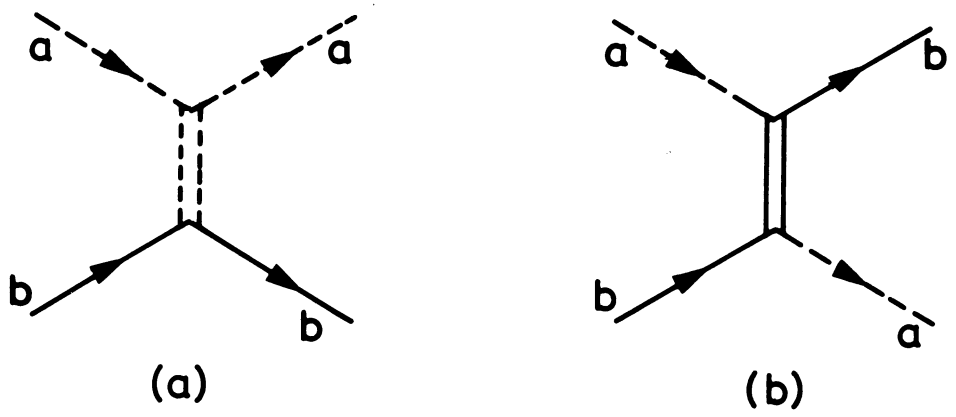

Fig. 10.2

Exchange diagram for the process a + b → a + b contributing to (a) the direct potential V_{dir} and (b) the exchange potential V_{ex}.

The potential that enters in the radial Schrödinger equation is then, in general, the sum of the usual (direct) potential and the exchange potential

$$V(r) = V_{dir}(r) + (-)^{\ell} V_{ex}(r) =$$

$$= \begin{cases} V_{dir} + V_{ex} \equiv V^{+} & \text{for } \ell \text{ even} \\ V_{dir} - V_{ex} \equiv V^{-} & \text{for } \ell \text{ odd} . \end{cases} \tag{10.7}$$

Now, the factor $(-)^{\ell}$ causes troubles when one studies solutions with ℓ complex. True, one could write, for example, $\exp(i\pi\ell)$ instead of $(-)^{\ell}$, but then one runs into difficulties with the asymptotic behaviour as $|\mathrm{Im}\ \ell| \to \infty$. In particular, the contribution from one of the circular pieces forming the path C', Fig. 9.5, will not vanish and the RSW representation will break down.

The procedure is instead to treat the even and the odd ℓ-values separately. Formally, this may be done as follows. Write

$$F(\cos\Theta, E) = \frac{1}{k} \sum_{\ell=0}^{\infty} (2\ell+1) f(\ell, E) P_{\ell}(\cos\Theta) =$$

$$= \frac{1}{k} \sum_{\ell=0}^{\infty} (2\ell+1) f(\ell, E) \left[\frac{1}{2} \{P_{\ell}(\cos\Theta) + P_{\ell}(-\cos\Theta)\} + \right. \tag{10.8}$$

$$\left. + \frac{1}{2} \{P_{\ell}(\cos\Theta) - P_{\ell}(-\cos\Theta)\} \right] =$$

$$= F^{(+)}(\cos\Theta, E) + F^{(-)}(\cos\Theta, E)$$

where

$$F^{(\pm)}(\cos\Theta, E) = \frac{1}{2k} \sum_{\ell=0}^{\infty} (2\ell+1) f^{(\pm)}(\ell, E) \{P_{\ell}(\cos\Theta) \pm P_{\ell}(-\cos\Theta)\} . \tag{10.9}$$

Obviously, $F^{(+)}$ is a sum only over even ℓ-values, since the two Legendre polynomials in the expansion of $F^{(+)}$ cancel for odd ℓ-values. We emphasize this by denoting the partial wave amplitude for even ℓ by $f^{(+)}(\ell, E)$. They are obtained from a radial Schrödinger equation with the potential $V^{(+)}$ of Eq. (10.7). In the same manner, $F^{(-)}$ is a sum only over odd ℓ-values, and the corresponding partial wave amplitudes $f^{(-)}(\ell, E)$ are determined from the potential $V^{(-)}$ of Eq. (10.7). The fact that $f^{(+)}$ and $f^{(-)}$ are obtained from different potentials implies that they are, in general, different analytic functions of ℓ. In particular, one expects $f^{(+)}$ and $f^{(-)}$ to have different Regge poles.

For $F^{(\pm)}$ one may now perform the RSW transform, since no factor $(-)^{\ell}$ enters explicitly. The result is a straightforward generalization of the representation (10.1) and reads

$$F^{(\pm)}(\cos\Theta, E) = \sum_i \frac{\beta_i(E)}{\sin \pi\alpha_i(E)} \left\{ P_{\alpha_i(E)}(-\cos\Theta) \pm P_{\alpha_i(E)}(\cos\Theta) \right\} + \\ + BI^{(\pm)}(\cos\Theta, E) . \tag{10.10}$$

Here, the extra factor ½ in Eq. (10.9) is incorporated in the functions $\beta_i(E)$ and in the background integrals. The total amplitude is, of course, still the sum of $F^{(+)}$ and $F^{(-)}$.

In summary, the existence of an exchange potential implies that the partial wave amplitudes $f^{(\pm)}(\ell, E)$ have different analytic continuations in ℓ, and, in particular, different Regge poles. One says that a Regge pole of $f^{(+)}(\ell, E)$ has <u>signature $\tau = +$</u>, while a pole of $f^{(-)}(\ell, E)$ has <u>signature $\tau = -$</u>. Thus, the signature of a Regge pole, sometimes also called j-parity, simply tells whether the pole occurs in the continuation of $f^{(+)}$ or of $f^{(-)}$. With this signature concept one may write

$$F(\cos\Theta, E) = F^{(+)} + F^{(-)} = \\ = \sum_i \frac{\beta_i(E)}{\sin \pi\alpha_i(E)} \left\{ P_{\alpha_i(E)}(-\cos\Theta) + \tau_i P_{\alpha_i(E)}(\cos\Theta) \right\} + BI(\cos\Theta, E) , \tag{10.11}$$

where τ_i is the signature of the Regge pole $\alpha_i(E)$. Moreover, the background integral is now the sum of $BI^{(+)}$ and $BI^{(-)}$, but we shall not emphasize this fact since it will be of no subsequent importance.

The signature concept for a Regge pole is extremely important. For the classification on trajectories it implies that a Regge pole manifests itself as a particle only at ℓ-values which differ by two units. To see how this comes about, let us concentrate on the contribution to the partial wave amplitude from one Regge pole in the RSW representation (10.11). From Eq. (A3.11) one finds [cf. also Eq. (9.25)]

$$f(\ell = n, E) = \frac{k\beta(E)}{\pi[\alpha(E) + n + 1]} \frac{1}{\alpha(E) - n} [1 + \tau(-)^n] + \ldots . \qquad (10.12)$$

Consequently, a Regge pole of even (odd) signature contributes only to a partial wave with even (odd) angular momentum and can, therefore, give an energy pole only if ℓ is even (odd). Thus, a <u>positive signature</u> Regge trajectory can only give a particle of <u>even angular momentum</u>, a <u>negative signature</u> pole only one of <u>odd angular momentum</u>. This $\Delta\ell = 2$ spacing rule is the first main conclusion to be drawn from the existence of exchange forces.

With this fact in mind, let us now return to $\pi\pi$- and $\pi\rho$-scattering. In $\pi\pi$-scattering, as we saw, Bose-Einstein statistics already gave the $\Delta\ell = 2$ spacing rule, so the signature concept is not really needed there. For $\pi\rho$-scattering, however, occurrence of exchange forces implies that the Regge partners to A_2 could only have spin 0, 4, 6, etc. If we again assume straight-line trajectories of slope $\sim 1\,(\mathrm{GeV})^{-2}$, we would get for the mass m_0 of the hypothetical spin-zero particle

$$m_0^2 \approx m_{A_2}^2 - 2 = -0.3 . \qquad (10.13)$$

Thus, spin 0 is ruled out since it would correspond to a particle of imaginary mass. For the spin 4 recurrence one obtains

$$m_4^2 \approx m_{A_2}^2 + 2 = (1.93)^2 , \qquad (10.14)$$

suspiciously in the vicinity of the S-meson.

In Fig. 10.3, all the known non-strange boson resonances are marked in a Chew-Frautschi plot. Those having well-established spins and parities occupy the proper places in the diagram, while those for which spins and other quantum numbers are not known are put below but at the appropriate energy. Throughout, horizontal bars indicate the measured full widths. If you like, this may be called a pessimist's Chew-Frautschi plot for the non-strange mesons. Also drawn in the diagram are the ρ- and A_2-trajectories, both assuming a straight-line form with a slope of $0.9\,(\mathrm{GeV})^{-2}$. The fact that the ρ-trajectory does not pass exactly through the position of the ρ-meson is connected to its determination at negative values of the squared energy: these points will be further elucidated in Chapter 14 below.

You have had essentially this picture, Fig. 10.3, discussed during the lectures by Prof. Goldhaber, who also treated the strange mesons in an analogous fashion. I have nothing new to add here. Let me only stress that the only reasonably well-established trajectories are the ρ- and the A_2-trajectories, where two particles might be present on each of them. For the other particles one is left with two possibilities: either they are alone on their respective trajectories - although this is not very exciting it is perfectly legitimate, since the trajectories may bend and turn downwards before reaching the next possible angular momentum (cf. Fig. 9.3 in this context): or one could attribute suitable quantum numbers, including spin-parity, to the resonances for which spin, parity, G-parity, isospin, etc., are not established. Such highly speculative considerations have indeed been carried out [see, e.g., D.G. Sutherland, CERN preprint TH-768 (1967) and references cited therein].

One final point about the ρ- and the A_2-trajectories. For the sake of argument let us assume that g(1650) is the first Regge recurrence of the ρ-meson and that S(1910) is the first recurrence of the A_2-meson. Experimentally, it seems as if all these four mesons lie approximately on the same straight line in the Chew-Frautschi diagram. In other words, the ρ- and the A_2-trajectories seem in fact to coincide so that one and the same trajectory could account for the four particles, spaced as they are by only one unit of spin. This would then indicate that exchange forces are not present, or at least play a minor role. In the fashionable language used at present this is referred to as "exchange degeneracy".

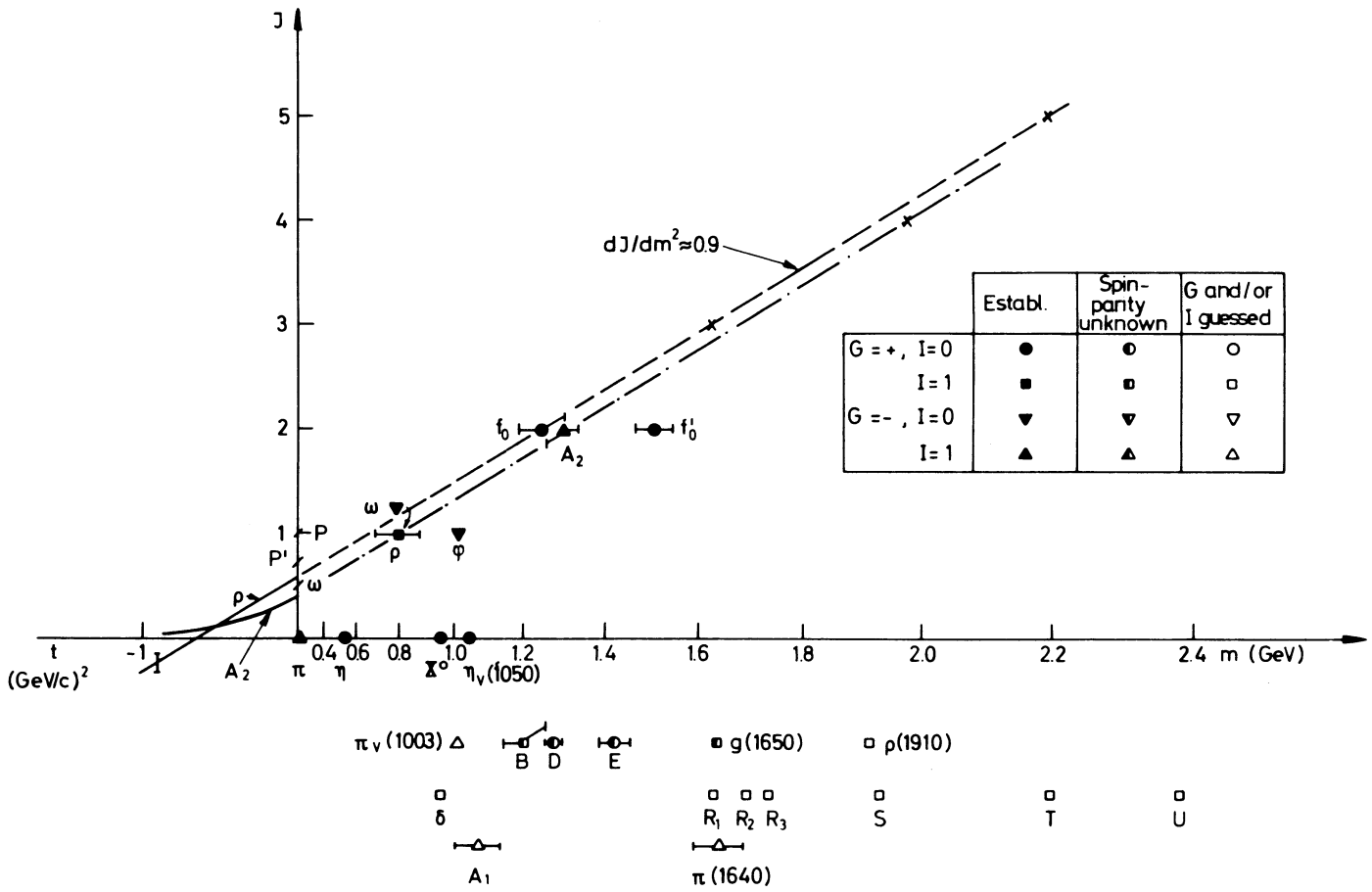

Fig. 10.3

Chew-Frautschi diagram for the non-strange bosons; note the quadratic mass scale. Particles with well-established spins and parities occupy the proper places, while unestablished ones are placed below at the appropriate energies. The notation and quantum number assignments of A.H. Rosenfeld et al. [Rev.Mod.Phys 39, 1 (1967)] are followed; the R-, S-, T- and U-mesons are taken from M.N. Focacci et al. [Phys.Rev. Letters 17, 890, 1209(E) (1966)]. Horizontal bars give the measured full widths. The ρ- and A_2-trajectories for $t \leq 0$ are obtained from high-energy charge-exchange and η-production reactions in π^- p collisions as explained in Chapter 14; only a typical statistical error on the ρ-trajectory is shown. These trajectories are extrapolated to the positive t-region, assuming constant slope. Also exhibited in the diagram are the $t = 0$ intercepts of the Pomeranchuk (P), the Pomeranchuk prime (P') and the ω-trajectories as obtained from fits to the total cross-section data at high-energy (see Chapters 13 and 15).

If one assumes a quark model, and attributes the bosons to Regge poles of the quark-antiquark scattering amplitude, one may give an argument for this exchange degeneracy. Namely, the direct forces are due to Feynman diagrams of the type given in Fig. 10.4(a), the exchange forces to diagrams as in Fig. 10.4(b). Since $\bar{q}q$ systems of low masses presumably exist (the mesons), while a qq system presumably would have rather large mass (and charge $^2/_3$), the direct potential is expected to dominate over the exchange one. Let me merely note that it is not really necessary to invoke quarks to explain the exchange degeneracy. The same argument would apply equally well to the (more realistic?) case of direct and exchange forces in nucleon-antinucleon scattering.

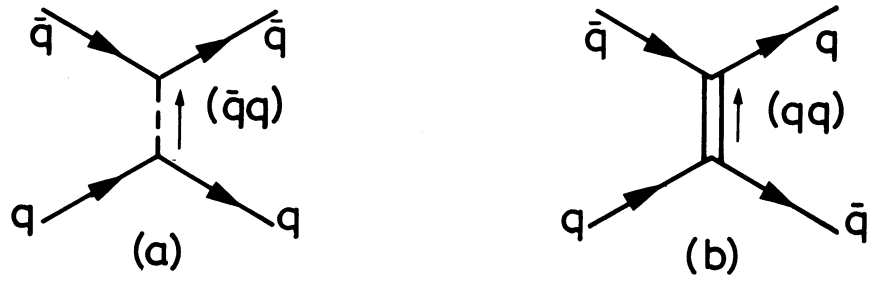

Fig. 10.4

Feynman diagrams contributing to quark-antiquark
(a) direct forces and (b) exchange forces.

10.2 Fermion Regge trajectories

Consider πN- (or KN-) scattering. There are now two partial wave amplitudes $f(\ell, \pm, E)$ for each value of ℓ, depending on whether $j = \ell + \frac{1}{2}$ or $\ell - \frac{1}{2}$, respectively. Since a potential now in general includes a spin-orbit part proportional to $\vec{\sigma} \cdot \vec{L}$, the amplitudes $f(\ell, \pm, E)$ would in a potential approach be determined from different potentials. In particular, the Regge poles of $f(\ell, +, E)$, which could give particles of spin-parity $^1/_2{}^-$, $^3/_2{}^+$, $^5/_2{}^-$, $^7/_2{}^+$, etc. (remember the negative intrinsic parity of the pion),

will in general be different from the Regge poles of $f(\ell, -, E)$, for which particles of spin-parity $\frac{1}{2}^+$, $\frac{3}{2}^-$, $\frac{5}{2}^+$, $\frac{7}{2}^-$, etc., may occur. Moreover, appearance of exchange forces implies the $\Delta\ell = 2$ spacing rule in each of the two groups. Summarizing, a fermion Regge pole is characterized by:

i) the relation between j and ℓ,

ii) the signature, i.e., whether ℓ is even or odd.

This gives the following four possibilities:

positive signature (ℓ even) and $j = \ell + \frac{1}{2}$: $\frac{1}{2}^-, \frac{5}{2}^-, \frac{9}{2}^-, \ldots$

positive signature (ℓ even) and $j = \ell - \frac{1}{2}$: $\frac{3}{2}^-, \frac{7}{2}^-, \frac{11}{2}^-, \ldots$

negative signature (ℓ odd) and $j = \ell + \frac{1}{2}$: $\frac{3}{2}^+, \frac{7}{2}^+, \frac{11}{2}^+, \ldots$

negative signature (ℓ odd) and $j = \ell - \frac{1}{2}$: $\frac{1}{2}^+, \frac{5}{2}^+, \frac{9}{2}^+, \ldots$.

Besides, each Regge trajectory carries isospin and strangeness. Consequently, in πN-scattering there are all in all eight possibilities for a Regge trajectory.

With these facts in mind, we turn to the experimental results as presented in the Chew-Frautschi plot of Fig. 10.5 for the strangeness-zero fermions. As for the bosons, Fig. 10.3, the well-established particles occupy their appropriate places in the diagram, while the non-settled ones are put below but at the proper energy. Again, horizontal bars give the full widths. Note also the different vertical scales for the $I = \frac{1}{2}$ and $I = \frac{3}{2}$ resonances.

The strange fermions may be exhibited in an analogous manner, as you have learned from Prof. Giacomelli.

The situation for the nucleon resonances is perhaps more encouraging than for the mesons. There seems to be three trajectories with at least two members. These are the N_α-trajectory through $N(938, \frac{1}{2}^+)$ and $N^*(1688, \frac{5}{2}^+)$, and the N_γ-trajectory representing $N^*(1525, \frac{3}{2}^-)$ and $N^*(2190, \frac{7}{2}^-)$; both these trajectories have isospin $I = \frac{1}{2}$. The third one is the $I = \frac{3}{2}$, Δ-trajectory with $\Delta(1236, \frac{3}{2}^+)$ and $\Delta(1920, \frac{7}{2}^+)$. Quite a few well-established resonances of spin $\frac{5}{2}$ or less, and mass below $\sim$ 1700 MeV, seem to be "Regge singlets", however. Note, though, the last remark of this chapter. [Note added in proof: It seems now established that $\Delta(2420)$ has spin-parity $\frac{11}{2}^+$; see Phys.Rev.Letters 19, 476 (1967).]

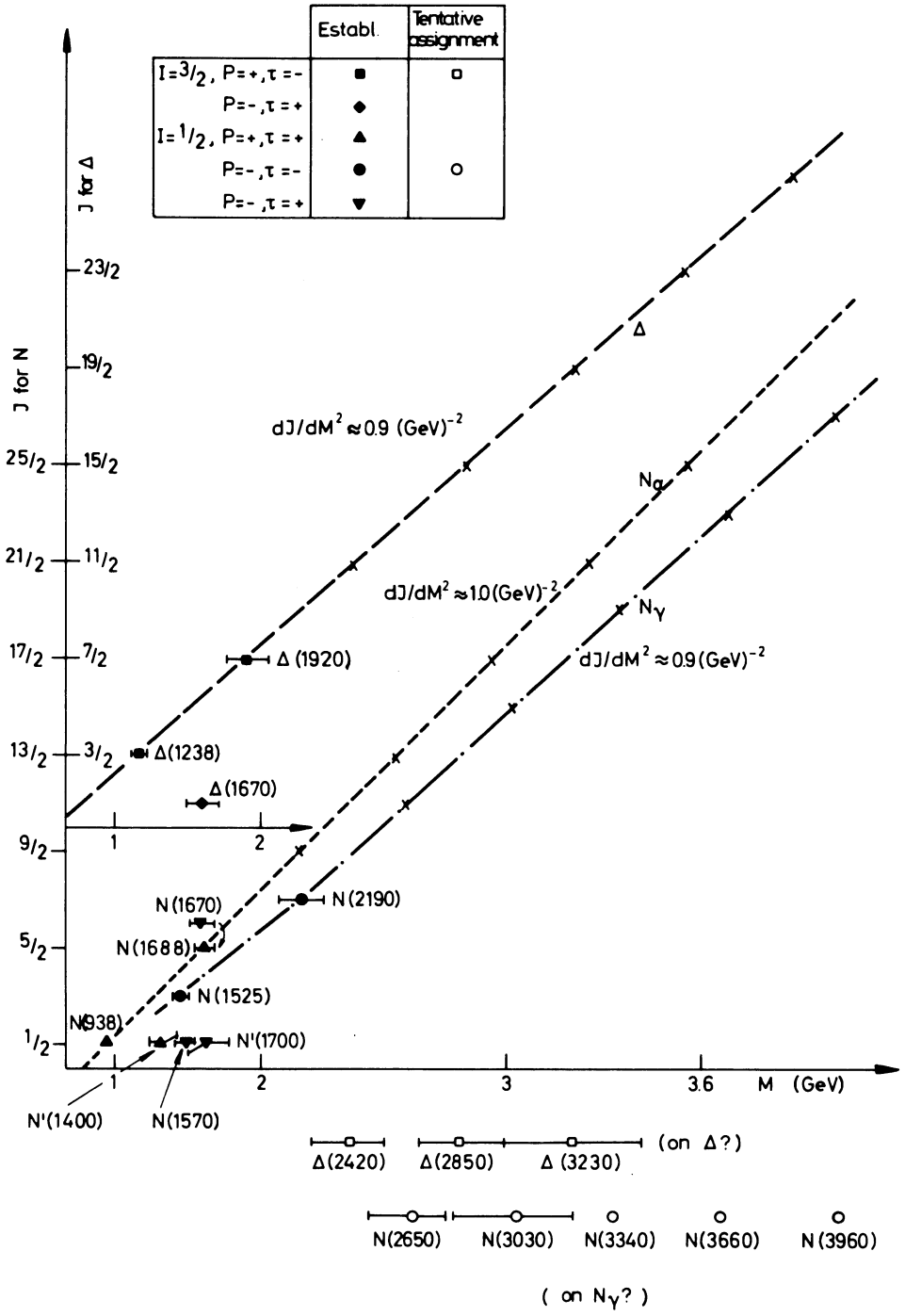

Fig. 10.5

Chew-Frautschi diagram for the non-strange fermions; note the quadratic mass scale and the different J-scales for the I = ½ and I = ³⁄₂ fermions. Well-established particles occupy their proper place, unestablished ones are placed below at the appropriate energies. The notation and quantum number assignments of Rosenfeld et al. (see caption to Fig. 10.3) are followed; see the text for further information. Horizontal bars give full widths.

Linear extrapolation of the presumed trajectories predicts resonances of higher and higher spins and masses, and the field is open for speculations. In fact, there has been a bump reported at the very high mass of ~ 3960 MeV, which would fit on the N_δ-trajectory if it is a resonance of spin-parity $^{27}/_2^-$(!!!). In πN-scattering, the position of this bump corresponds to $p_{lab} \sim 7$ GeV/c. However, this possible resonance, as well as those occuring in Fig. 10.5 at masses 3340 MeV and 3660 MeV, were not seen in elastic or total cross-sections measurements, but in a 16 GeV/c π^-p bubble chamber experiment by investigating the four prong events containing two or more neutrals

$$\pi^- p \to \pi^-\pi^+\pi^- p + MM \ , \qquad (10.15)$$

where MM denote the missing mass. From studies of the distribution in the invariant mass of p + MM, the above-mentioned bumps were found. [J. Ballam, Seminar at CERN on April 18, 1967; see also J. Ballam et al., Bull.Am.Phys.Soc. 12, 488 (Ref. BF11) (1967)]. As was pointed out to me at the School by Dr. Wojcik, the possible resonance at 3660 MeV has also been seen as a bump in the p + 7π invariant mass distribution in the reaction $\pi^+ p \to p + 8\pi$ at 8 GeV/c [J. Bartke et al., Physics Letters 24B, 118 (1967)].

Before we close this chapter, two remarks are appropriate. First, need a Regge trajectory be a straight line in the Chew-Frautschi diagram? The answer is no. There is no convincing theoretical argument favouring a straight-line trajectory, nor is there any definite argument against it within a limited energy interval. What is puzzling, however, is that the trajectories, in particular the non-strange fermion ones, seem to increase indefinitely. Of course, it should be kept in mind that these speculations are based on in fact rather scanty experimental evidences. However, they pose certain theoretical problems. From numerical computations using a Yukawa potential (9.1), one always finds trajectories that bend down rather quickly, something like the one drawn in Fig. 9.3. Moreover, an infinite increase of the trajectory seems in disagreement with the basic requirements of the Regge pole model and strong interaction dynamics in general [see N.N. Khuri, Phys.Rev.Letters 18, 1094 (1967)].

Second, a fermion trajectory shows some peculiarities that we have not mentioned so far. It originates from a general property, known as the McDowell symmetry, which a fermion partial wave amplitude has to satisfy [S.W. MacDowell, Phys.Rev. 116, 774 (1959)]. Namely, from very general assumptions one is able to show that

$$f(\ell, +, E) = f(\ell + 1, -, -E) . \qquad (10.16)$$

That is, the two partial waves with the same j but opposite parities transform into each other when the energy changes sign. In particular, if say $f(\ell, +, E)$ has an energy pole at negative energy, this is also a pole of $f(\ell + 1, -, E)$ but here at positive energy, so it corresponds to a particle. [Recall in this discussion that we now consider relativistic scattering, so the non-relativistic kinematics implied in the potential scattering treatment is totally inadequate. In particular, negative energy does not mean a bound state. In fact, in relativistic kinematics a negative energy is always unphysical. The condition for an energy pole to give a bound state or a resonance depends on whether it occurs below the scattering threshold or not.]

For a Regge trajectory, the McDowell symmetry means that a Regge pole at $\alpha(E)$ in $f(\ell, +, E)$ would at the same time be a Regge pole at $\alpha(-E)$ in $f(\ell + 1, -, E)$. If now $\alpha(E)$ depends only on E^2, the sign change of the energy is of no importance. Consequently, from the McDowell symmetry and straight-line trajectories in the Chew-Frautschi plot one expects the fermions to occur in parity doublets $(\frac{1}{2}^+, \frac{1}{2}^-)$, $(\frac{5}{2}^+, \frac{5}{2}^-)$, etc., the two particles in a doublet having (approximately) the same mass. If one relaxes the straight-line condition, one still obtains parity doublets, but now with different masses in general. For example, it could be that the $N^*_{\frac{1}{2}}(1670, \frac{5}{2}^-)$, which does not lie on any of the two $I = \frac{1}{2}$ trajectories in Fig. 10.5, is the parity doublet to $N^*_{\frac{1}{2}}(1688, \frac{5}{2}^+)$. The absence of an expected nucleon partner, of spin-parity $\frac{1}{2}^-$, would then be explained by a vanishing residue function at the energy (850 MeV according to the estimates) where it should appear. We refer to, for example, C.B. Chiu and J.D. Stack, Phys.Rev. 153, 1575 (1967) for further discussions and references.

P A R T IV

(Chapters 11-16)

REGGE POLES AND HIGH-ENERGY REACTIONS

We shall now turn to the other application of the Regge pole model, viz., to scattering of particles at high energy. Within this model, any high-energy two-body reaction, elastic as well as inelastic, is due to the exchange of one or a few Regge poles. In order to understand these ideas, one must first thoroughly be familiar with the concept of crossing relation, or crossing symmetry. Once we master this indeed very important general property of the scattering amplitude, we shall first treat some aspects of the one particle exchange (OPE) model as an application.

CHAPTER 11 - CROSSING SYMMETRY. THE OPE MODEL

What is crossing symmetry? In general terms, it is a relation which connects the scattering amplitude for particle-particle interaction to that of antiparticle-particle interaction. To make this more precise, we must introduce some formalism.

Consider a two-body reaction

$$a + b \to c + d \tag{11.1}$$

which is also illustrated in Fig. 11.1. As a definite example, we may take

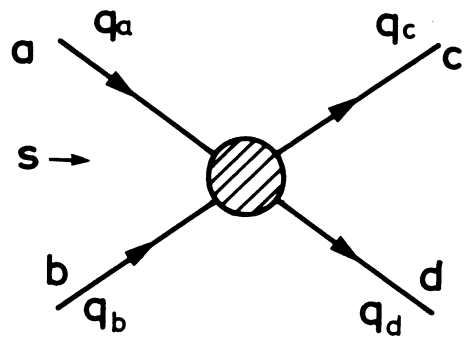

Fig. 11.1

The s-channel reaction (11.1) and the notation for the four-momenta.

pion-nucleon charge exchange scattering

$$\pi^- p \to \pi^0 n \,. \tag{11.2}$$

Neglecting possible spins, the reaction is described by one scattering amplitude. In order to arrive at the simplest formulation of the crossing relation, it is necessary to use the relativistic scattering amplitude T of Eq. (3.20); a similar definition of T applies to any two-body reaction. Moreover, it is convenient to consider T as a function of all the four-momenta $q_a, \ldots, q_d$

$$T = T(q_c, q_d; q_a, q_b) \,, \tag{11.3}$$

despite the fact that T is really a function only of the invariant variables

$$s = (q_a + q_b)^2 = (q_c + q_d)^2 \ , \tag{11.4}$$

$$t = (q_a - q_c)^2 = (q_b - q_d)^2 \ , \tag{11.5}$$

so that

$$T = T(s, t) \ . \tag{11.6}$$

We shall call the reaction (11.1) the s-channel reaction.

Besides the process (11.1), we shall also consider the reaction

$$a + \bar{c} \to \bar{b} + d \ , \tag{11.7}$$

where $\bar{c}$ and $\bar{b}$ are the antiparticles of c and b, respectively. It is illustrated in Fig. 11.2. For the example (11.2), the process (11.7) becomes

$$\pi^- \pi^0 \to \bar{p}n \tag{11.8}$$

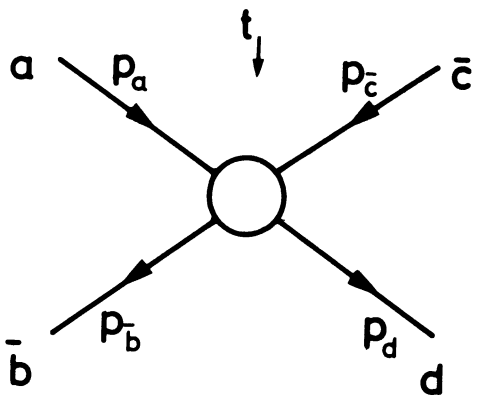

Fig. 11.2

The t-channel reaction (11.7) and the notation for the four-momenta.

since π^0 is its own antiparticle. The relativistic amplitude for this reaction as a function of the four-momenta is denoted

$$\bar{T} = \bar{T}(p_{\bar{b}}, p_d;\ p_a, p_{\bar{c}}) \ . \tag{11.9}$$

As for T, the amplitude $\bar{T}$ is in fact a function only of the relativistic variables

$$\bar{s} = (p_a + p_{\bar{c}})^2 = (p_{\bar{b}} + p_d)^2 \ , \tag{11.10}$$

$$\bar{t} = (p_a - p_{\bar{b}})^2 = (p_{\bar{c}} - p_d)^2 \ , \tag{11.11}$$

so that

$$\bar{T} = \bar{T}(\bar{s}, \bar{t}) \ . \tag{11.12}$$

The reaction (11.7) will be called the t-channel reaction.

A priori, there is no connection between the s- and the t-channel reactions (11.1) and (11.7). However, the principle of crossing symmetry tells that they are, indeed, connected. This principle can be formulated in the one equation

$$\bar{T}(p_{\bar{b}}, p_d;\ p_a, p_{\bar{c}}) = T(q_c = -p_{\bar{c}},\ q_d = p_d;\ q_a = p_a,\ q_b = -p_{\bar{b}}) \ . \tag{11.13}$$

It means the following. Assume that from some theory we are able to calculate the s-channel amplitude T as function of all the four-momenta. In other words, we assume that we know the analytic expression for T. Then we need not calculate separately the t-channel amplitude $\bar{T}$. We merely have to substitute in the analytic expression for T the t-channel momenta according to the rule given in Eq. (11.13), which is sometimes also called the substitution rule: change sign of the antiparticle momenta, but not of the particle momenta. Note that it is the four-momenta that enters; thus one must also change the sign of their zeroth components, i.e., the respective energies.

The crossing relation may be derived from general principles of quantum field theory. The basic ingredient of the proof is the following observation. You know from Prof. Veltman's lectures that in field theory a creation operator is always associated with a factor exp (ikx), an annihilation operator with a factor exp (-ikx); remember that $kx = k_0x_0 - kx$ in our

conventions. In an amplitude like T, the particles a and b must be annihilated, resulting in factors exp $(-iq_a x)$ and exp $(-iq_b x')$, while the created particles c and d are represented by factors exp $(iq_c y)$ and exp $(iq_d y')$; integration over the space-time coordinates x, x', y and y' is understood. A similar argument applied to $\bar{T}$ gives factors exp $(-ip_a x)$, exp $(ip_{\bar{b}} x')$, exp $(-ip_{\bar{c}} y)$ and exp $(ip_d y)$. Comparison of the exponents yields the substitution rule (11.13). A complete proof must, of course, also consider the factor in the integral over the space-time coordinates that multiplies the exponential functions, and also under which conditions one may consider T as an analytic function of the momenta.

The crossing relation is most easily understood in terms of the four-momenta. However, in most applications one is interested in how it looks in terms of the Mandelstam variables s, t and $\bar{s}$, $\bar{t}$. This form is easily derived. Indeed, the substitution rule (11.13) immediately yields

$$\bar{T}(\bar{s}, \bar{t}) = T[s = (p_a - p_{\bar{b}})^2 = \bar{t},\ t = (p_a + p_{\bar{c}})^2 = \bar{s}] \ . \qquad (11.14)$$

Consequently, in going from the s-channel to the t-channel, the energy variable s becomes a momentum transfer variable $\bar{t}$, and the momentum transfer variable t an energy variable $\bar{s}$. This may be illustrated in the Mandelstam plane (cf. Fig. 2.2). For simplicity, we shall only treat the particular example of pion-nucleon charge exchange. Without going into the kinematical details, it is clear that $\bar{s} = t$ must be greater than $(2M)^2$ for the t-channel reaction $\pi^- \pi^0 \to \bar{p}n$ to take place (M denotes the mass of the nucleon). Moreover, $\bar{t} = s$ is expected to be negative, since it is a momentum transfer variable. The exact shape of the t-channel physical region is indicated in Fig. 11.3. Note in particular that the physical regions for the s- and the t-channel reactions do not overlap.

The content of the crossing relation (11.14) may be summarized as follows. Suppose we know the analytic expression for the s-channel scattering amplitude T(s, t) as function of the two independent relativistic variables s and t, confined to the physical region of the s-channel (cf. Fig. 11.3). Then the t-channel scattering amplitude is given by the <u>same analytic expression</u>, only for <u>different values of the variables</u>, viz., confined to the t-channel physical region of Fig. 11.3. The argument applies also the

other way around: knowing the t-channel amplitude $\bar{T}(\bar{s}, \bar{t})$, the s-channel amplitude is given by the same analytic expression if one identifies $\bar{s} = t$, $\bar{t} = s$. Another way to express the same fact is to say that one and the same function $T(s, t)$ represents the scattering amplitude in both the s-channel and the t-channel, depending merely on whether it is evaluated in the physical region of the s- or the t-channel. Since these two regions do not overlap, it is very essential that $T(s, t)$ is an <u>analytic</u> function of its arguments in order that the continuation from the one physical region to the other should be possible. Moreover, since the analytic continuation of a function may depend on which particular path one chooses to continue along, the crossing relation may take slightly different forms depending on that choice. We shall not enter into any details here.

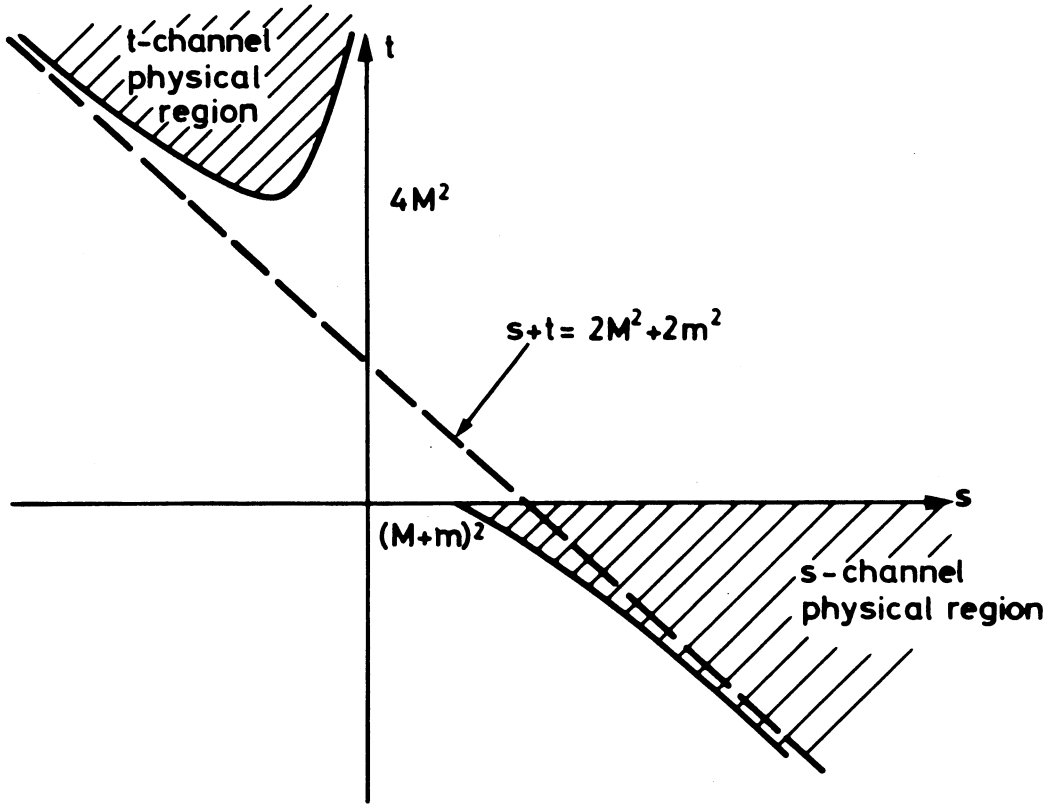

Fig. 11.3

The physical regions for the s-channel ($\pi^- p \to \pi^0 n$) and the t-channel ($\pi^- \pi^0 \to \bar{p} n$) reactions in the Mandelstam plane.

I am afraid all this was rather abstract, so let me try to illustrate how crossing symmetry is applied in a definite example. Consider the reaction $\pi^-\pi^0 \to \bar{p}n$. The amplitude for this (t-channel) reaction may be expanded in partial waves

$$\bar{T}(\bar{s},\bar{t}) = 8\pi\sqrt{\bar{s}}\,\frac{1}{\sqrt{k_t k_t'}}\sum_{\ell=0}^{\infty}(2\ell+1)\bar{f}(\ell,E_t)P_\ell(\cos\Theta_t)\ . \qquad (11.15)$$

Here, the partial wave expansion is introduced in analogy with Eqs. (4.4) and (3.20). Moreover, k_t and k_t' denote the c.m.s. three-momenta in the initial $(\pi^-\pi^0)$ and the final $(\bar{p}n)$ states, respectively, and the c.m.s. energy E_t and scattering angle Θ_t carry subscripts t to emphasize that they are t-channel quantities.

At an energy E_t near to the ρ-meson mass m_ρ (this is certainly an unphysical energy, being below the threshold $2M$), the scattering amplitude is expected to be dominated by the $\ell = 1$ partial wave in which the ρ-meson occurs as a resonance. The one ρ-meson exchange model for the s-channel reaction $\pi^-p \to \pi^0 n$ now amounts, essentially, to keeping <u>only</u> this resonating p-wave in the t-channel amplitude and to invoking crossing symmetry to get at the amplitude in the s-channel.

In more detail, one assumes that

$$\bar{T}(\bar{s},\bar{t}) \approx \bar{T}_\rho(\bar{s},\bar{t}) = K_\rho(\bar{s})P_{\ell=1}(\cos\Theta_t)\ , \qquad (11.16)$$

where

$$K_\rho(\bar{s}) = 8\pi\sqrt{\bar{s}}\,(k_t k_t')^{-1/2}\,3\bar{f}_\rho(\ell=1,E_t)\ , \qquad (11.17)$$

the partial wave amplitude $\bar{f}_\rho(\ell = 1, E_t)$ being a Breit-Wigner form similar to that of Eq. (4.65). Although it is possible to go into the details of the $\bar{s} = t$ dependence of $K_\rho(\bar{s})$, in particular to show that $K_\rho(\bar{s} = t)$ is proportional to the propagator denominator $(t - m_\rho^2)^{-1}$ characteristic of the one ρ-meson exchange Feynman diagram, it will take us too far to do so here. However, we call attention to the important fact that $K_\rho(\bar{s})$ is independent of the t-channel scattering angle $\cos\Theta_t$.

Using the crossing relation (11.14), the expression (11.16) is now assumed to be a good approximation to the scattering amplitude for the s-channel reaction $\pi^- p \to \pi^0 n$ at high energy. From the crossing rules, the function $K_\rho(\bar{s})$ is then replaced by $K_\rho(t)$; note that it is independent of s. To see what crossing symmetry means for $P_{\ell=1}(\cos\Theta_t) = \cos\Theta_t$, we must express it in terms of the invariant variables. In the same way as in Chapter 2 one easily derives

$$s = \bar{t} = (p_a - p_{\bar{b}})^2 = m^2 + M^2 - 2\epsilon_a\epsilon_{\bar{b}} + 2k_t k_t' \cos\Theta_t \ , \qquad (11.18)$$

where

$$\epsilon_a = \epsilon_{\bar{b}} = \frac{1}{2}\sqrt{\bar{s}} = \frac{1}{2}\sqrt{t} \ , \qquad (11.19)$$

$$k_t^2 = \frac{1}{4\bar{s}}\lambda(\bar{s}, m^2, m^2) = \frac{1}{4}(t - 4m^2) \ , \qquad (11.20)$$

$$k_t'^2 = \frac{1}{4\bar{s}}\lambda(\bar{s}, M^2, M^2) = \frac{1}{4}(t - 4M^2) \ . \qquad (11.21)$$

Thus

$$\frac{1}{2}\sqrt{(t-4M^2)(t-4m^2)}\cos\Theta_t = s + \frac{t}{2} - m^2 - M^2 \equiv s_t \ , \qquad (11.22)$$

thereby defining the new variable s_t. Equation (11.22) is the needed expression for $\cos\Theta_t$.

Consequently, the one ρ-meson exchange model, which is a special case of the OPE model, for the reaction $\pi^- p \to \pi^0 n$ amounts essentially (there are a few minor points which we ignore) to adopting the form

$$T(s,t) = K_\rho(t)P_{\ell=1}(\cos\Theta_t) = K_\rho(t)\frac{-2s_t}{\sqrt{4m^2 - t}\ \sqrt{4M^2 - t}}$$

for the scattering amplitude. Here, we extracted a factor $i = \sqrt{-1}$ from each square root in $\cos\Theta_t$ in order to get roots of positive numbers; to do this correctly, one must actually consider the path of continuation from the t-channel to the s-channel properly.

There are two important points about the form (11.23) which we want to emphasize. First, as mentioned above, $K_\rho(t)$ is proportional to $(t-m_\rho^2)^{-1}$. For t near to m_ρ^2, $K_\rho(t)$ thus becomes very large, and the assumption that the whole amplitude is given by the form (11.23) is reasonable. To the extent that t is not too far away from the position of the ρ-pole, the approximation of keeping only the ρ-exchange contribution is presumably all right, but becomes more and more dubious as t gets away from m_ρ^2. Anyhow, if it is true also for $t < 0$, the factor $(t-m_\rho^2)^{-1}$ produces an s-channel differential cross-section that is peaked at small $|t|$, in qualitative agreement with the experimental results. The conclusion holds provided there are no other factors in $K_\rho(t)$ that spoil this feature. Actually, such factors do occur.

The second point is that the energy dependence of the amplitude (11.23) is explicitly known. Namely, for fixed t and $s \to \infty$, the amplitude behaves as a constant times s. The result is, from Eq. (3.23), a differential cross-section which at fixed t behaves as a constant at high energy. This prediction is solely due to the fact that one keeps only the p-wave in the t-channel amplitude. It disagrees with the experimental findings as presented in Chapter 7, which rather show a decrease, roughly like $s^{-1} \sim p_{lab}^{-1}$ or stronger.

More generally, we see that the energy dependence of the differential cross-section predicted by the OPE model is entirely governed by the spin of the exchanged particle, i.e., the particular t-channel partial wave that is assumed to dominate. In fact, the ℓth t-channel partial wave, contributing the factor $P_\ell(\cos\Theta_t)$ to the full amplitude, yields a cross-section which at fixed t behaves as $s^{2\ell-2}$ for s tending to infinity. To see this, note that $\cos\Theta_t \sim s \to \infty$, and $P_\ell(x) \sim x^\ell$ for $x \to \infty$. For $\ell > 1$ this is disaster, since if the cross-section for one particular reaction goes to infinity with the energy, so does the total cross-section, in violent disagreement both with experiment and theory, the latter as represented by the Froissart bound. A solution to this dilemma was found through the introduction of the Regge pole model, as we shall see in Chapter 12 below.

Summarizing, the OPE model with exchange of a boson having spin ≥ 1 predicts an energy dependence which disagrees with the experimental results and, for spin ≥ 2, also with general theoretical requirements. Moreover,

the t-dependence of the OPE amplitude, which should reproduce the experimentally observed small angle peaking in $d\sigma/dt$ at fixed s, is in general not in very good agreement with the data either. While there are no means to cure the energy disease of the OPE model, unless by invoking the Regge pole model, there are some suggestions on how to remedy the bad features of the t-dependence.

We may refer to, for example, the lectures by N. Schmitz and by H. Pilkuhn at the 1965 CERN School of Physics [report CERN 65-24 (1965)] for further details and references on the OPE model.

CHAPTER 12 - THE HIGH-ENERGY SCATTERING AMPLITUDE IN THE REGGE POLE MODEL

To be precise, let us consider pion-nucleon scattering as illustrated in Fig. 12.1. The application of the Regge pole model to this reaction at high energy is based on the following procedure, closely related in fact to the way we developed the OPE model in the previous chapter:

i) Start with the RSW representation of the amplitude for the t-channel reaction $\pi\bar{\pi} \to \bar{N}N$.

ii) Use crossing symmetry to conclude that the same analytic expression also gives the s-channel amplitude.

iii) Consider the high-energy limit in the s-channel in order to isolate the contributions from the Regge poles with the largest real parts.

We now present these three steps in more detail.

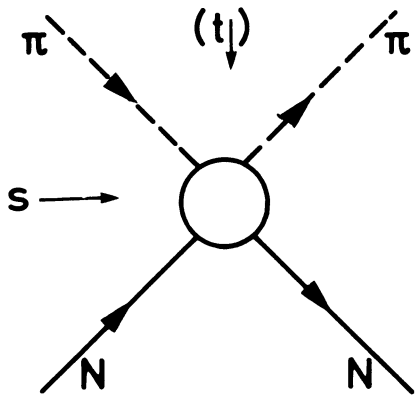

Fig. 12.1

The s- and the t-channels for pion-nucleon scattering.

First, we adopt the RSW representation (10.1) for the t-channel scattering amplitude, for the time being neglecting the modification due to the introduction of signature. Both the scattering angle and the energy should now carry a subscript t, and read Θ_t and E_t, respectively, to emphasize that they are t-channel quantities. Moreover, as in the OPE model, we must consider the relativistic amplitude $\bar{T}(\bar{s}, \bar{t})$, for which we write

$$\bar{T}(\bar{s}, \bar{t}) = \sum_i \frac{\beta_i(\bar{s})}{\sin \pi\alpha_i(\bar{s})} P_{\alpha_i(\bar{s})}(-\cos\Theta_t) + BI(\cos\Theta_t, \bar{s}) \ . \qquad (12.1)$$

Here we have made the modification of considering the trajectories α_i, the functions β_i and the background integral BI as functions of $\bar{s} = E_t^2$ instead of E_t. Moreover, the factor $8\pi\sqrt{\bar{s}}$ in the relation between the relativistic amplitude $\bar{T}$ and the "non-relativistic" one, $\bar{F}$, is taken care of by redefining β_i and BI in going from Eq. (10.1) to Eq. (12.1).

At first, the form (12.1) is valid only in the t-channel. However, the second step is to invoke crossing symmetry to conclude that the s-channel amplitude T(s, t) is given by the same expression. We only have to replace $\bar{s}$ by t, and to use Eq. (11.22) to obtain $\cos\Theta_t$ in terms of s and t.

Still, the formula does not look particularly simple. It should be noted, though, that it contains the energy-dependence rather explicitly. Namely, s appears only through the argument $\cos\Theta_t$ of the Legendre functions $P_{\alpha_i}(-\cos\Theta_t)$. The importance of this fact becomes more transparent if one performs the third step, that of going to high energy in the s-channel. This should be taken to mean that the masses m and M, and the momentum transfer $\sqrt{-t}$ can be neglected compared to the c.m.s. energy $\sqrt{s}$. In particular

$$\cos\Theta_t = \frac{2s_t}{\sqrt{t-4m^2}\ \sqrt{t-4M^2}} \approx \frac{-s}{\sqrt{4m^2-t}\ \sqrt{4M^2-t}} \propto -s \ . \qquad (12.2)$$

As above, we extracted here an $i = \sqrt{-1}$ from each square root in order to get roots of positive entities in the s-channel. Note also that Eq. (12.2) means that $\cos\Theta_t$ becomes numerically very large as s increases. This is of

course no contradiction, since Θ_t is the t-channel scattering angle and we now consider the s-channel physical region. The argument of the Legendre functions thus being very large, we may apply the result (A3.10) to obtain

$$P_{\alpha(t)}(-\cos\Theta_t) = \kappa(t)\left(\frac{s}{s_0}\right)^{\alpha(t)} \qquad \text{for} \qquad s \to \infty\ , \tag{12.3}$$

where all s-independent quantities are lumped into one function $\kappa(t)$, which is a known function of t if $\alpha(t)$ is so. The scale factor s_0, of the same dimension as s, is arbitrary and introduced only to have the power of a dimensionless number.

In this way we have isolated the energy-dependence of each individual Regge pole contribution. Since

$$\left(\frac{s}{s_0}\right)^{\alpha} = \left(\frac{s}{s_0}\right)^{\mathrm{Re}\,\alpha} \exp\left[\, i\ \mathrm{Im}\ \alpha\ \log\frac{s}{s_0}\right], \tag{12.4}$$

it follows that a Regge pole of larger Re α will at high energy dominate one with smaller Re α. Moreover, we may estimate the importance of the background integral (9.19) simply by noting that the only factor in $\mathrm{BI}(\cos\Theta_t, \bar{s})$ that depends on $\cos\Theta_t$ is $P_\ell(-\cos\Theta_t)$; this argument is not spoiled by the redefinitions that BI has undergone. Since the integral is along Re $\ell = -\frac{1}{2}(+\epsilon)$, it follows that

$$\mathrm{BI}(\cos\Theta_t, t) \propto s^{-\frac{1}{2}} \qquad \text{for} \qquad s \to \infty\ . \tag{12.5}$$

At high s-channel energy the RSW expansion of the t-channel amplitude thus reads

$$T(s, t) = \sum_i \frac{\gamma_i(t)}{\sin\pi\alpha_i(t)}\left(\frac{s}{s_0}\right)^{\alpha_i(t)} + O\left(s^{-\frac{1}{2}}\right)\ . \tag{12.6}$$

Here, the functions γ_i are the products of the respective β_i by the function κ of Eq. (12.3). If we order the Regge trajectories so that

$$\text{Re } \alpha_1 \geq \text{Re } \alpha_2 \geq \text{Re } \alpha_3 \geq \ldots \geq -\tfrac{1}{2} , \tag{12.7}$$

we may write

$$T(s,t) = \frac{\gamma_1(t)}{\sin \pi\alpha_1(t)} \left(\frac{s}{s_0}\right)^{\alpha_1(t)} + \frac{\gamma_2(t)}{\sin \pi\alpha_2(t)} \left(\frac{s}{s_0}\right)^{\alpha_2(t)} + \frac{\gamma_3(t)}{\sin \pi\alpha_3(t)} \left(\frac{s}{s_0}\right)^{\alpha_3(t)} + \ldots , \tag{12.8}$$

which is nothing but a representation of the s-channel scattering amplitude as a descending asymptotic series in powers of s, valid for large s.

A few comments on the representation (12.8) are appropriate. First, does one know something about the reality properties of $\alpha(t)$ and $\gamma(t)$? If we again refer to potential theory, we recall that the Regge trajectory and residue were real below the scattering threshold (see Chapter 9). Since $t = \bar{s} \leq 0$ in the s-channel physical region, it seems reasonable to assume that $\alpha(t)$ is real there. The argument is not straightforward, though, since $\bar{s} \leq 0$ corresponds to $E_t = \sqrt{\bar{s}}$ being complex. We shall not enter into a discussion but only mention that for boson trajectories the assumption that Im $\alpha(t) = 0$ for $t \leq 0$ seems to be all right, while for a fermion trajectory it certainly is not. We shall assume $\alpha(t)$ to be real in Eq. (12.8) unless we explicitly state otherwise.

Concerning $\gamma(t)$, it is related to the residue $R = R(E_t)$ by factors $[\kappa(t), \sqrt{t}\, k_t^{-1}$, etc.] which are real for $t \leq 0$ if $\alpha(t)$ is real; cf. Eqs. (9.3), (9.22), (12.1) and (12.3). Moreover, in potential theory the residue R is real below the scattering threshold [see point (iii), page 3-107]. In the same spirit in which $\alpha(t)$ was assumed real, one also assumes $\gamma(t)$ to be real for $t \leq 0$ [cf. also point (ii) below].

When deriving the high-energy form (12.8) we neglected exchange forces. They imply, from Eq. (10.11), that we must consider $P_\alpha(-\cos\Theta_t) + \tau P_\alpha(\cos\Theta_t)$

instead of $P_\alpha(-\cos\Theta_t)$ in Eq. (12.1); $\tau = \pm 1$ is the signature of the Regge pole $\alpha(t)$. In a straightforward way the high-energy approximation then reads

$$P_{\alpha(t)}(-\cos\Theta_t) + \tau P_{\alpha(t)}(\cos\Theta_t) \approx \kappa(t)\left[\left(\frac{s}{s_0}\right)^{\alpha(t)} + \tau\left(-\frac{s}{s_0}\right)^{\alpha(t)}\right] = \tag{12.9}$$

$$= \kappa(t)[1 + \tau \exp\{-i\pi\alpha(t)\}]\left(\frac{s}{s_0}\right)^{\alpha(t)} .$$

The fact that $(-)^{\alpha(t)}$ here equals $\exp[-i\pi\alpha(t)]$, and not $\exp[i\pi\alpha(t)]$, can only be proved by considering how the analytic continuation from the t-channel to the s-channel physical region is performed. Thus, the occurrence of exchange forces simply implies the extra parenthesis in Eq. (12.9). It is so important that one introduces a special notation for it, taken together with the factor $\sin\pi\alpha(t)$ of Eq. (12.8):

$$\zeta(t) = \frac{1 + \tau \exp\{-i\pi\alpha(t)\}}{\sin\pi\alpha(t)} . \tag{12.10}$$

One calls $\zeta(t)$ the "signature factor".

Summarizing, the Regge pole model implies a representation of the high-energy scattering amplitude that reads

$$T(s,t) = \gamma_1(t)\zeta_1(t)\left(\frac{s}{s_0}\right)^{\alpha_1(t)} + \gamma_2(t)\zeta_2(t)\left(\frac{s}{s_0}\right)^{\alpha_2(t)} + \tag{12.11}$$

$$+ \gamma_3(t)\zeta_3(t)\left(\frac{s}{s_0}\right)^{\alpha_3(t)} + \ldots ,$$

where:

i) $\alpha(t)$ is the trajectory of the t-channel Regge pole continued into the s-channel, i.e., the <u>exchanged Regge trajectory</u>; $\alpha(t)$ is assumed real for a boson trajectory.

ii) $\gamma(t)$ is the residue function; it is assumed real for a boson trajectory. In fact, assuming the high-energy form (12.11) with $\alpha(t)$ real, the reality of $\gamma(t)$ can be strictly proved from general principles of quantum field theory [see, for example, Van Hove's lecture notes, report CERN 65-22 (1965), Chapter IV]. In this proof, the signature concept is crucial.

iii) $\zeta(t)$ is the signature factor

$$\zeta(t) = \begin{cases} \dfrac{1}{\sin \frac{\pi}{2}\alpha(t)} \exp\left\{-i\frac{\pi}{2}\alpha(t)\right\} & \text{for} \quad \tau = + \\ \\ \dfrac{i}{\cos \frac{\pi}{2}\alpha(t)} \exp\left\{-i\frac{\pi}{2}\alpha(t)\right\} & \text{for} \quad \tau = - \,. \end{cases} \tag{12.12}$$

In particular, since both $\alpha(t)$ and $\gamma(t)$ are real, the phase of the contribution from one Regge pole of definite signature is uniquely related to its energy dependence.

The form (12.11) will from now on form the basis for our discussions.

We stress once more that the amplitude (12.11) is obtained by representing the t-channel amplitude as a sum of Regge poles. In that channel, the Regge trajectory is connected to bound states or resonances. In the amplitude it shows the dependence on $\cos \Theta_t$ through the Legendre functions. When continued to the physical region of the s-channel, in particular to high energy, the same Regge trajectory now tells the energy dependence, since $\cos \Theta_t$ is related to the s-channel energy. This property is illustrated in Fig. 12.2. In particular, a Regge trajectory $\alpha(t)$ is directly accessible to experiment at $t > \bar{s}_{th}$ only when it increases through a positive integer subjected to the $\Delta\ell = 2$ rule, but for (in principle) all values $t \leq 0$.

We now also see an important point where the Regge pole model differs from the one particle exchange model. In the latter, the energy dependence in the s-channel was given by $P_\ell(\cos \Theta_t) \sim s^\ell$, with ℓ equal to the angular momentum of the exchanged particle. For example, an A_2-exchange model for

the reaction $\pi^- p \to \eta n$ implies an amplitude behaving like s^2. In other words, the OPE model can be looked upon as a Regge pole model in which the Regge trajectory is constant = ℓ. For $\ell \geq 2$ this certainly disagrees with the theoretical and experimental findings. Only the fact that a Regge trajectory is allowed to vary with t in proceeding from the t- to the s-channel removes this discrepancy.

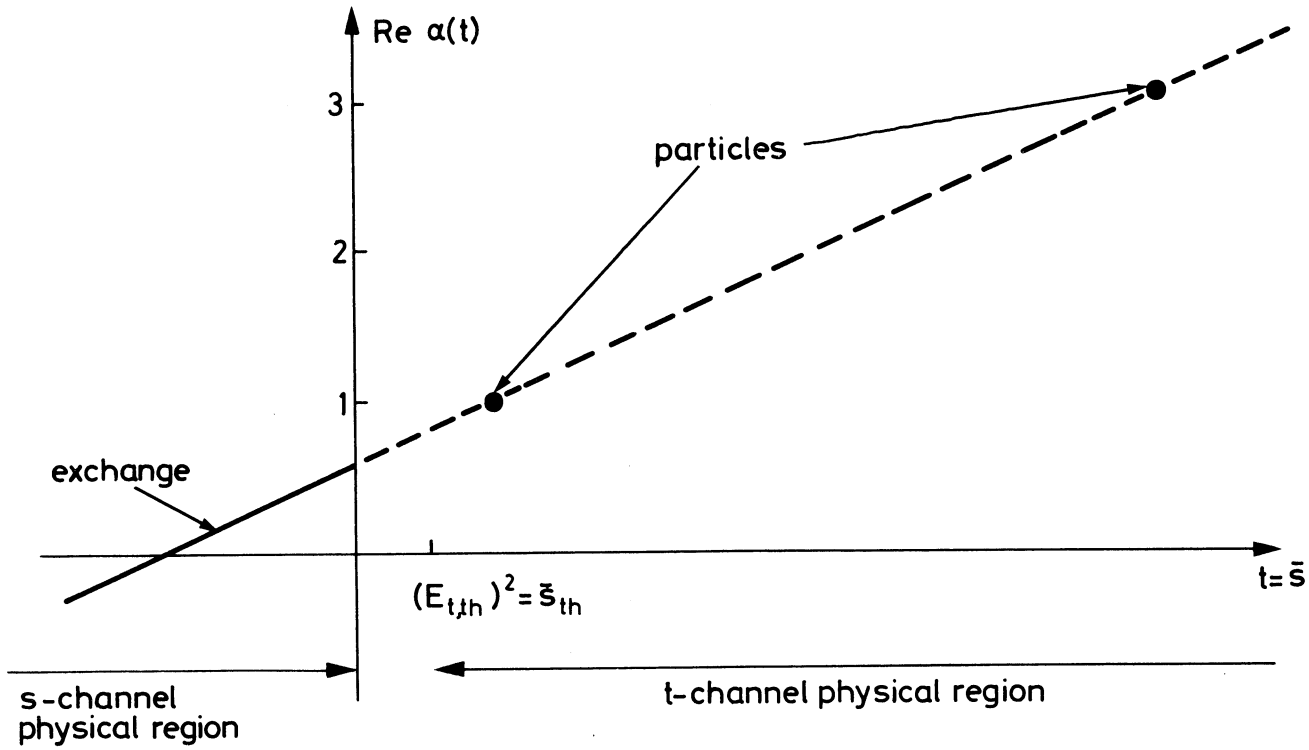

Fig. 12.2

The Chew-Frautschi diagram for an odd-signature straight-line trajectory which gives particles of spin 1 and 3 in the t-channel physical region, and which can be exchanged in the s-channel physical region. $E_{t,th}$ is the threshold energy for the t-channel reaction.

CHAPTER 13 - TOTAL CROSS-SECTIONS AND THE P-, P'- AND ρ-TRAJECTORIES

Equipped with the form (12.11) for the high-energy scattering amplitude, and its interpretation as contributions from different exchanged Regge poles, let us now turn to a more phenomenological discussion. Consider the total cross-section. The optical theorem (3.36) reads

$$\sigma_{tot} = \frac{1}{s} \text{Im } T_{el}(s, t = 0) \qquad (s \text{ large}) \ . \tag{13.1}$$

Consequently, only the values of the Regge pole parameters $\alpha(t)$ and $\gamma(t)$ at $t = 0$ matter, and we need for the time being not be concerned with their t-dependence. Let us first assume very high energy so that only $\alpha_1(t = 0)$, the Regge trajectory with the largest $t = 0$ intercept (the leading or "top-ranking" trajectory) contributes. If it is to reproduce the constancy of the total cross-sections (remember the Froissart bound), we must require

$$\alpha_1(0) = 1 \ . \tag{13.2}$$

What could be the signature of this trajectory? If it had $\tau_1 = -$, then the signature factor (12.12) would have a pole at $t = 0$, since $\cos(\frac{1}{2}\pi) = 0$. To avoid this, one assumes $\tau_1 = +$. We shall in a moment give another and better motivation for this assignment. We note in passing that the positive signature property and $\alpha_1(0) = 1$ implies a purely imaginary forward amplitude, in agreement with what is expected from the data (see Chapter 6, in particular Figs. 6.4-6.5).

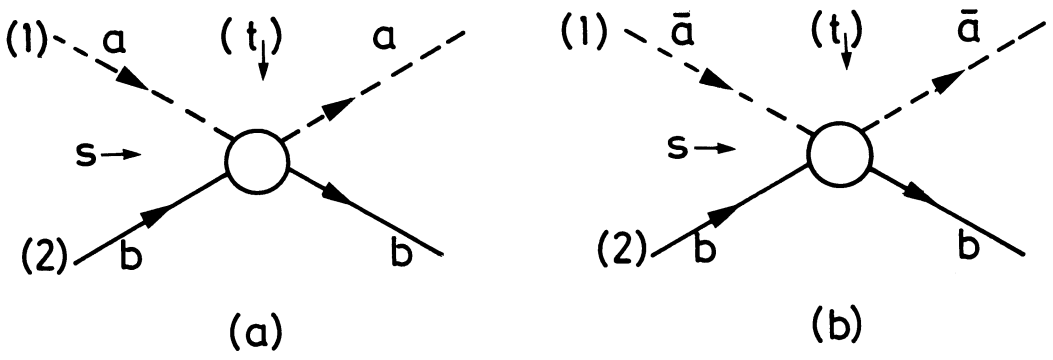

Fig. 13.1

Comparing the two reactions (a) $ab \to ab$ and (b) $\bar{a}b \to \bar{a}b$.

One calls this trajectory the Pomeranchuk trajectory, since it assures the validity of the Pomeranchuk theorem, which says that $\sigma_{tot}(ab)$ and $\sigma_{tot}(\bar{a}b)$ must become equal at asymptotic energies. This comes about as

follows. The t-channel reaction for ab → ab is $a\bar{a} \to \bar{b}b$, while for the process $\bar{a}b \to \bar{a}b$ it is $\bar{a}a \to \bar{b}b$ (see Fig. 13.1). Thus the t-channel reactions are the same except for one thing: the scattering angle Θ_t in the t-channel c.m.s. is always defined as the angle between the momenta of particles (1) and (2) of Fig. 13.1. But it means only that $\cos \Theta_t$ changes to $-\cos \Theta_t$ when going from Fig. 13.1 (a) to (b). Now, since a positive signature amplitude is symmetric as a function of $\cos \Theta_t$, containing as it does $P_\alpha(-\cos \Theta_t) + P_\alpha(\cos \Theta_t)$, the contribution of such a Regge pole to ab and $\bar{a}b$ elastic scattering is indeed the same. In summary, only a positive signature Pomeranchuk trajectory can account for the asymptotic equality of $\sigma_{tot}(ab)$ and $\sigma_{tot}(\bar{a}b)$. This is the most correct argument for the positive signature assignment of the Pomeranchuk trajectory.

In passing we note that a negative signature trajectory gives an amplitude that is antisymmetric in $\cos \Theta_t$, so it is equal in magnitude but has opposite sign for ab → ab and $\bar{a}b \to \bar{a}b$. Moreover, exactly the same argument can be applied to any two-body reaction ab → cd and its "crossed reaction" $\bar{c}b \to \bar{a}d$. This property of a Regge amplitude is sometimes called "line reversal". It is a direct consequence of the signature concept and crossing symmetry.

So, the Pomeranchuk pole $\alpha_P(t)$ must have positive signature. What other quantum numbers does it carry? Obviously, it must have baryon number B = 0 and strangeness S = 0 in order to be exchanged in an elastic reaction. It must have positive G-parity in order to contribute to pion-nucleon scattering. Its isospin could a priori be 0 or 1, but since it could give a $\pi\pi$-resonance with $\ell = 2$ (recall $\tau_P = +$), it must have I = 0; actually, the I = 0 assignment can be proved without invoking the occurrence of a particle on the trajectory. In summary, P has all the quantum numbers of the vacuum, except spin, so it is an example of a "vacuum trajectory". This property allows it to be exchanged in <u>all</u> elastic reactions.

From experiment we know that the total cross-sections are not constant at present accelerator energies. In the Regge pole model expression (12.11) this means that other trajectories besides $\alpha_1 = \alpha_P$ must be taken into account. Consider in particular pion-nucleon scattering. The $\pi^{\pm}p$ total cross-sections are given in Fig. 5.1. Here one needs at least two more trajectories. First, a negative signature one, contributing with different

signs to π^+p and π^-p scattering, in order to explain the finite difference $\sigma_{tot}(\pi^-p) - \sigma_{tot}(\pi^+p)$. This trajectory is identified with the ρ-trajectory, and has $\alpha_\rho(0) \approx 0.6$ as we shall discuss in more detail below. Second, one needs one more vacuum trajectory to explain the energy variation of $\sigma_{tot}(\pi^-p) + \sigma_{tot}(\pi^+p)$, to which the ρ-trajectory does not contribute. In other words, one must explain the fact that both cross-sections seem to approach their common Pomeranchuk limit from above. This trajectory is called P' ("Pomeranchuk prime") and has $\alpha_{P'}(0) \sim 0.7$. With these three trajectories, P, P' and ρ, one is able to reproduce the $\sigma_{tot}(\pi^\pm p)$ data very well, so no further trajectories are needed. Moreover, the ratios $\mathrm{Re}\ T_{el}(s, t = 0)/\mathrm{Im}\ T_{el}(s, t = 0)$ are also accounted for by these three exchanged Regge poles.

Are there any particles on these trajectories? Evidently, the ρ-trajectory is associated with the ρ-meson and, possibly, the g-meson as previously discussed in Chapter 10 (see in particular Figs. 10.1 and 10.3). Both P and P' could give mesons having $I = S = 0$, $G = +$ and spin-parity 2^+, $4^+, \ldots$. Indeed, there are two isoscalar mesons in the 2^+ nonet, $f_0(1250)$ and $f_0'(1500)$ (see Fig. 10.3). It seems more or less a matter of taste if one associates these with P and P'. Indeed, a straight-line trajectory would have a slope of $\sim 0.6\,(\mathrm{GeV})^{-2}$ if P is associated with f_0, of $\sim 0.8\,(\mathrm{GeV})^{-2}$ if f_0 lies on the P'-trajectory, and $\sim 0.6\,(\mathrm{GeV})^{-2}$ if P' is associated with f_0'. Now, as we shall see, it seems as if the slope of $\alpha_P(t)$ for $t < 0$ is still smaller [$\sim 0.3\,(\mathrm{GeV})^{-2}$ or less], so usually P is not associated with either f_0 or f_0'. Then P' could best be associated with f_0, since this would imply a slope of the trajectory nearest to the slopes for the ρ-, A_2- and fermion trajectories.

CHAPTER 14 - PION-NUCLEON ELASTIC AND CHARGE-EXCHANGE SCATTERING

Later on, we shall briefly discuss σ_{tot} also for NN, $\bar{N}N$, KN and $\bar{K}N$ collisions. Let us, however, first consider πN scattering also away from $t = 0$. Then things become more complicated. In fact, with P, P' and ρ contributing, the $\pi^\pm p$ elastic amplitudes are

$$T_{el;\,\pi^\pm p}(s, t) = P + P' \pm \rho \ . \qquad (14.1)$$

Here, each Regge contribution is a shorthand notation for $\gamma(t)\zeta(t)(s/s_0)^{\alpha(t)}$. Note that the ρ-trajectory, having negative signature, contributes with different signs to the $\pi^{\pm}p$ amplitudes. To be able to calculate $d\sigma_{el}/dt$, one must now know the trajectories and the residue functions as functions of t. The Regge pole model predicts essentially nothing concerning this t-dependence, so ignorance must be compensated for by assumptions. We shall return to these problems later.

It is evident that the complications mentioned are less severe if only one Regge pole contributes. With the Ansatz (14.1), this is the case for the charge exchange reaction $\pi^- p \to \pi^0 n$ [cf. Eq. (7.3)]

$$T_{c.e.}(s,t) = \frac{1}{\sqrt{2}} [T_{el;\pi^+p} - T_{el;\pi^-p}] = \sqrt{2}\,\rho \ . \tag{14.2}$$

Consequently

$$\frac{d\sigma_{c.e.}}{dt} = D(t) \left(\frac{s}{s_0}\right)^{2\alpha_\rho(t)-2} , \tag{14.3}$$

where D(t) comprises the t-dependence of $\sqrt{2}\gamma_\rho(t)$ and $\zeta_\rho(t)$ as well as a $(16\pi)^{-1}$ arising from the expression (3.23) for the differential cross-section. We emphasize that D(t) is an essentially unknown quantity from the theoretical point of view.

Still, the form (14.3) implies a non-trivial prediction, viz., the shrinkage of the forward charge-exchange peak. This may be seen as follows. Let us for simplicity assume a linear ρ-trajectory

$$\alpha_\rho(t) = \alpha_\rho(0) + t\,\alpha_\rho' , \tag{14.4}$$

where α_ρ' is $\sim 1\,(\mathrm{GeV})^{-2}$; what is actually needed for the discussion here is a trajectory that <u>increases</u> with t. It follows that

$$\left(\frac{s}{s_0}\right)^{2\alpha_\rho(t)-2} = \left(\frac{s}{s_0}\right)^{2\alpha_\rho(0)-2} \exp\left[2t\,\alpha_\rho' \log\frac{s}{s_0}\right] . \tag{14.5}$$

Now, the exponential factor here is the only one in the expression (14.3) for the cross-section that has a mixed s- and t-dependence. Neglecting the other factors, it implies at fixed s an exponentially decreasing cross-section as a function of $|t|$. Its slope, however, equals $2\alpha_\rho' \log (s/s_0)$ with $\alpha_\rho' > 0$, which increases with s and implies a peak that shrinks with energy. If the possible t-dependence of D(t) is taken into account this shrinkage could become superimposed upon an energy-independent "background peak", but the essence of the argument would still be true. Of course, it could happen that the background is so large that it more or less masks the shrinkage. In summary, a reaction which is dominated by the exchange of one Regge pole, the trajectory of which increases with t, will have an exponentially peaked cross-section that shrinks with energy.

How does this prediction match the experimental data? From Fig. 7.1 one sees indeed a shrinkage, albeit rather weak. Besides the influence of an energy-independent background peak, one must in this context also keep in mind that s changes only by a factor of ~ 2 when p_{lab} increases from ~ 4 GeV/c to ~ 18 GeV/c, so log s merely changes by a factor of ~ 1.6. Logarithmic variations are always very weak.

Actually, what one does is to consider

$$\log \left(\frac{d\sigma_{c.e.}}{dt} \right) = \log D(t) + [2\alpha_\rho(t) - 2] \log \frac{s}{s_0} \qquad (14.6)$$

as a function of log s at fixed t. In this way one may directly determine $\alpha_\rho(t)$ experimentally. The result is shown in Fig. 10.3. A very good parametrization of the trajectory is given by

$$\alpha_\rho(t) = 0.57 + 0.91\, t, \quad 0 \leq -t \leq 1\ (\text{GeV/c})^2 \ . \qquad (14.7)$$

It extrapolates to $\alpha_\rho[t = (760\ \text{MeV})^2] = 1.09$; alternatively, $\alpha_\rho(t) = 1$ for $t = (690\ \text{MeV})^2$.

Summarizing, the Regge pole model seems to give good agreement with the differential cross-section data for pion-nucleon charge exchange, assuming exchange of the ρ-trajectory having a constant slope. The trajectory extrapolates (approximately) to the position of the ρ-meson.

Let us just in passing note that another case where only one trajectory is expected to contribute is the reaction $\pi^- p \to \eta n$. As in the OPE model, among the established bosons only the A_2-trajectory could be exchanged. The Regge pole model then predicts a cross-section for η-production of the same form (14.3) as the charge exchange one. One could thus derive $\alpha_{A_2}(t)$ for $t < 0$ directly from the data. The A_2-trajectory determined in this way is also shown in Fig. 10.3. Note that $\alpha_{A_2}(t)$ seems to have a curvature, i.e., a varying slope. Caution is needed, though, since the data have rather large errors.

As soon as several trajectories contribute to a particular cross-section, the problem of shrinkage is no longer theoretically clear-cut. In fact, due to compensation between different Regge pole contributions, one may over a limited energy interval reproduce a constant slope of the forward cross-section, and even an expanding forward peak. However, the absence of an appreciable shrinkage for the $\pi^{\pm} p$ elastic diffraction peaks at the highest energies considered so far seems to indicate that the Pomeranchuk trajectory, which should more or less dominate here, has a fairly gentle slope, $\alpha_P' \lesssim 0.3\,(\mathrm{GeV})^{-2}$.

Historically, the first Regge pole boom in 1961-1962 was largely due to the shrinkage experimentally found in pp elastic scattering. When, however, πp showed no shrinkage, and $\bar{p}p$ even showed antishrinkage, i.e., expanding diffraction peak, the Regge pole model fell into disgrace. It should be clear from what we have said, though, that shrinkage or non-shrinkage in a limited s-interval for a reaction where several trajectories can be exchanged is really not a crucial test of the Regge pole model.

Since the Regge pole model seems to work well for the charge-exchange cross-section, it is really worthwhile to develop it further, in particular to take the so far neglected spin-complications into account. This will allows discussion of, for example, the polarization. One must now consider two amplitudes, the spin-non-flip one, G, and the spin-flip one, H. In the Regge pole model they should be obtained from the t-channel reaction $\pi^- \pi^0 \to \bar{p}n$, for which there are also two amplitudes. Namely, for each ℓ-value the $\bar{p}n$ system can be in a triplet or in a singlet spin state. Moreover, the situation is complicated by the fact that one must use relativistic amplitudes, not the "non-relativistic" G and H, in order to be able to formulate the crossing relations properly.

We shall not derive the expressions for G and H in the Regge pole model, but merely state the results and give some plausibility arguments for them. The 1966 Erice lecture notes by R.J.N. Phillips quoted in the bibliography may be consulted for some more details. The result reads, under the assumption that only one Regge pole contributes

$$8\pi\sqrt{s}\, G(\cos\Theta, E) = g(t)\zeta(t)\left(\frac{s}{s_0}\right)^{\alpha(t)} \tag{14.8}$$

$$8\pi\sqrt{s}\, H(\cos\Theta, E) = \sqrt{-t}\, h(t)\zeta(t)\alpha(t)\left(\frac{s}{s_0}\right)^{\alpha(t)} . \tag{14.9}$$

As before, the function $\zeta(t)$ is the signature factor, while $g(t)$ and $h(t)$ are residue functions. The extra factors $8\pi\sqrt{s}$ in front of G and H convert them into relativistic amplitudes. Note that G takes the same form as if the particles had zero spins; this is not unreasonable, since G has the same partial wave expansion as had the amplitude F previously. However, this argument is dubious, to say the least, since the Regge pole expression originates from considerations of the t-channel partial wave expansion. On the other hand, there are two extra factors, $\sqrt{-t}$ and $\alpha(t)$, in the expression for H as compared to G. The factor $\sqrt{-t}$ is explicitly extracted, since H is proportional to $\sin\Theta \propto \sqrt{-t}$ (Θ is the s-channel scattering angle); in other words, $\sqrt{-t}$ assures the vanishing of H in the very forward direction. The factor $\alpha(t)$ comes about as follows. The t-channel amplitude from which H is obtained by crossing symmetry has, like H itself, a partial wave expansion in terms of $\sin\Theta_t P'_\ell(\cos\Theta_t)$. The RSW representation therefore contains $\sin\Theta_t\, P'_{\alpha(t)}(-\cos\Theta_t)$. At high energy

$$\sin\Theta_t = \sqrt{1-\cos^2\Theta_t} \sim \cos\Theta_t \sim s\ , \quad s \text{ large}\ , \tag{14.10}$$

$$P'_\alpha(-\cos\Theta_t) = \frac{d}{d(\cos\Theta_t)} P_\alpha(-\cos\Theta_t) \sim \frac{d}{ds}\, s^\alpha = \alpha s^{\alpha-1}\ , \quad s \text{ large}\ . \tag{14.11}$$

This explains the factor $\alpha(t)(s/s_0)^{\alpha(t)}$ in H.

We note two important features of the amplitudes (14.8), (14.9):

i) the spin-non-flip and the spin-flip amplitudes have the same energy dependence;

ii) if $\alpha(t)$ is assumed to be real, the residue functions $g(t)$ and $h(t)$ are both real. The phases of G and H are thus the same, since they are both given by the signature factor $\zeta(t)$.

The cross-section obtained from the amplitudes (14.8), (14.9) reads

$$\frac{d\sigma}{dt} = \frac{1}{16\pi} |\zeta(t)|^2 \left[|g(t)|^2 + (-t)\alpha(t)^2 |h(t)|^2 \right] \left(\frac{s}{s_0}\right)^{2\alpha(t)-2} , \qquad (14.12)$$

while the polarization as given by

$$P = \frac{2 \operatorname{Im} GH^*}{|G|^2 + |H|^2} \qquad (14.13)$$

is zero, from point (ii) above.

Let us now apply these results, which are valid for any reaction of spin-parity structure $0^- + \frac{1}{2}^+ \to 0^- + \frac{1}{2}^+$, to the particular reaction $\pi^- p \to \pi^0 n$. The prediction of the ρ-exchange Regge pole model is unambiguous: there should be no charge exchange polarization. Experimentally, $P_{c.e.} \approx 15\%$ even at $p_{lab} \approx 11$ GeV/c (see Fig. 6.9), in definite disagreement with the prediction. We shall in a moment discuss how the theory can be twisted to obtain a non-vanishing polarization.

Before that, however, let us consider the expression (14.12) for the differential cross-section. It is of the general form (14.3), due to point (i) above. Fits to the data reveal that a large spin-flip residue function $h(t)$ is needed in order to reproduce in the simplest way the experimental flattening off at very small t. Actually, one finds that h is comparable in magnitude, or even greater than g. This fact has the following interesting consequence. Due to the factor $\alpha(t)$, the spin-flip term vanishes whenever $\alpha(t) = 0$. For the ρ-trajectory (14.7) this happens at $-t \approx 0.6\,(\mathrm{GeV/c})^2$. One then expects the differential cross-section to show a minimum around $-t = 0.6\,(\mathrm{GeV/c})^2$. This compares very favourably with the experimental findings, Fig. 7.1. In summary,

the dip-secondary bump structure in the pion-nucleon charge exchange differential cross-section is, in the ρ-exchange Regge pole model, explained by the fact that the otherwise large spin-flip amplitude is proportional to $\alpha_\rho(t)$ and therefore vanishes at $-t \approx 0.6\,(\mathrm{GeV/c})^2$ where $\alpha_\rho(t) = 0$.

What could be invoked to explain the non-vanishing polarization in $\pi^- p \to \pi^0 n$? Evidently, if one sticks to the Regge pole model one need something more than pure ρ-exchange. Several suggestions have been put forward, among them:

i) contribution from a secondary trajectory, sometimes referred to as the ρ';
ii) influence of direct channel resonances;
iii) a complex trajectory, $\mathrm{Im}\,\alpha_\rho(t) \neq 0$ for $t < 0$;
iv) contribution from a cut in the angular momentum plane.

We shall briefly discuss the first two possibilities, and refer to the bibliography for further details.

A ρ'-trajectory would add contributions to G and H of the same form as the ρ-trajectory. In an obvious notation we may write

$$G = G_\rho + G_{\rho'} \,, \tag{14.14}$$

$$H = H_\rho + H_{\rho'} \,. \tag{14.15}$$

The polarization then reads

$$P_{c.e.} = \frac{2\ \mathrm{Im}\,[G_\rho H_\rho^* + G_{\rho'} H_\rho^*]}{|G|^2 + |H|^2} \,. \tag{14.16}$$

Remember here that $G_\rho H_\rho^*$ and $G_{\rho'} H_\rho^*$ are both real. Now, $d\sigma_{c.e.}/dt$ is well reproduced by the ρ-term alone. Consequently, $G_{\rho'}$ and $H_{\rho'}$ must be rather small. In particular, one needs $\alpha_{\rho'} < \alpha_\rho$. The polarization may then be written

$$P_{c.e.} \propto \frac{\left(\frac{s}{s_0}\right)^{\alpha_\rho + \alpha_{\rho'}} \sin \pi(\alpha_\rho - \alpha_{\rho'})}{\left(\frac{s}{s_0}\right)^{2\alpha_\rho}} = \left(\frac{s}{s_0}\right)^{\alpha_{\rho'} - \alpha_\rho} \sin \pi(\alpha_\rho - \alpha_{\rho'}) \,. \tag{14.17}$$

Thus, $P_{c.e.}$ is predicted to decrease with energy in this model. For $\alpha_\rho - \alpha_{\rho'} \sim 0.5$ and reasonable ρ' residue functions, the cross-section is virtually the same with and without the ρ'-contribution. The polarization at 6 GeV/c could, however, be 15-20% and will at 11 GeV/c only have decreased by a factor $\sim \frac{3}{4}$. Such a gentle energy-dependence is not ruled out by the present data.

Another explanation invokes direct channel resonances. That is to say, besides the ρ-trajectory exchange one includes contributions from the N* resonances that can be formed by the incident $\pi^- p$ system and decay into the final $\pi^0 n$ state. In other words, one assumes amplitudes of the form

$$F = F_\rho + F_{res} \ , \tag{14.18}$$

(F stands for G and H) where the ρ-contribution is of the forms (14.8), (14.9) while F_{res} is a sum over resonating partial waves in the s-channel. That is, for G_{res} and H_{res} one uses the expressions (4.38), (4.39) with partial wave amplitudes of the Breit-Wigner form [cf. Eqs. (4.63)-(4.65)]

$$f = - \frac{\frac{1}{2}\Gamma_{tot}\sqrt{x_{el} \cdot x_{c.e.}}}{E - E_{res} + i\,\frac{1}{2}\Gamma_{tot}} \ . \tag{14.19}$$

Here, x_{el} is the resonance elasticity and $x_{c.e.}$ the probability for its decay into $\pi^0 n$, related in fact to x_{el} by isospin invariance. If only the well-established resonances of masses $\lesssim 2$ GeV (corresponding to $p_{lab} \lesssim 2$ GeV/c) are used, one obtains a total amplitude $\sqrt{s}\, F_{res}$ behaving like $s^{-\frac{1}{2}}$, if one makes the rather drastic assumption that the form (14.19) extrapolates far away from the resonance position. An argument like the one used above for the ρ'-trajectory shows that the polarization $P_{c.e.}$ now behaves as $s^{-\frac{1}{2} - \alpha_\rho} \sim s^{-1}$, hardly in agreement with experiment. If, on the other hand, one assumes resonances all along the straight line fermion trajectories in Fig. 10.5, there will certainly be resonances even at, say, $p_{lab} = 11$ GeV/c. However, one does not know their elasticities. Arguments based on the experimental values of $(j + \frac{1}{2})x_{el}$, and on the spin assignments of the resonances, indicate an exponential decrease of the elasticities with energy, though. So once more one expects a decreasing polarization, even

if the decrease may be rather gentle. In summary, the ρ + res explanation of the charge exchange polarization is marginally tenable. The non-vanishing, almost energy-independent πN charge-exchange polarization poses great difficulties for the Regge pole model.

To close this chapter, let us return to $\pi^{\pm}$p elastic scattering. As we saw, three Regge poles are needed, the P, P′ and ρ. Even if the trajectories were known as functions of t, one spin-non-flip and one spin-flip residue function for each pole remain unknown. So one assumes some parametrization, in the simplest cases, for instance

$$h(t) = [\alpha(t) + 1]D_0 \exp(D_1 t) . \qquad (14.20)$$

Here we only point out the fact that many unknown parameters are introduced in this way, so one starts to leave even the modest amount of theory one has and approaches curve-fitting. Still, some non-trivial predictions emerge. For example, one finds in fitting $d\sigma_{el}/dt$ for $\pi^{\pm}$p that P and P′ give very small contributions to the spin-flip amplitude. Since ρ has a large spin-flip part, the main contribution to the polarization is given by

$$P_{el} \propto \mathrm{Im}\,[(G_P + G_{P'})H_\rho^*] . \qquad (14.21)$$

Consequently, since the ρ-contribution has opposite signs for π^+p and π^-p, while G_P and $G_{P'}$ stay the same, the model predicts

$$P_{el;\pi^+p} = - P_{el;\pi^-p} . \qquad (14.22)$$

One may even invoke arguments in favour of a positive $P_{el;\pi^+p}$ at small $|t|$. These predictions compare favourably with experiment, Fig. 6.9. Note also that the polarization is predicted to change sign around $-t = 0.6\,(\mathrm{GeV/c})^2$, since H_ρ changes sign here according to the discussion above. This is also in agreement with the experimental data.

CHAPTER 15 - SOME OTHER TWO-BODY AND QUASI-TWO-BODY REACTIONS

In the same manner as πN scattering is discussed, one may treat KN and NN scattering. Consider, for example, NN and $\bar{N}N$ reactions, in particular the four elastic processes pp → pp, pn → pn, $\bar{p}p \to \bar{p}p$ and $\bar{p}n \to \bar{p}n$ as well as the two charge exchange reactions pn → np and $\bar{p}p \to \bar{n}n$, all of which have been measured. Which Regge poles can be exchanged? For the elastic processes one expects, besides P, P′ and ρ, the A_2 (in this context sometimes called the R-trajectory) and also the ω; the last two are excluded from $\pi^{\pm}$p elastic scattering due to G-parity conservation. By considering the appropriate t-channel reactions, one is able to deduce the following results

$$T_{el;\,pp} = P + P' - \omega - \rho + A_2 \,, \tag{15.1}$$

$$T_{el;\,pn} = P + P' - \omega + \rho - A_2 \,, \tag{15.2}$$

$$T_{el;\,\bar{p}p} = P + P' + \omega + \rho + A_2 \,, \tag{15.3}$$

$$T_{el;\,\bar{p}n} = P + P' + \omega - \rho - A_2 \,, \tag{15.4}$$

$$T_{c.e.;\,pn} = -2\rho + 2A_2 \,, \tag{15.5}$$

$$T_{c.e.;\,\bar{p}p} = 2\rho + 2A_2 \,. \tag{15.6}$$

Neglecting spin complications, each pole here contributes the form $\gamma(t)\zeta(t)(s/s_0)^{\alpha(t)}$ to the amplitude. The absolute sign in front of each contribution in these equations is of little importance, since the sign of $\gamma(t)$ is, in general, unknown. What is important, though, is how the sign changes in going from one reaction to another. For example, P and P′ contribute the same amount to all elastic reactions; this is so because they are vacuum trajectories. The ω-trajectory is an isosinglet of negative signature, so it changes sign in going from pp to $\bar{p}p$, and from pn to $\bar{p}n$ elastic scattering. It contributes the same sign to the pp and pn amplitudes, since the t-channel, I = 0, $\bar{N}N$ state is given by the combination $(\bar{p}p + \bar{n}n)/\sqrt{2}$ implying equality of the amplitudes for $\bar{p}p \to \omega \to \bar{p}p$ and $\bar{p}p \to \omega \to \bar{n}n$. On the other hand, since ρ and A_2 have I = 1 and signatures

$\tau_\rho = -$, $\tau_{A_2} = +$, one easily deduces the contributions from these poles. Or, once knowing their contributions to the elastic amplitudes, one may use the results of Exercise 7.2 to obtain the charge exchange amplitudes.

The table yields

$$\sigma_{tot}(pn) - \sigma_{tot}(pp) \propto 2[\text{Im } \rho - \text{Im } A_2] \ , \tag{15.7}$$

$$\sigma_{tot}(\bar{p}p) - \sigma_{tot}(\bar{p}n) \propto 2[\text{Im } \rho + \text{Im } A_2] \ . \tag{15.8}$$

Experimentally (see Fig. 5.1) both these differences are small. Thus, the contribution of the ρ- and A_2-trajectories to the NN and $\bar{N}N$ elastic scattering is small. Then

$$\sigma_{tot}(\bar{p}p) - \sigma_{tot}(pp) \sim 2 \text{ Im } \omega \ . \tag{15.9}$$

Since this difference is large ($\sim$ 20 mb) experimentally according to Fig. 5.1, the ω-trajectory gives an appreciable contribution. Moreover, for the same reason as in πN scattering, both P and P′ must contribute. Thus, in order to treat NN and $\bar{N}N$ elastic scattering one needs at least three trajectories, P, P′ and ω. Observe, though, that in order to treat the charge-exchange reactions one must take also the ρ- and A_2-poles into account. Experiments on σ_{tot} can be fitted with the values for $\alpha_P(0)$ and $\alpha_{P'}(0)$ taken from πN scattering and an ω-intercept of $\alpha_\omega(0) \sim 0.5$.

The discussion of the differential cross-sections is even more involved than in the πN case, since there are now more trajectories contributing and, in a consistent treatment, also several spin amplitudes, actually five for each reaction. We shall not go into details. Let us just remark that one has great difficulties in reproducing the two charge-exchange reactions by the $\rho \pm A_2$ exchange model. Remember here that the pn charge exchange showed a very steep decrease for increasing $|t|$ in the nearly forward direction, while $\bar{p}p$ charge exchange was more "well-behaved" (see Figs. 7.4 and 7.5), features which seem impossible to fit with only ρ and A_2 contributing. Moreover, the energy-dependence of the charge-exchange cross-sections causes troubles. We refer to the bibliography for further reading.

KN and $\bar{K}N$ elastic and charge exchange reactions can also be treated in the same way. One finds the same five trajectories contributing here as in the nucleon-nucleon processes. We shall not enter into the details but again refer to the bibliography for those interested.

Many inelastic reactions have also been treated in the Regge pole model. In fact, we have already discussed the charge-exchange processes and η-production in $\pi^- p$ collisions. One could proceed to treat associated production (strange meson exchange), backward scattering (baryon exchange) and resonance production processes in meson-nucleon collisions, photoproduction of mesons, etc. In general, the Regge pole model replaces the one-particle exchange model for these inelastic reactions. Note in particular the different criteria for the exchanged object in the two models. In the OPE model, implying an amplitude proportional to $(t - m_e^2)^{-1}$ with m_e the mass of the exchanged particle, exchange of the lightest particle is thought to dominate. In the Regge pole model, on the other hand, the trajectory with largest $\alpha(t)$ dominates at high energy. These two prescriptions very often give different results. For example, π-exchange should play a minor role in the Regge pole model, while it is supposed to give the main contribution in the OPE model as soon as it can be exchanged.

The prescription for the Regge pole model is thus that any trajectory which may contribute to a particular reaction also should be exchanged. This "universality principle" for Regge trajectories implies, among other things, that reactions which are dominated by the exchange of the same Regge pole should have the same energy dependence. Let us see how this prediction works in a few examples.

If the Pomeranchuk trajectory can be exchanged in an inelastic reaction, the cross-section should remain constant. Examples of such reactions are $pp \to pN^*_{1/2}$, where the P-trajectory is indeed allowed and which, from Fig. 7.11, seem to show an almost energy-independent cross-section. Note that P cannot contribute to $pp \to pN^*_{3/2}$, which requires exchange of an object with I = 1. We also note that the spins and parities of those $N^*_{1/2}$ that have a constant production rate are $1/2^+$, $3/2^-$ and $5/2^+$, so the P-exchange just conserves the relation $j = \ell - 1/2$, merely adding some units of orbital angular momentum (0, 1 and 2, respectively), when transforming the incoming proton into an outgoing $N^*_{1/2}$. The theoretical basis for this empirical rule is not well understood.

The charge exchange reactions, being dominated by ρ- and A_2-exchange, should show forward cross-sections with an energy dependence

$$\frac{d\sigma_{c.e.}}{dt}(t = 0) \sim \frac{1}{s^2}\, s \sim s^{-1} \sim p_{lab}^{-1} \qquad (15.10)$$

in rough agreement with the experimental findings.

In associated production processes, the exchanged object is one of the strange mesons $K^*(890)$ and $K^*(1400)$. A straight-line extrapolation from the position of these resonances to the $t \leq 0$ region, assuming a trajectory slope of $\sim 1\,(GeV)^{-2}$, leads to $\alpha_{K^*}(0) \sim 0.2$, implying a forward differential cross-section behaving like $\sim p_{lab}^{-1.6}$. The present experimental data do not allow a stringent test of this prediction.

The reactions $\pi^{\pm} p \to \rho^{\pm} p$ may have ω- and A_2-exchange dominating, while $\pi^- p \to \rho^0 n$ allows only A_2-exchange. The energy-dependence of the forward cross-section predicted from ω- and/or A_2-exchange is $\sim p_{lab}^{-1}$, while the experimental finding is $\sim p_{lab}^{-2}$, the errors being rather large, though. Moreover, ω or A_2-exchange will give predictions for the decay distribution of the outgoing ρ-meson which are not in agreement with the data; besides, these decay distributions seem experimentally the same for $\rho^{\pm}$ and ρ^0 production, again within experimental uncertainties. Thus, the ρ-production processes seem to cause troubles to the Regge pole model. In fact, these reactions are excellently accounted for by the OPE model, assuming pion exchange and so-called absorptive corrections.

CHAPTER 16 - FURTHER PROPERTIES OF THE REGGE POLE MODEL

In this chapter we collect some more or less disconnected theoretical topics, related to the discussion of high-energy reactions in the Regge pole model. The treatment here is more condensed than in previous chapters.

16.1 Factorization

One characteristic property of the OPE model is the occurrence of two coupling constants, one related to the vertex aec (see Fig. 16.1) the other to the vertex bed. Indeed the OPE model amplitude is proportional to $g_{aec}\, g_{bed}$, i.e., it "factorizes" into one contribution from each vertex.

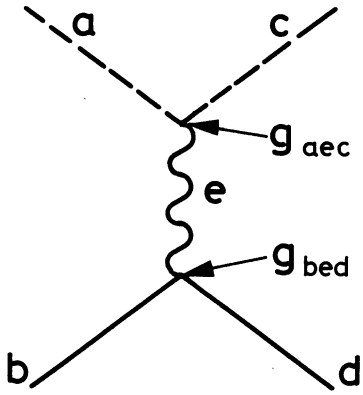

Fig. 16.1

An illustration of the factorization in the OPE model.

A similar factorization property can be proved for the one-pole contribution

$$\gamma(t)\zeta(t)\left(\frac{s}{s_0}\right)^{\alpha(t)} \tag{16.1}$$

to the amplitude in the Regge pole model. More precisely, it turns out that the residue function $\gamma(t)$ can be written

$$\gamma(t) = (\text{known kinematical factors})\gamma_{aRc}(t)\gamma_{bRd}(t)\,. \tag{16.2}$$

Here, $\gamma_{aRc}(t)$ refers to the coupling of the Regge pole R to the t-channel initial state $a\bar{c}$, while $\gamma_{bRd}(t)$ refers to the coupling of R to $\bar{b}d$.

The practical importance of this factorization property lies in the fact that one and the same Regge pole coupling $\gamma_{aRc}(t)$ may occur in different reactions, since it is independent of how the Regge pole couples to the other two particles. Let us illustrate this property by an example. Consider pp, πp and $\pi\pi$ elastic scattering and assume asymptotic energies so that only the P trajectory contributes. The factorization principle implies

$$T_{el;pp} \propto \gamma_{pPp}\,\gamma_{pPp} \ , \tag{16.3}$$

$$T_{el;\pi p} \propto \gamma_{\pi P\pi}\,\gamma_{pPp} \ , \tag{16.4}$$

$$T_{el;\pi\pi} \propto \gamma_{\pi P\pi}\,\gamma_{\pi P\pi} \ , \tag{16.5}$$

which yield the relation

$$\sigma_{tot}(pp)\sigma_{tot}(\pi\pi) = [\sigma_{tot}(\pi p)]^2 \ , \tag{16.6}$$

between the total cross-sections, and a similar relation for the elastic ones. Although this is a pretty safe theoretical prediction, the $\pi\pi$ cross-section not being measured so far, it is by no means uninteresting. For example, it could happen that $\sigma_{tot}(\pi\pi)$ may be within reach in an intersecting storage rings arrangement.

The factorization property has further important consequences. As in the OPE model, one may use different internal symmetry schemes, such as isospin invariance, SU(3) etc., to relate the coupling of one exchanged object to different members of the multiplets. For example, once knowing how the ρ-trajectory couples to the t-channel state $\pi^-\pi^0$, one may use SU(3) Clebsch-Gordan coefficients to obtain its coupling to the $K^-\bar{K}^0$ state, assuming of course that SU(3) is a good symmetry. This reduces the number of arbitrary functions needed in a phenomenological fit. Other applications of the factorization principle occurs in, for example, considerations of different polarization parameters in NN scattering, since the factorization refers not only to coupling of a Regge pole to different particles but also to different spin states of the same particles. It will take us much too far to go into details here, and we refer to the bibliography for further studies. We only emphasize that factorization is a property of a one-Regge-pole contribution. As soon as several trajectories are exchanged, there is, in general, no clear-cut prediction from this principle.

16.2 Ghosts

Consider the signature factor $\zeta(t)$ for, say, a positive signature Regge trajectory

$$\zeta(t) = \left[\sin\frac{\pi}{2}\alpha(t)\right]^{-1} \exp\left[-i\frac{\pi}{2}\alpha(t)\right], \qquad \tau = + \ . \tag{16.7}$$

This factor has a pole for $\alpha(t) = 0$. If this happens for t greater than zero, it gives a bound state. However, it cannot be tolerated for $t \leq 0$, since it would mean an infinite differential cross-section at that t-value. One way to get rid of the undesired pole (the "ghost") is to assume that the residue function $\gamma(t)$ is proportional to $\alpha(t)$

$$\gamma(t) = \alpha(t)[\alpha(t)+1]\tilde{\gamma}(t) \ . \tag{16.8}$$

It is then the factor $\tilde{\gamma}(t)$ which obeys the factorization principle (16.2). Here, we also extracted a factor $\alpha(t)+1$. This is not needed to kill any ghost, like the factor $\alpha(t)$ is. However, one may show that it still has to be there, the reason being that the residue function must vanish at $\alpha(t)$-values which are symmetric with respect to $\alpha(t) = -\frac{1}{2}$. It produces a zero in the amplitude, which should be detectable as a minimum (if other poles contribute) in the cross-section.

16.3 Fermion Regge poles. Daughter trajectories and conspiracy

A fermion Regge pole is expected to contribute to, for example, backward πN elastic and charge-exchange scattering. As already mentioned, one peculiar property of a fermion trajectory is that it is complex for $t \leq 0$. As a consequence, one does not have the simple relation between the trajectory and the phase of the amplitude that one had for a real trajectory, and one does expect a non-vanishing polarization even if only one Regge pole contributes. In fact, one may show that if a fermion trajectory $\alpha_f(t)$ contributes to a particular scattering process, so does its complex conjugate trajectory, $\alpha_f(t)^*$.

There is one more hitherto overlooked characteristic of πN backward scattering which is merely due to kinematical considerations. This property is shared by all reactions that do not have the masses pairwise equal as in elastic scattering. It comes about as follows. Consider $\pi^- p \to \pi^0 n$

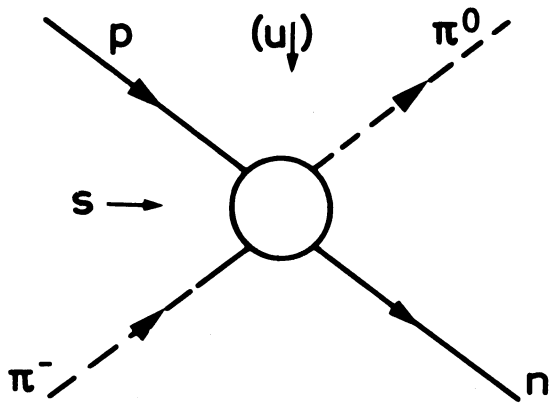

Fig. 16.2

The s- and the u-channels for
pion-nucleon charge-exchange scattering.

backward scattering, as illustrated in Fig. 16.2. We adopt here the usual convention to call the u-channel that channel in which the RSW representation of the scattering amplitude is performed. For our purpose this is merely a matter of notation, but the reason is that the t-channel is reserved for the reaction $\pi^-\pi^0 \to \bar{p}n$. In the u-channel, the variable s is a momentum transfer variable. Defining the u-channel scattering angle Θ_u to be the one between the incoming proton momentum and the outgoing positive pion momentum, one easily derives [cf. Eq. (2.9)]

$$s = -2k_u^2(1 - \cos\Theta_u) \tag{16.9}$$

where

$$k_u^2 = \frac{1}{4u}\lambda(u, m^2, M^2) \ . \tag{16.10}$$

Consequently

$$\cos\Theta_u = 1 + \frac{2u}{\lambda(u, m^2, M^2)}\, s \tag{16.11}$$

It is this variable that appears as an argument in the Legendre functions when the RSW representation of the u-channel amplitude is analytically continued to the s-channel. But in the backward direction of the s-channel, the variable u can take the value zero and may even be positive

(cf. Figs. 6.10, 6.11 and Exercise 2.6). It follows that $\cos\Theta_u$ does not become large as s tends to infinity if $u = 0$. In fact, for any finite s, however large, there is always an interval in u near to the backward direction where $\cos\Theta_u$ is bounded. The high-energy approximation corresponding to Eq. (12.3) can then not be derived in a straightforward way.

Still, it could happen that the characteristic behaviour $(s/s_0)^{\alpha(u)}$ is valid even at $u = 0$, only that it must be derived in another way. A simple continuity argument supports this suggestion: if the form $(s/s_0)^{\alpha(u)}$ is valid for $u < 0$, it is not unlikely to be true also for $u = 0$. To give a more convincing argument requires much more involved thinking. In fact, one may prove that the suggestion is true.

This has a very interesting consequence, though. Namely, in order to arrange the Regge pole behaviour, one must assume the occurrence of so called daughter trajectories. This amounts to the following. Let $\alpha_0(u)$ be the trajectory that is assumed responsible for the backward scattering. The correct Regge behaviour is obtained only if this pole is accompanied by another trajectory, $\alpha_1(u)$ of opposite signature to $\alpha_0(u)$ and such that $\alpha_1(u = 0) = \alpha_0(u = 0) - 1$. This pole is called the first daughter trajectory to $\alpha_0(u)$; it has also a daughter, etc. This set of trajectories gives a contribution to the amplitudes which individually do not have the desired energy-behaviour but which add in such a way as to produce the Regge pole form for the amplitude. The fundamental reason for this compensation is the requirement that the Regge pole contribution to the scattering amplitude should fulfil the analyticity properties implied by the Mandelstam representation. An analogous situation occurs in, for example, N-N scattering. Here, due to the spin complications, Mandelstam analyticity implies either "conspiracy" between two trajectories, now having the same intercept at $t = 0$, or the vanishing of some (combination of) residue functions at that point ("evasion"). We refer to the bibliography for further studies.

16.4 Cuts in the angular momentum plane

One important conclusion from potential theory, which was taken over to hadron interactions, was the fact that the only singularities occurring in the angular momentum plane to the right of the line $\mathrm{Re}\ J = -\frac{1}{2}$ are the Regge poles. Only under this assumption can the MSW representation (10.1) and the high-energy form (12.6) be derived.

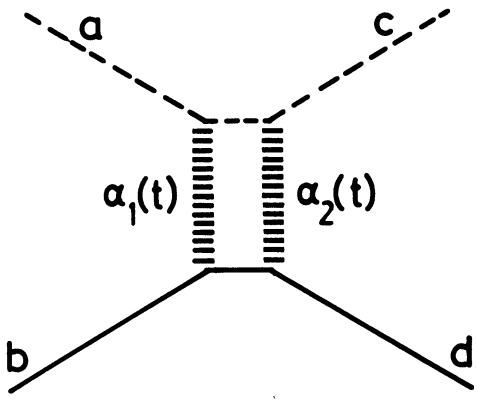

Fig. 16.3

Double Regge pole exchange in a two-body process.

Are there some theoretical arguments for or against this assumption? The answer is that, once having assumed the existence of Regge poles in hadron interactions, one is more or less naturally led to the existence of cuts in the angular momentum plane; namely, the exchange of <u>two</u> Regge poles, symbolically indicated in Fig. 16.3, having trajectories $\alpha_i(t)$, $i = 1, 2$, implies a cut going to the left from a position $\alpha_c(t)$ in the complex ℓ-plane given by

$$\alpha_c(t) = \alpha_1(0) + \alpha_2(0) - 1 + \frac{\alpha_1' \cdot \alpha_2'}{\alpha_1' + \alpha_2'}\, t \ , \qquad (16.12)$$

where for simplicity straight-line trajectories $\alpha_i(t)$ are assumed. We illustrate this in Fig. 16.4. Summarizing, a cut in the angular momentum plane seems almost unavoidable in hadronic interactions.

What is the influence of a cut on the high-energy scattering amplitude (12.1)? Without going into details, we merely state that the dominating contribution from the cut is given by

$$\gamma_c(t)(s/s_0)^{\alpha_c(t)} \left[\log s/s_0\right]^{-\nu} \ , \quad \nu > 0 \ . \qquad (16.13)$$

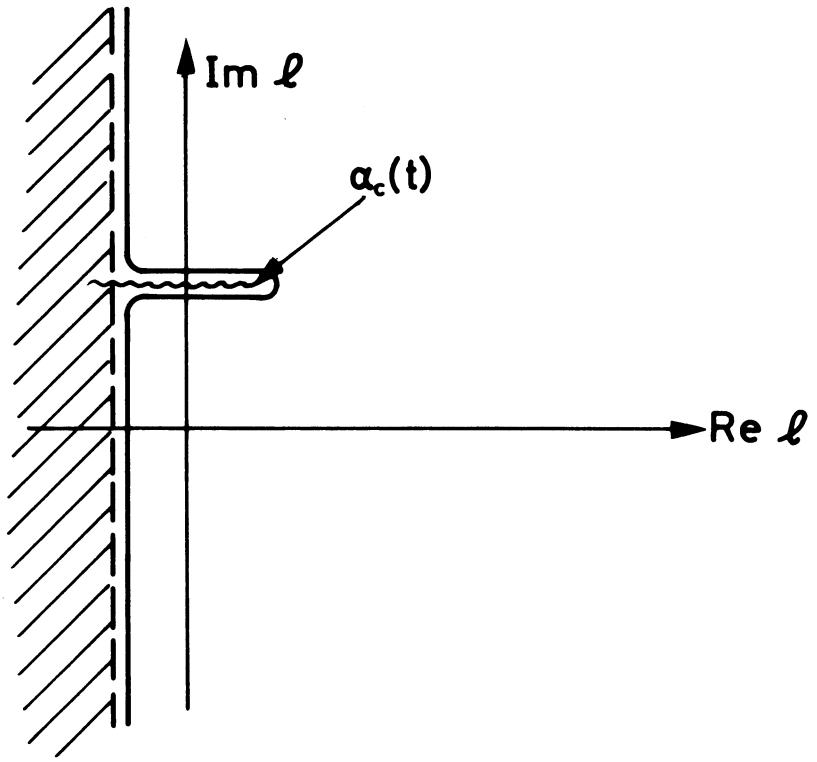

Fig. 16.4

An illustration of the appearance of a cut in the angular momentum plane.

Consider for example pion-nucleon charge exchange. Here, the cut could be due to joint exchange of P and ρ. But this would mean, from Eq. (16.12), that $\alpha_c(t) > \alpha_\rho(t)$ as soon as $t < 0$. In other words, the contribution of the cut is expected to dominate over the ρ-exchange contribution for all values of t except possibly for $t = 0$. Of course, it could happen that, for some miraculous reason, the factor multiplying the cut contribution vanishes. However one feels rather uneasy about the occurrence of cuts. They pose a very intriguing theoretical problem.

APPENDIX 1

ANALYTIC FUNCTIONS

We adopt the following definition of an analytic function (more "minimal" definitions, i.e., requiring less assumptions, exist).

A function $g(z)$ of the complex variable z is analytic (or holomorphic) in the neighbourhood of a point $z = a$ if it allows a Taylor series expansion

$$g(z) = \sum_{n=0}^{\infty} b_n (z-a)^n \,, \tag{A1.1}$$

(with coefficients b_n independent of z), which has a radius of convergence $R > 0$.

It is permitted to differentiate term by term in the series to get

$$g^{(k)}(a) = \left\{ \frac{d^k}{dz^k} g(z) \right\}_{z=a} = k!\, b_k \,. \tag{A1.2}$$

Next we give a few examples of analytic functions.

i) The function

$$g(z) = \sum_{n=0}^{\infty} \frac{1}{n!} z^n = e^z \tag{A1.3}$$

is an example of an entire function: since the series expansion converges for all z, it is analytic in the whole complex plane.

ii) Consider

$$g_\nu(z) = \sum_{n=0}^{\infty} z^n \frac{\nu(\nu-1)\ldots(\nu-n+1)}{1 \cdot 2 \ldots n} = (1-z)^\nu \,. \tag{A1.4}$$

For $\nu = 0, 1, 2, 3, \ldots$, the series reduces to a polynomial, which evidently represents an entire function. For all other ν values, the radius of convergence is $R = 1$. However, since the series may be summed to give $(1 - z)^{\nu}$, the function which for $|z| < 1$ is defined by the series can be defined for all values of z, except possibly at $z = 1$. This is a particular example of how an <u>analytic continuation</u> may be performed: the original definition of the function has a meaning only for certain values of the variable; by some trick, however, one is able to extend the definition to other z values and, consequently, to obtain a function which is identical to the original one where this was defined, but which has a larger domain of definition.

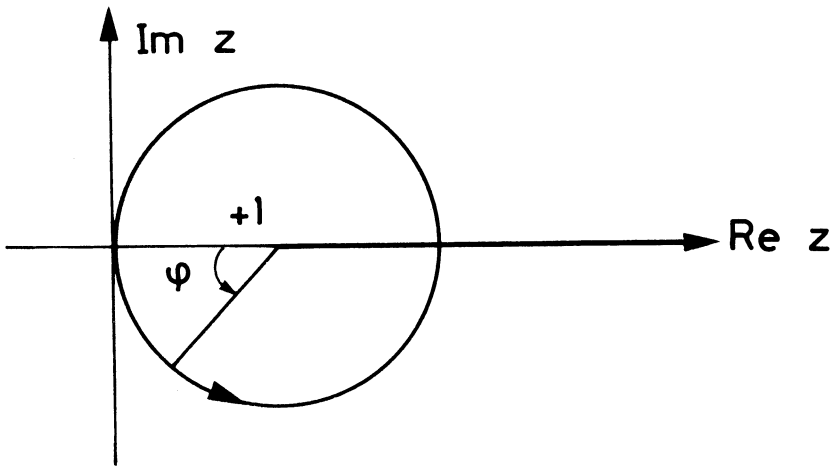

Fig. A1.1

An illustration of the multi-valuedness of the functions (A1.4).

The behaviour near $z = 1$ of the particular function (A1.4) requires detailed study. To this end, let us consider a circle of unit radius centred at $z = 1$ (see Fig. A1.1). For points on the circle, one has

$$z = 1 - \exp(i\varphi) \quad , \quad 0 \leq \varphi < 2\pi \quad , \tag{A1.5}$$

so that

$$(1 - z)^{\nu} = [\exp(i\varphi)]^{\nu} \quad . \tag{A1.6}$$

Now, start at the origin, $\varphi = 0$, where $g_\nu(z = 0) = 1$, and go one turn around the circle back to the origin to end up with $\varphi = 2\pi$. Then

$$g_\nu(z) = [\exp(2i\pi)]^\nu = \exp(2i\pi\nu) . \qquad (A1.7)$$

This value differs from the original one, unless ν is an integer, positive, negative or zero. For non-integer ν, one is thus forced to specify not only that one considers the points $z = 0$ but also what value one gives to $g_\nu(z)$ at that point, and how the different values hang together (this gives the different "branches" of the function). One way to avoid ambiguities of this kind is to forbid a complete tour around the circle by cutting it at some point; where is completely arbitrary. Since the same discussion can be carried through for all circles centred at $z = 1$, one thus has to forbid encircling all of them, that is, to have a cut running from the point $z = 1$ out to infinity. Usually (but not necessarily!), this cut is taken along the real axis, either from $z = 1$ to $z = +\infty$ or from $z = 1$ to $z = -\infty$. The first of these choices is illustrated in Fig. A1.1.

Summarizing, for non-integer ν the function defined by the series (A1.4) can be continued to all values of z, except possibly $z = 1$, provided one cuts the plane from $z = 1$ to infinity. This is necessary in order to have a single-valued function. The function is said to be analytic in the cut plane.

A cut is a particular example of a singularity of an analytic function. Another, more well-known, type is a pole. In our example (A1.4) with $\nu = -1, -2, -3, \ldots$, there are no troubles with the multi-valuedness of the function; thus, no cut is needed. However, the function is infinite at $z = 1$, to be precise in a manner such that

$$\lim_{z \to 1} (1 - z)^{|\nu|} g_\nu(z) = 1 \quad , \quad \nu = -1, -2, \ldots . \qquad (A1.8)$$

This situation is characterized by saying that the function has a pole at $z = 1$. This ends our examples.

The concept of a pole for an analytic function is a very important one: if for $0 < |z-a| < R$, a function $g(z)$ allows the representation

$$g(z) = \sum_{n=0}^{\infty} b_n (z-a)^n + \sum_{n=1}^{N\geq 1} d_n \frac{1}{(z-a)^n} \quad , \quad d_N \neq 0 \; , \tag{A1.9}$$

then it is said to have a pole of order N at $z = a$; d_1 is called the residue of the pole at $z = a$

$$d_1 = \text{Res } g(z = a) \; . \tag{A1.10}$$

The function (A1.9) is said to be meromorphic at $z = a$, i.e., analytic except for a (isolated) pole.

One of the most important properties of analytic functions is given in a theorem due to Cauchy, which we formulate as follows.

Cauchy's theorem

Let $g(z)$ be meromorphic, i.e., analytic except for isolated poles, in a (bounded) domain D of the complex z plane, and let C be a closed contour in D such that an arbitrary point in D is encircled at most once by C. Then

$$\oint_C dz\, g(z) = 2\pi i \sum_{m=1}^{M} \text{Res } g(z_m) \; . \tag{A1.11}$$

Here, z_m, $m = 1, 2, \ldots, M$, are the positions of those poles of $g(z)$ that are enclosed by the curve D. Moreover, it is assumed that C is encircled in the positive (counter-clockwise) sense (cf. Fig. A1.2).

We indicate the proof of this theorem in the special case when $g(z)$ is of the form (A1.9); it is easily generalized. The situation in the complex z plane is illustrated in Fig. A1.3. Let $z = z_0$ be an arbitrary point on C. Then, for integer $k \neq -1$, one has

$$\oint_C dz(z-a)^k = \int_{\substack{z=z_0 \\ \text{along } C}}^{z=z_0} dz(z-a)^k = \left[\frac{1}{k+1}(z-a)^{k+1}\right]_{z=z_0}^{z=z_0} = 0 \ , \quad \text{(A1.12)}$$

since $(z-a)^{k+1}$ assumes the same value after a complete tour around C.

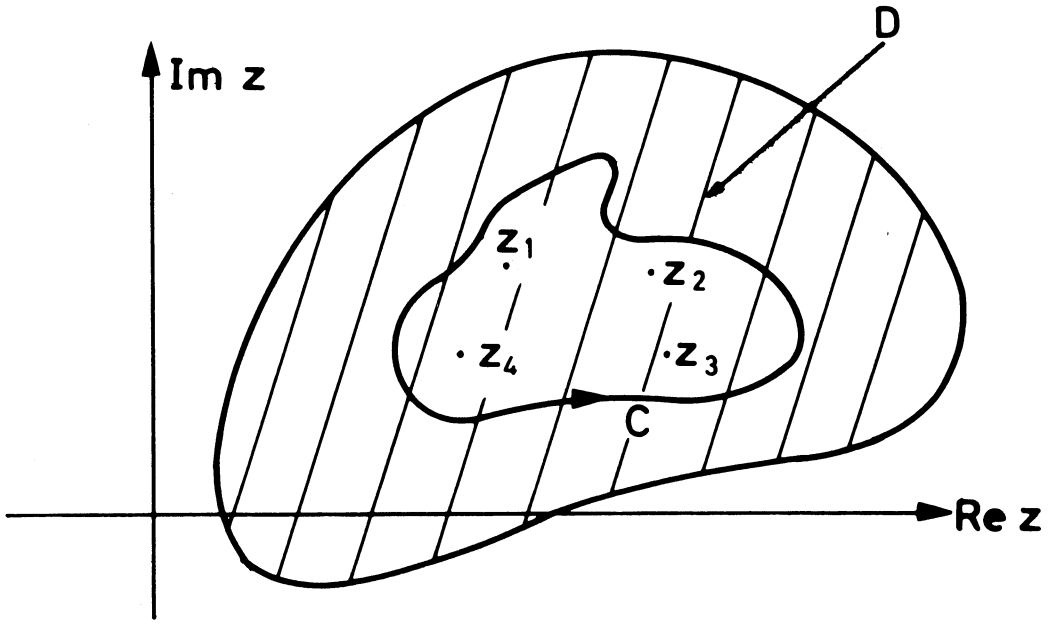

Fig. A1.2

The situation in the complex z plane where the Cauchy theorem applies in the form (A1.11).

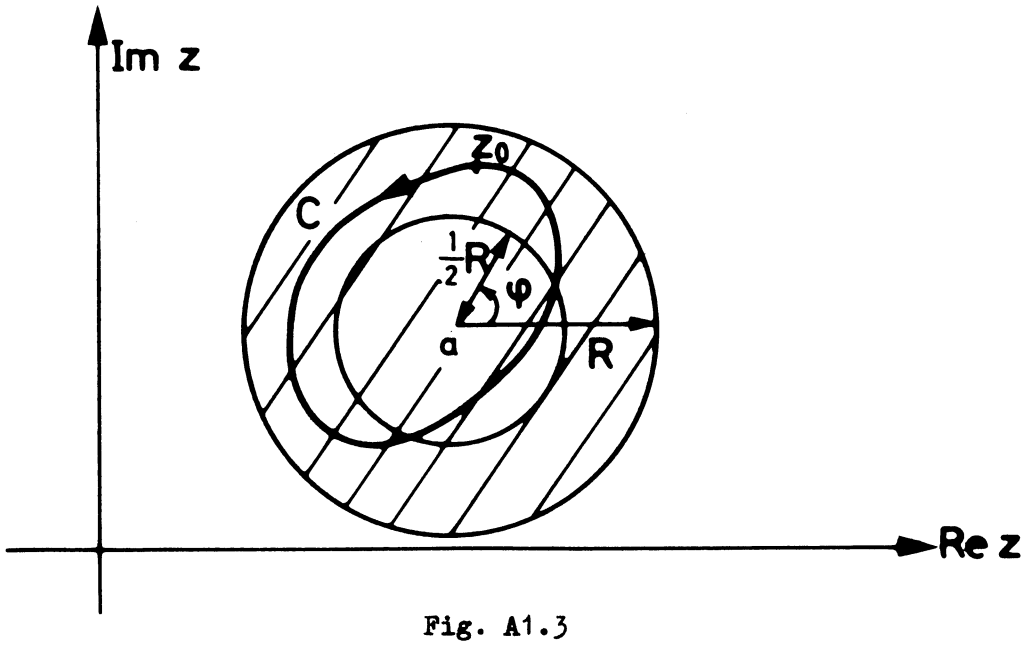

Fig. A1.3

An illustration of the proof of the Cauchy theorem for the function (A1.9).

Consequently, since term-by-term integration is allowed, one obtains

$$\oint_C dz\, g(z) = d_1 \oint_C \frac{dz}{z-a} . \tag{A1.13}$$

So, if the residue d_1 vanishes, the integral vanishes. In particular if $g(z)$ is holomorphic (no poles) in D, and C′ is any contour in D, then

$$\oint_{C'} dz\, g(z) = 0 . \tag{A1.14}$$

This part of the Cauchy theorem may be used to prove (do this!) that the contour C in Eq. (A1.13) may be deformed into the circle

$$z = a + \frac{1}{2} R \exp(i\varphi) \quad , \quad 0 \leq \varphi < 2\pi . \tag{A1.15}$$

Then

$$\oint_{\text{circle}} \frac{dz}{z-a} = \int_0^{2\pi} \frac{\frac{1}{2} R\, id\varphi \exp(i\varphi)}{\frac{1}{2} R \exp(i\varphi)} = 2\pi i . \tag{A1.16}$$

This ends our physicist's proof of the theorem (A1.11).

The following result is an immediate corollary of the theorem (A1.11).

If $g(z)$ is holomorphic (analytic with no poles) in a domain D, and C any positive contour inside D that encircles any point at most once, then

$$\frac{1}{2\pi i} \oint_C dz \frac{g(z)}{z-a} = \begin{cases} g(a) & \text{if a is inside C} \\ 0 & \text{if a is outside C} . \end{cases} \tag{A1.17}$$

Exercise A1.1: Prove Eq. (A1.17)!

APPENDIX 2

BESSEL FUNCTIONS

The Bessel functions $J_0(x)$ and $J_1(x)$ of order zero and one, respectively, are defined by

$$J_0(x) = \frac{1}{\pi} \int_0^{\pi} d\varphi \exp (ix \cos \varphi) , \tag{A2.1}$$

$$J_1(x) = - \frac{d}{dx} J_0(x) = \frac{1}{i\pi} \int_0^{\pi} d\varphi \cos \varphi \exp (ix \cos \varphi) . \tag{A2.2}$$

By expanding the exponential

$$\exp (ix \cos \varphi) = \sum_{n=0}^{\infty} \frac{1}{n!} (ix)^n \cos^n \varphi , \tag{A2.3}$$

and using

$$\int_0^{\pi} d\varphi \cos^n \varphi = \begin{cases} \dfrac{\pi(2m-1)!!}{2^m m!} & \text{if } n = 2m \text{ is even,} \\ 0 & \text{if } n \text{ is odd,} \end{cases} \tag{A2.4}$$

where $(2m-1)!!$ equals $(2m-1)(2m-3)(2m-5) \ldots 3.1$, one easily derives the series expansions of $J_0(x)$ and $J_1(x)$. In particular, for small values of x it suffices with the first few terms:

$$J_0(x) = 1 - \frac{1}{2}\frac{1}{2}x^2 + \frac{1}{4!}\frac{3}{2^3}x^4 + O(x^6) = \exp\left(-\frac{1}{4}x^2\right) + O(x^4)\,, \quad \text{(A2.5)}$$

an approximation which is good to $\lesssim 10\%$ for $x \leq 1.5$. Moreover, by differentiation

$$\frac{2}{x}J_1(x) = \frac{2}{x}(-1)\left[-\frac{1}{2}x + \frac{1}{16}x^3 + O(x^5)\right] = \exp\left(-\frac{1}{8}x^2\right) + O(x^4), \quad \text{(A2.6)}$$

which is accurate to $\lesssim 10\%$ for $x \lesssim 2.5$. Note the different constant factors in the exponent for J_0 and J_1!

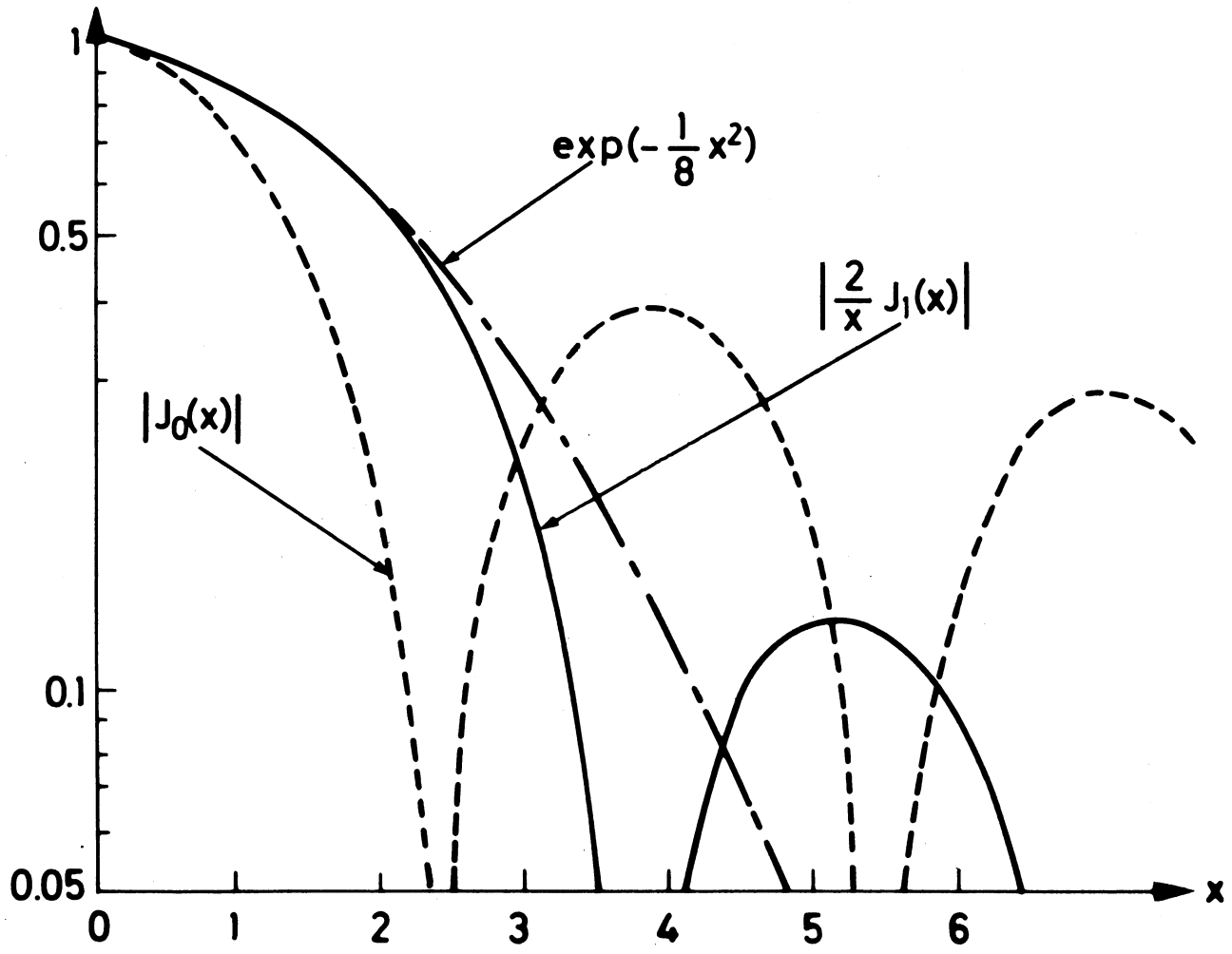

Fig. A2.1

The x-dependence of the Bessel functions [cf. Eq. (A2.6)].

Besides the relation (A2.2), one also has

$$\frac{d}{dx}\left[x J_1(x)\right] = x J_0(x) \ . \qquad \text{(A2.7)}$$

Exercise A2.1: Prove Eq. (A2.7). [Hint: use the defining integral (A2.2) for $J_1(x)$, differentiate, and perform a partial integration.]

In the same way as an "arbitrary" function $f(x)$ can be represented by a Fourier integral, it can also be represented by a Fourier-Bessel integral which reads

$$f(x) = \int_0^\infty y\,dy\, J_0(xy) g(y) \ , \qquad \text{(A2.8)}$$

where

$$g(y) = \int_0^\infty x'\,dx'\, J_0(x'y) f(x') \ . \qquad \text{(A2.9)}$$

These two relations can be summarized in

$$\int_0^\infty x' y\,dy\, J_0(xy) J_0(x'y) = \delta(x - x') \ . \qquad \text{(A2.10)}$$

For a proof of the Fourier-Bessel theorem, we refer to G.N. Watson, Theory of Bessel Functions, Cambridge University Press (1952). The impact parameter expansion (4.50) is an example of a Fourier-Bessel transform.

A Fourier-Bessel transform used in Chapter 6 is

$$\kappa(x) = \int_0^\infty y\,dy\, J_0(xy)\, \exp(-y^2) = \frac{1}{2} \exp\left(-\frac{1}{4} x^2\right) . \qquad (A2.11)$$

Exercise A2.2: Prove Eq. (A2.11)! [Hint: prove that

a) $\kappa(0) = \frac{1}{2}$;

b) $(d\kappa/dx) = -(x/2)\,\kappa(x)$ by suitable partial integrations.]

APPENDIX 3

LEGENDRE FUNCTIONS

The Legendre polynomials are defined by

$$P_\ell(x) = \frac{1}{2^\ell \ell!} \frac{d^\ell}{dx^\ell} (x^2 - 1)^\ell \ . \tag{A3.1}$$

One may derive an integral representation of $P_\ell(x)$ as follows. Let

$$f(x) = \frac{1}{2^\ell \ell!} (x^2 - 1)^\ell \ . \tag{A3.2}$$

Being a polynomial, $f(x)$ can be written as a Cauchy integral

$$f(x) = \frac{1}{2\pi i} \oint d\xi \, \frac{f(\xi)}{\xi - x} \ , \tag{A3.3}$$

where the integration path is any closed curve in the complex ξ plane which once goes around the point $\xi = x$. Then

$$P_\ell(x) = \frac{d^\ell}{dx^\ell} f(x) = \frac{\ell!}{2\pi i} \oint d\xi \, \frac{f(\xi)}{(\xi - x)^{\ell+1}} = \tag{A3.4}$$

$$= \frac{1}{2\pi i} \frac{1}{2^\ell} \oint d\xi \, \frac{(\xi^2 - 1)^\ell}{(\xi - x)^{\ell+1}} \ .$$

In particular, if the integration path is chosen as a circle of radius $\sqrt{x^2 - 1}$ around x (we assume for the time being that $x^2 > 1$), as is illustrated in Fig. A3.1, we may write

$$\xi = x + \sqrt{x^2 - 1} \exp(i\varphi) \quad , \quad -\pi < \varphi \leq \pi \ . \tag{A3.5}$$

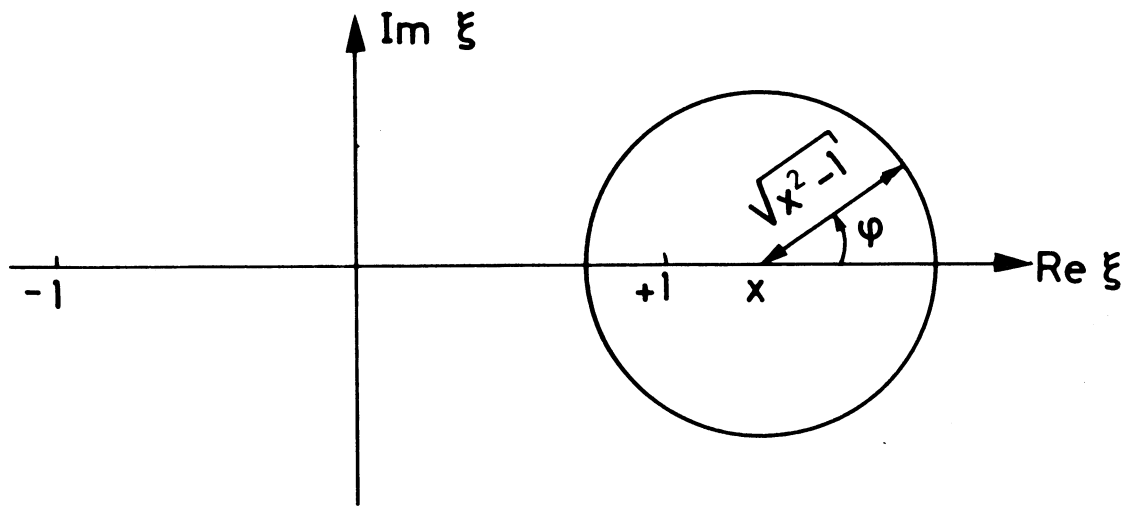

Fig. A3.1

The path of integration used in deriving Eq. (A3.6).

Finally, introducing φ as the integration variable instead of ξ, one derives from Eq. (A3.4)

$$P_\ell(x) = \frac{1}{\pi}\int_0^\pi d\varphi\,[x+\sqrt{x^2-1}\,\cos\varphi]^\ell \ . \qquad \text{(A3.6)}$$

Exercise A3.1: Derive Eq. (A3.6)!

This is the desired integral representation of $P_\ell(x)$. It is valid for all values of x, also complex ones (provided $|\arg x| < \frac{1}{2}\pi$), if proper care is taken of the square root; if $-1 \leq x \leq +1$, for example, one must define $\sqrt{x^2-1} = i\sqrt{1-x^2}$. Moreover, the integral representation may be used to define $P_\ell(x)$ for <u>any ℓ value</u>, be it positive-integral as in the derivation, arbitrary real or arbitrary complex. Some care is needed though, in defining which are the branches of the multi-valued function that are chosen.

From the form (A3.6) many useful relations for the Legendre functions $P_\ell(x)$ may be derived. We now give some of the formulae used in the main discussion.

i) For $0 \leq 1 - x << 1$, writing $\sqrt{1 - x^2}$ as $\approx \sqrt{2(1 - x)}$ and using

$$\left[1 + i\sqrt{2(1-x)}\cos\varphi\right]^\ell = \left[1 + \frac{1}{\ell}\left\{i\ell\sqrt{2(1-x)}\cos\varphi\right\}\right]^\ell \approx$$

$$\approx \exp\left[i\ell\sqrt{2(1-x)}\cos\varphi\right], \quad (\ell \text{ large}), \tag{A3.7}$$

one finds, noting the definition (A2.1)

$$P_\ell(x) \approx J_0\left(\ell\sqrt{2[1-x]}\right), \quad (0 \leq 1 - x << 1, \ \ell \text{ large}). \tag{A3.8}$$

This approximation is accurate to $\lesssim 10\%$ for $0 \lesssim 1 - x \lesssim 0.2$ already for $\ell = 1$.

ii) For $x \to \pm \infty$ one finds

$$P_\ell(x) = x^\ell \frac{1}{\pi}\int_0^\pi d\varphi \left[1 \pm \sqrt{1 - x^{-2}}\cos\varphi\right]^\ell \approx$$

$$\approx \frac{1}{\pi} x^\ell \int_0^\pi (1 + \cos\varphi)^\ell d\varphi, \quad \text{Re } \ell > -\frac{1}{2}. \tag{A3.9}$$

The restriction Re $\ell > -\frac{1}{2}$ applies, since otherwise the x independent integral does not converge. The integral may be evaluated explicitly to give

$$P_\ell(x) \approx (2x)^\ell \frac{\Gamma(\ell + \frac{1}{2})}{\sqrt{\pi}\,\Gamma(\ell + 1)} , \qquad \begin{matrix} x \to \pm\infty \\ \mathrm{Re}\ \ell > -\frac{1}{2} , \end{matrix} \tag{A3.10}$$

where $\Gamma(z)$ is the conventional Euler gamma function.

iii) For $n \geq 0$ an integer, one has

$$\frac{1}{2}\int_{-1}^{+1} dx\, P_n(x)P_\ell(x) = \frac{\sin \pi\ell}{\pi(\ell - n)(n + \ell + 1)} . \tag{A3.11}$$

This formula is discussed in Section 3.12 of the Bateman Manuscript Project "Higher Transcendental Functions", Vol. 1 (Mc Graw-Hill, New York, 1953).

BIBLIOGRAPHY OF THE REGGE POLE LITERATURE

As a substitute for the almost complete lack of references in the text, I have collected here the titles of some 300 articles on complex angular momenta and the Regge-pole model. This list is certainly not complete. Items which are particularly incomplete are complex angular momentum in potential theory, Regge poles and sum rules, large angle scattering, and papers from the period 1961 to 1965. On the other hand, I hope that the recent (approximately 1965 to 1967) phenomenological treatments are well covered. The systematic literature survey was completed on June 30, 1967.

I. Some pioneering articles. Books and reviews.

H.M. Chan, High-energy reactions and Regge poles, Report CERN 67-16 (1967).

G.F. Chew and S.C. Frautschi, Principle of equivalence for all strongly interacting particles within the S matrix framework, Phys.Rev.Letters 7, 394 (1961).

V. de Alfaro and T. Regge, Potential scattering (North Holland Publ.Comp., Amsterdam, 1965).

S.C. Frautschi, Regge poles and S-matrix theory (W.A. Benjamin, New York and Amsterdam, 1963).

S.C. Frautschi, M. Gell-Mann and F. Zachariasen, Experimental consequences of the hypothesis of Regge poles, Phys.Rev. 126, 2204 (1962).

M. Gell-Mann, Application of Regge poles, Proceedings of the International Conference on High-Energy Physics at CERN Geneva, 1962 (edited by J. Prentki), (CERN, Geneva, 1962), p.533.

V.N. Gribov, Possible asymptotic behaviour of elastic scattering, Zh.Eksp.Teor.Fiz. 41, 667 (1961), English translation in Soviet Physics JETP (USA) 14, 478 (1962).

W. Kummer, Speculations on experimental consequences of Regge poles, Report CERN 62-13 (1962).

W. Kummer, Introduction to Regge poles, Fortschr.Phys. 14, 429 (1966).

E. Leader, Present phenomenological status of the Regge-pole model, Rev.Mod.Phys. 38, 476 (1966).

S. Mandelstam, An extension of the Regge formula, Ann.Phys. (N.Y.) 19, 254 (1962).

A. Martin, Analyticity in potential scattering, Progr.Element.Particle Cosmic Ray Phys., Vol. VIII (North Holland Publ.Comp., Amsterdam, 1965).

R.G. Newton, The complex j-plane (W.A. Benjamin, New York 1966).

R.L. Omnès, Regge poles, Ann.Rev.Nucl.Sci. 16, 263 (1966).

R.L. Omnès and M. Froissart, Mandelstam theory and Regge poles (W.A. Benjamin, New York and Amsterdam, 1963).

R.J.N. Phillips, Regge poles in high-energy scattering, Proceedings 1966 International School of Physics "Ettore Majorana" at Erice (Acad.Press, New York, 1966), (edited by A. Zichichi), p.268.

J. Prentki (editor), Proceedings of the International Conference on High-Energy Physics at CERN, Geneva, 1962 [Section R: Regge poles and related topics (p.503-525). Section H1: High-energy physics (theoretical) (p.533-568)].

T. Regge, Singularities in the angular momentum and high-energy phenomena, Proceedings of the Sienna International Conference on Elementary Particles, Sept. 30 - October 5, 1963 (Società Italiana di Fisica, Bologna, 1963)(edited by G. Bernardini and G.P. Puppi), p. 153-155.

Ya.A. Smorodinsky (editor), Proceedings of the XII International Conference on High-Energy Physics, Dubna, August 5-15, 1964 (Atomizdat, Moscow, 1966). [Session: Methods of complex angular momenta in field theory (p.353-394)].

E.J. Squires, Complex angular momenta and particle physics (W.A. Benjamin, New York and Amsterdam, 1963).

L. Van Hove, Theory of strong interactions of elementary particles in the GeV region, Springer Tracts in Modern Physics, Ergeb.Exakt. Naturwiss., Vol. 39 (Springer Verlag, Berlin/Heidelberg/New York, 1965)(edited by G. Höhler).

L. Van Hove, General theoretical situation in high-energy two-body reactions, Lecture given at the Stony Brook Conference on High-Energy Two-body Reactions, April 23-24, 1966 CERN Preprint.

L. Van Hove, Very high-energy scattering of strongly interacting particles, in Particle interactions at high energies (Scottish Universities' Summer School 1966), (Oliver and Boyd, Edinburgh/London, 1967), p.63.

L. Van Hove, Hadron collisions at very high energies, Proceedings of the XIIIth International Conference on High-Energy Physics, Berkeley, California, Aug.31 - Sept.7, 1966 (Univ. of California Press, Berkeley, 1967), p.253.

K.C. Wali (editor), Talks presented at the Symposium on Regge Poles, Dec. 15-16, 1966, Argonne Preprint, March 1967.

T.R. Walsh (editor), Proceedings of the Oxford International Conference on Elementary Particles, Sept. 19-25, 1965 (The Rutherford High-Energy Laboratory, 1966).

Added in Proof:

R.J. Eden, High-energy collisions of elementary particles (Cambridge Univ.Press, 1967).

Proceedings of the Heidelberg International Conference on Elementary Particles, Sept. 20-27, 1967 (to be published by North Holland Publ.Comp., Amsterdam).

II. Trajectory phenomenology

A. Ahmadzadeh, Exchange degeneracy classification of Regge trajectories and the total cross-section, Phys.Rev.Letters 16, 953 (1966).

A. Ahmadzadeh, Possible Regge recurrences of the vector and tensor mesons, Nuovo Cimento 467, 415 (1966).

R.C. Arnold, Meson symmetries, Phys.Rev.Letters 14, 657 (1965).

D. Cline, Isotopic-spin one-boson Regge trajectories, Nuovo Cimento 45A, 750 (1966).

P. di Vecchia and F. Drago, A note on the 10* and 27 Regge trajectories, Nuovo Cimento 50A, 181 (1967).

S. Minami, Remarks on Regge trajectories, Nuovo Cimento 46A, 545 (1966).

S. Minami, Isotopic-spin-zero mesons, Osaka City Univ. Preprint, Oct. 1966.

A. Pignotti, Hitherto overlooked SU(3) octet of Regge poles implied by bootstrap dynamics, Phys.Rev. 134, B630 (1964).

R. Ramachandran, Fermion trajectory parametrization and superconvergence, International Centre for Theoretical Physics, Preprint IC/67/30, Trieste, May 1967.

J. Scanio, New determination of the ρ' Regge-trajectory intercepts, Phys.Rev. 152, 1337 (1966).

D.G. Sutherland, Some remarks on higher mesons, CERN Preprint TH.768, May 1967.

III. Forward elastic πN-scattering, and πN reactions in general

A. Ahmadzadeh, Regge-pole model of quark-quark amplitudes and total cross-sections of the hadrons, Physics Letters 22, 96 (1966).

V. Barger and M. Olsson, Analysis of total cross-section differences at high-energies, Phys.Rev.Letters 15, 930 (1965).

V. Barger and M. Olsson, Real part of the pn scattering amplitudes from an SU(3) Regge-pole model, Phys.Rev.Letters 16, 545 (1966).

V. Barger and M. Olsson, Forward elastic scattering at high energy in an SU(3) Regge-pole model, Phys.Rev. 146, 1080 (1966).

V. Barger and M. Olsson, Regge-pole model and σ_{tot} in the laboratory momentum range 2-6 GeV/c, Phys.Rev. 148, 1428 (1966).

V. Barger and M. Olsson, Interference of Regge ρ-exchange with direct channel fermion resonances, Phys.Rev. 151, 1123 (1967).

A. Biaℓas, E. Biaℓas, O. Czyzewski and A. Kotanski, Regge recurrences and πp elastic scattering at high-momentum transfers, Nuovo Cimento 48A, 1111 (1967).

T.O. Binford and B.P. Desai, High-energy elastic scattering at low momentum transfers, Phys.Rev. 138, B1167 (1965).

C.B. Chiu, R.J.N. Phillips and W. Rarita, πN polarization and Regge poles, Phys.Rev. 153, 1485 (1967).

G. Cohen-Tannoudji, A. Morel and H. Navelet, A phenomenological analysis of high-energy data in πN and $\bar{K}$N systems: shadow scattering and Regge singularities, Nuovo Cimento 48A, 1075 (1967).

Y. Futami and T. Sawada, The Fermi-Yang model for the pion and the high-energy behaviour of the πN scattering, Nuovo Cimento, 48A, 843 (1967).

G.T. Hoff, Proof that the near-forward minimum and secondary peak in π^-p elastic scattering are resonance effects, Phys.Rev.Letters 18, 816 (1967).

Meng Ta-Chung, Fermion Regge poles and relations between phase shifts in πN scattering, Z.Phys. 198, 538 (1967).

R.J.N. Phillips and W. Rarita, Regge poles and the phase of the forward-scattering amplitudes, Phys.Rev.Letters 14, 502 (1965).

R.J.N. Phillips and W. Rarita, Regge-pole models for high-energy πN, K$\bar{N}$ and $\bar{K}$N scattering, Phys.Rev. 139, B1336 (1965).

D.L. Pursey and L. Sertorio, Regge cuts and πp total cross-sections, Phys.Rev. 155, 1591 (1967).

W. Rarita, R.J. Riddell, Jr., C.B. Chiu and R.J.N. Phillips, Regge-pole model for πp, pp and $\bar{p}$p scattering, University of California Preprint UCRL 17523, April 1967.

M. Restignoli, L. Sertorio and M. Toller, Regge-pole phenomenology and forward dispersion relations, Phys.Rev. 150, 1389 (1966).

V. Singh, Regge poles in πN scattering and in $\pi\pi \to N\bar{N}$, Phys.Rev. 129, 1889 (1963).

IV. Fermion exchange in elastic, charge-exchange and strangeness-exchange πN reactions

D. Amati, A. Stanghellini and K. Wilson, Theory of fermion Regge poles, Nuovo Cimento 28, 639 (1963).

V. Barger and D. Cline, Regge recurrences and π^-p elastic scattering at 180°, Phys.Rev.Letters 16, 931 (1966).

V. Barger and D. Cline, Backward π^+p elastic scattering from a direct channel Δ_δ resonance model, Physics Letters 22, 666 (1966).

V. Barger and D. Cline, Fermion Regge-pole model and the structure of pion-nucleon elastic scattering in the backward hemisphere, Phys.Rev. 155, 1792 (1967).

C.B. Chiu and J.D. Stack, Regge-pole model for high-energy backward $\pi^\pm$p scattering, Phys.Rev. 153, 1575 (1967).

B.R. Desai, Exchange of even- and odd-parity baryon-meson resonances and the backward elastic scattering, Phys.Rev.Letters 17, 498 (1966).

F.N. Dikmen, Critique of Regge-poles interpretation of backward π^-p elastic scattering, Phys.Rev.Letters 18, 798 (1967).

J. Dreitlein and K. Mahanthappa, Some comments on phenomenological aspects of Regge theory, Nuovo Cimento 48A, 275 (1967).

V.N. Gribov, Fermion Regge poles and the asymptotic behaviour of meson-nucleon large-angle scattering, Zh.Eksper.Teor.Fiz. 43, 1529 (1962); English translation in Soviet Physics JETP (USA) 16, 1080 (1963).

H. Högaasen, Models for backward associated production in $\pi^- p \to \Lambda K^\circ$, CERN Preprint TH.777.

T. Kinoshita, Fermion Regge poles and the asymptotic behaviour of backward meson-nucleon scattering, Report CERN 62-33 (1962).

J.D. Stack, Polarization as a test for Regge behaviour in the backward $\pi^\pm p$ elastic scattering, Phys.Rev.Letters 16, 286 (1966).

N. Thibault, Amplitude de diffusion en théorie de Regge dans le domaine cinématique du pic arrière πN, Nuovo Cimento 50A, 135 (1967).

Y. Yamamoto, Backward $\pi^\pm p$ scattering and the Y = 1 fermion Regge-pole hypothesis, Progr.Theor.Physics 38, 382 (1967).

V. Charge-exchange and η-production (not polarization), and associated production in πN reactions

A. Ahmadzadeh and C.H. Chan, Sum rules for high-energy scattering phenomena, Physics Letters 22, 692 (1966).

F. Arbab, N.F. Bali and J. Dash, Ambiguities in the phenomenological determination of Regge-pole parameters, Phys.Rev. 158, 1515 (1967).

F. Arbab and C.B. Chiu, Association between the dip in the $\pi^- p \to \pi^\circ n$ high-energy angular distribution and the zero of the ρ trajectory, Phys.Rev. 147, 1045 (1966).

R.C. Arnold, Double-octet Regge-pole model with exchange degeneracy for charge and hypercharge exchange reactions, Phys.Rev. 153, 1506 (1967).

V. Barger and D. Cline, SU(3) sum rules for meson-nucleon charge exchange reactions, Phys.Rev. 156, 1522 (1967).

M. Barmawi, Application of a Regge-pole model to the reactions $\pi^- p \to \pi^0 n$, $\pi^- p \to \eta n$ and $\pi^+ p \to \omega p$, University of Chicago Preprint EFINS 67-40, May 1967.

F.S. Chen-Cheung, Relation among the πN and KN charge exchange cross-sections from the SU(3) Regge-pole theory, Phys.Rev. 156, 1520 (1967).

B. Desai, πN charge-exchange scattering and the ρ trajectory, Phys.Rev. 142, 1255 (1966).

H. Högaasen and W. Fischer. The ρ'-trajectory and its contribution to NN and πN charge exchange, Physics Letters 22, 516 (1966).

G. Höhler, J. Baacke and G. Eisenbeiss, The parameters of the Regge-pole model for πN charge exchange scattering. Physics Letters 22, 203 (1966).

G. Höhler, J. Baacke, H. Schaile and P. Sonderegger, Analysis of πN charge exchange from 4 to 18 GeV/c, Physics Letters 20, 79 (1965).

G. Höhler, J. Baacke and R. Strauss, High-energy behaviour of the πN forward charge-exchange scattering amplitudes, Physics Letters 21, 223 (1966).

D. Horn, C. Schmid and M. Suzuki, Finite energy sum rules and the Regge analysis of the πN charge-exchange amplitude, Cal.Tech. Preprint CALT 68-124, March 1967.

R.K. Logan, Single Regge-pole analysis of $\pi^- p$ charge-exchange scattering, Phys.Rev.Letters 14, 414 (1965).

R.J.N. Phillips, Two-Reggeon branch points and double charge exchange, Physics Letters 24B, 342 (1967).

R.J.N. Phillips, Kinematic corrections to Regge-pole analysis of $\pi^- p \to \eta n$, Nuclear Phys. B1, 572 (1967).

R.J.N. Phillips and W. Rarita, Single Regge-pole analysis of $\pi^- p \to \eta^0 n$, Phys.Rev.Letters 15, 807 (1965).

R.J.N. Phillips and W. Rarita, Regge trajectories from $\pi^- p \to \eta^0 n$ data, Physics Letters 19, 598 (1965).

R.J.N. Phillips and W. Rarita, Predictions for $\pi^- p \to \eta^0 n$ from Regge poles and SU(3), Phys.Rev. 140, B200 (1965).

I.A. Sakmar and J.H. Wojtaszek, Regge analysis of the reaction $\pi^- p \to \eta n$, Univ. of Miami Preprint, April 1967.

Ph. Salin, Inelastic meson-baryon scattering with Regge poles and SU(3) symmetry, Nuclear Phys. B3, 323 (1967).

K.A. Ter-Martirosyan, The simplest inelastic processes at high energies, Yadernaya Fizika 4, 1067 (1966), English translation in Soviet J. Nuclear Phys. (USA) 4, 766 (1967).

A. Yokosawa, Regge behaviour in $\pi^- p$ charge-exchange process at the region around N(2190), Phys.Rev. 159, 1431 (1967).

VI. Polarization in πN charge-exchange and η-production reactions

G. Altarelli, A. Borgese, F. Buccella and M. Colocci, Regge recurrences and πp charge-exchange polarization at high-energy, Nuovo Cimento 48A, 245 (1967).

J. Beaupre and L. Sertorio, The effect of a sum rule on the ρ' and a cut, to be published in Nuovo Cimento.

C.B. Chiu and J. Finkelstein, Suggestive features in πN charge-exchange polarization associated with Regge cuts, Nuovo Cimento 48A, 820 (1967).

V.M. de Lany, D.J. Gross, I.J. Muzinich and V.L. Teplitz, Polarization test for cuts in angular momentum, Phys.Rev.Letters 18, 149 (1967).

B.R. Desai, D.T. Gregorich and R. Ramachandran, πN charge-exchange polarization and the baryon trajectories in the direct channel, Phys.Rev.Letters 18, 565 (1967).

D. Horn, C. Schmid and M. Suzuki, Finite energy sum rules and the Regge analysis of the πN charge-exchange amplitude, Cal.Tech. Preprint 68-124, March 1967.

R.K. Logan, J. Beaupre and L. Sertorio, $\pi^- p$ charge exchange polarization and the possibility of a second ρ-meson, Phys.Rev.Letters 18, 259 (1967).

R.K. Logan and L. Sertorio, Regge-pole analysis of πp charge exchange polarization, Phys.Rev.Letters 17, 834 (1966).

R.K. Logan and L. Sertorio, A Regge-pole model of $\pi^- p \to \eta n$ polarization to be published in Nuovo Cimento.

R.J.N. Phillips, Resonance tails and high-energy πN charge exchange, Nuovo Cimento, 45A, 245 (1966).

W. Rarita and B.M. Schwarzschild, $K^+ n$ charge exchange and the ρ' Regge trajectories, to be published in Phys.Rev.

VII. Resonance production, in particular in πN reactions

R.C. Arnold, Application of $SU(6)_W$ in a model for vector-meson production at high energies, Argonne Preprint, May 1967 (Rev.version).

M. Barmawi, Regge-pole analysis of $\pi^+ n \to \omega p$, Phys.Rev.Letters 16, 595 (1966).

M. Barmawi, The Regge-pole contribution to vector meson production, Phys.Rev. 142, 1088 (1966).

M. Barmawi, Application of a Regge-pole model to the reactions $\pi^- p \to \pi^0 n$, $\pi^- p \to \eta n$ and $\pi^+ n \to \omega p$, University of Chicago Preprint EFINS 67-40, May 1967.

I. Bender, V. Linke and H.J. Rothe, Study of angular decay correlations for the process $\pi N \to \rho N$ in the Regge-pole model, I, University of Heidelberg Preprint, May 1967.

A.V. Berkov, Yu P. Nikitin and M.V. Terent'ev, Regge poles in vector meson production amplitudes, Zh.Eksper.Teor.Fiz. 46, 2202 (1964), English translation in Soviet Phys. JETP (USA) 19, 1487 (1964).

A. Borgese, F. Buccella, E. Celeghini and M. Colocci, Symmetry and Regge poles for high-energy inelastic two-body reactions, University of Florence Preprint, April 1967.

H. Caprasse and H. Stremnitzer, A Regge-pole analysis of $\pi^+ p \to \pi^0 N^{*++}$, Nuovo Cimento 44A, 1245 (1966).

L. Jones, Information about Regge-pole couplings from vector meson production, to be published in Phys.Rev.

L. Jones, Implication of unequal mass kinematics for the Regge-pole model of vector meson production, to be published in Phys.Rev.

A.B. Kaidalov, Factorization of amplitudes and pair production of resonances at high energy, Zh.Eksper.Teor.Fiz. Pis'ma 4, 484 (1966), English translation in JETP Letters (USA) 4, 325 (1966).

M. Krammer and U. Maor, Regge-pole parameters for the reaction $\pi^+p \to \pi^0\Delta^{++}$ (1238), Nuovo Cimento 50A, 963 (1967).

M.L. Paciello and A. Pugliese, A Regge-pole analysis of ρ^- decay angular distributions and production in $\pi^- p \to \rho^- p$, Physics Letters 24B, 431 (1967).

G.L. Ringland and R.L. Thews, Bound for effective polarization in ρ-production in a Regge-pole exchange model, Univ. of California preprint UCRL 17474, March 1967.

D.P. Roy, N^* production in high energy πp and Kp collisions by Regge-pole model, Nuovo Cimento 40A, 513 (1965).

D.G. Sutherland, δ^- production in a Regge pole and L-excitation scheme model, Nuovo Cimento 46A, 551 (1966).

R. Thews, Regge poles in resonance production, Phys.Rev. 155, 1624 (1967).

Ling-Lie Wang, Prediction of a minimum in the high energy $\pi N \to \omega N$ differential cross-section, Phys.Rev.Letters 16, 756 (1966).

Ling-Lie Wang, Regge-pole formulae for differential cross-sections of quasi-two-body πN and NN interaction, Phys.Rev. 153, 1664 (1967).

VIII. NN and $\bar{N}N$ reactions

A. Ahmadzadeh, Zero-energy intercepts of the ρ and R trajectories, the pn charge-exchange scattering and difference in pp and np total cross-sections, Phys.Rev. 134, B633 (1964).

A. Ahmadzadeh, Regge-pole model of quark-quark amplitudes and total cross-sections of the hadrons, Physics Letters 22, 96 (1966).

A. Ahmadzadeh and C.H. Chan, Sum rules for high-energy scattering phenomena, Physics Letters 22, 692 (1966).

F. Arbab and J.W. Dash, Regge-pole analysis of $pn \to np$ and $p\bar{p} \to n\bar{n}$ scattering, to be published in Phys.Rev.

V. Barger and M. Olsson, Real part of the pn scattering amplitudes from an SU(3) Regge-pole model, Phys.Rev.Letters 16, 545 (1966).

V. Barger and M. Olsson, Regge-pole model and σ_{tot} in the laboratory momentum range 2-6 GeV/c, Phys.Rev. 148, 1428 (1966).

V. Barger and M. Olsson, Forward elastic scattering at high energy in an SU(3) Regge-pole model, Phys.Rev. 146, 1080 (1966).

T.O. Binford and B.P. Desai, High-energy elastic scattering at low momentum transfers, Phys.Rev. 138, B1167 (1965).

P. Dita and B. Nicolescu, $p\bar{p} \to n\bar{n}$ charge-exchange scattering, Phys. Rev. 160, 1395 (1967).

K. Fiałkowski, Factorization theorem of Regge residues and spin dependence of the $p\bar{p} \to \Delta\bar{\Delta}$ amplitudes at high energies, Jagellonian University Preprint, June 1967.

V. Flores-Maldonado, High-energy NN scattering from Regge poles, Phys.Rev. 155, 1773 (1967).

V. Flores-Maldonado, Regge-pole theory and pn and $\bar{p}n$ charge-exchange scattering at small angles, Phys.Rev.Letters 17, 113 (1966).

H. Högaasen and W. Fischer, The ρ'-trajectory and its contribution to NN and πN charge exchange, Physics Letters 22, 516 (1966).

H. Högaasen and Å. Frisk, The ρ + R model and np charge exchange, Physics Letters 22, 90 (1966).

A.B. Kaidalov and B.M. Karnakov, Spin effects in high-energy NN scattering, Zh.Eksper.Teor.Fiz. 50, 691 (1966), English translation in Soviet Physics JETP (USA) 23, 459 (1966).

E. Leader and R.C. Slansky, General analysis of NN scattering; critical test for Regge-pole theory, Phys.Rev. 148, 1491 (1966). [Erratum ibid 156, 1742 (1967)].

V.N. Mel'nikov and K.H. Ter-Martirosyan, The experimental data on charge transfer of K mesons on nucleons at high energies and the theory of complex angular momenta, Yadernaya Fizika 4, 1072 (1966), English translation in Soviet J. Nuclear Phys. (USA) 4, 770 (1967).

R.J.N. Phillips, Is there a pion conspiracy?, Nuclear Phys. B2, 394 (1967).

R.J.N. Phillips and W. Rarita, Regge poles and the phase of the forward-scattering amplitudes, Phys.Rev.Letters 14, 502 (1965).

W. Rarita, R.J. Riddell, Jr., C.B. Chiu and R.J.N. Phillips, Regge-pole model for πp, pp and $\bar{p}$p scattering, University of California preprint UCRL 17523, April 1967.

W. Rarita and V.L. Teplitz, Regge-pole model for high-energy pp and $\bar{p}$p scattering, Phys.Rev.Letters 12, 206 (1964).

D.P. Roy, Study of the reaction $\bar{p}p \to Y\bar{Y}$ by Regge-pole exchange model, Phys.Rev. 146, 1218 (1966).

Ling-Lie Wang, Regge-pole formulae for differential cross-sections of quasi-two-body πN and NN interaction, Phys.Rev. 153, 1664 (1967).

IX. KN and $\bar{K}$N reactions

A. Ahmadzadeh, Regge-pole model of quark-quark amplitudes and total cross-sections of the hadrons, Physics Letters 22, 96 (1966).

A. Ahmadzadeh, Branching ratio predictions for high-energy reactions involving strange particles, Physics Letters 22, 669 (1966).

A. Ahmadzadeh and C.H. Chan, Sum rules for high-energy scattering phenomena, Physics Letters 22, 692 (1966).

F. Arbab, N.F. Bali and J. Dash, Ambiguities in the phenomenological determination of Regge-pole parameters, Phys.Rev. 158, 1515 (1967).

R.C. Arnold, Double-octet Regge-pole model with exchange degeneracy for charge and hypercharge exchange reactions, Phys.Rev. 153, 1506 (1967).

V. Barger and D. Cline, SU(3) sum rules for meson-nucleon charge exchange reactions, Phys.Rev. 156, 1522 (1967).

V. Barger and M. Olsson, Forward elastic scattering at high energy in an SU(3) Regge-pole model, Phys.Rev. 146, 1080 (1966).

V. Barger and M. Olsson, Regge-pole model and σ_{tot} in the laboratory momentum range 2-6 GeV/c, Phys.Rev. 148, 1428 (1966).

T.O. Binford and B.P. Desai, High-energy elastic scattering at low momentum transfers, Phys.Rev. 138, B1167 (1965).

A. Borgese, F. Buccella, E. Caleghini and M. Colocci, Symmetry and Regge poles for high-energy inelastic two-body reactions, University of Florence Preprint, April 1967.

N. Cabibbo, Phase of $K_L - K_S$ regeneration in a simple Regge-pole model, Physics Letters 22, 212 (1966).

F.S. Chen-Cheung, Relation among the πN and KN charge-exchange cross-sections from the SU(3) Regge-pole theory, Phys.Rev. 156, 1520 (1967).

G. Cohen-Tannoudji, A. Morel and H. Navelet, A phenomenological analysis of high-energy data in πN and KN systems: shadow scattering and Regge singularities, Nuovo Cimento 48A, 1075 (1967).

A. Derem, Analyse de l'échange de charge $K^- p$ à haute énergie à l'aide de deux pôles de Regge ρ et R, Nuclear Phys. B3, 106 (1967).

V.N. Mel'nikov and K.A. Ter-Martirosyan, The experimental data on charge transfer of K mesons on nucleons at high energies and the theory of complex angular momenta, Yadernaya Fizika 4, 1072 (1966), English translation in Soviet J. Nuclear Phys. (USA) 4, 770 (1967).

R.J.N. Phillips, Two-Reggeon branch points and double charge exchange, Physics Letters 24B, 342 (1967).

R.J.N. Phillips and W. Rarita, Further evidence for Pignotti's R-trajectories, Phys.Rev. 138, B723 (1965).

R.J.N. Phillips and W. Rarita, Regge-pole models for high-energy πN, KN and $\bar{K}N$ scattering, Phys.Rev. 139, B1336 (1965).

W. Rarita and B.M. Schwarzschild, $K^+ n$ charge exchange and the ρ' Regge trajectories, to be published in Phys.Rev.

D.D. Reeder and K.V.L. Sarma, Prediction of polarization in $K^- p \to \bar{K}^0 n$ at high energies, Nuovo Cimento 51A, 169 (1967).

M. Restignoli, L. Sertorio and M. Toller, Regge-pole phenomenology and forward dispersion relations, Phys.Rev. 150, 1389 (1966).

D.P. Roy, N* production in high energy πp and Kp collisions by Regge-pole model, Nuovo Cimento 40A, 513 (1965).

D.P. Roy, Single Regge-pole analysis of $K^- p \to \bar{K}^0 n$, Nuovo Cimento 40A, 1212 (1965).

Ph. Salin, Inelastic meson-baryon scattering with Regge poles and SU(3) symmetry, Nuclear Phys. B3, 323 (1967).

X. Photo-induced reactions

H.D.I. Abarbanel, F.E. Low, I.J. Muzinich, S. Nussinov and J.E. Schwarz, High-energy limit of photon scattering on hadrons, Phys.Rev. 160, 1329 (1967).

H.D. Abarbanel and S. Nussinov, Implications of Regge behaviour for processes involving photons, Phys.Rev. 158, 1462 (1967).

J.P. Ader, M. Capdeville and Ph. Salin, A Regge-pole model fit of pion and K-meson photoproduction, Nuclear Phys. B3, 407 (1967).

A. Ahmadzadeh and R.J. Jacob, High-energy photoproduction branching ratios in the Regge-pole model, Phys.Rev. 160, 1359 (1967).

F. Buccella and M. Colocci, High-energy photoproduction of vector mesons and Regge poles, Physics Letters 24B, 61 (1967).

B. Diu and M. Le Bellac, Photoproduction of charged pions in a Regge-pole model, Physics Letters 24B, 416 (1967).

P. di Vecchia and F. Drago, Neutral non-strange 0^--meson photoproduction and Regge poles, Physics Letters 24B, 405 (1967).

W. Drechsler, X^0-photoproduction in Regge-pole model, Nuovo Cimento 45A, 263 (1966).

W. Drechsler, Regge-pole contribution to ω° photoproduction, Physics Letters 23, 272 (1966).

S. Frautschi and L. Jones, Small angle photoproduction and conspiracy, to be published in Phys.Rev.

P.G.O. Freund, Photoproduction of vector mesons as virtual vector meson-proton scattering, Nuovo Cimento 48A, 541 (1967).

M.B. Halpern, Conspiracy and superconvergence in pion photoproduction, Phys.Rev. 160, 1441 (1967).

Y.S. Jin and H.A. Rashid, Regge-Khuri representation for photoproduction, Nuclear Phys. 58, 611 (1964).

G. Kramer and P. Stichel, Photoproduction of pions in forward direction and Regge poles, Zeitschr.Phys. 178, 519 (1964).

M.P. Locher and H. Rollnik, Reggeized vector-meson exchange for π° photoproduction, Physics Letters 22, 696 (1966).

R. Musto and F. Nicodemi, Gauge invariance and Regge-pole sum rules for pion photoproduction, Syracuse Univ. Preprint NYO 3399-104, March 1967.

H.K. Shepard, Pomeranchuk exchange contribution to forward photon processes, Phys.Rev. 159, 1362 (1967).

G. Zweig, The reaction $\gamma N \to \pi N$ at high energies, Nuovo Cimento 32, 689 (1964).

XI. Reactions involving nuclei

E. Abers, H. Burkhardt, V. Teplitz and C. Wilkin, Regge-pole dominance at high energies: an experimental test, Physics Letters 21, 339 (1966).

T.C. Hsien and E.C. Mihul, The process $\pi^- p \to \bar{p}d$ and Regge poles, Nuclear Phys. 76, 491 (1966).

P.B. James, R.K. Logan and H.D.D. Watson, Particle nucleus interactions and the Regge-pole model, Phys.Rev. 160, 1539 (1967).

T.B. Treacy, On complex angular momentum in nuclear reactions, Univ. of Canberra Preprint, March 1967.

XII. Reactions with multi-particle final states

Chan Hong-Mo, K. Kajantie and G. Ranft, A Regge model for high-energy collisions producing three final particles, Nuovo Cimento 49A, 157 (1967).

Chan Hong-Mo, K. Kajantie, G. Ranft, W. Beusch and E. Flaminio, Double Regge analysis of high-energy experiments producing three final particles, Nuovo Cimento, 51A, 696 (1967).

I.T. Drummond, Some aspects of complex angular momentum and 3-particle states, Phys.Rev. 153, 1565 (1967).

R.G. Roberts and G.M. Fraser, Regge poles and high-energy single particle production, Phys.Rev. 159, 1297 (1967).

I.A. Verdiyev, Regge hypothesis and spin structure of five-point amplitudes, Nuclear Phys. 68, 675 (1967).

F. Zachariasen and G. Zweig, Bounded momentum transfer restrictions on high-energy interactions, Phys.Rev. 160, 1322 (1967).

F. Zachariasen and G. Zweig, High-energy interactions and multi-Regge-pole hypothesis, Phys.Rev. 160, 1326 (1967).

XIII. Regge poles and higher symmetries

R.C. Arnold, Application of $SU(6)_W$ in a model for vector-meson production at high energies, Argonne Preprint, May 1967.

V. Barger and L. Durand, III, Experimental evaluation of quark and Regge-pole models for high-energy scattering, Phys.Rev. 156, 1525 (1967).

V. Barger and M. Olsson, SU(3) symmetry test for Regge residues, Phys.Rev.Letters 18, 294 (1967).

A. Borgese, F. Buccella, E. Celeghini and M. Colocci, Symmetry and Regge poles for high-energy inelastic two-body reactions, University of Florence Preprint, April 1967.

N. Cabibbo, L. Horwitz and Y. Ne'eman, The algebra of scalar and vector vertex strengths in Regge residues, Physics Letters 22, 336 (1966).

N. Cabibbo, J.J.J. Kokkedee, L. Horwitz and Y. Ne'eman, Possible vanishing of strong interaction cross-sections at infinite energies, Nuovo Cimento 45A, 275 (1966).

F.S. Chen-Cheung, Relation among the πN and KN charge-exchange cross-sections from the SU(3) Regge-pole theory, Phys.Rev. 156, 1520 (1967).

J. Daboul, Compatibility of quark and Regge-pole models, Nuovo Cimento 50A, 850 (1967).

P.G.O. Freund, Symmetry, universality and non-vanishing asymptotic total cross-sections, Nuovo Cimento 46A, 563 (1966).

P.G.O. Freund, A.N. Maheshwari and E. Schonberg, Baryonic Regge recurrences and $U(6)_W \otimes O(2)_W$ symmetry with application to decays and photoproduction, Phys.Rev. 159, 1232 (1967).

P.B. James and R.K. Logan, A Regge quark model of hadron scattering, Physics Letters 25B, 38 (1967).

V.G. Kadyshevskij and R.M. Mir-Kasimov, Regge trajectory splitting and relations between high-energy cross-sections, Dubna Preprint P2-3251, May 1967.

Y. Ne'eman and J.D. Reichert, Charge exchange and associated production in the algebra of factorized residues, Phys.Rev.Letters 18, 1226 (1967).

R.J.N. Phillips and W. Rarita, Prediction for $\pi^- p \to \eta^0 n$ from Regge poles and SU(3), Phys.Rev. 140, B200 (1965).

A. Salam and J. Strathdee, Reggeization of internal symmetries, Phys.Rev.Letters 19, 339 (1967).

Ph. Salin, Inelastic meson-baryon scattering with Regge poles and SU(3) symmetry, Nuclear Phys. B3, 323 (1967).

H. Yabuki, On relations between total cross-sections at high-energy, Nuovo Cimento 48A, 229 (1967).

XIV. The Regge pole versus the one-particle-exchange model

L. Durand, III, Connection between Regge pole and single particle exchange models for high-energy reactions, Phys.Rev. 161, 1610 (1967).

L. Van Hove, Regge pole and single particle exchange mechanism in high-energy collisions, Physics Letters 24B, 183 (1967).

XV. Properties of trajectories and residue functions

R.C. Arnold, Bound states and Regge trajectories in a vector meson exchange model, Nuovo Cimento 37, 589 (1965).

N.F. Bali, Shu-Yuan Chu, R.W. Haymaker and Chung-I Tan, Regge trajectories for two Yukawa potentials, Phys.Rev. 161, 1450 (1967).

A.O. Barut and D.E. Zwanziger, Complex angular momentum in relativistic S-matrix theory, Phys.Rev. 127, 974 (1962).

P. Carruthers and M.M. Nieto, Dynamical model for negative parity Regge trajectories in the πN system, Cornell University Preprint, January 1967.

Shu-Yuan Chu and Chung-I Tan, The high-energy behaviour of Regge trajectories in a bootstrap model, Univ. of California Preprint UCRL 17511, April 1967.

R. Dashen and S. Frautschi, Chew-Low model for Regge-pole couplings, Phys.Rev. 152, 1450 (1966).

B.R. Desai, Residues of Regge poles and the diffraction peaks, Phys.Rev. 138, B1174 (1965).

I.T. Drummond, Simplified model for a three-particle Regge trajectory, Phys.Rev. 155, 1749 (1967).

C.E. Jones and V.L. Teplitz, Investigation of the hypothesis of Khuri's theorem on Regge-pole asymptotes, Phys.Rev.Letters 19, 135 (1967).

N.N. Khuri, On the possibility of an infinite sequence of Regge recurrences, Phys.Rev.Letters 18, 1094 (1967).

H.J.W. Müller, Determination of Regge trajectories in a bootstrap model of pion-pion scattering, Zeitschr.Phys. 205, 145 (1967).

T. Sawada, Mesons as Regge dipoles, Nuovo Cimento 48A, 534 (1967).

T. Sawada, Dipole nature of the leading Regge trajectory, Tokyo Univ. of Education Preprint, March 1967.

J.R. Taylor, Analyticity of the position and the residue of Regge poles, Phys.Rev. 127, 2257 (1962).

XVI. Complex angular momenta in presence of spin

F. Calogero, J.M. Charap and E.J. Squires, The continuation in total angular momentum of partial wave amplitudes for particles with spin, Ann.Phys. (N.Y.) 25, 325 (1963).

W. Drechsler, Reggeization of helicity amplitudes, to be published in Nuovo Cimento.

M. Gell-Mann, M. Goldberger, F. Low, E. Marx and F. Zachariasen, Elementary particles of conventional field theory as Regge poles, III, Phys.Rev. 133, B145 (1964).

S. Mandelstam, The Regge formalism for relativistic particles with spin, Nuovo Cimento 30, 1113 (1963).

V. Singh, Regge poles in πN scattering and in $\pi\pi \to N\bar{N}$, Phys.Rev. 129, 1889 (1963).

W.G. Wagner, Simplicity of Regge asymptotic amplitudes, Phys.Rev. Letters 10, 202 (1963).

XVII. Factorization and spin-dependence

J.M. Charap and E.J. Squires, Factorization of the residues of Regge poles, Phys.Rev. 127, 1387 (1962).

G.C. Fox and E. Leader, Factorization of helicity amplitudes at high energies, Phys.Rev.Letters 18, 628 (1967).

M. Gell-Mann, Factorization of couplings to Regge poles, Phys.Rev. Letters 8, 263 (1962).

V.N. Gribov and I.Ya. Pomeranchuk, Complex angular momentum and the relation between the cross-sections of various processes at high energies, Phys.Rev.Letters 8, 343 (1962).

V.N. Gribov and I.Ya. Pomeranchuk, Spin structure of the meson-nucleon and nucleon-nucleon scattering amplitude at high energies, Phys.Rev.Letters 8, 412 (1962).

Y. Hara, Spin independence of total cross-sections, Physics Letters 23, 696 (1966).

Y. Hara, Total cross-sections at high energies, Progr.Theor.Phys. 37, 941 (1967).

T. Kawai, A generalized factorization theorem and the asymptotic behaviour of the scattering amplitude, Nuovo Cimento 50A, 176 (1967).

Keh Ying Lin, Regge-pole theory and spin-independence of the total cross-sections, Phys.Rev. 159, 1362 (1967).

A.H. Mueller and T.L. Trueman, Spin dependence of high-energy scattering amplitudes, I and II, Phys.Rev. 160, 1296 and 1306 (1967).

XVIII. Ghost-killing mechanisms and dips in cross-sections

F. Arbab and C.B. Chiu, Association between the dip in the $\pi^- p \to \pi^0 n$ high-energy angular distribution and the zero of the ρ trajectory, Phys.Rev. 147, 1045 (1966).

G.F. Chew, Decreasing $I = 0$, $J = 0$ $\pi\pi$ phase shift and Regge ghosts, Phys.Rev.Letters 16, 60 (1966).

C.B. Chiu, Shu-Yuan Chu and Ling-Lie Wang, Regge-pole model for πN and NN secondary maxima and the no-compensation mechanism, Phys.Rev. 161, 1563 (1967).

S. Frautschi, Regge trajectories and minima in differential cross-sections, Phys.Rev.Letters 17, 722 (1966).

M. Gell-Mann, Applications of Regge poles, Proceedings of the International Conference on High-Energy Physics at CERN, Geneva 1962 (edited by J. Prentki), p.533.

Ling-Lie Wang, Prediction of a minimum in the high-energy $\pi N \to \omega N$ differential cross-section, Phys.Rev.Letters 16, 756 (1966).

Ling-Lie Wang, Regge-pole formulas for differential cross-sections of quasi two-body πN and NN interaction, Phys.Rev. 153, 1664 (1967).

XIX. Cuts in the angular momentum plane

A.A. Anselm and I.T. Dyatlov, Mandelstam branch points and scattering of particles at high energies and large momentum transfers, Physics Letters 24B, 479 (1967).

J.B. Bronzan and C.E. Jones, Elastic unitarity and Regge-cut discontinuities, Phys.Rev. 160, 1494 (1967).

C.B. Chiu and J. Finkelstein, Suggestive features in πN charge-exchange polarization associated with Regge cuts, Nuovo Cimento 48A, 820 (1967).

V.N. Gribov, On the possible experimental investigations of Regge branch points, Yadernaya Fizika 5, 197 (1967). English translation in Soviet J. Nuclear Phys. 5, 138 (1967).

V.N. Gribov, I.Ya. Pomeranchuk and K.A. Ter-Martirosyan, Moving branch points in j-plane and Regge-pole unitarity condition, Phys.Rev. 139, B184 (1965).

C.E. Jones and V.L. Teplitz, Branch points, fixed poles and falling trajectories in the complex j-plane, Phys.Rev. 159, 1271 (1967).

S. Mandelstam, Cuts in the angular-momentum plane, I, Nuovo Cimento 30, 1127 (1963); II, Nuovo Cimento 30, 1148 (1963).

S. Mandelstam and Ling-Lie Wang, Gribov-Pomeranchuk poles in scattering amplitudes, Phys.Rev. 160, 1490 (1967).

R. Oehme, Fixed poles in the complex angular momentum plane, Phys. Rev.Letters 18, 1222 (1967).

P. Osborne and J.C. Polkinghorne, Double Regge poles and Regge cuts, Nuovo Cimento 47A, 526 (1967).

D.L. Pursey and L. Sertorio, Regge cuts and πp total cross-sections, Phys.Rev. 155, 1591 (1967).

H.J. Rothe, Study of branch points in the angular-momentum plane, Phys.Rev. 159, 1471 (1967).

Y. Srivastava, Asymptotic unitarity constraints on Regge multipoles and cuts, University of Rome Preprint, May 1967.

Y. Srivastava, Condensation of Regge cuts, vanishing total cross-sections and twisting trajectories, Phys.Rev.Letters 19, 47 (1967).

XX. Unequal mass reactions (see also point XXI)

V. Barger, Regge exchange mechanism for inelastic reactions, Nuovo Cimento 35, 700 (1965).

L. Durand, III, Regge poles in the scattering of particles of unequal mass - Remark on a paper by Freedman and Wang, Phys.Rev. 154, 1537 (1967).

H.W. Fearing, Daughter trajectories and Regge formalism for scatterings of unequal mass particles, Stanford University Preprint ITP 253, March 1967.

D.Z. Freedman, C.E. Jones and Jiunn-Ming Wang, Daughter trajectories and unequal-mass scattering, Phys.Rev. 155, 1645 (1967).

D.Z. Freedman and Jiunn-Ming Wang, Regge poles and unequal-mass scattering processes, Phys.Rev. 153, 1596 (1967).

M.L. Goldberger and C.E. Jones, Analyticity constraints on unequal-mass Regge formulas, Phys.Rev. 150, 1269 (1966).

N. Nakanishi, On the validity of the Regge formula in the unequal-mass case, Progr.Theor.Phys. 37, 618 (1967).

R.J. Oakes, Regge poles and the scattering of unequal-mass particles Physics Letters 24B, 154 (1967).

I.A. Sakmar, The difference in the kinematics of high-energy crossing in the Regge formalism for equal (m+m → m+m) and non-equal (m+M → m+ M) masses, Nuovo Cimento 40A, 76 (1965).

I.A. Sakmar and J. Wojtaszek, Four mass kinematics for Regge crossing, to be published in Phys.Rev.

XXI. Mandelstam analyticity and complex angular momentum. Daughter trajectories and conspiracy. (See also point XX.)

E. Abers and V. Teplitz, On kinematic constraints, crossing and the Reggeization of scattering amplitudes, Phys.Rev. 158, 1365 (1967).

G. Cohen-Tannoudji, A. Morel and H. Navelet, Kinematical singularities, crossing matrix and kinematical constraints for two-body helicity amplitudes, Saclay Preprint, April 1967.

B. Diu and M. LeBellac, Kinematical constraints on Regge-pole residues, to be published in Nuovo Cimento.

L. Durand, III, Subsidiary Regge trajectories with singular residues; nucleon-nucleon scattering, Phys.Rev.Letters 18, 58 (1967).

J. Finkelstein and Jiunn-Ming Wang, A proof of the Lorentz pole hypothesis, Univ. of California Preprint UCRL 17500, April 1967.

S. Frautschi and L. Jones, Small angle photoproduction and conspiracy, to be published in Phys.Rev.

M.B. Halpern, Conspiracy and superconvergence in pion photoproduction, Phys.Rev. 160, 1441 (1967).

H. Högaasen and Ph. Salin, General classification of conspiracy relations, Nuclear Phys. B2, 615 (1967).

R.J.N. Phillips, Is there a pion conspiracy?, Nuclear Phys. B2, 394 (1967).

A.R. Swift, A daughter Regge trajectory in a field theory model, Univ. of Wisconsin Preprint, March 1967.

A.R. Swift, A relativistic model of daughter Regge trajectories, Phys.Rev.Letters 18, 813 (1967).

J.C. Taylor, Regge poles in invariant amplitudes and families of trajectories, Oxford University Preprint, April 1967.

J.C. Taylor, Regge trajectories and singularities at t = 0, Oxford University Preprint 19-67, May 1967.

D.V. Volkov and V.N. Gribov, Regge poles in nucleon-nucleon and nucleon-antinucleon scattering amplitude, Zh.Eksper.Teor.Fiz. 44, 1068 (1963), English translation: Soviet Phys. JETP (USA) 17, 720 (1963).

XXII. Group-theoretical approach to complex angular momentum

N.F. Bali, J.S. Ball, G.F. Chew and A. Pignotti, Analytic S-matrix approach to zero-momentum transfer symmetry, Phys.Rev. 161, 1459 (1967).

E.G. Beltrametti and G. Luzzatto, A general treatment of the complex-angular-momentum SU(2) representations, Nuovo Cimento 51A, 147 (1967).

R. Delbourgo, A. Salam and J. Strathdee, Partial wave analysis in terms of the homogeneous Lorentz group, to be published in Phys. Rev.

R. Delbourgo, A. Salam and J. Strathdee, Harmonic analysis in terms of the homogeneous Lorentz group, Physics Letters 25B, 230 (1967).

G. Domokos, Four-dimensional symmetry, Phys.Rev. 159, 1387 (1967).

D.Z. Freedman and Jiunn-Ming Wang, O(4) symmetry and Regge-pole theory, Phys.Rev. 160, 1560 (1967).

G.I. Iverson, A group-theoretical interpretation of complex angular momentum, Nuovo Cimento, 51A, 289 (1967).

J.-M. Levy-Leblond, Regge poles and/or group theory, Nuovo Cimento 45A, 772 (1966).

E.H. Roffman, Complex inhomogeneous Lorentz group and complex angular momentum, Phys.Rev.Letters 16, 210 (1966).

M.H. Rubin, An expansion of the two particle scattering amplitude in terms of the matrix elements of the Lorentz group, Univ. of Wisconsin Preprint, February 1967.

R.F. Sawyer, O(4) and forward production processes at high energies, Phys.Rev.Letters 18, 1212 (1967).

J. Strathdee, J.F. Boyce, R. Delbourgo and A. Salam, Partial wave analysis, I, International Centre for Theoretical Physics, Trieste, Preprint IC/67/9, February 1967.

M. Toller, On the group theoretical approach to complex angular momentum and signature, CERN Preprint TH.770, May 1967.

M. Toller, An expansion of the scattering amplitude at vanishing four-momentum transfer using representations of the Lorentz group, CERN Preprint TH.780, April 1967.

XXIII. Regge poles and sum rules

J.B. Bronzan, I.S. Gerstein, B.W. Lee and F.F. Low, Current algebra and non-Regge behaviour of weak amplitudes, Phys.Rev. Letters 18, 32 (1967).

J.B. Bronzan, I.S. Gerstein, B.W. Lee and F.E. Low, Current algebra and non-Regge behaviour of weak amplitudes, Phys.Rev. 157, 1448 (1967).

V. de Alfaro, S. Fubini, G. Rossetti and G. Furlan, Sum rules for strong interactions, Physics Letters 21, 576 (1966).

R. Gatto, New sum rules for superconvergence, Phys.Rev.Letters 18, 803 (1967).

R. Gatto, Convergence relations from Regge behaviour, Nuovo Cimento 49A, 747 (1967).

R.H. Graham and M. Huq, Superconvergence relations for the process $\pi N \to \rho N$, Phys.Rev. 160, 1421 (1967).

M.B. Halpern, Conspiracy and superconvergence in pion photoproduction, Phys.Rev. 160, 1441 (1967).

D. Horn, C. Schmid and M. Suzuki, Finite energy sum rules and the Regge analysis of the πN charge-exchange amplitude, Cal.Tech. Preprint CALT 68-124, March 1967.

Jong-Ping Hsu and S. Okubo, Tests of sum rules based upon Regge-pole model, Physics Letters 24B, 179 (1967).

K. Igi and S. Matsuda, New sum rules and singularities in the complex j-plane, Phys.Rev.Letters 18, 625 (1967).

K. Kikkawa, Regge-pole residues and superconvergence hypothesis in the baryon-meson scattering, Nuovo Cimento 51A, 852 (1967).

R. Musto and F. Nicodemi, Gauge invariance and Regge-pole sum rules for pion photoproduction, Syracuse Univ. Preprint NYO 3399-104, March 1967.

S. Okubo, Generalized algebra of currents and Regge poles, Univ. of Rochester Preprint, November 1966.

S. Okubo, Regge pole and generalized algebra of currents, presented at the 4th Coral Gables Conf. on Symmetry, Univ. of Miami, Jan. 1967, Univ. of Rochester Preprint UR 875-179, January 1967.

R.J.N. Phillips, Two-Reggeon branch points and double charge exchange, Physics Letters 24B, 342 (1967).

R. Ramachandran, Fermion trajectory parametrization and superconvergence, International Centre for Theoretical Physics, Trieste, Preprint IC/67/30, May 1967.

H.R. Rubinstein and G. Veneziano, Connection between Regge-pole parameters and local commutation relations, Phys.Rev. 160, 1286 (1967).

J.H. Schwarz, Superconvergence relations from Regge-pole theory, Phys.Rev. 159, 1268 (1967).

V. Singh, Fubini sum rule and analyticity in angular momentum plane, Phys.Rev.Letters 18, 36 (1967).

XXIV. Modified Regge representations

W.J. Abbe and G.A. Gary, Further studies of a recent Regge representation, Phys.Rev. 160, 1510 (1967).

N.W. Dean, Regge-like poles in the impact parameter plane, to be published in Nuovo Cimento.

A. Gersten, On the expansion of the scattering amplitude in functions interpolating Legendre polynomials, Ann.Phys.(N.Y.) 44, 112 (1967).

Y.S. Jin and H.A. Rashid, Regge-Khuri representation for photoproduction, Nuclear Phys. 58, 611 (1964).

M. Kretzschmar, On the modified Regge representation of the Khuri type, Max-Planck Inst., Munich, Preprint, April 1966.

S. Mukherjee, Modified Regge representation, Phys.Rev. 160, 1546 (1967).

XXV. Miscellaneous

W.J. Abbe, P. Nath and Y.N. Srivastava, Theory of Reggeized bootstrap, Nuovo Cimento 49A, 716 (1967).

I.T. Drummond and G.A. Winbow, Complex angular momenta and infinite helicity sums, Phys.Rev. 161, 1401 (1967).

G. Konisi and T. Saito, Reggeization of particles with identical quantum numbers, Osaka University Preprint, March 1967.

S. Okubo, Reggeized tadpole model and electromagnetic mass differences, Univ. of Rochester Preprint, December 1966.

T. Pradhan and J.N. Passi, Reggeization of elementary particles, Phys.Rev. 160, 1336 (1967).

Meng Ta-Chung, On the Regge-pole model for isovector nucleon form factor, Tech. Hochschule Karlsruhe, Preprint, December 1966.